Platelet Rich Plasma in Regenerative Tendon Repair

Mechanobiological Interactions and Clinical Application

Joseph Alsousou



Supervisors

Dr Mark Thompson | Dr Sarah Franklin | Professor Keith Willett

Nuffield Department of Orthopaedics, Rheumatology
and Musculoskeletal Sciences (NDORMS)

A thesis submitted for the degree of
Doctor of Philosophy

Wolfson College
Michaelmas Term 2013

This thesis is submitted to the Nuffield Department of Orthopaedics, Rheumatology and Musculoskeletal Science (NDORMS), University of Oxford, in partial fulfilment of the requirements for the degree of Doctor of Philosophy. The thesis is entirely my own work and, except where otherwise stated, describes my own research.

Joseph Alsousou, Wolfson College, Oxford

Copyright©2013 by Joseph Alsousou

All Rights Reserved

Platelet Rich Plasma in Regenerative Tendon Repair:
Mechanobiological Interactions and Clinical Application

Joseph Alsousou, Wolfson College, Oxford
Submitted for the degree of Doctor of Philosophy
Michaelmas Term 2013

Tendon injury prevalence in both athletic and occupational settings is on the increase. Tendon healing properties are poor, despite the complex biological process triggered by the injury, which makes those injuries incapacitating for months. A significant proportion of these injuries remain difficult to treat, and many patients suffer from decreased performance and longstanding sequelae. While mechanical stabilization has been a hallmark of tendon surgical management, orthobiologics are playing an increasing role in optimizing tendon healing. Platelet rich Plasma (PRP), which is a volume of autologous plasma having platelet concentration above baseline, has been suggested as an accelerant orthobiological agent rich in supraphysiological concentration of growth factors. However, strong evidence of its mode of action and of its clinical efficacy is lacking.

The purpose of this thesis is to identify the role of PRP in tendon regeneration in *in vitro* and clinical studies. Firstly, the viability and biological components of clinically-prepared PRP were studied in novel experiments. This PRP was used in linked *in-vitro* studies to investigate the possible mechanism of PRP effect on the injured Achilles tendon cells and tissues. Cell count, viability, proliferation and DNA content were studied. The clinical application of PRP in Achilles tendon rupture was assessed in a randomised clinical pilot study using a combination of PROMs, objective outcome measures and a novel imaging modality called functional ultrasound elastography. This non-invasive technique was developed in a healthy-tendons volunteer study and its feasibility in ruptured tendons was assessed in the pilot trial. In another unique study, the immunohistochemical response to PRP was assessed in biopsies taken under US guidance at week 6 and compared to control to explore the possible mechanism of PRP effects.

The findings confirmed that PRP is a viable activatable autologous blood product rich in growth factors. The results also confirmed that leukocytes and platelets are present in very high concentration with reversal of lymphocyte neutrophil ratio. Elastography volunteer study confirmed that FUSE is feasible using clinically applicable ultrasound scan. The improved algorithm allowed visualisation of localised strain within the studied tissues. The clinical application of PRP in Achilles tendon rupture revealed positive efficacy signal that PRP led to faster healing, improved pain and earlier restoration of function. However, the findings of this pilot trial were indicative and not confirmative. Immunohistochemistry analysis showed that PRP enhanced the maturity of the healing tendon tissues by promoting better collagen I deposition, improved Collagen III/Collagen I ratio, reduced cellularity, better vascular structure and higher GAGs content when compared with control. The finding may explain the clinical improvement observed in these patients at week 6 onwards. Linked *in-vitro* studies showed that autologous PRP with its cellular components, which include platelets, leukocytes and erythrocytes, has the ability to stimulate tendon cell migration to the injury site and stimulate proliferation in the injured human tendon. Additionally, it may maintain tissue viability in the hypoxic environment that follows tendon injury. Promoting migration and proliferation of cells and maintain tissue viability may play an important role to accelerate tendon healing.

The findings of this project has informed the design of a phase II large multi-centre randomised controlled trial and helped secure major funding from the National Institute of Health Research (NIHR). This trial will set the scene for PRP use tendon treatment.

To my family, my brave idols
and to Sian Newbury, my beautiful partner;

for their unwavering support and unconditional love

Acknowledgements

It is with great pleasure that I thank everyone who participated in the adventure of this thesis. From the early meetings in 2008 at the John Radcliffe hospital with my supervisor Professor Keith Willett to the final research study in 2012, this journey has been made possible by many great people.

First and foremost, incredible thanks are due to my supervisor Prof Keith Willett. He has championed both me and my work from the very beginning, and has always made the necessary resources available. His expertise in research and clinical fields has been invaluable in ensuring this work was well resourced and well justified. Special thanks are in order for his continued support throughout the difficult times that I faced whilst writing this thesis.

Great thanks to my supervisor Mark Thompson for his invaluable support in each of the studies performed to complete this project. His expertise in mechanobiology did not only help in completing the elastography work but also augmented the link with the engineering department to take this work further into other fields. His guidance and support in refining the work in each chapter is highly valued.

Another great thanks to Sarah Franklin, who has been an amazing supervisor who trained me to perform all the laboratory work including cell culture assays and histology. Her close supervision meant I was able to perform these experiments swiftly and within tight time frame.

Dr Paul Harrison (haematology scientist) contribution to this project has also been essential to complete PRP assays. His experienced opinion has allowed me to refine the design of this project experiments. Also thanks to Dr Eugene McNally (Musculoskeletal Radiologist) for his time and effort towards training me on Ultrasound technique in this field.

Congratulations and thanks are owed to the Trauma Unit of the Oxford University Hospitals NHS Trust, for supporting the clinical trial successfully completing the pilot study. The participation of all the trauma orthopaedic consultants has made this trial successful. A particular thanks to Mr Robert Handley who has taught me the operative technique and supported this project throughout.

The collaboration with Professor Alison Noble and her team at the Institute of Biomedical Engineering (IBME) has been essential to the elastography work. I have worked closely with Prof Noble team to collect, analyse and process elastography data. Dr Larry Li (Engineering scientists) and Mr Phil Brown (Engineering D-Phil student) provided amazing support to this project. My work with P Brown is forming the backbone of his thesis on elastography in musculoskeletal system. His hard work and determination led to improved elastography algorithm and imaging.

Thank you to the friends and staff at Kadoorie research centre for all the support and endless discussions throughout this project. In particular, thanks to Liz Tutton, Susana Symonds and Bridget Gray for their continuing support during the clinical trial and at the writing stage. A sincere thank-you also to all the proof-readers of this thesis in parts or full: Liz Tutton, Sarah Franklin and Sian Newbury.
«Merge Record #»
Ultimately, thank you to my parents, Amina and Ahmed, and my brothers and sisters; Susana, Raed, Rana, Basel and Zoha for their lifetime of support and faith. Despite the terrible situation in their homeland in Syria, they continued to support my work and give me the inspiration to continue.

This work would not have been possible without the financial support of the National Institute of Health Research (NIHR), BOA Joint Action, Oxford Biomedical Research Centre and the International Olympic Committee (IOC).

Also this work would not have possible without the support of the National Health Service (NHS) at clinical, management, R&D and staff levels.









INTERNATIONAL
OLYMPIC
COMMITTEE



Abbreviations

ATR	Achilles Tendon Rupture
TA	Tendo Achilles
FUSE	Functional Ultrasound Elastography
PRP	Platelet Rich Plasma
GF	Growth Factors
US	Ultrasound
MRI	Magnetic Resonance Imaging
RF	Radio Frequency
ATRS	Achilles Tendon Rupture Score
VISA-A	Victoria Institute of Sport Activity – Achilles score
FAOS	Foot and Ankle Outcome Score
DF	Dorsal flexion
PF	Planter Flexion
ELISA	Enzyme-linked Immunosorbent Assay
FCS	Fetal Calf Serum
DMEM	Dulbecco's Modified Eagle Medium

Publications and contributions

The following peer-reviewed papers were written and presented during and based upon the contents of this D.Phil thesis:

Journal Papers

Alsousou J, Ali A, Willett K, Harrison P. The role of Platelet Rich Plasma in Tissue regeneration. Platelet Journal. 2013;24(3):173-82.

Alsousou J, Thompson M, Huley P, Willett K. The Biology of Platelet Rich Plasma and its Application in Trauma and Orthopaedic surgery. A review article. J Bone Joint Surg Br 2009 51-B (8): 987.

Alsousou J, Thompson M, Harrison P, Franklin S, Willett K. Platelet Rich Plasma with its cellular component enhances Tenycyte proliferation. Manuscript in writing.

Brown PG, Alsousou J, Cooper A, Thompson MS, Noble JA. The AutoQual ultrasound elastography method for quantitative assessment of lateral strain in post-rupture Achilles tendons. Journal of Biomechanics. 2013;46(15):2695-700.

Alsousou J, Thompson M, Willett K, Franklin S. Platelet Rich Plasma enhances Achilles tendon rupture healing: an Immunohistochemical Study in human. Manuscript in writing.

Conference Papers

Alsousou J, Thompson M, Willett K, Franklin S. The Effect of PRP on tenocytes in human tendon cultures: an in-vitro study. EFFORT, Istanbul, 2013

Alsousou J, Thompson M, Franklin S, Handley R, McNally E, Willett K. Platelet Rich Plasma in Accelerated Achilles Tendon healing: A Randomised Controlled Trial-Pilot Phase. EFFORT, Istanbul, 2013

Alsousou J, Thompson M, McNally E, Willett K, Noble AJ. Functional Ultra Sound Elastograph (FUSE) of tendon: a novel mechanical and clinical tool. EFFORT, Istanbul, 2013.

Alsousou J, Thompson M, McNally E, Willett K, Noble AJ.Functional Ultra Sound Elastograph (FUSE) of Achilles tendon: a novel tool. ORS, California 2011

Alsousou J, Thompson M, Willett K, Franklin S. The effect of Platelet Rich Plasma (PRP) on Tendon
Alsousou J, Thompson M, McNally E, Willett K, Noble AJ. Regeneration: an in vitro culture study. ORS, California 2011.

Alsousou J, Thompson M, McNally E, Willett K, Noble AJ. Functional Ultrasound Elastography (FUSE) of Achilles tendon: a novel technique. EORS, Davos, 2011

Alsousou J, Thompson M, McNally E, Handley R,Willett K. PATH: Platelet rich plasma in Accelerated Tendo-Achilles Healing. International Olympic Committee consensus meeting, Lausanne, 2010

Awards

The following Awards were presented based upon contents of this thesis:

ARUK Young Investigator Award

ARUK, BOA Congress 2012

Platelet Rich Plasma in Accelerated Achilles Tendon healing: A Randomised Controlled Trial-Pilot Phase

Duthie Award - Basic science

Oxfordshire Deanery and Nuffield Orthopaedic Centre Trust, 2011

The Effect of Platelet Rich Plasma on Tenocytes in Human Achilles Tendon Tissues

Duthie Award - Clinical science

Oxfordshire Deanery and Nuffield Orthopaedic Centre Trust 2010

Platelet Rich Plasma in Accelerated Achilles Tendon healing: A Randomised Controlled Trial

Savio L. Woo Young Researcher Award finalist

Orthopaedic Research Society, California, 2011

Functional Ultrasound Elastography (FUSE) of Achilles tendon: a novel technique of tendon mechanical property measurement

Best Poster Presentation Award

20th European Student Conference, Berlin, 2009

Functional Ultrasound Elastography (FUSE) of Achilles Tendon: developing an outcome tool

Table of Content

LIST OF FIGURES ..... **XIV**

LIST OF TABLES ..... **XVI**

CHAPTER 1 INTRODUCTION **1**

1.1 THE ACHILLES TENDON 4
1.1.1 Etymology - Achilles myth *4*
1.1.2 Anatomy *5*
1.2 TENDON STRUCTURE 8
1.2.1 Macroscopic Tendon Architecture *8*
1.2.2 Ultrastructural Architecture of Tendon *9*
1.2.3 Molecular Composition of Tendon *11*
1.2.4 Cellular Components of Tendon *13*
1.3 MECHANICAL PROPERTIES OF TENDON 15
1.3.1 Ultrastructure Morphological response to loading *15*
1.3.2 Stress-Strain properties of the tendon *17*
1.3.3 In vivo Achilles Tendon Mechanical Properties *18*
1.4 ACHILLES TENDON RUPTURE (ATR) 20
1.4.1 Terminology *20*
1.4.2 Epidemiology *20*
1.4.3 ATR Aetiology *21*
1.4.4 Diagnosis and Imaging *23*
1.4.5 Concepts of Achilles Tendon Rupture Treatment *24*
1.4.6 Tendon Healing *27*
1.5 ACHILLES TENDON RUPTURE – THE DILEMMA 31
1.6 PRESENT STUDY SYSTEM 32
1.7 AIMS OF THE PRESENT THESIS 35
1.8 OUTLINE OF THIS CURRENT THESIS 36

CHAPTER 2 PLATELET RICH PLASMA **37**

2.1 INTRODUCTION 37
2.2 METHODS 38
2.3 DEFINITION 38
2.4 BIOLOGICAL PROPERTIES OF PLATELETS 39
2.5 CELLULAR COMPONENT OF PRP 41
2.6 BIOACTIVE PROTEINS AND GROWTH FACTORS IN PRP 42
2.6.1 Growth Factors *43*
2.6.2 Other Bioactive proteins *45*
2.7 PRP PREPARATION 48
2.7.1 Preparation Methods *48*
2.7.2 Handling and Activation of PRP *51*
2.8 IN VITRO AND ANIMAL STUDIES OF PRP 53
2.8.1 In Vitro Cell and tissue culture *53*
2.8.2 In Vivo Animal Studies *55*
2.9 CLINICAL STUDIES OF PRP 56
2.10 ORTHOPAEDIC APPLICATIONS 57
2.10.1 Bone *57*
2.10.2 Wound Healing *58*
2.10.3 Tendon *59*
2.10.4 Tendon Disorders and PRP clinical studies *59*
2.11 POTENTIAL ADVERSE RISKS OF PRP 62
2.12 DISCUSSION 63
2.12.1 Clinical Studies Design *63*
2.13 PRP CLASSIFICATION SYSTEM 64
2.14 CONCLUSION 67

CHAPTER 3 FUNCTIONAL ULTRASOUND ELASTOGRAPHY (FUSE) 68

3.1 CHAPTER INTRODUCTION 68
3.1.1 Elastography Principles 70
3.1.2 Elastography Algorithm 71
3.1.3 Developing Standardised Foot and Ankle Movement Device 74
3.1.4 Functional Ultrasound Elastography of Achilles Tendon Studies 76
3.1.5 FUSE Volunteers Study 77
3.1.6 Volunteers Study Design and Protocol 77
3.1.7 Volunteers Study Results 81
3.1.8 FUSE Patients study 87
3.2 CHAPTER CONCLUSION 89

CHAPTER 4 PRP BIOLOGICAL CONTENTS, VIABILITY AND FUNCTION 91

4.1 CHAPTER INTRODUCTION 91
4.2 METHODS 93
4.2.1 Whole Blood Collection and PRP Preparation Technique 93
4.2.2 Blood Cells count assay 95
4.2.3 Growth Factors Concentration 95
4.2.4 Aggregation analysis 96
4.2.5 Platelet Function Assay: CD62p marker expression 97
4.3 RESULTS 98
4.3.1 Blood Cells count 98
4.3.2 Growth Factors Concentration 100
4.3.3 Aggregation analysis 100
4.3.4 Platelet Function Assay: CD62p marker expression 101
4.4 CHAPTER DISCUSSION 102
4.5 CHAPTER CONCLUSION 105

CHAPTER 5 PLATELET RICH PLASMA IN ACCELERATED TENDO-ACHILLES HEALING (PATH) TRIAL 106

5.1 INTRODUCTION 106
5.2 BACKGROUND AND RATIONALE 106
5.2.1 Achilles tendon Rupture 106
5.2.2 Platelet Rich Plasma 107
5.2.3 Achilles tendon Rupture and PRP 108
5.3 HYPOTHESIS 109
5.4 METHODS 110
5.4.1 Aims and Objectives 110
5.4.2 PATH Trial 111
5.4.3 Study Population 112
5.4.4 Outcome Measures 113
5.4.5 Trial Flow Chart 115
5.4.6 Interventions 122
5.4.7 PRP Preparation Technique 124
5.4.8 Follow-up assessments 124
5.4.9 Statistical Analysis 125
5.5 RESULTS 126
5.5.1 ATRS 127
5.5.2 VISA-A 129
5.5.3 Foot and Ankle Outcome Score (FAOS) 131
5.5.4 FAOS – Sport 132
5.5.5 FAOS- QOL 133
5.5.6 Functional Ultrasound Elastography 134
5.5.7 Maximum Heel Raise at 6 months 139
5.5.8 Time to return to Work and sport 139
5.5.9 Calf Girth ratio 140
5.5.10 SF-36 141

5.5.11 Adverse Events *142*
5.6 Chapter conclusion 143

CHAPTER 6 THE ACHILLES TENDON HISTOLOGICAL RESPONSE TO PRP: IN VIVO HUMAN STUDY 144

6.1 Chapter Introduction 144
6.2 Methods 146
6.2.1 Patient Groups *146*
6.2.2 Biopsy Procedure *146*
6.2.3 Samples processing *146*
6.2.4 Histological stains *147*
6.2.5 Immunohistochemistry stains *150*
6.2.6 Imaging and Analysis *152*
6.2.7 Statistical Analysis *153*
6.3 Results 153
6.3.1 Histological stains *153*
6.3.2 Immunohistochemistry stains *157*
6.3.3 Modified Bonar Score results *164*
6.4 Chapter discussion 164
6.5 Chapter conclusion 166

CHAPTER 7 PRP IN VITRO EFFECT ON TISSUE AND TENOCYTE CULTURES 167

7.1 Introduction 167
7.2 Methods 168
7.2.1 Tissue culture *169*
7.2.2 Tendon cell culture *170*
7.2.3 PRP preparation *170*
7.3 Preparation of medium for Tenocyte culture Assays 171
7.3.2 PRP Function assay *173*
7.3.3 Growth Factors Concentration Assay *173*
7.3.4 Tissue Culture Cell Counting Assay *174*
7.3.5 Tissue Viability Assay *175*
7.3.6 Alamar Blue Assay- Tenocyte count *176*
7.3.7 DNA Content in Tenocytes Assay *176*
7.3.8 Tenocytes Proliferation Assay *177*
7.4 Results 178
7.4.1 PRP Function assay *178*
7.4.2 Growth Factors concentration Assay *178*
7.4.3 Cell Count Assay *179*
7.4.4 Tendon Tissue Viability Assay *180*
7.4.5 Alamar Blue Assay- Tenocyte count *181*
7.4.6 DNA Content in Tenocytes Assay *182*
7.4.7 Tenocytes Proliferation Assay *183*
7.5 Chapter Discussion 183
7.5.2 Limitations of the in-vitro studies *186*
7.6 Chapter Conclusion 187

CHAPTER 8 GENERAL DISCUSSION AND FUTURE WORK 188

8.1 Platelets Rich Plasma Biological properties 188
8.1.1 PRP potential bioactive componenets *189*
8.1.2 Platelets viability *190*
8.1.3 PRP Activation *191*
8.1.4 PRP classification *191*
8.2 Functional Ultrasound Elstography: An outcome tool 192
8.2.1 FUSE use in ATR *192*
8.3 Clinical efficacy of PRP in ATR: Pilot study 193
8.3.1 Feasibility assessment *193*
8.3.2 PROMS signal *193*

8.3.3 Objective outcome measure *194*
8.4 TENDON IMMUNOHISTOCHEMICAL RESPONSE TO PRP 194
8.5 IN-VITRO PRP EFFECT ON CELLS AND TISSUES 195
8.6 THE EFFICACY SIGNAL OF PRP IN ATR: IN –VITRO AND IN-VIVO 195
8.7 LIMITATIONS 196
8.7.1 Limitations of Elastography Studies *196*
8.7.2 Limitations of PRP Biological Properties studies *197*
8.7.3 Limitations of the clinical pilot study *197*
8.7.4 Limitations of the histology studies *198*
8.7.5 Limitations of in-vitro cell and tissue studies *199*
8.8 FUTURE WORK 200
8.8.1 Multi-Centre Randomised Controlled Trial *200*
8.9 CONCLUSION 208

BIBLIOGRAPHY 209

APPENDICES 228

APPENDIX 3.1 ACHILLES TENDON STUDY DATA MANAGEMENT PROTOCOLS 228
APPENDIX 4.1: AUTOLOGOUS BLOOD WITHDRAWAL PROTOCOL 230
APPENDIX 4.2: PLATELET RICH PLASMA GROWTH FACTORS SAMPLE PREPARATION 231
APPENDIX 4.6 TGF-B1 ELISA IMMUNOASSAY 232
APPENDIX 4.7 PDGF-AB ELISA IMMUNOASSAY 234
APPENDIX 4.5 VEGF ELISA IMMUNOASSAY 236
APPENDIX 4.8 IGF-1 ELISA IMMUNOASSAY 238
APPENDIX 4.6 PLATELET AGGREGATION ASSAY PROTOCOL 240
APPENDIX 4.7 FLOW CYTOMETRY CD62P EXPRESSION ASSAY PROTOCOL 241
APPENDIX 5.2: DYNAMIC USS PROTOCOL 242
APPENDIX 5.3 SHEFFIELD REGIME FOR NON OPERATIVE T.A RUPTURES 243
APPENDIX 5.4 PROTOCOL FOR CUTANEOUS REPAIR OF RUPTURED TA 244
APPENDIX 5.5: ACHILLES TENDON RUPTURE SCORE (ATRS) 245
APPENDIX 5.6: VISA-A QUESTIONNAIRE 246
APPENDIX 5.7 FOOT AND ANKLE OUTCOME SCORE (FAOS – UK) 248
APPENDIX 5.8 FUNCTIONAL USS ELASTOGRAPHY (FUSE) PROTOCOL 252
APPENDIX 5.9 SF – 36 QUESIONNAIRE 253
APPENDIX 6.1 : HAEMATOXYLIN EOSIN STAIN 257
APPENDIX 6.2: ALCIAN BLUE STAINING PROTOCOL 258
APPENDIX 6.3 IMMUNOHISTOCHEMISTERY PROTOCOL 259
APPENDIX 7.1: TENDON EXPLANT PROTOCOL 261
APPENDIX 7.2: LIVE/DEAD VIABILITY STAIN PROTOCOL 263
APPENDIX 7.3: ALAMAR BLUE ASSAY 264
APPENDIX 7.4: PICOGREEN DSDNA CONTENT ASSAY PROTOCOL 265
APPENDIX 7.5: ZIVA™ ULTRASENSITIVE BRDU CELL PROLIFERATION ASSAY 266

List of Figures

Figure 1 .1 Peter Paul Rubens. Achilles Dipped into the River Styx, c. 1650-1655. 5
Figure 1 .2 Anatomy of the Achilles tendon. 7
Figure 1 .3 Low magnification cross section of the tendon in H&E stain (left image) and x20 magnification ... 9
Figure 1 .4 Hierarchical ultrastructure of the tendon..... 10
Figure 1 .5 Extracellular matrix of rat tail tendon imaged by tapping mode AFM. 13
Figure 1 .6 tenocytes position between fibres. 14
Figure 1 .7 Electron micrograph of stretched Achilles tendon.. 16
Figure 1 .8 Typical tendon stress-strain curve.. 16
Figure 1 .9 Dynamic USS of ruptured Achilles tendon.. 24
Figure 1 .10 Achilles tendon and PRP study system 34
Figure 2 .1 Upon activation granules appear to migrate to the platelet periphery where they leave the platelet interior through platelet plasma membrane blebs. 40
Figure 3.1. The principle of ultrasound elastography 70
Figure 3.2. Details of a compression elastography method.. 73
Figure 3.3. FUSE method and strain vector. 74
Figure 3.4. The Oxford Foot and Ankle Moving device (OFAM). 75
Figure 3.5. Tendon sections 78
Figure 3.6. Strain index measurement..... 80
Figure 3.7. Examples of scan images of the same tendon. 83
Figure 3.8. Average stain measurements for the Achilles tendon and fat pad in both axial and longitudinal directions. 85
Figure 3.9. The results of strain index measurement of controlled and freehand FUSE. 85
Figure 3.10. Examples of displacement images of the same tendon. 86
Figure 3.11. An example of acutely ruptured Achilles tendon FUSE scan. 89
Figure 4 .1 PRP preparation using Magellan autologous platelet separator system. 94
Figure 4 .2 Illustration of CD62p expression flowcytometry assay. 98
Figure 4 .3 Examples of histogram analysis of PRP (left) and whole blood (right).. 99
Figure 4 .4 Three examples of electrical impedance graphs 101
Figure 4 .5 an example of PRP function analysis using flowcytometry 102
Figure 4 .6 PRP is mounted in a dual syringe ready for clinical application 104
Figure 5 .1 CONSORT Flow chart. 115
Figure 5 .2 Flow chart of the non-operative leg of the trial 116
Figure 5 .3 Flow chart of the operative leg of the trial... 117
Figure 5 .4 The Oxford Achilles Tendon Rupture treatment selection pathway. 118
Figure 5 .5 Patient blinding method.. 120
Figure 5 .6 Percutaneous surgical TA repair.. 123
Figure 5 .7 ATRS linear regression analysis for all treatment pathways. 128
Figure 5 .8 ATRS linear regression analysis for operative treatment pathway. 129
Figure 5 .9 VISA-A linear regression analysis.. 130
Figure 5 .10 shows the analysis of VISA-A progression in the operative treatment pathway.. 130
Figure 5 .11 The analysis of FOAS- Pain score.. 131
Figure 5 .12 The analysis of FOAS- ADL score. 132
Figure 5 .13 The analysis of FAOS- sport score. 133
Figure 5 .14 Example of B-mode longitudinal images output for ruptured Achilles tendon throughout the follow-up period between rupture diagnosis at week0 to final scan at week 24. 135
Figure 5 .15 Zonare real-time elastography scanning of a PATH trial patient at the time of acute diagnosis (week 0)..... 136

Figure 5 .16 The progression of the ruptured tendon from acute presentation at week0 to healing at week-12……137
Figure 5 .17 The results of elastography strain compared to clinical outcome. 138
Figure 5 .18 Average strain measurement using FUSE algorithm and Elastography index progression throughout tendon healing..... 139
Figure 5 .19 The results of Maximum heel-raise test in PRP and control groups.. 140
Figure 5 .20 Calf girth ratio analysis.. 140
Figure 5 .21 SF-36 scores plot for baseline and final follow up at week 24.. 142
Figure 6 .1 The percutaneous US guided needle biopsy..... 147
Figure 6 .2 General Immunohistochemistry (IHC) protocol outline.. 151
Figure 6 .3 H&E stained samples cell count in PRP and control group tendon tissues. 154
Figure 6 .4 H&E stain grading of fibre structure represented as mean ±SD. 154
Figure 6 .5 H&E stain light microscopy examples 155
Figure 6 .6 Achilles tendon tissue Alcian blue stain. 156
Figure 6 .7 The results of Alcian Blue stain. 156
Figure 6 .8 Collagen I immunohistochemistry staining examples 157
Figure 6 .9 Collagen III immunohistochemistry staining examples 158
Figure 6 .10 The results of collagen I and III immune stain 158
Figure 6 .11 The ratio of collagen III / collagen I in both groups. 159
Figure 6 .12 IHC staining with KI-67.. 160
Figure 6 .13 Proliferation index: the number of KI67+cells/ all cells in the PRP and control groups. There is no significant difference between the two groups. 160
Figure 6 .14 CD 45 stain of the tendon samples. 161
Figure 6 .15 A plot of CD 45 positive cells in the tendon samples of both groups. 162
Figure 6 .16 CD 34 IHC stain of the tendon samples.. 163
Figure 6 .17 Shows the vascularity grade as defined by the modified Bonar score.. 163
Figure 7 .1 Flowchart of tendon tissue cultures using the three medium types 169
Figure 7 .2 The layout of the 96-well plate used in tenocyte culture experiments with different type of medium in each column. 173
Figure 7 .3 Photomicrographs demonstrating the semi-quantitative scoring system.. 174
Figure 7 .4 The cell count average score in the three types of culture media 179
Figure 7 .5 Live & Dead staining in three samples cultured in the three media types.. 180
Figure 7 .6 Live dead cell tissue index in the three culture media types 100% PRP, 50% PRP and control. .. 180
Figure 7 .7 Alamar Blue assay results after 48 hours incubation with culture medias. 181
Figure 7 .8 The effect of media on dsDNA content of tenocytes after 48-hour and 96-hour incubation. ... 182
Figure 7 .9 The results of cell proliferation assay after 48 hour incubation. 183
Figure 7 .10 Light microscopy image of tenocytes cultured with PRP in this study. 185

List of Tables

TABLE 2.1 A LIST OF SOME OF THE GROWTH FACTORS IN THE PLATELET ALPHA GRANULES 46
TABLE 2.2 LIST OF THE IDENTIFIED BIOACTIVE FACTORS IN THE CELL MEMBRANE AND INSIDE THE PLATELET**.** 47
TABLE 2.3 LIST OF PRP PREPARATION DEVICES AND THEIR PRP PRODUCTS 50
TABLE 2.4 PRP AND ACHILLES TENDON RUPTURE CLINICAL STUDIES SUMMARY. 61
TABLE 2.5 EHRENFEST CLASSIFICATION SYSTEM OF THE MAIN AVAILABLE PRP PRODUCTS 64
TABLE 2.6 MISHRA CLASSIFICATION IS DIVIDED INTO 4 TYPES 65
TABLE 2.7 THE MODIFIED PRP CLASSIFICATION SYSTEM. 66
TABLE 4.1: THE AVERAGE CELL COUNT IN PRP AND INITIAL WHOLE BLOOD. 99
TABLE 4.2: THE CONCENTRATION OF GROWTH FACTORS IN WHOLE BLOOD AND PRP. 100
TABLE 4.3: THE MEAN AGGREGATION UNITS AND STANDARD DEVIATION OF THROMBIN, COLLAGEN AND CONTROL IN PRP 101
TABLE 4.4: THE RESULTS OF PLATELET FUNCTION ASSAY IN PRP 102
TABLE 5.1: PATIENTS' RECRUITMENT SUMMARY 126
TABLE 6.1: THE MODIFIED BONAR SCORING SYSTEM 149
TABLE 6.2: ANTIBODIES USED FOR IMMUNOHISTOCHEMISTRY 150
TABLE 6.3 SUMMARISES BONAR SCORE RESULTS IN EACH CATEGORY 164
TABLE 7.1 SHOWS THE CULTURE MEDIUM USED IN OUR EXPERIMENTS. 172
TABLE 7.2 THE SEMI-QUANTATIVE SCORE USED TO QUANTIFY CELL COUNT AROUND EACH EXPLANT. 174
TABLE 7.3 THE CONCENTRATION OF GROWTH FACTORS IN 100% PRP AND 50% FCS 178

Chapter 1 Introduction

Tendons are uniaxial connective tissues interposed between muscles and bones. They transmit contractile forces created in the muscle to bone, resulting in joint movement. Some tendons have the capability of storing energy and releasing it when it is needed. Tendon injuries are common in both athletics and occupational settings. Although most tendons have the ability to heal after injury, mechanobiological properties of healed tendon appear never to match those of intact tendon leading to higher risk of further injury.(1)

Tendon injuries cause major morbidity in the aging but physically active population. 20% of all tendon ruptures involve the Achilles tendon. The incidence of Achilles tendon rupture (ATR) is increasing; reported at 8.5-12 per 100,000 per year with a peak at 30-40 years of age (2). This results from a combination of poor vascularity, changes to the collagen matrix and alteration in the mechanical environment (2). Therefore, even with the best available clinical management, tendon injuries give rise to substantial morbidity that may last for several months and pose a considerable challenge for clinicians (3).

A significant proportion of these injuries remain difficult to treat, and many patients suffer from decreased performance and longstanding pain and discomfort (4). Return to functional activity and minimization of recurrence are the goal of any management intervention. Therapies are currently dominated by the conflicting priorities of rapid rehabilitation and a return to work versus the risk of re-rupture and/or surgery. New cost-effective treatments that reduce both the risk of re-rupture and time to functional healing are needed to address this challenge. Within this scope novel orthobiological agents such as Platelet Rich Plasma (PRP) have become potential treatments for tendon injuries. (5)

PRP, a blood derivative with supraphysiological concentration of platelets, has increasing scientific attention for its potential in safely treating musculoskeletal injury (6). Platelets play an important role in haemostasis, host defense and tissue healing (7). Platelet cellular membrane and granules contain >1100 bioactive proteins, which play an important role in promoting local angiogenesis, cell homing, migration, proliferation, differentiation and collagen deposition, all key in tissue regeneration (8). The full array of potential bioactive growth factors and chemokines released upon platelet activation is becoming well defined (8, 9). These include transforming growth factor (TGF-ß1 and ß2), platelet-derived growth factor (PDGF-AA AB and BB), vascular endothelial growth factor (VEGF A and C), Insulin growth factor (IGF-1), Fibroblast growth factor (FGF) and epidermal growth factor (EGF).

Disruption of the vascular structure as a result of injury leads to fibrin formation and platelet aggregation. A stable blood clot is then formed by blood coagulation. Subsequently, bioactive proteins and growth factors are released into the injured tissue from the platelets and other cells (such as leukocytes) that induce and support cell proliferation, matrix production and vascularisation to achieve tissue healing. (10, 11).

Application of autologous PRP to enhance tendon healing is becoming widely used in clinical practice (12), including tendon and ligament injury repair (13, 14), despite the lack of clinical trials to support its use. The drive of its clinical use has been the evidence provided by cell, tissue and animal studies on PRP effect on proliferation (15), migration (16), protection (17, 18), collagen production (19) and laying of matrix (20). However, most cellular and tissue experiments may not resemble or replicate PRP treatment within clinical settings. Within the published non-clinical literature there are numerous methods of preparing PRP conditioned medium. The most common method is centrifugation at varying speed, which produces highly concentrated platelet plasma. PRP will be activated to form a clot then diluted and filtered of any cells to produce a non-cellular medium that is rich in platelet-produced growth factors (18). In comparison, clinically prepared PRP is in fact a

term that include of wide range of products that have varying biological components (21). Most of these products have varying concentration of blood cells (platelets, leukocytes and erythrocytes). Ehernfest et al classified the different platelet concentrates into four categories, depending on their leucocyte and fibrin content: pure platelet-rich plasma (P-PRP), leukocyte- and platelet-rich plasma (L-PRP), pure platelet-rich fibrin (P-PRF), and leucocyte and platelet-rich fibrin (L-PRF) (21). In addition, platelets are very sensitive to *in vitro* manipulation and can be easily activated during preparation methods therefore prematurely releasing their bioactive contents before application to the targeted tissues considering that platelets release 90% of their functioning molecules within the first hour of activation (12, 13, 22).

Therefore, there are four important factors that need to be assessed when trying to take PRP biological experiments to bedside: firstly the PRP preparation method and its resemblance to clinical preparation techniques, secondly the actual biological components of platelet concentrates, thirdly the viability of platelets within the PRP preparation and fourthly the use of autologous products. To our knowledge, there is no published human tissue culture study that addresses all the above mentioned points.

In addition, the clinical use of PRP for a wide variety of applications has been reported, most prevalently in the periodontal and craniofacial literature. Collectively, these studies provide evidence to support the clinical use of PRP in enhancing bone-graft integration; however, there are few insufficiently studies of the clinical efficacy of PRP application in tendon injuries and their evidence is far from conclusive (7, 13, 23).

Obtaining information about the effect of platelets and their bioactive proteins on tendon tissues and cells in well-designed *in vitro* studies, which incorporate the aforementioned factors, will enormously improve our understanding of healing tendon tissue response to PRP therapy. This then can be linked to *in vivo* human studies to investigate the clinical application of PRP and its histological interactions. The clinical study design should include robust outcome measures that are

able to evaluate the tendon mechanical and functional response to PRP therapy and compare it to a control.

The reminder of this chapter aims to give an introduction to the key areas related to the work that has been undertaken in this thesis:

1. Tendon biomechanical structure
2. Tendon acute injuries
3. Concepts of tendon injury treatment
4. Potential regenerative therapies
5. Platelet Rich Plasma

The rational for laboratory studies and clinical trial and the aims and outline of the thesis have also been discussed.

1.1 The Achilles Tendon

1.1.1 Etymology - Achilles myth

Achilles' name can be analysed as a combination of ἄχος (*akhos*) "grief" and λαός (*Laos*) "a people, tribe, nation, etc." In other words, Achilles is an embodiment of the grief of the people, grief being a theme raised numerous times in the *Iliad*.

In the Greek mythology a boy named Achilles, son of king Peleus and a goddess, the Nereid Thetis, was to be a hero. According to the *Achilleid*, written by Statius in the 1st century AD, when Achilles was born Thetis tried to make him immortal by dipping him in the river Styx. However, he was left vulnerable at the part of the body by which she held him, his heel (figure 1)(24). In another version of this story, Thetis anointed the boy in ambrosia and put him on top of a fire, to burn away the mortal parts of his body. Peleus interrupted her and pulled the boy away by his heel.



Figure 1 .1 Peter Paul Rubens. Achilles Dipped into the River Styx, c. 1650-1655. Oil on panel, 43 5/8" by 35 5/16". Ringling Museum of Art, Sarasota, Florida

Achilles was later in his life wounded in his right heel by an arrow shot by the Trojan prince Paris during the Trojan War. He eventually died from this wound. The story gave rise to the expression “Achilles heel”, meaning a person’s principal weakness.

The oldest known written record of the tendon inserting into the calcaneal bone being named for Achilles tendon, is in 1693 by the Flemish/Dutch anatomist Philip Verheyen. In his widely used text *Corporis Humani Anatomia*, Chapter XV, page 328, he described the tendon's location and termed it "the cord of Achilles" ("quae vulgo dicitur chorda Achillis").

1.1.2 Anatomy

The Achilles tendon (Tendo Calcaneus or tendo Achillis) is the largest tendon of the human body. It is the common tendon of the gastrocnemius and soleus muscles (Triceps Surae muscle). The muscle

originates from the medial and lateral femoral condyles as the two heads of gastrocnemius and continues as the gastrocnemius merges with the soleus distally. The soleus muscle originates from the upper third of the fibula and central third of the tibia. The plantaris muscle, absent in 6%-8%, is a small 5-10 centimetre rudimentary muscle which originates from the lateral femoral condyle, by its long tendon inserts medially (together with the Achilles tendon or alone) on the tuber calcaneii or at the plantar aponeurosis (25).

The tendon fibres from the gastrocnemius extend 11–26 cm above the calcaneus and those of the soleus 3–11 cm above it (25). The tendon is rounded and narrow in shape at its midpoint and finally fans out at the insertion. The cross –section area varies from 0.8-1.4cm^2 along the course of the tendon.(26) The narrowest part of the tendon is approximately 4 cm above the insertion. As the tendon descends, its fibres rotate by up to 90° so that the posterior gastrocnemius tendon fibres rotate anterolaterally and the anterior soleus fibres run posteromedially (25) (Fig. 1). This results in less fibre buckling when the tendon is lax and less deformation of individual strands when under tension. Therefore, fibre distortion and interfibre friction may decrease resulting in increase of strength. (27) The tendon inserts into the central part of the posterior surface of the calcaneus. There is one superficial and one deep bursa at the distal part of the tendon, which is separated from the deep muscles and vessels by a considerable interval filled up with areolar and adipose tissue. Along its lateral side, but superficial to it, is the small saphenous vein.

The tendon does not have a true synovial sheath, but is covered by the paratenon a thin layer of loose areolar tissue that acts to reduce friction. The spaces between these are rich in mucopolysaccharides, which are necessary for the gliding function. On the ventral side the paratenon consists of fatty areolar tissue and contains blood vessels and connective tissues.

The tendon insertion into the calcaneal bone is intimately related to the retrocalcaneal bursa and the collagen fibres are interspersed into the calcaneal bone forming a stiff fibrocartilaginous expansion (28) called the osteotendinous junction, also described as an enthesis (29). Anteriorly to

the horseshoe-shaped retrocalcaneal bursa, the Kager´s fat pad protects the bursa and tendon against the posterior tip of the calcaneal bone. The retrocalcaneal bursa contains synovial fluid that reduces the friction between the bursa walls and subsequently between the Achilles tendon and the calcaneal bone.

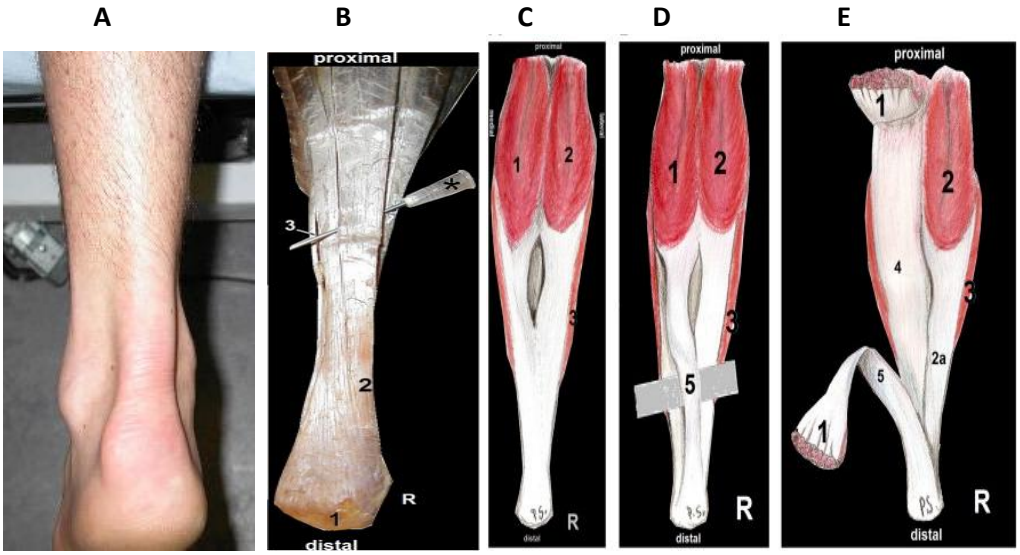


Figure 1 .2 Anatomy of the Achilles tendon. A) The right Achilles tendon subcutaneous projection at the posterior aspect of the heel. B) Achilles tendon anatomy (1) Tuber calcanei, (2) (and above the syringe) the fibres from the lateral part of the medial head of the gastrocnemius and (3) plantaris muscle tendon; * marks syringe. (C–E) The stages of dissection (1) Medial head of the gastrocnemius muscle, (2) lateral head of the gastrocnemius muscle, (2a) fibres from the lateral head of the gastrocnemius, (3) soleus muscle, (3a) fibres from the soleus muscle, (4) aponeurosis of soleus muscle and (5) fascicle from the medial head of the gastrocnemius muscle. Some of the images adapted from Szaro et al (30)

The blood supply of the Achilles tendon is provided by branches of the peroneal and posterior tibial arteries. Vessels originating from the gastrocnemius and soleus muscles supply the tendon at the musculotendinous junction. The blood vessels to the distal part of the tendon, at the region of the enthesis, originate from an arterial plexus at the posterior part of the calcaneal bone. This supply starts at the margin of the insertion and extends up the endotenon for about 2 cm proximally (31). Qualitative and quantitative histological analyses have shown that the Achilles tendon proper (the central parts of tendons) has a rather poor blood supply throughout its length, as determined by the small number of blood vessels per cross-sectional area. This may suggest that poor vascularity may prevent adequate tissue repair following trauma, leading to further weakening of the tendon (32).

1.2 Tendon structure

1.2.1 Macroscopic Tendon Architecture

The tendon is highly fibrous connective tissue, which has a brilliant white colour with a glistening appearance. Tendons are considerably varied in shape and in the way that they are attached to bone and muscles. Tendon shape ranges from cylindrical to flattened ribbons. The tendons for large, powerful muscles like the quadriceps are short and broad whereas those attached to muscles which control delicate movements such as finger flexors are long and thin. This variation in shape is due to varying functional roles depending on the anatomical position.

Small tendons are surrounded by a dense connective tissue called a tendon sheath (33). In contrast, large human tendons such as the Achilles tendon are surrounded by a loose areolar connective tissue, called the paratenon and closest to the tendon tissue proper the tissue has the structure of a fine connective tissue sheath called the epitenon. Together the epitenon and paratenon form parts of the peritenon (28). The peritenon (also called paratendon) has both a visceral, inner layer continuous with the epitenon and a parietal layer, continuous with the deeper fascia (26). The middle layer between the paratenon and epitenon is called the mesotenon. The three layers are supplied with fine blood vessels, lymphatic vessels and nerves form the peritenon (figure 1.3).

There are thus three layers consisting of fibrous connective tissue with fine blood vessels, lymphatic vessels and nerves, and forming the entity described as the peritenon (34). The peritenon forms an elastic sleeve around the tendon, which is able to lengthen during tendon movement allowing the tendon to smoothly glide against surrounding tissues (33).

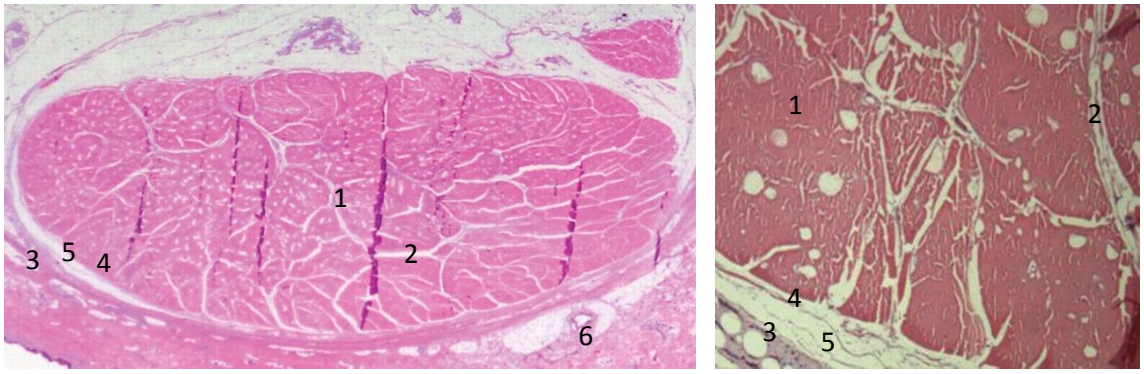


Figure 1 .3 Low magnification cross section of the tendon in H&E stain (left image) and x20 magnification (right). (1) The actual tendon is the heavily stained pink areas. (2) Endotendon (3) Paratenon (4) Epitenon (5) Mesotenon. (6) depicts blood vessels. (34)

The Achilles tendon fibres originating from the gastrocnemius and soleus muscles rotate 90 degrees about the tendon's long axis on descending to the calcaneus (figure 1.2). It has been speculated that this rotation of the tendon portions results in an internal stress especially in the midportion 2-6 cm proximal to the insertion (28).

1.2.2 Ultrastructural Architecture of Tendon

The dense packing of collagen fibrils (typical diameter 10-300 nm) forms collagen fibres, which in turn progressively aggregate into units forming collagen fibre bundles, namely primary (collagen subfascicles), secondary (collagen fascicles) and tertiary (collagen fascicle bundles) ultimately defining the tendon (figure 1.4). The tropocollagen or "collagen molecule" is a subunit of larger collagen aggregates called fibrils, which are held together by electrostatic chemical cross-linking.

In human tendons, the diameter of the tertiary bundles varies from 1000 mm to 3000 mm. The diameter of the secondary bundles ranges from 150 µm to 1000 µm. The diameter of both types of bundles is directly related to the macroscopic size of the tendon so that the lowest values are seen in the small tendons, such as the flexors and extensors of the fingers and toes, and the largest diameters in the big tendons, such as the Achilles, tibialis anterior, and extensor hallucis longus tendons. (28)

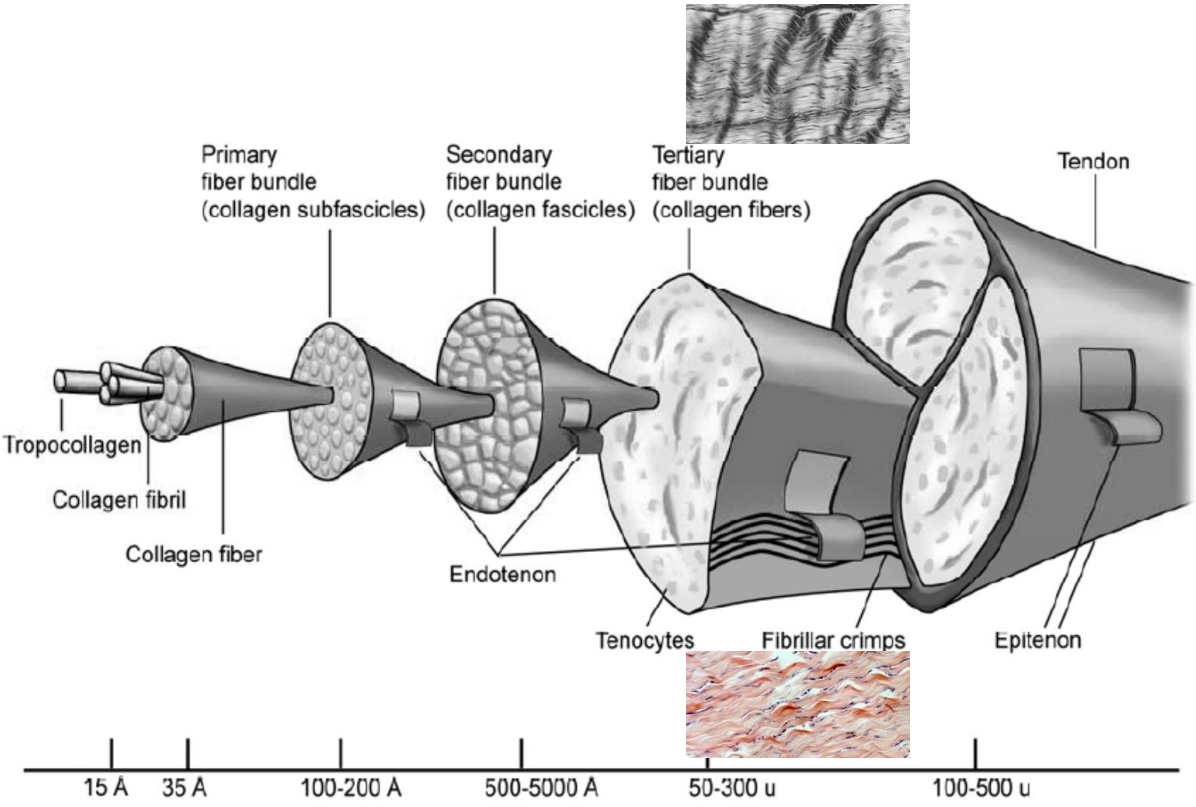


Figure 1 .4 Hierarchical ultrastructure of the tendon. Adapted from Kastelic et al. (35)

The complex structure of tendons at both micro and macro levels mean that the tissue is able to withstand high and varying mechanical demands to which it is subjected during activities of everyday living. Tendons are exposed to longitudinal, transverse and torsion forces *in vivo*. However, in the majority of tendons tensile stress along the longitudinal axis is the greatest; therefore most of the collagen fibres are aligned longitudinally in the tensile regions. Under polarized light microscopy, the collagen fibre bundles appear crimped with alternative dark and light transverse at approximately 100 µm (35). This pattern disappears when the tendon is stretched about 2 % and is thought to be related to the straightening of the fibres (28).

Either within one fascicle or between different fascicles crimping is a characteristic phenomenon. Along the course of individual fibres, or between the superficial and midsubstance fibres of a fascicle, crimping is, however, a rather varying, irregular phenomenon, the crimp angle varying between 0° and 60° (28). This may be due to varying contribution of the proteoglycan cross-linking to the collagen crimp. The direction of the fibre crimping or the phase of the wave pattern may be

completely reversed between the front and back surfaces of the fascicles and subfascicles. Fibrillar crimps conform with the overall complex ultrastructure of the tendon that provides high buffer capacity in harbouring large forces of different directions but mainly in the longitudinal direction (36).

Primary, secondary and tertiary bundles are held together by a Glycosaminoglycan (GAG)-rich layer called endotenon (figure 1.5 and 1.6). The endotenon envelops each tendon fibre and binds individual fibres, and in larger units fibre bundles, together (33). The epitenon is a relatively dense fibrillar network of collagen with strands of 8–10 nm in thickness (33). This network contains longitudinal, oblique, as well as transversal fibrils and shows little variation in density or fibril orientation. Occasionally, the fibrils of the epitenon are fused with the superficially located tendon fibrils via cross linking and GAG links (28). Along with its important function of binding, the endotenon network allows the fibre groups to glide on each other and carries blood vessels, nerves, and lymphatics to the deeper portion of the tendon (37).

1.2.3 Molecular Composition of Tendon

The composition of human tendon can be outlined under four categories: 1. Collagen 2. Elastin 3. Proteoglycans (Hyaluronan, glycosaminoglycans) and 4. Inorganic components.

Water accounts for 65-70% of the total weight of the tendon and is closely associated with large chain glycosaminoglycans which are highly hydrophilic (33). This combination is thought to provide the gliding function of fibrils. Also since water is almost incompressible,the resistance of the tendon against hydrostatic compression forces is high (38).

The dry mass of normal tendons, which makes up about 30% of the total mass, is composed of about 86% collagen, 2% elastin, 1–5% proteoglycans, and 0.2% inorganic components such as copper, manganese, and calcium (39). The collagen portion is made up of 97–98% type I collagen, with small amounts of other collagen types. These include type II collagen in the cartilaginous zones, type III

collagen in the reticulin fibres of the vascular walls, type IX collagen, type IV collagen in the basement membranes of the capillaries, type V collagen in the vascular walls, the pericellular type VI collagen and type X collagen in the mineralized fibrocartilage near the interface with the bone. (40)

The function of elastic fibres is not entirely clear, but they may contribute to the recovery of the crimp configuration of the collagen fibres after tendon stretch (41). Elastic fibres are scarcely present in human tendons and even then can only be found in 10% of healthy human tendons (42). Electron microscopy reveals that elastic fibres are approximately 0.3–2.0 μm in diameter and consist of two distinct morphological components: an amorphous central bulk (core) and electro-dense filaments (43). In some human pathological conditions, such as Ehlers-Danlos syndrome and chronic uremia, the number and volume of the tendinous elastic fibers is clearly increased (38).

The collagen in tendons is held together with proteoglycan components, including decorin and, in compressed regions of tendon, aggrecan, which are capable of binding to the collagen fibrils at specific locations (44). The proteoglycans are interwoven with the collagen fibrils—their glycosaminoglycan (GAG) side chains have multiple interactions with the surface of the fibrils—showing that the proteoglycans are important structurally in the interconnection of the fibrils (45). The major GAG components of the tendon are dermatan sulfate and chondroitin sulfate, which associate with collagen and are involved in the fibril assembly process during tendon development. Dermatan sulfate is thought to be responsible for forming associations between fibrils, while chondroitin sulfate is thought to be more involved with occupying volume between the fibrils to keep them separated and help withstand deformation. Dermatan sulfate chains may extend and associate with other dermatan sulfate chains on decorin that is bound to fibrils, therefore creating interfibrillar bridges and eventually causing parallel alignment of the fibrils (figure 1.5).

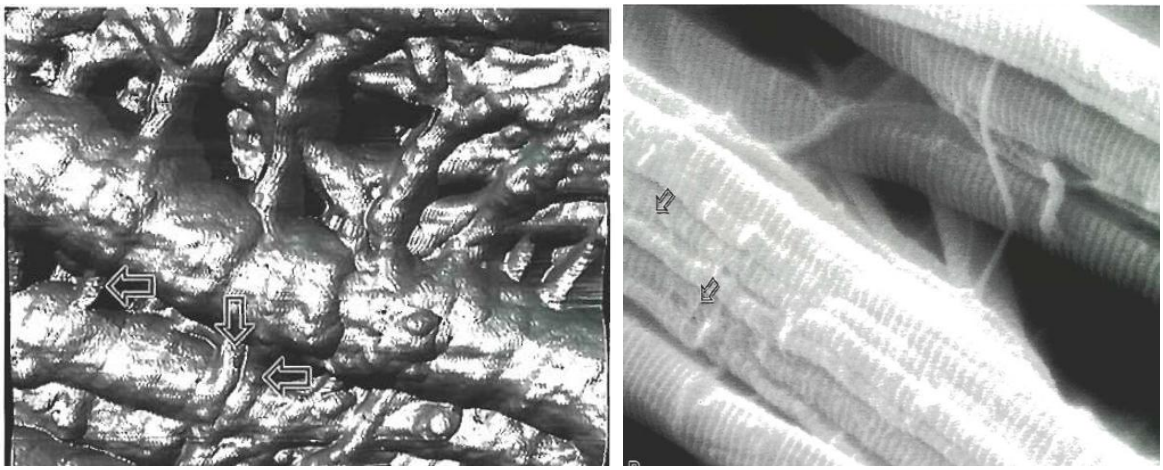


Figure 1 .5 Extracellular matrix of rat tail tendon imaged by tapping mode AFM. Right: Collagen fibrils running from top left to bottom right are covered with a webbing of small glycosaminoglycan filaments (arrow), which are running orthogonal to the collagen fibril and passing from fibril to fibril. Left: Image by high resolution SEM: GAG can easily be seen to wind around collagen fibril rather than radiate from them. Image adapted from Raspanti et al (45)

The inorganic components role in the tendon biomechanical and functional role is largely unknown. Calcium is found in the highest concentrations (0.001–0.01% of dry weight in the tendon proper, and 0.05– 0.1% in the insertion). In pathological conditions such as calcifying tendinopathy, a 10 to 20 fold increase can be detected (46). Other detected components have been magnesium, manganese, cadmium, cobalt, copper, zinc, nickel, lithium, lead, fluoride, phosphor, and silicon. The trace elements are usually in a concentration of 0.02–120 ppm in tendon tissue (33, 46).

1.2.4 Cellular Components of Tendon

The majority of cells in tendons are tenocytes (90-95%) and Immature tenocytes active in the deposition of matrix, known as tenoblasts. Other cells include: chondrocytes (5-10%) usually located at the insertion, synovial cells and vascular cells (33). Many other types of cells such as inflammatory cells, macrophages and cells with myofibroblastic appearances can be found in a pathologically changed tendon (47), but not in healthy tendons (48).

Tenocytes are specialised fibroblasts that are situated within the collagen fascicles. They appear as cells lying in parallel with and inbetween, the tendon fibres in histological longitudinal sections (figure 1.6). Tenocytes are slender, spindle shaped, elongated cells with a sparse cytoplasm (49). The cells have three dimensional networks of processes that run laterally delineating the collagen fibres and longitudinally within the tendon (50). Intracellular communication takes place within this network via gap-junction proteins (connexins 32 and 43). These form distinct networks – tenocyte rows are linked by both longitudinally, but only by connexin 43 laterally. Tenocytes communication via connexin 32 and 43 have differential effects on the load response, with connexin 32 being stimulatory of collagen synthesis and connexin 43 being inhibitory. Cells coordinate and control their response to mechanical signals at least in part by differential actions of these two types of gap junction (51).

There are few cell markers that may be used to mark tenocytes (52). COL-I is the most important protein and should be highly expressed. COL-III, biglycan, decorin, tenomodulin and tenascin C should also be expressed while COL-II and osteocalcin expression should be present just in low amounts (53).

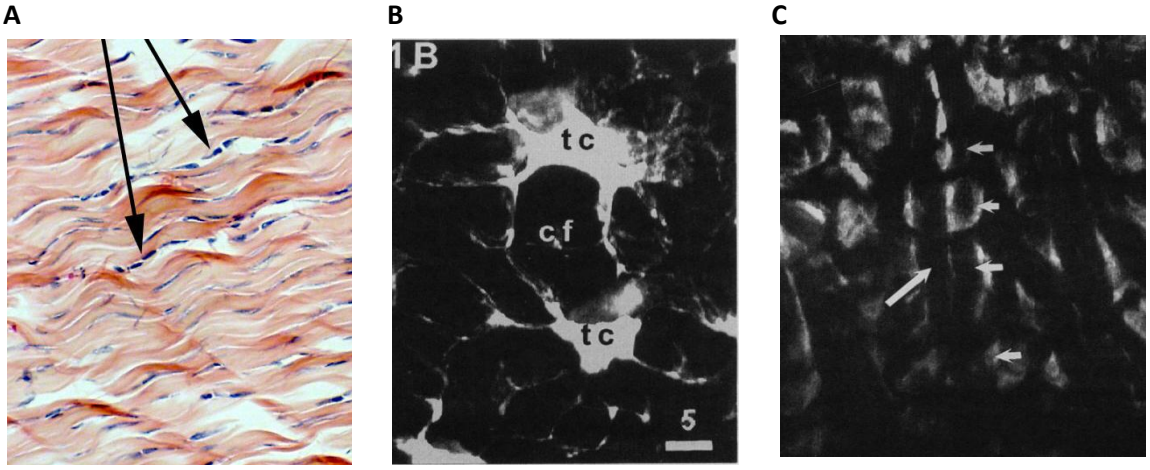


Figure 1 .6 Tenocytes position between tendon fibres. A) Tenocytes in H&E stain. B) Confocal microscopy images of tendon cross section shows tenocytes of tenocyte (tc) with extended broad lateral processes meeting those of adjacent cells. C) Longitudinal projection showing processes extending longitudinally from the cell body. Image adapted from McNeilly et al (50).

1.3 Mechanical properties of tendon

1.3.1 Ultrastructure Morphological response to loading

The primary mechanical strength of tendons is dependent upon extracellular formation of triple-helical collagen fibrils with stabilizing molecular cross-links (54, 55) (Fig 1.4). This intricate architecture means that the tissue is able to withstand high and varying mechanical demands to which it is subjected to during activities of everyday living. The largest component is the longitudinal tensile forces.

The collagen fibres are assembled in highly ordered parallel bundles to respond better to mechanical loading and are aligned along the long axis of the tendon. The collagen crimp changes when the tendon is stretched by tensile loading. Biomechanical studies investigating the physiological function of tendon crimps have demonstrated that they disappeared when tendons were slightly stretched (~2% strain) (figure 1.8) (37). In stretched tendons the crimps pattern began to disappear progressively, i.e. individually rather than simultaneously, from the ends toward the centre of the collagen fascicle. It was also suggested that the initial non-linear toe region of the stress–strain curve of the tendon may correspond to straightening of the crimps (figure 1.7) (56).

SEM studies suggest that fibril and fibres crimps are different terms that describe the wavy configuration of collagen fibrils and fibres inside the tendon structure. Some authors suggested that fibril and fibre crimps response differently to stretching. Franchi et al in a recent publication showed that when tendon is physiologically stretched *in vivo* the fibre crimps decrease in number (46%) and appear more flattened with an increase in the crimp top angle (165° in stretched tendons vs. 148° in relaxed tendons). Under SEM and TEM, the 'fibrillar crimps' are still present, never losing their structural identity in straightened collagen fibril bundles of stretched tendons even where tendon crimps are not detectable. These data suggest that the 'fibrillar crimp' may be the true structural component of the tendon crimp acting as a shock absorber during physiological stretching of Achilles tendon (figure 1.7).(36) Once the collagen fibres have straightened, they stretch linearly with

increasing tendon loads. If the strain placed on the tendon remains at less than 4%, which is within the limits of most physiological loads, the fibres regain their original configuration on removal of the load, but at strain levels 4-8% the collagen fibres start to slide past one another as the intermolecular cross-links fail, and at strain levels > 8% macroscopic ruptures occur because of tensile failure of the fibres and interfibrillar shear failure (figure 1.8) (27). Interestingly, local strains within collagen fibres are smaller than the externally applied strains, never exceeding 1.2% of axial strain, even at 8% gross applied strain (57).

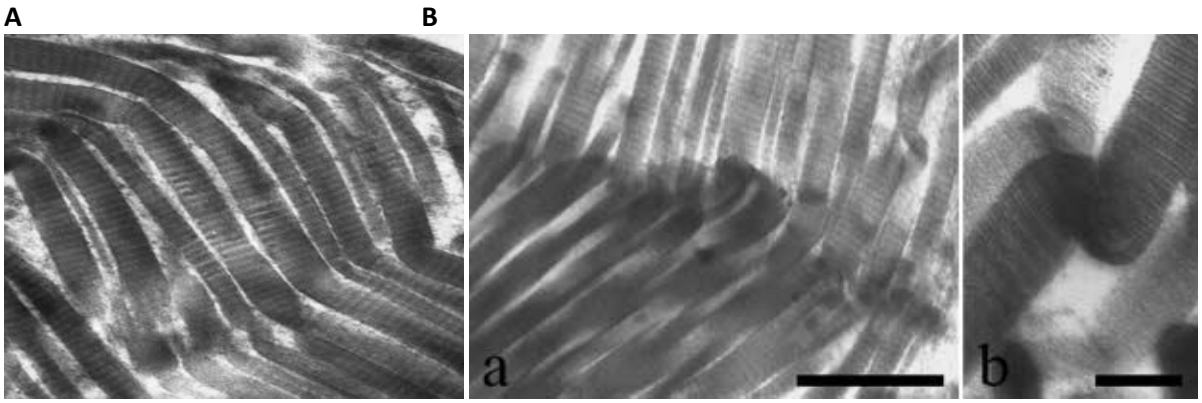


Figure 1 .7 ***A) Electron micrograph of stretched Achilles tendon showing that the same tendon crimp is composed of more than one 'fibrillar crimp' and that each collagen fibril includes many 'fibrillar crimps'. Scale bar = 1 µm. B) Electron micrographs of stretched Achilles tendon showing few crimped collagen bundles and their relative 'fibrillar crimps' (a). Scale bar = 1 µm. See in (b) a twisted and bent collagen fibril. Scale bar = 250 nm(36).***

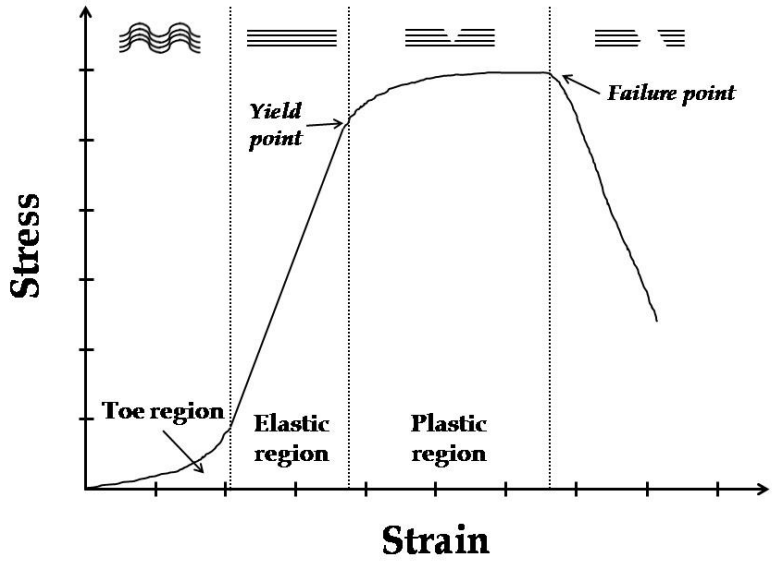


Figure 1 .8 ***Typical tendon stress-strain curve (58). Crimping occurs at the micrometre scale and can be seen using light microscopy (57).***

1.3.2 Stress-Strain properties of the tendon

The mechanical testing of tendons has traditionally been studied using methodologies involving stretching the isolated tendon to failure; with both tendon elongation and the applied force recorded throughout the testing. The strain is determined by the change in length $\frac{\Delta l}{L}$. The Young's modulus, (E), is the slope of the linear part of the stress-strain curve (fig 1.8). It is a measure of stiffness of the tendon, and is dominated by the material behaviour of the straightened collagen. E can be calculated using the following equation:

$$E = \frac{\text{Tensile Stress}}{\text{Tensile strain}} = \frac{\sigma}{\varepsilon} = \frac{F/_{L0}}{A0/_{\Delta L}}$$

Where F is the force applied, A_0 is the original cross-sectional area through which the force is applied, ΔL is the change in length of the tissue, and L_0 is the original length of the tissue. Four different regions can be identified in the tendon stress-train curve (figure 1.8). Region II; referred to as the tendon "toe" region, is associated with tensile stress that reduce the resting crimp of collagen fibres as discussed previously (this is usually under 2% strain). In region II, or the "linear region", loading causes stretching of fibres and at the end of this region some fibres starts to break. Further stress brings the tendon to region III, where additional fibres failure occurs at unpredictable manner. Complete failure occurs at region IV. The most common material properties obtained from the stress-strain curve are Young's modulus (GPa), the ultimate stress (MPa) and the ultimate strain (%). Yong's modulus ranges between 1-2 GPa. Ultimate tendon stress (i.e tensile stress at failure) is ~100MPa. Ultimate tendon strain (i.e. strain at failure) ranges between 4 and 10% (59). The material properties of tendons depend, in part, on the rate at which the tendon or ligament is loaded. Most studies find higher failure stresses and failure strains as faster strain rates although changes in the modulus are often not observed (60).

1.3.3 In vivo Achilles Tendon Mechanical Properties

Despite the fact that an “Achilles heel” reflects “a weakness”, the tendon is by necessity the largest, toughest and strongest tendon in the human body. The tendon transmits the tensile force generated by the gastrocnemius and soleus muscles to the calcaneus. To do this effectively, the tendons must be capable of resisting high tensile forces with limited elongation (61). The biomechanical loading of the Achilles Tendon during normal locomotion varies from 600N in cycling to 4kN in sub-maximal hopping and up to 9kN (110MPa) in running at a speed of 6m/sec (62).

It has been suggested that the human Achilles tendon experiences higher in vivo stresses than most other tendons. Komi et al (63) used cross-sectional area ratios to estimate the in vivo stresses imposed on various tendons. They estimated that while most tendons experience peak stresses below 30 MPa, the human Achilles tendon experiences peak stresses around 67 MPa. Buckle transducer data also suggest that in vivo stresses are high in the human Achilles tendon. It is reported peak stresses of 59 MPa for walking and 111 MPa for running in two subjects who had buckle transducers attached to their Achilles tendons (64).

The age of the individual and the size of the AT are important factors for its biomechanical properties and its capability to cope with high stress levels. Younger individuals have significantly higher tensile rupture stress and lower stiffness (65), while increased age, body height and cross-sectional calf muscle size correlate significantly with thicker Achilles tendons (26, 66, 67). The tendon has the ability to adapt to mechanical loading. Immobilization of tendon during treatment protocols decreases collagen synthesis and increases its degradation. The number and size of the collagen fibre bundles, the water content and the total glycosaminoglycan content diminishes (68, 69). Therefore, the tensile strength of the tendon is markedly reduced. The histochemical changes leading to the atrophy of tendon begin a few hours after cast immobilization (70). The low metabolic rate of the tendon nevertheless means that the atrophy effects are slow and not as dramatic as in muscle. On the other hand, exercise can lead to increases in tendon modulus and strength (71).

Magnetic resonance imaging (MRI) studies have recently reported strains of the AT ranging from 5–10% during isometric contractions at forces below the maximum possible force during dynamic movements.(72) It has previously been thought that such high strain would cause tendon rupture and failure; however real-life activities such as one-legged hopping can induce much larger stresses and strains on the AT without inducing acute rupture (63, 73).

The human Achilles tendon also stores and returns energy during strain loading. Lichtwrack et al (73) study demonstrated the energy storing capabilities of the AT, whereby the tendon stretches in proportion to the force applied during the downward motion of the body and then recoils to release most of the energy stored (74%) during the upward movement. This provides a substantial amount of the total mechanical energy of the on-leg hop (16%). This mechanism has been thought to provide an energy saving mechanism during human walking, running and jumping (73) and has recently been suggested to account for up to 6% of the total mechanical work produced during walking (74).

Despite the advantages of testing a tendon in its physiological environment, the in vivo measurement has some inherent unavoidable problems. One problem relates to the incorporation of heat losses by the tendon. More important is the problem of nonhomogeneous stress application across the tendon since this tendon is formed by the merge of gastrocnemius and soleus muscles. Another issue is the use of invasive techniques previously required to make measurements, such as tantalum bead implementation, which could change the mechanical properties of the tendon or induce errors due to beads migration. The use of externally induced muscle contraction may also result in inaccurate non-symmetrical contraction of the muscle, which does not represent actual muscle contraction. A non-invasive harmless and cost effective in vivo human mechanical property measurement method, which can capture data in real time of dynamic active or passive contraction, will be able to enormously increase our knowledge of tendon material properties.

1.4 Achilles Tendon Rupture (ATR)

1.4.1 Terminology

Achilles tendon rupture may be total or partial, closed or open and acute or late. The term ATR in this thesis will refer to an acute, closed, total rupture of Achilles tendon. An acute or early rupture is one which is diagnosed within one week of injury, while the terms late or chronic rupture have been used to describe a rupture with a delay in treatment of 4 weeks or more. Diagnosis within 1-4weeks is called neglected or subacute rupture. Re-rupture means a repeated rupture, often occurring within the first 12 weeks post treatment.

1.4.2 Epidemiology

The incidence of ATR is on the increase since the 1950s (75). The rupture incidence accelerated in the 1970s to reach 8.5 per 10^5 per year (76). According to Leppilahti *et al.* (1996) the average incidence of ATR, increased from 2 /10^5 inhabitants in 1979 to 1986 to 12 in 1987 to 1994, with a peak incidence of 18 in 1994 (77, 78). The main reason for the rapid increase in ATRs is probably an increase in the popularity of recreational sports since 1980s. The prevalence is approximately 18 per 10^5 per year and is thought to be rising (79).

Acute TA ruptures occur most commonly in males in their third and fourth decades who play sport intermittently; the left TA is more commonly ruptured than the right (80). Bilateral total ATRs are infrequent and only case reports have been published on simultaneous bilateral ATRs. This usually occurs in older patients with systemic disease or a history of long-term corticosteroid medication (81).

About 75% of all ATRs are related to recreational sports demanding sudden acceleration and jumping. Ball games provide more than 60% of cases in many series. Only 8 to 20% of ATR patients are competitive athletes, while 75% are recreational athletes and 10 to 12% do not take part in any sports. ATRs typically occur 2 to 6 cm proximal to the tendon insertion on the calcaneus, and with

decreasing frequency proximally and distally (82). The pathological mechanism is not understood. Only a very few patients have symptoms in their AT before rupture. Maffulli et al (83) reported that only 5% of 176 ATR patients had previous AT symptoms. However, Nestorson et al (84)reported that in elderly patients (>65) a significant proportion of ATR patients (44%) had symptoms before rupture. In this age group, the affected patients differed significantly with respect to age, sports activity and injury mechanism from those without previous AT symptoms.(78) A number of etiological theories have been proposed which include the adverse influence of oral and topical corticosteroids (85), fluoroquinolone antibiotics (e.g. ciprofloxacin) (86), exercise-induced hyperthermia (87) and mechanical abnormalities of the foot (80).

1.4.3 ATR Aetiology

The exact pathogenesis of ATR is unknown. Most authors refer to two etiological theories: 1. The degenerative theory 2. The mechanical theory. According to the degeneration theory repetitive microtrauma and hypovascularity in the tendon are predisposing factors to the chronic degeneration, which leads to a rupture without excessive loads being applied. This theory has been supported by angiographic (88) and histological (89) findings. The mechanical theory is based on the loading of tendon beyond its ultimate strain. The mechanisms of injury include sudden forced plantar flexion of the foot for example during sporting activities; unexpected dorsiflexion of the foot for example during a fall downstairs; and violent dorsiflexion of a plantar flexed foot, for example a fall from a ladder (90).

Histological evidence of collagen degeneration was found in all seventy-four ruptured Achilles tendons described in a study by Arner et al (91). However, nearly two-thirds of the specimens were obtained more than two days after the rupture. Davidsson and Salo (92) reported marked degenerative changes in two patients with a rupture of the Achilles tendon who had an operation on the day of the injury. The changes, therefore, should be regarded as having developed before the

rupture. In a study by Waterston (93), all tendons that were operated on within twenty four hours after the injury showed marked degenerative changes and collagen disruption, in accordance with the findings in another recent study. Alternating exercise with inactivity could produce the degenerative changes seen in tendons (94).

McMaster (95) proposed that a healthy tendon would not rupture, even when subjected to severe strain. However, Barfred (75) demonstrated that, if straight traction were applied to a tendon, as in McMaster's experiments, the risk of rupture would be distributed equally to all parts of the muscle-tendon-bone complex. If oblique tensile loadings were applied, the risk of rupture would be concentrated on the tendon. He calculated that, if a 1.5-centimeter-wide Achilles tendon in a human were subjected to traction with 30 degrees of supination on the calcaneus, the fibres on the convex aspect of the tendon would be under 10% strain before the fibres on the concave side would be strained. Therefore, the risk of rupture would be greatest when the tendon was obliquely loaded, when the muscle was in maximum contraction, and when the initial length of the tendon was short. Such factors are probably all present in movements occurring in many sports that require rapid push-off.

Arner and Lindholm (91) classified the trauma resulting in the rupture into three main categories. The first category was pushing off with the weight-bearing forefoot while extending the knee. This movement is seen in sprint starts and in jumping in sports such as basketball. This mechanism accounted for 53% of the ruptures in their series. The second category was sudden, unexpected dorsiflexion of the ankle, such as that occurring when the foot slips into a hole or the individual falls down stairs (17% of cases). The third category was violent dorsiflexion of a plantar flexed foot, such as may occur after a fall from a height. This mechanism was reported by 10% of patients.

1.4.4 Diagnosis and Imaging

In most cases the history of ATR is typical and diagnosis of an acute rupture can usually be made clinically (83). The patients usually report a sudden pain in the calcaneal area, and have often heard a "pop" or snap in the AT region. Occasionally the pain may be slight or even absent. The majority of patients do not have any symptoms prior to rupture. It is suggested that 4-18% report symptoms such as pain, tenderness or stiffness prior to rupture.(96) Almost always there is a palpable gap in the tendon. The longer the time elapsing between the rupture and examination, the more difficult it may be to palpate the gap at the rupture site because of oedema and haematoma.

There are many diagnostic tests available. In 80% of ATR active planter flexion is absent. However, in 20% of ruptures the flexor digitorum longus is able to actively planter flex the foot leading to 12-28% of misdiagnosis. In Simmonds test (97) there is absent or reduced plantar flexion, while Thompson's test involves squeezing the calf, with consequent failure to achieve plantar flexion (98). In the sphygmomanometer cuff test described by Copeland et al (99), the sphygmomanometer is applied around the bulk of the calf muscle with the knee flexed 90°. The cuff is inflated to approximately 100 mm Hg with the ankle plantar flexed. Passive dorsiflexion of the ankle is then performed by pressing on the sole of the foot. Only a flicker of movement is seen in the column of mercury if the AT is completely ruptured, while if the tendon is intact, the column will rise to match the normal value, as tested on the contralateral calf. This test has only historic value and is not recommended in clinical practice due to the severe pain it may cause.

Ultrasound (US) (80) or magnetic resonance imaging (MRI) (100) may be used if confirmation is necessary or more details of the rupture is required. US dynamic scanning is an inexpensive non-invasive technique, which can be performed in the clinical setting. Our group has previously performed a study to investigate the use of Dynamic US as a selective tool for ATR treatment.(101) The size of rupture gap was identified using dynamic US scan and measured with the foot in planter flexion (figure 1.9). Patients with a gap of 5 mm or more in equinus on ultrasound underwent

surgery; those with a gap of less than 5 mm received non-operative treatment. All patients were followed up to a minimum of 12 months. The results demonstrated that dynamic US scan may be used to determine the optimal management option to reduce the risk of re-rupture. This work allowed us to confirm the clinical diagnosis and introduce a standardised protocol for Achilles tendon treatment selection and progressive rehabilitation protocols for both surgical and non-surgical management.

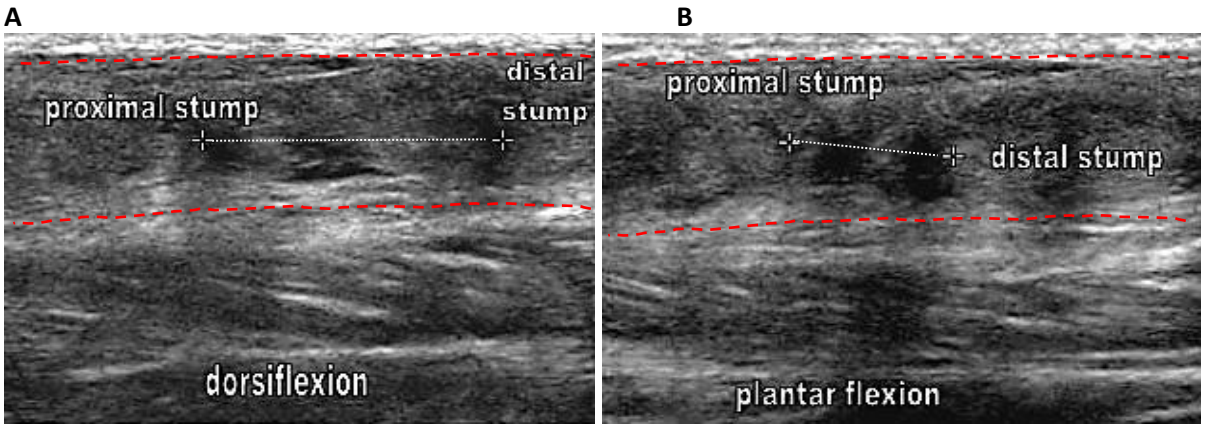


Figure 1 .9 Dynamic USS of ruptured Achilles tendon. A) Measurement of rupture gap in dorsiflexion 2.8mm. B) Minimum approximation of the tendon ends in planter flexion 11mm.

1.4.5 Concepts of Achilles Tendon Rupture Treatment

There is a lack of consensus on the best management of the acute Achilles tendon rupture. Treatment can be broadly classified into operative (open or percutaneous) (102) and non-operative (cast immobilisation or functional bracing) (103). There is on-going controversy regarding the best techniques to manage subcutaneous ruptures of the Achilles tendon. Two recent reviews have concluded that operative management has a lower re-rupture rate (4% vs 15%) but must be balanced by the risks associated with surgery such as infection, adhesion and numbness (104). In all types of treatment the average time off work is 12 weeks while the average time to return to sport or normal activities is 18 weeks (105). Those figures are based on incomplete reported outcome measures and small numbers in few clinical trials. The choice of optimal treatment is usually based on surgeon expert opinion or patient choice. Generally, open surgical management has been used in athletes and young fit patients, percutaneous surgical intervention in those who do not wish to have

an open repair (e.g. for scar avoidance or cosmesis), and non-surgical management in older or less active adults (83). Different surgical techniques exist such as the six-strand repair, the less bulky two-strand repair (Mortensen method) (106), augmentation of the primary repair with the use of a gastrocnemius flap as proposed by Silfverskiold or with plantaris tendon (Aktas technique) (107). The most common open surgical method is direct augmentation of the tendon with Kessler or Web non-absorbable suture. However, in recent years there has been an increase in percutaneous surgical repair in surgical practice, which has been reported to have less infection and skin dehiscence risk.

1.4.5.1 Open Operative Repair

Several authors have opposed operative repair, noting that the high rate of complications is the main disadvantage (80, 108). Soldatis et al (109), in a study of twenty-three patients who had operative repair, reported only two complications, both delayed wound-healing. However, wound problems should not be unexpected when open repair is used, as the most commonly used longitudinal incision passes through poorly vascularized skin. A transverse incision just distal to the gap in the tendon has been reported with only one wound breakdown (110). After the operation, the leg is immobilized in a cast for four to six weeks(111). Some surgeons have advocated the use of a functional orthosis after several days of immobilization in a cast. This orthosis allows plantar flexion but restricts dorsiflexion and is designed to help to prevent atrophy of the triceps surae (112). Some surgeons allow free motion of the ankle but no weight-bearing after operative repair (113).

There is a continuing controversy regarding the use of open operative techniques to manage subcutaneous ruptures of the Achilles tendon, with some investigators reporting a high overall rate of complications (infection 18.2%) and others noting few complications and a low rate of repeat rupture (5-10%) (114).

1.4.5.2 Percutaneous Surgical repair

This technique was first reported by Ma and Griffith (115) who developed a method for percutaneous repair as a compromise between open operative methods and nonoperative treatment. Although this method has less infection and wound dehiscence risk (3.9%), the risk of sural nerve entrapment is reported to be as high as 10% with persistent paresthesia and the necessity of a formal operative exploration to remove the suture and free the nerve (116). There is no difference in re-rupture rate between open and percutaneous TA repair (114).

Percutaneously repaired Achilles tendons are less thick than are those repaired with open procedures, and some patients may prefer the better appearance that this may offer (112).

1.4.5.3 Non-operative Treatment

The most commonly used form of non-operative treatment is immobilization in a plaster cast, usually for a period of six to eight weeks. Immobilization has been advocated by those who think that it produces results similar to those achieved with operative treatment. When the Achilles tendon ruptures, the paratenon generally remains intact. Stripping of the paratenon during an operation reduces the amount of reactive tissue that is produced later at the site of the injury (117). Lea et at (118) reported 13% rerupture rate in a study of ruptured Achilles tendons treated with eight weeks of immobilization in a plaster cast.

1.4.5.4 Rehabilitation controversies

Traditional rehabilitation following Achilles tendon injury has involved prolonged protection of the tendon, usually in a plaster cast, followed by an extensive period of physiotherapy to regain lost muscle function and range of movement. Early mobilisation and weight-bearing has been introduced more recently to reduce complications of stiffness and weakness from muscle wasting and adhesions. Sceptics remain concerned about increased re-rupture rates from early tendon loading.

Recently, on the basis of results reported with use of functional postoperative bracing, McComis et al (119) managed fifteen patients non-operatively with a functional bracing protocol to repair a

rupture of the Achilles tendon. They achieved good functional results, proving that, for selected patients, nonoperative functional bracing may be a viable alternative to operative intervention or to use of a plaster cast for the treatment of an acute rupture of the Achilles tendon. In clinical practice, rehabilitation protocols vary depending on the experience of the treating physiotherapist or surgeon preference (114).

1.4.6 Tendon Healing

1.4.6.1 Healing stages

There are three main stages of tendon healing: inflammation, repair or proliferation, and remodelling, which can be further divided into consolidation and maturation. These stages can overlap with each other. In the first stage, inflammatory cells such as neutrophils are recruited to the injury site, along with erythrocytes. Monocytes and macrophages are recruited within the first 24 hours, and phagocytosis of necrotic materials at the injury site occurs. After the release of vasoactive and chemotactic factors, angiogenesis and the proliferation of tenocytes are initiated. Tenocytes migrate to the site and start to synthesize collagen III (120). This stage lasts 3 days and the repair or proliferation stage then begins and lasts for about six weeks. During this stage tenocytes are involved in the synthesis of large amounts of collagen and proteoglycans at the site of injury, and the levels of GAG and water are high (121). After approximately 6 weeks, the remodelling stage commences. During this stage, the healing tissue is resized and reshaped. A corresponding decrease in cellularity, collagen and glycosaminoglycan synthesis occurs and the repair tissue changes from cellular to fibrous. Tenocyte metabolism remains high during this period, and tenocytes and collagen fibres become aligned in the direction of stress. A higher proportion of type I collagen is synthesized during this stage (120). This is followed by the maturation phase, with gradual change of fibrous tissue to scar-like tendon tissue over the course of one year. At the end of this phase tenocyte metabolism and tendon vascularity decline (121). Tendon healing can occur intrinsically, via proliferation of epitenon and endotenon and intrafibres tenocytes, or extrinsically, by migration of

cells from the surrounding sheath and synovium (122). The variation in phenotypic expression of tenocytes has not been extensively investigated, and this information may prove useful for optimizing repair strategies.

There are five growth factors that have been shown to be significantly upregulated and active during tendon healing: insulin-like growth factor 1 (IGF-I), platelet-derived growth factor (PDGF), vascular endothelial growth factor (VEGF), basic fibroblast growth factor (bFGF), and transforming growth factor beta (TGF-β).(123) The role of those factors will be discussed later in this study.

1.4.6.2 Mechanical Stimulus

Remodelling adapts the tendon to the mechanical loads placed on it, and prevents the tendons from incurring injuries. An increase in the tendon mass and cross-sectional area occurs during modelling phase of healing (120). While stretching can disrupt healing during the initial inflammatory phase, it has been shown that early controlled movement of the tendons following an acute injury can help to promote the synthesis of collagen by the tenocytes, leading to increased tensile strength and diameter of the healed tendons and fewer adhesions than what is seen in tendons which are immobilized.

Several mechanobiological mechanisms have been proposed as reasons for the response of tenocytes to mechanical force that enable them to alter their gene expression, protein synthesis, and cell phenotype, and eventually cause changes in tendon structure. A major factor is mechanical deformation of the extracellular matrix, which can affect the actin cytoskeleton (connexin 32 and 43) and therefore affect tenocytes. G-proteins, which induce intracellular signalling cascades, may also be important, as well as ion channels which are activated by stretching to allow ions such as calcium, sodium, or potassium to enter the cell (121).

1.4.6.3 Treatment strategies and healing of Tendon

Open surgery enables direct approximation (abutment) of disrupted tendon ends and an assessment of tendon length, but disrupts the blood supply to the tendon by damaging the paratenon (a thin lining containing the blood vessels which supply the tendon proper). This is minimised by a percutaneous approach (minimal incisions with a suture passed blindly and tied) but there are concerns about the integrity of this repair and reports of increased sural nerve injury (116). The approximation of the tendon ends allows the intrinsic biological healing process to start the healing. Tendon may heal even if there is a gap between the tendon ends, however the working mechanical length of the tendon may be affected.

1.4.6.4 Tendon Healing Limitations

Adhesion formation after tendon injury poses a major clinical problem (124). Paratenon disruption at the time of injury or surgery allows granulation tissue and tenocytes from surrounding tissue to invade the repair site. The surrounding tissues attach to the repair site resulting in adhesion formation. Despite remodelling, the biochemical and mechanical properties of healed tendon tissue never match those of intact tendon (125). One possible reason for this may be the absence of mechanical loading during the period of immobilization. However the most likely cause is failure at multi levels in this complex healing process. In human Achilles tendon re-rupture rate varies depending on treatment strategy. Reportedly 10-15% in non-operative treatment and 5-10% in operative treatment. However surgical interventions are associated with complications that can be devastating to the tendon and its function (e.g. infection risk).

Although most tendons have the ability to heal after injury, mechanobiological properties of healed tendon never appear to match those of intact tendon leading to higher risk of further injury (65, 126). This limited healing capacity of tendon appears to be caused by poor vascularisation, changes to the matrix structure and alteration in the mechanical environment of this connective tissue (32, 69, 127, 128). Therefore, even with the best available clinical management, tendon injuries give rise

to substantial morbidity that may last for several months and pose a considerable challenge for clinicians(3).

The optimal treatment of acute tendo-Achilles ruptures continues to be debated.

1.4.6.5 Regenerative therapies

Tendon recovery of its functional ability is slow and is subjected to the risk of rerupture. Even with mechanical surgical fixation with sutures to achieve approximation of the rupture tendon edges, the biological repair processes follow at the same pace as non-interventional treatment. Consequently, there is no difference in full function recovery and rehabilitation periods between surgical and conservative treatment. (114) Therefore, the key to accelerate the healing process and improve the mechanobiological properties of healing tendons may lie in the ability to alter part or all of the complex biological healing pathway.

Faster return to functional activity and minimization of recurrence are the goal of any management pathway. Within this scope novel orthobiological agents such as Platelet Rich Plasma (PRP) have become potential treatments for tendon injuries (6, 13). In recent times there has been an increase in orthobiological therapies used to enhance the biological response to musculoskeletal injuries. Our knowledge of the effective mechanism at cellular and tissue level in human is still limited but it is evolving rapidly with increasing number of laboratory and clinical studies to investigate various potential orthobiological agents. The orthobiologics field is the fastest growing segment of orthopaedic sciences. The constant need for enhanced biological repair of musculoskeletal defects has been felt by both surgeons and patients. Globally it is estimated that orthobiologics are incorporated in approximately 2.2 million orthopaedic procedures annually. The following is a list of potential orthobiological regenerative therapies:

1. Cytokines
2. Growth Factors
3. Platelet Rich Plasma

4. Allografts and Autografts
5. Mesenchymal Stem cell (MSCs)
6. Gene therapy
7. Tissue engineering products (e.g. Collagen-rich ECM)

Platelet-Rich Plasma, an autologous derivative of whole blood that contains a supraphysiological concentration of platelets, has gained increasing attention in both the scientific literature and the wider media for its potential application in the treatment of traumatic musculoskeletal injury (6). The potential of PRP as an orthobiological agent in tendon repair will be discussed in chapter 2.

1.5 Achilles tendon Rupture – The Dilemma

The increasing Achilles tendon injuries cause major morbidity that lead to long term reduction of function and rerupture risk (114). The slow regenerative ability of the tendon leads to healing tendon tissue with encumbered mechanobiological properties. Although mechanical stimulation by moving the tendon early stimulate tendon regeneration but increase the risk of re-injury. Therapies have to address the conflicting priorities of rapid rehabilitation versus re-rupture risk.

Furthermore, there is lack of consensus on the best treatment of the acute Achilles tendon rupture. Opinion is divided as to whether surgical on non-surgical intervention is optimal and which surgical method or repair technique is best (114). However, the hallmark of all current treatment strategies has been mechanical augmentation with suture or immobilization in cast, both of which do not alter the existing biological regenerative pathway of the tendon leading to long rehabilitation, reduced function and high rerupture risk. New cost-effective treatments that reduce both the risk of re-rupture and time to functional healing are needed to address this challenge. Biological agents that are able to kick start the regenerative process and accelerate it offer a potential adjunct therapy that may lead to accelerated healing and restoration of tendon function with reduced re-rupture rate. Platelets are blood cells that form blood clots in the injured tissues. Platelets and platelet derived growth factors play important roles in the healthy response to injury, promoting healing of tissues, and have been proposed as therapeutic agents. Although in-vitro studies demonstrate the synergetic

effect of PRP on tendon healing clinical evidence is lacking. A study of PRP augmenting surgery for ATR found 6 athletes resumed training earlier than controls (10). However, a similar 30-patient RCT of PRP found no benefit (11). Two recent reviews concluded that the poor methodological quality of trials assessing PRP for tendon injury meant evidence for effectiveness is limited (12,13). A 2012 systematic review/meta-analysis of PRP for orthopaedic conditions (14) stated the need for adequately powered studies using disease-specific and patient-important outcomes and to investigate the effect of platelet concentration.

In the current study the role of platelet rich plasma as an autologous biological agent, which may be able to enhance the regeneration of Achilles tendon, will be studied at cellular, tissue, mechanical and clinical levels.

1.6 Present Study System

The subcutaneous Achilles tendon rupture and its unsatisfactory current treatment present an opportunity to study the effect of PRP as a regenerative therapy that may improve the outcome and may allow us to transfer the acquired knowledge to other tendons disorders.

Tendon healing occurs at various stages of biological repair. The regenerative repair process result in significant changes at various levels, which we can group under three categories:

1. Tendon Structure changes: at Microscopic and macroscopic levels
2. Mechanobiological changes: changes in mechanical properties
3. Clinical changes: improvement in pain and clinical tendon function.

Assessing the effect of any regenerative treatment at one or all of the above levels of change will enormously advance our knowledge of this therapy efficacy. It will identify the level of action and allow targeted manipulation of one or more healing pathway to further enhance the healing pathway.

In order to establish the biological and clinical efficacy of PRP it is necessary for this study to include experiments that will allow the exploration of the aforementioned healing levels. Therefore this study includes human cellular and tissue laboratory experiments, which are linked to *in vivo* mechanical and clinical studies. Critically, this study has to include robust tissue and cellular studies that provide information on some of the potential PRP mechanism cascade. In addition, the clinical trial has to have validated reliable subjective and objective outcome measures to investigate tendon healing clinically. The lack of non-invasive cost effective versatile mechanical testing method, which is available in clinical settings, has prompted the development and validation of a novel mechanical outcome measure tool (Functional Ultrasound Elastography). This tool facilitates the exploration of mechanical property changes throughout the healing phases.

In addition, considering the variability in PRP products and the lack of information about the bioactive proteins and growth factors' concentrations in PRP, it is important to quantify both viability and concentrations.

The strength of this project lies in the robust repeatability and measurability of the system and the capacity to quantify the clinical and mechanobiological properties of the healing tissue.

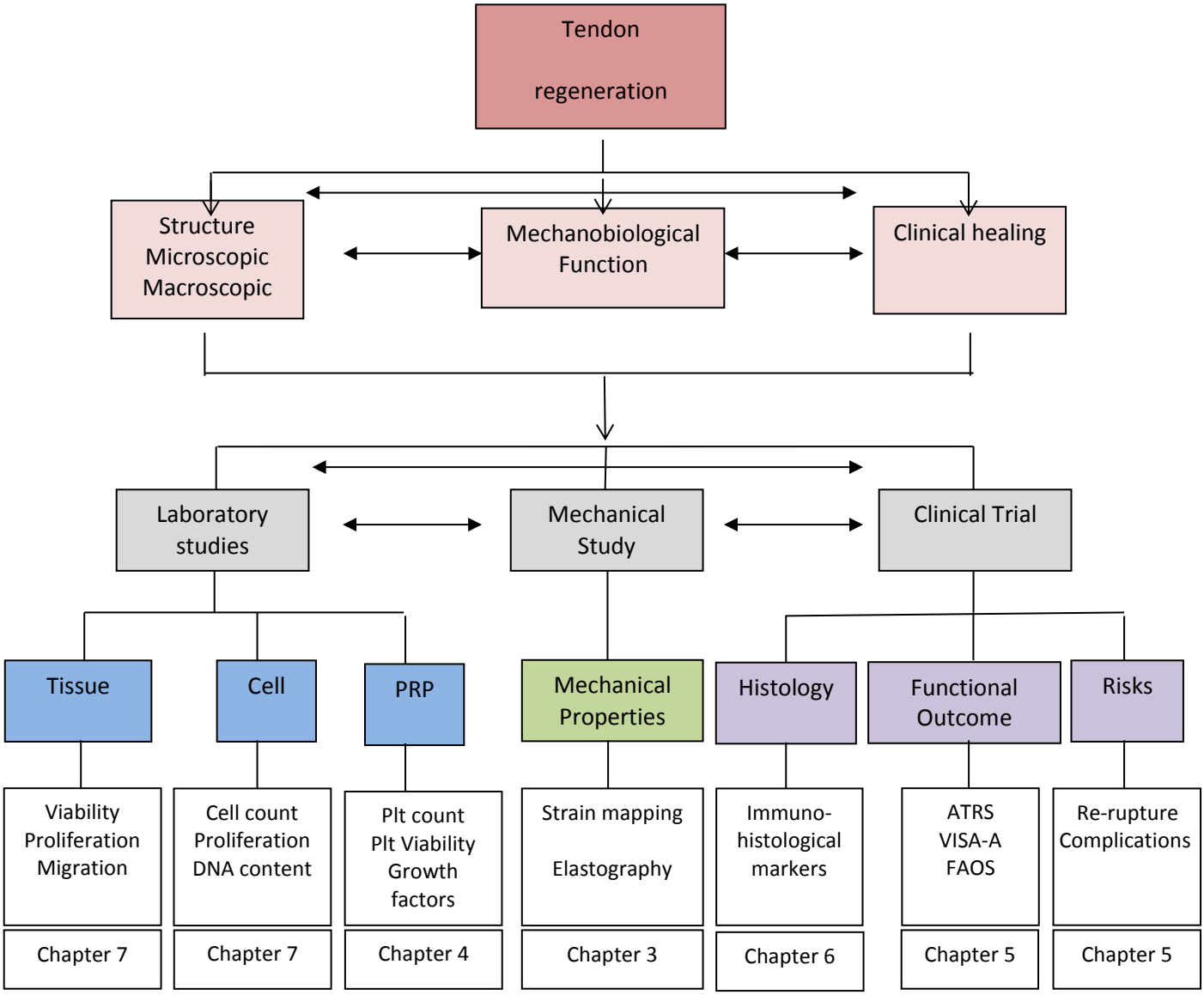


Figure 1 .10 Achilles tendon and PRP study system. The level of changes will be assessed in the three components of the study (i.e laboratory, mechanical and clinical). Samples for the laboratory work will be obtained from ATR patients recruited in the clinical trials. PRP and tissues used in laboratory experiments are autologous samples obtained from the same patients. (Plt = platelet).

1.7 Aims of the Present Thesis

The overall aim of this project is to understand the biological, mechanical and clinical effect of Platelet Rich Plasma in Achilles tendon rupture. This is achieved via multidimensional linked studies to investigate in vitro cellular and tissue response, *in vivo* histological changes, *in vivo* tendon mechanical alterations, and clinical outcome measures progression as a response to PRP application as an adjunct therapy. With this background, this project has following aims:

1) To study the clinical application of PRP in Achilles tendon rupture. This is achieved via the following objectives:
   - **a)** To design and conduct a prospective randomised clinical trial to study the feasibility of PRP clinical application in acute Achilles tendon rupture.
   - **b)** To study platelets function in autologous clinically prepared PRP before and after activation.
   - **c)** To study the concentration of growth factors (GF) in PRP obtained from patients.
   - **d)** To study the histological changes associated with PRP application *in vivo*. This will be facilitated by tissue samples obtained from trial patients.
2) To develop and investigate a novel imaging modularity as an outcome measure able to assess the mechanical properties of healing tendon.
3) To study the effect of PRP on injured tendon cells and tissues by modelling tendon healing *in vitro*. This is achieved via the following experiments:
   - **a)** Study injured tendon tissue response to autologous PRP application
   - **b)** Study injured tendon cultured tenocyte response to PRP in terms of proliferation, migration and DNA content.
4) Finally, to combine the above studies to support the ultimate goal of the project, which is investigating the mechanobiological effect and clinical application of PRP in tendon regeneration.

1.8 Outline of this current thesis

The introduction in this chapter aims to understand tendon structure and healing issues. However, understanding PRP biology variations, cell studies and clinical application in the current literature is fundamental to the deisgn and conduct of each experiment to achieve the abovementioned aims. With this in mind, Chapter 2 presents a systematic review of the current literature of basic and clinical studies of PRP and its effect on tissue and tendon regeneration. The variation in available products and suggested classifications will also be discussed in Chapter 2.

In the following chapter, the development of functional ultrasound elastography as an outcome measure tool will be detailed. The use of this tool in the clinical trial will be also discussed. Quantifying platelet function and activity and growth factors in the product we used in all our experiments will be discussed in Chapter 4. Having established a mechanical outcome tool and studied PRP characteristics, a clinical trial will incorporate those findings to study the clinical application of PRP in Achilles tendon patients. Trial design, method and results will be detailed in Chapter 5. To explore the *in vivo* histological response of ruptured tendo Achilles to PRP treatment, immunohistochemical markers will be compared to a control in Chapter 6. The following chapter (chapter 7) describes the effect of PRP and its cellular components on tenocytes and tendon tissues in cellular and tissue culture. The combined findings will be discussed and summarised in chapter 8. The prospects for future work are proposed in the final chapter (Chapter 8).

Chapter 2 Platelet Rich Plasma

2.1 Introduction

Platelet-Rich Plasma (PRP), an autologous derivative of whole blood that contains a supraphysiological concentration of platelets, has gained increasing attention in both the scientific literature and the wider media for its potential application in the treatment of traumatic musculoskeletal injury (6, 13). The theoretical benefit of PRP in providing a local environment for tissue regeneration which is rich in growth factors and other cytokines has been supported by *in vitro* and animal studies which suggest a positive influence on the migration and proliferation of a number of cell types. Furthermore, the full array of potential bioactive growth factors and chemokines released upon platelet activation is becoming well defined (8, 9). These include transforming growth factor (TGF-ß1 and -ß2), platelet-derived growth factor (PDGF-AA, -AB and -BB), vascular endothelial growth factor (VEGF A and C), Insulin growth factor (IGF-1) and epidermal growth factor (EGF) etc. These factors promote local angiogenesis, stem cell homing, local cell migration, proliferation and differentiation coupled with the deposition of proteins such as collagen which play a key role in enabling the restoration of normal tissue structure and function [table 2.1] (8, 9).

The reported clinical use of PRP is largely confined to the last two decades and initially centred around its application in dental and maxillofacial surgery where autologous fibrin gel is already being used as an operative sealant (13, 129-131). More recently, developments in research regarding the regenerative effects of PRP in a range of tissue types including bone, cartilage, tendon and muscle, particularly in the context of traumatic injury, have attracted interest in fields such as orthopaedic and plastic surgery where effective union of sometimes poorly vascularised and damaged tissue is a critical determinant of successful clinical outcome (12, 132). Despite the lack of appropriately powered trials, results from feasibility clinical studies have been encouraging, and PRP

administration remains an attractive strategy given its cost-effective and minimally invasive nature; moreover, the autologous nature of PRP eliminates concerns about the potential for disease transmission or immunological reactions although adverse risks may appear with the wider use of PRP preperations. The aim of this literature review is to describe PRP bioactivities, to elucidate the different techniques for PRP preparation, to review animal and human studies, to evaluate the evidence regarding the use of PRP in Trauma and Orthopaedic surgery with focus on tendon, to clarify risks, and to provide background for the purpose of this research thesis.

2.2 Methods

Multiple databases (including EMBASE, CINAHL, and MEDLINE) were searched as well as reference lists of articles and contacted authors up till 2012. Keywords included platelet-rich plasma, platelet concentrates, platelet gel, PRP preparation, PRP and trauma, PRP and bone, PRP and tendon. Only articles published in peer reviewed journals that met the following criteria were included: (1) *In vitro* studies that have reported on the effect of PRP on primary cell cultures; (2) *In vivo* animal studies that have evaluated the effect of PRP on hard or soft tissue regeneration; (3) clinical articles on PRP treatment; and (4) related outcome studies. The eligibility criteria were applied to titles and abstracts and potentially eligible studies were chosen for retrieval. The reference lists of all eligible articles were reviewed for additional eligible papers.

2.3 Definition

Platelet rich plasma (PRP), which is also known as platelet enriched plasma (PeRP), platelet rich concentrate (PRC), Platelet concentrate, Platelet Rich Fibrin(PRF), Platelet Rich in Growth Factors (PRGF), Platelet Rich Fibrin Matrix (PRFM), Autologous Concentrated Plasma (ACP), platelet gel, or platelet releasate, may be defined as a volume of the plasma fraction of autologous blood having a platelet concentration above baseline (133). A concentration of (1,407,640±320,100/µl) of platelets in plasma has been suggested to be the working definition of PRP (134). This is a platelet count 5 times higher than in the blood (normally 150,000/µl to 350,000/µl, with an approximate mean of

200,000/µl). Platelet rich plasma refers to autologous preparations. However, the preparation of allogeneic PRP (aPRP) might not be excluded. The use of aPRP may serve as an alternative option in the case of patients who refuse to be subjected to a blood drawing procedure or have contraindications to autologous PRP (135).

There are a large number of PRP products, which are obtained via different preparation methods, available for clinical application. However, not all “PRP” labelled products are PRP. The commercially available products have subtle difference between them that is partially represented in the product name. However, this is causing confusion for researchers and clinicians. Several clinical trials have been conducted without clear quantification of the potential biological properties of the used PRP, which may differ significantly leading to varying outcomes. Therefore, when investigating the effect of a PRP product it is important to link the outcome of any PRP research study to the type of PRP preparation. Table 2.3 shows a list of PRP preparation devices and the related product content. In this chapter, the author will also describe recently suggested classifications and suggest a new system to classify PRP based on this review information.

2.4 Biological Properties of Platelets

Platelets, or thrombocytes (from Greek θρόμβος, "clot" and κύτος, "cell"), are cytoplasmic fragments of megakaryocytes, a type of white blood cell, and are formed in the marrow. They are the smallest of the blood cells, irregularly round or oval in shape (approximately 2-3 µm in diameter). The average life span is 5-9 days. They lack nuclei but contain organelles and structures such as mitochondria, microtubules, and granules (alpha, delta, and lambda). The α granules (200 to 500 nm in diameter), bound by a membrane, are formed during megakaryocytes maturation (136). Each platelet cell contains approximately 50 to 80 granule of all types [figure 2.1] (136). Platelets contain more than 1100 bioactive proteins in the granules or on cell surface, many of which have a fundamental role in haemostasis or tissue healing.(6, 137) These two functional roles of platelets are a somewhat arbitrary division because haemostasis can be considered to be the first stage of healing

(7, 10). Platelets begin actively secreting these proteins within 10 minutes of clotting,(11) with more than 95% of the resynthesized growth factors secreted within 1 hour (23). After the initial burst of growth factors, the platelets synthesize and secrete additional growth factors for the remaining several days of their life span (23). However, the determinants of the biologic properties of PRP are unknown, and there is insufficient understanding of the clinical effects of PRP application.(133) The combined action of all these growth factors is complex, and each growth factor may have a different effect on a particular tissue. Growth factors may also interact with each other, activating different sets of signalling pathways. Different growth factors isoforms have varying effects that may enhance or inhibit tissue repair depending on the mode of growth factor release, as well as the dynamics of the wound environment.(10)

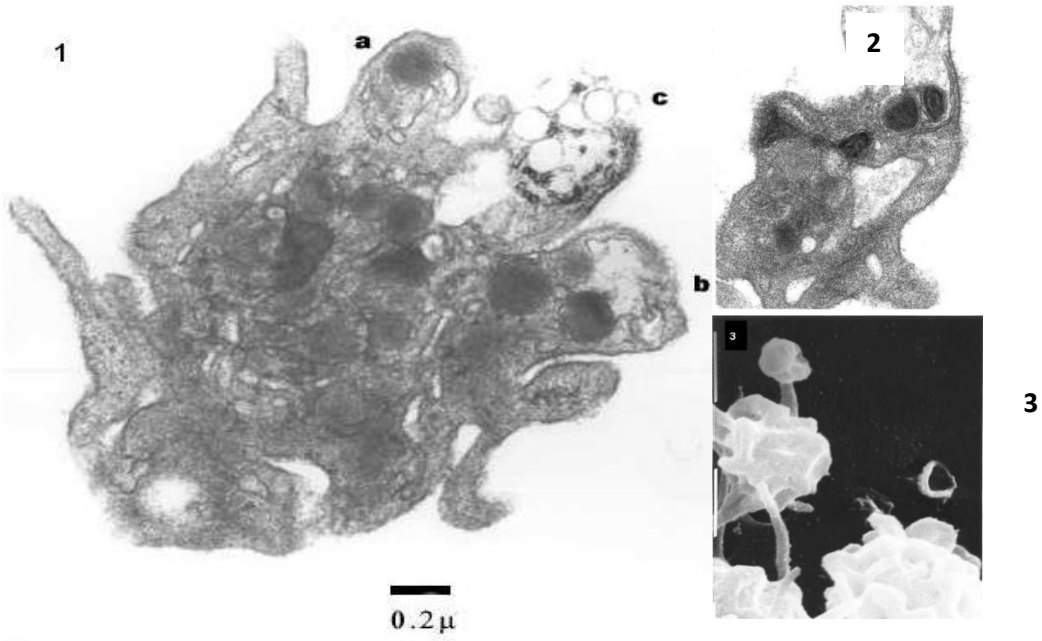


Figure 2 .1 Upon activation granules appear to migrate to the platelet periphery where they leave the platelet interior through platelet plasma membrane blebs (a)– protrusions (b) rupture the limiting membranes with loss of electron density(c). 2. Enlarged section shows blebbing of the alpha granule. 3. SEM picture of an activated platelet shows multivesicular bleb at the tip of a pseudopod with another remnant of an alpha granule lying on the filter(138) .

Platelet activation is achieved by collagen or thrombin. Under normal physiological conditions, collagen in blood vessels is covered with endothelial cells, which adhere to it via Von Willebrand factor (VWF), and prevent collagen from activating platelets. When the endothelial layer is stripped

in an injury, collagen, vWF and tissue factor from the subendothelium is exposed leading to platelet adhesion to collagen via glycoprotein Ia (GP Ia) and subsequent aggregation and activation. Thrombin is a powerful platelet activator, which can lead within minutes to clot formation and platelet degranulation. Platelets can also be activated by a negatively charged surface, such as glass. Non-physiological flow conditions (especially high values of shear stress) caused by arterial stenosis or artificial devices (Mechanical Heart Valves, blood pumps etc) can also lead to platelet activation (139). During activation, platelet change shape from spherical to irregular cell with pseudopods extending from their surface [figure 2.1]. Platelets α granules (contains containing P-selectin, platelet factor 4, transforming growth factor-β1, platelet-derived growth factor, fibronectin, B-thromboglobulin, vWF, fibrinogen, and coagulation factors V and XIII) and dense granules (containing ADP, ATP, Calcium and Serotonin) migrate to the periphery and bleb merging with cell membrane and releasing their content.

Platelets aggregate to form a clot using fibrinogen and von Willebrand factor (vWF) as a connecting agent. The most abundant platelet aggregation receptor is glycoprotein IIb/IIIa (gpIIb/IIIa); this is a calcium-dependent receptor for fibrinogen, fibronectin, vitronectin, thrombospondin, and vWF. Other receptors include GPIb-V-IX complex (vWF) and GPVI (collagen) (22).

2.5 Cellular component of PRP

The properties of PRP are based on the production and release of bioactive proteins including multiple growth and differentiation factors upon platelet activation. However, the role of other cells that may exist in PRP such as leukocytes is still under investigation (5). The presence of leukocytes has a great impact on the biology of these products, not only because of their immune and antibacterial properties, but also because they are key players in tissue healing and the local factor regulation.

Clinically prepared PRP is in fact a term that includes a wide range of products that have varying biological components [table 2.3] (21). Most of these products have varying concentration of blood

cells (platelets, leukocytes and erythrocytes) and many of them have high leukocytes concentration. The direct cellular interaction between platelets, leukocytes and target tissues is still largely unknown.(140) Polymorphonuclear leukocyte (PMN) adhesion to activated platelets is important for the recruitment of PMN at sites of tissue damage. The binding of activated platelets to PMN involves P-selectin and the activated β_2-integrin CD11b/CD18. (141) The effect of PRP components on cells and tissues is a complex process that involves growth factors and cytokines produced by both platelets and leukocytes. In addition, there may be direct cellular interactions that regulate the intracellular signalling pathways in the resident tissue cells (e.g ERK and AkT pathways for proliferation) (142).

2.6 Bioactive Proteins and Growth Factors in PRP

Researchers have identified more than 1100 bioactive proteins inside platelets or on their surface [table 2.1 and 2.2] (8). The most commonly studied platelet proteins include platelet-derived growth factor (PDGF), transforming growth factor (TGF-β), platelet-derived epidermal growth factor (PDEGF), vascular endothelial growth factor (VEGF), insulin-like growth factor 1 (IGF-1), fibroblastic growth factor (FGF), epidermal growth factor (EGF) and cytokines including proteins such as platelet factor 4 (PF4) and CD40L. Chemokines and newly synthesized metabolites are also released. The level of growth factors released from the platelets upon activation is commonly quantified by enzyme-linked immunosorbent assay (ELISA) and is shown in table 2.1.(138, 143, 144). PRP facilitates the application of autologous plasma and platelet-derived proteins. In addition, it promotes the development of a fibrin scaffold at the desired location that can act as a temporary matrix for cell growth and differentiation to assist repair in the injured tissue. Studying the role of those bioactive factors is essential to understand the biological activities of PRP. Below is a description of some of the growth factors in the alpha granules, which play an important role in tissue regeneration:

2.6.1 Growth Factors

2.6.1.1 PDGF

PDGF was first found in platelets and especially in the alpha granules.(145) PDGF can also be found in other cells, such as macrophages,(146) endothelial cells,(147) monocytes, and fibroblasts, as well as in bone matrix (148). In chemical terms, platelet-derived growth factor is dimeric glycoprotein composed of two A (-AA) or two B (-BB) chains or a combination of the two (-AB). There are five different isoforms of PDGF that activate cellular response through two different receptors. Known ligands include A (PDGFA), B (PDGFB), C (PDGFC), and D (PDGFD), and an AB heterodimer and receptors alpha (PDGFRA) and beta (PDGFRB) (149). The reason for three distinct forms remains unclear, but differential binding by various receptor cells such as endothelium, fibroblasts, macrophages, and marrow stem cells has been suggested (148). The most important specific activities of PDGF include angiogenesis and macrophage activation (149), proliferative activity on fibroblasts (150), chemotaxis for fibroblasts, and collagen synthesis (151). Furthermore, PDGF-AA enhances the proliferation of osteoblasts (152). Weibrich et al (134) measured the levels of PDGF- AB and PDGF-BB in PRP and found minimum and maximum values of 117.5±63.4 ng/ml and 9.9±7.5 ng/ml respectively. There was little, or no, correlation between the levels of these individual proteins with donor age and gender attributes.

2.6.1.2 TGF-β

TGF- β has been referred to as member of a super-family of growth and differentiation factors including the bone morphogenetic proteins (153). TGF-β has three different isoforms: β1, β2, and β3 (154). TGF-β has been observed to promote extracellular matrix production (155), to enhance the proliferative activity of fibroblasts (150), to stimulate biosynthesis of type I collagen and fibronectin, and to induce deposition of bone matrix (156). TGF-β may inhibit osteoclast formation and bone resorption, thus favoring bone formation over resorption (157). The level of TGF- β1 in PRP prepared using centrifusion is 169.4±84.5 ng/ml and TGF- β2 is 0.4±0.3 ng/ml according to Weibrich et al (134).

2.6.1.3 IGF-1

IGF-I is a protein similar in molecular structure to insulin and binds to insulin and IGF-1R receptors. This protein is also chemotactic for fibroblasts and stimulates protein synthesis (157). IGF-1 activates phosphatidylinositol-3 kinase (PI3K) signalling pathway and subsequently upregulates Akt. IGF-1 enhances bone formation by proliferation and differentiation of osteoblasts (157). Its concentration in PRP is reported to be 84.2±23.6 ng/ml (134).

2.6.1.4 PDEGF

Cohen discovered PDEGF in 1962 (158). It stimulates epidermal regeneration, promotes wound healing by stimulating the proliferation of keratinocytes and dermal fibroblasts, and enhances the production and effects of other growth factors (159). It plays a significant role in blood vessel formation (angiogenesis) (145). PDEGF has the capacity to induce vascularization by stimulating vascular endothelial cells. Several cytokines and growth factors, including IGF-1, TGF-α, TGF-β, PDGF, and interleukin 1b up-regulate PDEGF (143).

2.6.1.5 PF-4

Platelet factor 4 (PF4) is a small cytokine belonging to the CXC chemokine family that is also known as chemokine (C-X-C motif) ligand 4 (CXCL4) . This chemokine is released from alpha-granules of activated platelets during platelet aggregation.PF-4 may be partially responsible for the initial influx of neutrophils into wounds. It also acts as a chemoattractant for fibroblasts and promotes blood coagulation by moderating the effects of heparin-like molecules (160).

2.6.1.6 VEGF

VEGF is a sub-family of growth factors, more specifically of platelet-derived growth factor family of cystine-knot growth factors. The most important member is VEGF-A. Other members are Placenta growth factor (PGF), VEGF-B, VEGF-C and VEGF-D. The latter ones were discovered later than VEGF-A, and, before their discovery, VEGF-A was called just VEGF. They are important signalling proteins involved in both vasculogenesis (the formation of new blood vessels when there are no pre-existing

ones) and angiogenesis (the formation of new blood vessels from pre-existing ones), which paves the way for the healing process (161). *In vitro*, VEGF-A has been shown to stimulate endothelial cell mitogenesis and cell migration. It is also a vasodilator and increases microvascular permeability.

2.6.1.7 EGF

The discovery of EGF won Dr Stanley Cohen a Nobel Prize in Physiology and Medicine in 1986. EGF acts by binding with high affinity to epidermal growth factor receptor (EGFR) on the cell surface triggering an increase in the expression of certain genes that ultimately lead to DNA synthesis and cell proliferation (162).

2.6.1.8 FGF

Fibroblast growth factors (FGFs) make up a large family of polypeptide growth factors that are found in organisms ranging from nematodes to humans. 22 members of the FGF family have been identified, all of which are structurally related signaling molecules but effect cells via different pathways (163). FGFs are homeostatic factors and function in tissue repair and response to injury. One important function of FGF1 and FGF2 is the promotion of endothelial cell proliferation and the physical organization of endothelial cells into tube-like structures. They are very potent angiogenesis factors (164).

2.6.2 Other Bioactive proteins

Researchers have identified approximately 1100 proteins on platelet surface and inside the cell (165). They include: IL-1, RANTES (CCL5), IL-8 (CXCL8), MIP-1α (CCL3), MIP-2 (CXCL2), LIX (CXCL6) GRO-α (CXCL1), ENA-78 (CXCL5), SDF-1α (CXCL12), MCP-1 (CCL2), MCP-3, (CCL7), PF4 (CXCL4), pro-platelet basic protein (PBP), β-TG, NAP-2, connective-tissue activating peptide III CTAPs, thymus and activation-regulated chemokine (TARC, CCL17), angiopoietin-1, High mobility group box 1 (HMGB1), IL-6sR, endostatin*, osteonectin*, bone sialoprotein, dickkopf-1, osteoprotegerin [table 2.2].

Table 2.1 A list of some of the growth factors in the platelet alpha granules, which are released upon activation, and the presence of related receptors in the target tissues .

Growth Factor	Effect	Receptor expression (166)				PRP concentration
		Tendon	Bone	Cartilage	muscles	
TGF-β	Fibroblast proliferation(167) Synthesis of type I collagen and fibronectin Induce deposition of bone matrix, inhibits bone resorption	±	+	+	±	β1: 169.4±84.5 ng/ml β2: 0.4±0.3 ng/ml
PDGF	Angiogenesis(145) Macrophage activation Fibroblasts: proliferation, chemotaxis, collagen synthesis Enhances the proliferation of bone cells	±	±	-	-	AB 117.5±63.4 ng/ml BB 9.9±7.5 ng/ml
IGF-I	Chemotactic for fibroblasts (1) Stimulates protein synthesis. Proliferation and differentiation of osteoblasts	2+	+	+	+	84.2±23.6 ng/ml
PDEGF	Stimulates epidermal regeneration(1) Promotes wound healing by stimulating the proliferation of keratinocytes and dermal fibroblasts	+	-	-	+	470±320 pg/ml
PF-4	Stimulate the initial influx of neutrophils Chemoattractant for fibroblasts(1)	+	+	-	+	0.189±0.07 nmol/ml
EGF	Epithelial cell proliferation(168) differentiation of epithelial cells	?	-	-	+	51 ± 5 pmol/l
VEGF	Angiogenesis (15) Migration and mitosis of endothelial cells creation of blood vessel lumen creates fenestrations Chemotactic for macrophages Vasodilation	±	-	-	+	76 to 854 pg/ml

±present in small quantities, + = present, - = absent?.

Table 2.2 list of the identified bioactive factors in the cell membrane and inside the platelet**.**

Type	Bioactive factor	Function
Adhesion proteins	VWF, Pro-peptide, Fg, Fn, Vn, TSP-1, TSP-2, laminin-8	Cell contact interactions Haemostasis and clotting extracellular matrix constituents
Clotting factors and their inhibitors	Factor V/Va, factor XI, multimerin, protein S, high-molecular-weight kininogen, protease, nexin-1 and -2, Protein C inhibitor	Thrombin production and clotting. Cell proliferation
Fibrinolytic factors and their inhibitors	Plasminogen, PAI-1, u-PA, α2-antiplasmin, Histidine-rich glycoprotein, thrombin-activatable fibrinolysis inhibitor (TAFI,) α2-macroglobulin	Plasmin production Vascular modelling
Proteases and antiproteases	MMP-1,2,4,9, ADAMTS13, ADAMS10, ADAMS17 (TACE), TIMPs 1–4, platelet inhibitor of FIX, C1 inhibitor, α 1-antitrypsin	Angiogenesis, vascular modelling, regulation of coagulation, regulation of cellular behaviour
Growth and mitogenic factors	PDGF (A, B and C), EGF, IGF-1, VEGF (A and C), bFGF (FGF-2), HGF, BMP-2,4,6, CTGF, SCUBE1, IGFBP3	Chemotaxis, cell proliferation and differentiation, angiogenesis
Chemokines, cytokines and others	TGF-□1 and -□2, IL-1, RANTES (CCL5), IL-8 (CXCL8), MIP-1□□□CCL□□, MIP-2 (CXCL2), LIX (CXCL6) GRO-□□(CXCL1), ENA-78 (CXCL5), SDF-1□□(CXCL12), MCP-1 (CCL2), MCP-3 (CCL7), PF4 (CXCL4), Pro-Platelet Basic Protein (PBP),TG, NAP-2, connective-tissue activating peptide III T(CXCL7), Thymus and activation-regulated chemokine (TARC, CCL17), Angiopoietin-1, High Mobility Group Box 1 (HMGB1), IL-6sR, Bone Sialoprotein, Dickkopf-1, Osteoprote Gerin	Regulation of angiogenesis, Chemotaxis, vascular modelling, cellular interactions, bone formation
Anti-microbial proteins	Thrombocidins and kinocidins	Bactericidal and fungicidal properties
Others	Chondroitin 4-sulfate, Albumin, Immunoglobulins G and M, Amyloid β-protein precurser, Disabled-2, Complement factor H, Bile Saltdependent Lipase (BSDL), Semaphorin 3A, PrPC	Function depends on the factor and target tissue
Membrane glycoproteins	αIIb□3, αvβ3, GPIb, PECAM-1, most plasma membrane constituents, receptors for primary agonists, **P-selectin**, TLT-1, Semaphorin 4D, CD63, CD40L, LIGHT, TNF-related apoptosis inducing ligand (TRAIL), FasL, furin, GLUT3, cellubrevin, SANP23, syntaxin-2, clathrin	Platelet aggregation and adhesion, endocytosis of proteins, secretion, inflammation, thrombin generation, platelet-leukocyte and platelet-vascular cell interactions

2.7 PRP Preparation

2.7.1 Preparation Methods

Autologous PRP can be prepared in a laboratory or an operating theatre or clinic room from anticoagulated blood collected in the immediate pre-therapeutic period. There are several choices of anticoagulants that can use for blood collection. Trisodium citrate solution is the most widely used anticoagulant (citrate is a weak chelator of calcium thus inhibiting coagulation and platelet function) with few negative effects on PRP preparation (13). ACD (acid citrate dextrose) and CPD (citrate phosphate dextrose) with and without adenine (ACD-A and CPD-A) are also effective anticoagulants. The use of Ethylene Diamine Tetra Acetic acid (EDTA) is potentially more harmful in the preparation of PRP, and a large number of damaged/activated platelets have been observed during preparation. Therefore it is not recommended for PRP preparation.

Traditionally, a relatively pure preparation and good yield of PRP can be easily obtained by low g centrifugation (170 – 200 g) of anticoagulated blood for 10 minutes at room temperature (169). For clinical applications there is no such standardization and there are 3 essential main methods available which can rapidly provide a sterile product suitable for clinical application: 1). The Gravitational Platelet Sequestration (GPS) or centrifuging technique 2) Standard cell separators and 3) Autologous selective filtration technology (plateletpheresis).

The GPS method depends on the centrifugal forces to separate blood cells. Upon centrifugation; three layers become evident: the bottom layer comprised of red blood cells (specific gravity = 1.09), the middle layer comprised of platelets and white blood cells (buffy coat, specific gravity = 1.06), and the top plasma layer (specific gravity = 1.03). Various methods to collect platelet layer have been developed with varying degrees of red and leukocyte contamination [table 2.3]. Platelet concentration, yield and recovery are also dependent on the centrifuge protocol and collection method (170). Applied mechanical forces may damage or activate platelets, with the consequence of degranulation resulting in lower concentrations of growth factors. One study evaluated the effect

of different centrifugal forces and showed that centrifugation at greater than 800 g may decrease the amount of releasable TGF-β from the PRP (171).

Standard cell separators and salvage devices generally operate on a full unit of blood. In general, they use continuous flow centrifuge bowl or continuous flow disk separation technology coupled with a hard and soft centrifugation steps. Weibrich et al. described a discontinuous technique with a cell separator that produces a five-fold increase in platelet count (134). The red blood cells, and some, or all, of the platelet poor plasma (PPP) can also be returned to the patient to maintain circulating volume.

Selective filtration technology or plateletpheresis depends on a single-use proprietary filter designed to concentrate platelets from whole blood. The platelets are captured on the filter and are then harvested to provide a platelet rich concentrate (PRC). Although this technique reduces platelet lysis, which may be induced during centrifugation, platelet fragmentation and activation have also been shown in filtration-based systems (170, 172).

In general, most systems do not concentrate the plasma proteins of the coagulation cascade (170). Plasma protein concentrations above baseline can be achieved through secondary ultrafiltration. The Autologous Growth Factor Filter (AGF) is a microporous, hollow, cellulose fiber filtration device with a volume of 8ml and uses PRP as a baseline product that has been manufactured by the cell separator device. The device filters water after multiple passes of PRP through the filtration device. As much as two-thirds of the aqueous phase is removed by filtration, thus the concentrations of the retained plasma proteins and formed elements are correspondingly increased (173). Evidently each preparation technique will result in significant differences in yields, concentration, purity, viability and activation status of the isolated platelets. Each of these variables will therefore not only influence the eventual concentrations of the bioactive proteins released from the platelet granules [Table 2.3] but also affect the eventual clinical efficacy of each PRP preparation (131).

Table 2.3 List of PRP preparation devices and their PRP products. Concentration increase is the platelet count in PRP divided by Platelet count in the blood (count in PRP/ count in blood). ACP: autologous concentrated plasma; PCP: platelet concentrated plasma; PRF: platelet-rich fibrin; PRFM: platelet-rich fibrin matrix; PRGF: plasma-rich in growth factors; PRP: platelet-rich plasma; RBC: red blood cells; WBC: white blood cells. * Increase above baseline is based on a collection volume of 50-60ml whole blood with a single pass (except for the cell saver device that uses 450ml).

Technology	Device Name	Product name	Concentration Increase *	% Platelet Recovery	Product content
Floating Buoy or shelf	Biomet GPS™	PCP	3.2 x	70%	Manual collection of buffy coat which contains Platelets, WBC and minimal amount of RBC
	Harvest® SmartPrep2 BMAC™ Depuy Symphony II 3i PCCS	PRP	4.6x 4.0x 4.0x	65-72%	
Cell Saver Based Systems	Electa, Haemonetics, CATS, BRAT	PRP	4-6x	75%	Platelet concentrate only with plasma. No WBC or RBC contamination.
Computer Aided System	Sorin Angel	PRP	4.3x	70%	Automated buffy coat collection, which contains concentrated Platelets, WBC fractions and minimal amount of RBC
	Arteriocyte Medical (Magellan™)	PRP	5.1x	76%	
Standard Centrifugation	AutoloGel System Smart PReP	PRP PReP	1-2x	78%	Platelets in plasma suspension with minimum white cells and low concentration of Platelets
	Cascade PRFM Fibrinet system	PRFM	1-2x	78%	Platelet rich fibrin membrane
	Choukroun's PRF	PRF	1-2x	70%	Leukocyte and Platelet rich fibrin
Direct Siphoning	GenesisCS	PRP	6x	68 %	concentrates of platelets, leukocytes through siphoning device
Direct Aspiration	Secquire Arthrex ACP	PRP	1.6x	31 %	Manual aspiration of platelet and plasma after centrifuging
Platelet Separation	Vivostat	PRF FS	6x	65%	Platelet Rich Fibrin Fibrin Sealant without Platelet
Platelet Filtration	Caption Advanced Tissue Regeneration (ART)-Curasan Set	PC	4.3x	-	Concentrated platelets without plasma.

2.7.2 Handling and Activation of PRP

Once the PRP is prepared, it is stable for clinical use, in the anticoagulated state, for 8 hours, or longer (133). Some authors advocate using PRP within no longer than 6 hours if it is kept at room temperature (174). However, Sweeney et al (175) suggested using a specific method, which included adding low-pH glucose-containing additive solution with $NaHCO_3$ to platelet in ELX bag, to keep PRP viable for up to 7 days by lowering PH to allow sterilization and provide energy to platelet from glucose.

PRP must be activated for the platelets to release their α-granule contents, with the clot providing a vehicle to capture the secreted proteins and maintain their presence at the application site. Activation with bovine thrombin is no longer recommended as this was reported to cause coagulopathy resulting from cross-reactivity of anti-bovine factor V antibodies with human factor V (176, 177). Calcium chloride is therefore a much safer but slower alternative without any risk of prion or virus exposure. Platelet activation via this method takes at least 20 minutes (7). Recently, autologous thrombin preparation kits have been introduced as a safe and faster activation alternative. Briefly, active autologous thrombin is generated by combining 10% calcium chloride with a small volume of PRP or blood in a syringe containing negatively charged particles (e.g. glass fibres). The mixture is typically incubated for 10-15 minutes and then filtered to remove cells and fibrin leaving a solution that contains significant thrombin activity. This autologous thrombin preparation is then combined with the autologous PRP preparation during injection via a dual syringe resulting in platelet activation (178).

Furthermore, injecting inactive PRP into collagen rich tissues may also result in direct platelet activation resulting in degranulation (179, 180). Harrison et al. found that thrombin activated the platelets leading to immediate release of TGF-β1 and PDGF-AB. While the collagen activated PRP clots resulted in 80% greater cumulative release of TGF-β1, VEGF and PDGF than thrombin over 7 days (179).

Platelet Concentration effect on PRP efficiency

The effect of PRP on tissue healing is likely a function of many variables, including the platelet concentration, PRP volume delivered, the extent and type of injury, and perhaps the overall medical condition of the patient. A concentration of (1,407,640±320,100/µl or 10%) of plasma has been suggested to be the working definition of PRP (153). However, Anitua et al stated that the platelet count of PRP should be just above 300,000/µL (7). On the other hand, Choi and others showed that high PRP concentrations (>10%) suppressed, but that low PRP concentrations (1–5%) stimulated, the viability and proliferation of alveolar bone cells (181).

The concentration of PRP is correlated to the platelet count in the blood from which it is derived. Weibrich et al (134) examined the platelet concentration of different donors and found that the platelet concentration of PRP was correlated to platelet count in donor whole blood. They also found a significant effect of gender on platelet concentration, although no effect of age was detected. The concentration of growth factors also increased with increasing platelet number (144).

The method used to measure platelet concentration can add uncertainty to concentration ratio determination. Manual counts of stained platelet smears, as well as automated machine methods, may be used (11). The manual method counts individual platelets, whereas automated scanning techniques, such as used by the Coulter Counter, may count clumps of platelets as a single platelet, providing an underestimate. This stresses the importance of using consistent methods and properly interpreting the results of other investigators whose counting methods may differ. Weibrich et al (182) suggest that different individuals may require different platelet concentration ratios to achieve comparable biological effect. Although, the dependence of clinical benefit on platelet concentration versus total number of platelets delivered may need to await further investigation, quantifying PRP properties it is highly recommended when conducting PRP related research.

2.8 In Vitro and Animal Studies of PRP

2.8.1 In Vitro Cell and tissue culture

PRP influences the migration, proliferation and differentiation of a number of cell types, although the temporal features and molecular basis of this effect remain unclear. Castelnovo et al (183) demonstrated an 80-fold enhancement of porcine retinal cell migration 48 hours after the application of human platelet suspension and PRP has been shown to promote the recruitment of circulation-derived cells for tendon healing *in vivo (184)*. It has a mitogenic effect on endothelial cells (185), bone (186), cartilage (20, 187) and periodontal ligament (188) as well as on mesenchymal and dental stem cells (189, 190). However, there are conflicting reports concerning its effect on cell differentiation. While several studies indicate a positive influence (186, 190-192), PRP has been shown to inhibit the osteogenic differentiation of marrow derived pre-osteoblasts in a dose-dependent manner (193) and has an inhibitory effect on mesenchymal stem cell differentiation when applied in isolation but a stimulatory effect with 1,25(OH)2vitamin D3 co-treatment (189).

The effect of PRP on cellular activity appears to be highly time- and dose-dependent. Soffer et al (194) showed that whilst short term exposure to human platelet lysate (<24 hours) promotes bone cell proliferation and chemotaxis, long-term exposure results in decreased levels of alkaline phosphatase and mineral formation. Other studies indicate that PRP stimulates the growth of bone marrow cells for 4-8 days (143) and that, beyond 6 days, washed platelet solution has a stronger influence on mesenchymal cell proliferation than PRP (195). The concentration of PRP also appears to be critical in determining its effect. Some authors suggest that high concentrations adversely affect fibroblast cell viability and proliferation (181, 196). This conclusion was not found supported by other research studies. In an animal model, Weibrich et al (197) found that platelet concentration required for a positive PRP effect on bone regeneration seems to span a very limited range (Average 1,000,000 platelets/µl, range 9,53,000–1,729,000 platelets/µl). At lower concentrations, the effect is suboptimal, while higher concentrations might have a paradoxically inhibitory effect.

Although the mechanism by which PRP exerts its cellular effect is poorly understood, the presence of a combination of growth factors, chemokines and other bioactive factors [table 2.3] may also be important considering that isolated administration of TGFβ or PDGF does not have the same mitogenic effect as PRP (6). Cheng et al demonstrated the significance of both the platelet and plasma protein constituents of PRP as these fail to significantly enhance gene expression of collagen types 1 and 3 in cultured ligament cells when applied in isolation but only succeed in combination (198).

Several studies have confirmed the ability of PRP to induce local gene expression. The growth factors TGF-β1 and PDGF appear to play an important role in tendon and ligament regeneration by promoting expression of proteins including collagen and cartilage oligomeric matrix protein (19, 167, 198-200). Histologically, PRP has been shown to promote gross ligamentisation of tendons (201) and increases the maximum breaking strength and stiffness of healing tendons *in vitro* when used with a bone-marrow derived stromal cell-seeded graft (202). Activation of the Nrf2-anti-oxidant response element pathway has been implicated in the increase in tenocyte growth due to addition of platelet-released growth factor (17). Further, Lyras et al (203, 204) showed that a single application of PRP to Achilles and patellar tendon defects significantly enhances IGF-1 protein expression and is associated histological with a faster healing process (thicker tendons with organised fibre structure).

The effect on gene expression and mRNA may also be an important factor in PRP mechanism. PRP increases mRNA expression of bone matrix protein (BMP) (205) and may also contain novel potentiators for BMP-dependent osteoblastic differentiation (206). Anitua et al. demonstrated that PRP application results in increased expression and production of VEGF and HGF in cultured tenocytes (207). Other *in vitro* studies confirmed that the ability of PRP to promote angiogenesis, which is crucial in acute tissue injury repair, may be an important reason for its regenerative effects (208-210).

It is unclear whether the mitogenic effects of PRP are dependent upon the presence of intact platelets or not. Lysed solutions have been shown to have a positive effect on osteogenic activity (211) and bone marrow stem cells (16), but other studies suggest that platelets rendered damaged or non-viable by processing may have impaired growth factor secretion (11, 23). Platelets synthesise and secrete additional growth factors after the initial burst, targeting the affected tissues for the remaining 7-9 days of their life span (190). Therefore, the continuing activity of platelets after the initial release of bioactive factors may be lost if they are not intact following preparation (212).

2.8.2 In Vivo Animal Studies

The effect of PRP on tissue regeneration has also been studied in animal models. It has been shown to promote bone regeneration in rat and rabbit calvarial defects (213), the alveolar sockets of Cebus apella monkeys (214) and porcine tibial metaphyseal defects (215), as well as promoting the incorporation of mandibular bone grafts in goats (216) and tibial grafts in rabbits (217). However, other studies suggest that PRP has no effect on bone healing and may actually be detrimental when used as a supplement to bone grafts. In a study looking at craniofacial bone repair in rabbits, where PRP-treated grafts were associated with diffuse fibrous tissue deposition that inhibited bone formation when compared with untreated grafts (218), and Broggini et al showed that PRP alone or when used in combination with autogenous bone failed to promote remodelling in rabbit calvaria whereas autogenous bone without PRP leads to accelerated remodelling (219).

PRP injection into transected rat Achilles tendons increases callous strength and stiffness by 30% after 1 week (220), and Bosch et al showed that lesioned equine superficial digital flexor tendons treated with PRP have significantly higher strength at failure, improved collagen network organisation and increased metabolic activity than saline-treated controls (221). The same author also demonstrated that a single intratendinous PRP injection induces significantly more neovascularisation than placebo control until at least 23 weeks after treatment (222), confirming other animal and *in vitro* studies suggesting a key role for angiogenesis as a mechanism underlying

the regenerative effects of PRP(207, 209, 210, 212, 223, 224). In a porcine model, Hadad et al showed that adipose-derived stem cells and PRP significantly enhance healing of perfusion-depleted tissue when applied in combination but not in isolation, lending support to the hypothesis that the growth factors contained in activated PRP have a permissive effect in enabling regeneration (225).

Animal studies have also shown that PRP application improves left ventricular function following ischaemia-reperfusion (226), promotes fat-graft survival (227) and enhances the repair of cartilage (228), skin (229), corneal epithelium (230), liver (231), intestine (232) and peripheral nerves(233).

2.9 Clinical Studies of PRP

The clinical research studies are predominantly case studies or limited case series. There have been several randomised trials (RCT) investigations investigating the use of Platelet Rich Plasma, with a recent systematic review and meta-analysis identifying 23 trials in 13 conditions (234). Pathologies studied including arthroplasty, spinal fusion and a range of tendon pathologies. This 2012 review used the GRADE evaluation method and found the quality of evidence to be very low. The authors concluded 'the current literature is complicated by a lack of standardization of study protocols, platelet separation techniques, and outcome measures'. Despite this uncertainty about the evidence there is increasing clinical use of platelet-rich plasma in the clinical practice and mainly in sport medicine.

In the following sections, the published clinical evidence in relation to the musculoskeletal system will be summarised. Within the tendon section, the existing clinical studies on ATR and PRP will be discussed in more detail.

2.10 Orthopaedic Applications

2.10.1 Bone

There are few clinical studies examining the role of PRP in bone healing after orthopaedic trauma (13, 235). Most of the published studies are related to the use of PRP in oral and cranial surgery. Currently, it is common to combine the platelet-rich material with autograft, allograft, demineralized bone matrix, or other graft material to fill bony defects in the mandible or cranium (133).

Percutaneous injection of autologous platelet-leukocyte-rich gel has been shown to be an effective and less invasive alternative to bone marrow injection in the treatment of delayed bone union and non-union provided it is given within 11 months from the time of injury (140). Platelet-rich products promote faster fusion in spinal surgery (236, 237). The successful healing of clavicle fracture non-union was recently reported in a single case (238).

In intrabony defects, PRP reduces the time taken for bone regeneration (239, 240) and has been used to treat mandibular osteonecrosis resulting from radiotherapy (241) or the use of bisphosphonates (242). Cenni et al recently provided a possible biological explanation for this through the demonstration that growth factor release from platelets is maintained within regions of osteonecrosis (243). In one series, researchers were able to measure levels of PDGF and TGF-β in the fracture hematoma of 24 patients who had fresh fractures of the foot and ankle; however, the investigators were unable to detect these same proteins in the nonunion tissue of 7 patients presenting with similar fractures. After PRP application of the non-union during revision surgery, radiographic union was observed by an average of 8.5 weeks (244).

The use of PRP in maxillofacial surgery is well supported with recently published level 1 and 2 evidence (Meta analysis or Randomised controlled trials). However, there is no Level 1 or level 2 evidence showing that cortical bone benefits from PRP. Few anecdotal reports studied the effect on a mix of corticocancellous bone or a mixture of PRP and bone substitutes.

2.10.2 Wound Healing

As early as 1990, autologous human platelet-derived wound healing factors (HPDWHF) were proposed to regulate wound healing of recalcitrant skin ulcers by promoting the formation of granulation tissue in the early healing phase (245). PRP and other platelet-rich products have been shown to promote healing in a range of cutaneous lesions (246-248) and have therefore attracted interest in fields such as plastic surgery where structured approaches to the use of PRP are beginning to emerge (132). In a randomised controlled trial, diabetic foot ulcers treated with PRP gel showed significantly reduced time to healing compared with controls (249). Whilst there have been reports of negative results with the use of platelet-derived wound healing factors in ulceration, most notably in a trial by Krupski et al (250), more recent studies using autologous PRP have supported its beneficial role in chronic wound healing and provided evidence that it may actually reverse non-healing trends (246, 251).

Post-traumatically, PRP promotes ulcer healing (252), faster re-epithelialisation of lower extremity wounds with bone exposure (253) and, in combination with hyaluronic acid, can act as an effective scaffold for cellular growth in covering exposed tendons in acute and chronic open wounds of the foot and ankle (254). In a 5-year study assessing the effect of applying platelet gel to patients presenting with traumatic loss of finger substance, Balbo et al reported better aesthetic results and a shorter recovery time in the PRP-treated group (255). However, although an early case report suggested that PRP promotes healing even in the presence of infection (256), recent randomised studies have shown that it fails to actually prevent infection if administered during inguinal surgery (257) or during wound closure following venous harvesting (258).

2.10.3 Tendon

2.10.4 Tendon Disorders and PRP clinical studies

In small-numbered series, PRP has also been shown to reduce pain in patients with chronic tendinopathy (259, 260), with a persisting effect for at least 2 years from the time of treatment despite normalisation of VEGF, EGF and CCL2 blood levels after 24 hours (168). More recently, in the 2-year follow-up of a double-blind randomized controlled trial comparing PRP with corticosteroid injection for the treatment of chronic lateral epicondylitis, Gosens et al reported significantly increased function and reduced pain in the PRP-treated group compared to those treated with steroids (261). The benefit of PRP as a second-line, surgery-sparing therapy in the treatment of elbow tendinopathy resistant to physical therapy has been further demonstrated in a prospective randomised trial reported earlier this year (262). Creaney et al study showed that injecting PRP in chronic tendinopathy reduced the need for surgery from 20% to 10% when compared with autologous blood injection alone.

Despite the evidence that PRP may be effective in treating tendinopathy, there is also a growing body of evidence to the contrary. The most significant trial in this regard was a double-blind randomised controlled trial carried out by De Vos et al which showed no difference in pain or function in patients with chronic Achilles tendinopathy treated with PRP compared with those treated with saline (263). A recent study identified no significant difference in the degree of neovascularisation or tendon structure (using colour Doppler ultrasonography and ultrasonic tissue characterisation) in patients with chronic Achilles tendinopathy treated with PRP compared with those receiving a saline placebo (264). Another application of PRP that has gained significant attention is its use in anterior cruciate ligament (ACL) reconstruction using hamstring tendon grafting following traumatic injury. In a randomised, double-blind trial, Vogrin et al used contrast-enhanced MRI to demonstrate that ACL grafts treated with platelet gel had a significantly higher level of vascularisation at the osteoligamentous interface 4-6 weeks post-operatively compared to

control grafts (265). PRP gel has also been shown to reduce the time taken for a homogenous appearance on MRI following ACL reconstruction by 48% (266), although contrary to this Silva and Sampaio demonstrated a failure of PRP to affect the signal intensity of the fibrous interzone in femoral tunnels following grafting(267). Functionally, the application of platelet gel to grafts has been shown to significantly improve anteroposterior knee stability following surgery (268).

With regards to the use of PRP in treating rotator cuff tears, a pilot study of patients undergoing arthroscopic rotator cuff repair showed that intraoperative PRP administration was associated with significantly increased function and reduced pain at 6, 12 and 24 months post-operatively with no adverse events (269). However, a recent randomised controlled trial demonstrated that platelet-rich fibrin matrix has no benefit in enhancing healing of small and medium-sized rotator cuff tears (270): as with tendinopathy, the consensus in the literature is that further trials are needed to determine whether neutral results regarding the benefit of platelet-rich mediums indicate a lack of benefit from having additional growth factors in certain healing environments or whether they reflect suboptimal preparation and administration techniques (6, 271). Two recent reviews conclude that the poor methodological quality of trials assessing the use of PRP in treating chronic tendinopathy mean the evidence supporting its effectiveness is limited and thus insufficient to recommend its routine clinical use (272, 273).

2.10.4.1 Achilles tendon and PRP – the current evidence

A thorough literature search of the application of PRP in Achilles tendon rupture in both animal and human studies was conducted. Nine studies present results for the use of platelets in Achilles tendon rupture treatment, seven from animal experiments and two from human trials (table 2.4)(14, 274). Six of the animal studies used a rat model, and one used an ovine model. All animal studies, using biomechanical and histological assessments, are in agreement showing a beneficial effect of platelets. Only two human studies have tested the effect of platelets on the treatment of Achilles tendon rupture based on imaging techniques and clinical results [table 2.4]. Sanchez et al (14) found

positive effects in a group of 12 athletes treated with PRP augmented suture repair at 32 months in a case-control study. In ultrasonographic assessment, there was less tendon thickening, higher concentrations of TFG-beta and other growth factors and patients regained range of motion faster and returned to sports (gentle running) earlier. In a randomised study of 30 patients, Schepull et al (274) found no effect of platelets on radioisometrical tendon contraction or clinical outcomes. Both of these underpowered clinical studies used PRP as an adjunct to open surgical repair and this may have obscured any effect of PRP on healing.

There are three other studies that report on the use of platelets in human Achilles tendinopathy however the results of these trials have little bearing on Achilles tendon rupture, which has a very different pathology, regenerative properties and treatment pathways. Therefore there is only one underpowered randomised clinical trial that has assessed PRP in Achilles tendon rupture (14, 274). The authors of that recognised a limitation in their platelet preparation technique and storage (of up to 20 hours) resulted in only a 20% release of growth factors from the platelets. In our 20-patient pilot study, described later in this thesis, we achieved an average 69% growth factors release.

Table 2.4 PRP and Achilles tendon rupture clinical studies summary.

Author	Year	Random-ised	Blinded	Power Calculation	PRP	Follow-up (month)	Platelet Group	Control Group
Schepull et al	2011	Yes	Yes	No	PRC	12	12 (4 lost to FU)	14
Sanchez et al	2007	No	No	No	PRGF	12	6	6

Recently published systematic reviews (275, 276) have concluded that there are encouraging signs that PRP could be developed as an effective therapy. Sadoghi et al (275) concluded that there is evidence in support of a positive effect of platelet concentrates in the treatment of Achilles tendon ruptures in vivo in animal models and human application, consistent with a medium- to large-sized effect. This effect is most likely attributed to enhanced scar tissue maturation. In another systematic review, Taylor et al (276) concluded that PRP use in tendon and ligament injuries has several potential advantages, including faster recovery and, possibly, a reduction in recurrence, with no adverse reactions described.

2.11 Potential Adverse Risks of PRP

PRP is prepared from autologous blood, therefore it is inherently safe, and any concerns of disease transmission such HIV, hepatitis, or Creutzfeldt-Jacob disease or immunogenic reactions that exist with allograft or xenograft preparations are eliminated (13). However, using calcium chloride and bovine thrombin preparations, which contain bovine factor V to activate the platelets may lead to immunogenic reaction. The systemic use of bovine thrombin in cardiovascular surgery to promote clotting has been reported to be associated with coagulopathies resulting from cross-reactivity of anti-bovine factor V antibodies with human factor V (176, 177). The bovine thrombin preparations used in those reported cases were high dose (>10,000 units) and were applied directly onto open wounds where absorption into systemic circulation is certain. There have been no similar reports since 1997 due to the use of highly purified bovine thrombin. Conversely, the very small dose of bovine thrombin (<200 units) used to activate PRP before application will be consumed during clot formation and digested by macrophages. Hence, bovine thrombin activated PRP is unlikely to produce anti factor V antibodies.

The use of bovine thrombin for activation is therefore avoided in modern preparation techniques. Some authors proposed that PRP gel formation can be performed only with the addition of calcium, but this usually takes longer to complete (277). An effective alternative is thrombin receptor agonist peptide (TRAP) that mimics the effect of thrombin. Most current techniques use autologous thrombin or calcium chloride to activate PRP.

To date, there is no compelling evidence of any systemic effect of local PRP injection. Furthermore, there are no scientific reports suggesting potential cause–effect relationships between growth factors present in PRP and carcinogenesis. Some potential arguments for these considerations include the limited need of PRP injections in clinics (as PRP is not chronically administered) and the short *in-vivo* half-lives and local bioavailability of growth factors produced by PRP.

2.12 Discussion

Based on the inconclusive results in the current literature, this review cannot provide solid evidence in favour of the application of PRP in tendon disorders and in particular Achilles tendon rupture. However, because the majority of the reviewed clinical trials reported encouraging outcomes, further controlled clinical trials are warranted to elucidate the effects of PRP.

Clinical trials should include a sufficient number of patients and a proper design (randomized controlled trials), including a test group similar to control except for the application of PRP. Also, proper description of the PRP procurement techniques must be included, amount of blood collected, baseline number of platelets, amount of PRP obtained, number of platelets increase above baseline, coagulation promoters, doses and mixing ratio to PRP.

2.12.1 Clinical Studies Design

Given the rudimentary knowledge of the mechanism of action of PRP in clinical settings and the limitations of current studies, it is important that any future clinical trial should be carefully designed, adequately powered to study the effect of PRP on that tendon disorder and use disease-specific outcome tools. This has been highlighted by several authors (272, 278), who have shown that the imprecision in effect size estimates from underpowered studies into PRP have led to unsafe conclusions.

A study powered to determine if there are clinically important effects while furthering the understanding of PRP mechanism in clinical settings, would add significantly to the science of PRP clinical application. In a consensus paper published recently (6), a panel of experts listed important elements of clinical trials of PRP: 1). RCT design 2). Clear inclusion/exclusion criteria 3). Homogenous study population 4). Standardised clinical assessment 5). Validated PRP production method and delivery 6). Robust outcome measures and 7). Standardised post treatment follow-up protocol.

2.13 PRP Classification System

"Not all PRP is in fact PRP"

In the field of platelet concentrates, most products are termed Platelet-Rich Plasma (PRP). Unfortunately, this term is very general and incomplete, leading to confusion in the scientific literature and misleading conclusions. Currently, there are more than 12 platelet concentrate products available commercially and although they have varying preparation method and components [table 2.3] they are all labelled Platelet Rich Plasma.

Accurate use of the terminology to reflect the product properties is required in both: clinical and scientific applications. The terminology must be simple, accurate and pragmatic. It also must avoid commercial interests and thus remain scientifically homogeneous (279). Clinically prepared PRP is in fact a term that include of wide range of products that have varying biological components (21). Most of these products have varying concentration of blood cells (platelets, leukocytes and erythrocytes). Two authors have tried to classify PRP products according to their biological content, of which are described below.

Ehrenfest et al (21) classified the different platelet concentrates into four categories, depending on their leucocyte and fibrin content: pure platelet-rich plasma (P-PRP), leukocyte- and platelet-rich plasma (L-PRP), pure platelet-rich fibrin (P-PRF), and leucocyte and platelet-rich fibrin (L-PRF) [table 2.5]. Yet, Mishra et al (280) used the presence of Leukocytes and method of activation to classify PRP into four types [table 2.6].

Table 2.5 Ehrenfest classification system of the main available PRP products (21).

PRP Class	Leukocytes	Fibrin Content
P-PRP	No	Low
L-PRP	Yes	Low
P-PRF	No	High
L-PRF	Yes	High

Table 2.6 Mishra classification is divided into 4 types (1-4) and two subtypes (A and B) (280).

	White Cells	Activation	Platelet Concentration
Type 1	Increased	No activation	A >5x B <5x
Type 2	Increased	Activated	A >5x B <5x
Type 3	Minimal or no WBC	No activation	A >5x B <5x
Type 4	Minimal or no WBC	Activation	A >5x B <5x

In addition to the aforementioned factors, platelets are very sensitive to *in vitro* manipulation and can be easily activated during preparation methods therefore prematurely releasing their bioactive contents before application to the targeted tissues. (12, 13, 22). Therefore including the preparation method may be important to stratify PRP product effects.

Building on the conclusions from the literature systematic review, the author of this thesis suggests a new classification system, which incorporate the above two classification systems, and include the preparation method technique. This new system will use a combination of numeric and alphabetical characters to identify the class of PRP product. In addition to the above two identifiers in Ehernfest and Mishra classifications: Leukocytes, Fibrin, the new system will also include: activation, platelet concentration and preparation method categories.

Activation is divided into two subcategories:

I for the use of activation

II for PRP application without activator

Unlike Mishra classification, platelet concentrate is subdivided into three categories (A, B and C) based on platelet count range in the samples. This is in line with evidence presented previously in this chapter (197), which states that the most effective platelet count range is (900 – 1700 $x10^3$ /µl). The three categories are:

A Platelet count < 900 $x10^3$ /µl

B Platelet count 900 – 1700 $x10^3$ /µl

C Platelet count > 1700 $x10^3$ /µl

The preparation methods are classified into three categories:

1 The Gravitational Platelet Sequestration (GPS) technique

2 Standard cell separators

3 Autologous selective filtration technology (plateletpheresis)

The modified classification is presented in table 2.6. For example, the PRP used in conducting research in this thesis will be classified as: L-PRP IB1, which is indicates that this PRP is prepared using GPS method, contained leukocytes with platelet count range 900-1700 and it is activated before application.

Table 2.7 The modified PRP classification system. The subcategories of activation, platelet concentration and preparation technique is added after the main class (e.g L-PRP IB1).

Class	**Leukocytes**	**Fibrin**	**Activation**	**Platelet Concentration**	**Preparation category**
P-PRP	**-**	**Low**	**I**	**A**	**1**
			II	**B**	**2**
				C	**3**
L-PRP	**+**	**Low**	**I**	**A**	**1**
			II	**B**	**2**
				C	**3**
P-PRF	**-**	**High**	**I**	**A**	**1**
			II	**B**	**2**
				C	**3**
L-PRF	**+**	**High**	**I**	**A**	**1**
			II	**B**	**2**
				C	**3**

2.14 Conclusion

Based on the inconclusive results in the current literature, this review cannot provide solid evidence in favour of the application of PRP in tendon disorders and in particular Achilles tendon rupture. However, because the majority of the reviewed clinical trials reported encouraging outcomes, further controlled clinical trials are warranted to elucidate the effects of PRP.

Clinical trials should include a sufficient number of patients and a proper design (randomized, controlled, clinical trials), including a test group similar to control except for the application of PRP. Also, proper description of the PRP procurement techniques must be included, amount of blood collected, baseline number of platelets, amount of PRP obtained, number of platelets increase above baseline, coagulation promoters, doses and mixing ratio to PRP. This may be facilitated easily by a new evidence-based PRP classification system to aid interpreting the result of scientific and clinical studies.

Chapter 3 Functional Ultrasound Elastography (FUSE)

3.1 Chapter Introduction

Tendons are exquisite mechanical systems able to transfer force and store energy as part of the complex coordinated mechanical function of the musculoskeletal system. Characterization of tendon mechanical properties enables clinicians and researchers to have a better understanding of tendon function and the mechanisms responsible for tendon tear or complete rupture following acute or chronic mechanical loading. The ability to measure these mechanical properties of a tendon system *in vivo* will facilitate monitoring of the healing tendon and allow customisation of related rehabilitation protocols. Additionally, it may offer an invaluable objective outcome measure tool in clinical trials.

Current experimental techniques to study the mechanical behaviour of tendon *in vivo*, such as RadioStereometric Analysis (RSA) measurement of implanted tantalum beads, are invasive and carry the risk of further injury to the tendon. The accuracy of those methods may be compromised by bead migration in the tendon. RSA method provides global mechanical properties of the muscle tendon unit without differentiation of the involved structures or detection of local mechanical variation within each structure (281). Thus, new non-invasive imaging techniques are needed to elucidate the implications of localized tendon damage on function, and to quantitatively assess the effects of tissue repair or regeneration as a measure of treatment efficacy (282). The development and use of new ultrasound analysis techniques can contribute to this goal by providing inexpensive noninvasive assessments of tissue mechanics.

Elasticity imaging, a technique that utilises ultrasound versatility to image the mechanical variables of tissues, is a recent development. The aim of elasticity imaging is to use more of the information contained in image data to quantify clinically relevant tissue properties, such as those experienced in manual palpation. Theoretically, any imaging modality can be used for elasticity imaging. However, due to the necessity of either static or dynamic deformation, ultrasound (283-286) and magnetic

resonance imaging (MRI) (287, 288) are particularly well suited. Ultrasound is the most popular modality for elasticity imaging due to its high frame rates, low latencies, low cost and widespread availability. Compressional elasticity imaging, which is performed with compression, is desirable because it may be carried out straightforwardly with commercially available probes.

Elastography is a new ultrasound imaging method, first introduced by Ophir et al in 1991(289), by applying static axial compression on inhomogeneous tissue and computing the partial derivative of ultrasound-detected tissue displacements along the axial orientation of the ultrasound probe. In 1999, Pesavento et al (290) developed a fast cross-sectional technique based on real-time elastography to allow its use in clinical practice. Elastography has proven effective for detecting anomalies in soft tissues such as the breast, liver and thyroid, with deformation induced via simple manual compression of the tissue with the probe (291, 292). However, there is no validated elastography technique in musculoskeletal tissues. A major challenge in elastographic imaging of muscles, ligaments and tendons is that the primary direction of tissue motion is perpendicular to the compression forces and to the ultrasound beam direction (293). Further, the spatial resolution of ultrasound is much lower in this perpendicular direction, being determined by the number of transducers in the probe.

The aim of this chapter is to propose and develop a new elastography technique that is able to measure and image strain distribution of Achilles tendon *in vivo*. This includes the following: develop new elastography algorithm able to track tendon movement, compare various methods of elastography imaging methods, and develop a new technique to control tendon movement, validate the use of this technique in healthy volunteers and experiment on its use in Achilles tendon rupture.

3.1.1 Elastography Principles

The principle of conventional ultrasound elastography methods is as follows: tissue compression produces displacement within the tissue correlated to its stiffness. Less displacement is produced in stiff (hard) tissues than in compliant (soft) tissues. Elastography measures these displacements by tracking the speckle patterns within the tissues (figure 3.1).

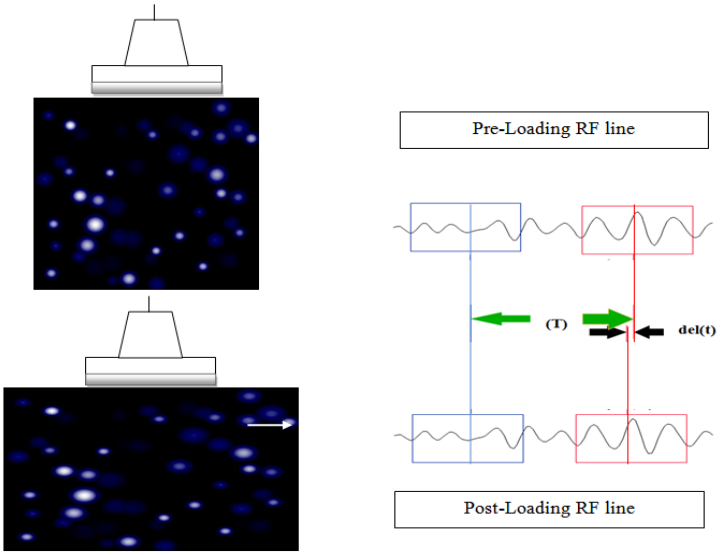


Figure 3.1. ***The principle of ultrasound elastography. Compression and decompression of tissues causes displacement which changes the timing of the echo signals received at the transducer. The radio frequency (RF) signal is compared and displacement is calculated to generate local strain.***

For the mechanical properties to be measurable, the tissue must undergo deformation. Thus broad categories of elasticity imaging have developed around different forms of induced deformation: vibrational, compressional, and acoustic force. In vibrational elasticity imaging, low-amplitude, low-frequency shear waves (less than 0.1 mm displacement and less than 1 kHz frequency) are propagated through the tissues, while real-time Doppler techniques are used to image the shear wave velocity. Compressional elasticity imaging requires only two images, one before and one after deformation, but is often conducted with several intermediate images. It was introduced just after vibrational elasticity imaging by Ophir et al., and is the most researched and commercialized form of elasticity imaging undoubtedly due to its straightforward image acquisition and processing (289). In acoustic elastography, acoustic radiation force is generated by the transfer of momentum of the

acoustic wave to the tissues. The acoustic force of ultrasound is used to develop a shear wave from which the shear modulus can be estimated in way similar to the vibrational elasticity imaging techniques (294).

All of those methods were tested on large organs such as liver, spleen and breast. They all measure the displacement in the axis of the beam, which in large organs such as the liver and the breast is able to provide clinically relevant information. However in tendons the major functional and clinically interesting direction is along the axis of the tendon and perpendicular to the ultrasound beam.

3.1.2 Elastography Algorithm

Although elastography has proven effective for detecting anomalies in soft tissue such as the breast, liver and thyroid, with deformation induced via simple manual compression of the tissue with the transducer (292), tendon elastography imaging has so far failed to show the same success. Drakonaki et al (295) used commercial real-time elastography technique with compression to study Achilles tendon with limited success. However, manual compression does not provide insights into how tendinous tissue will deform with muscle loading, and thus likely does not represent the deformation patterns relevant to injury and rehabilitation.

Elastography of human tendons presents several challenges: firstly the direction of loading is parallel to the skin and therefore perpendicular to the ultrasound beam direction. Secondly; healthy tendons are stiff tissues and so require larger forces in order to produce measurable displacements. Thirdly; the lateral resolution of ultrasound probe is substantially lower than along-beam resolution (296). And fourthly; the tendon can undergo large motion with muscle contraction or passive movement and care need to be taken to ensure tissue remains within the imaging plane. Therefore the current elastography algorithms do not offer accurate elastography imaging of tendons. Developing a specific tendon elastography technique needs to take into account the aforementioned factors.

We developed a novel technique to address all the aforementioned factors to produce strain mapping images of the Achilles tendon in its functional loading direction.

The algorithm matches small overlapping blocks of image in successive frames, calculate the 2D displacement vector in the direction of the tendon movement for each block to obtain a dense frame to frame displacement map and then to sum the displacement maps of successive frames to infer the total displacement of the sequence. Using the strain formula $= \frac{\mathrm{d2}-\mathrm{d1}}{L} = \frac{\Delta d}{L}$, The strain is calculated as the spatial gradient of a polynomial fitted to the displacement over a range of points (297). The strain values at each point may be plotted using a colour gradient generating a so-called strain map, which represents the spatial distribution of strain in the tendon and surrounding tissues. This may be superimposed over the B-mode grey scale image to show the anatomical structures of the strain map. Figure 3.2 shows the simplified flowchart of the modified compressional elastography processing algorithm which was developed within the Biomedical Image Analysis (BioMedIA) laboratory led by Prof Alison Noble at the Institute of Biomedical Engineering at the University of Oxford. The algorithm uses block tracking of non-overlapping regions throughout the B-mode movie sequence to calculate a displacement map. The gradients of the interpolated displacement map are then used to create the strain image (294, 298). This algorithm was originally developed and validated for breast tissues.

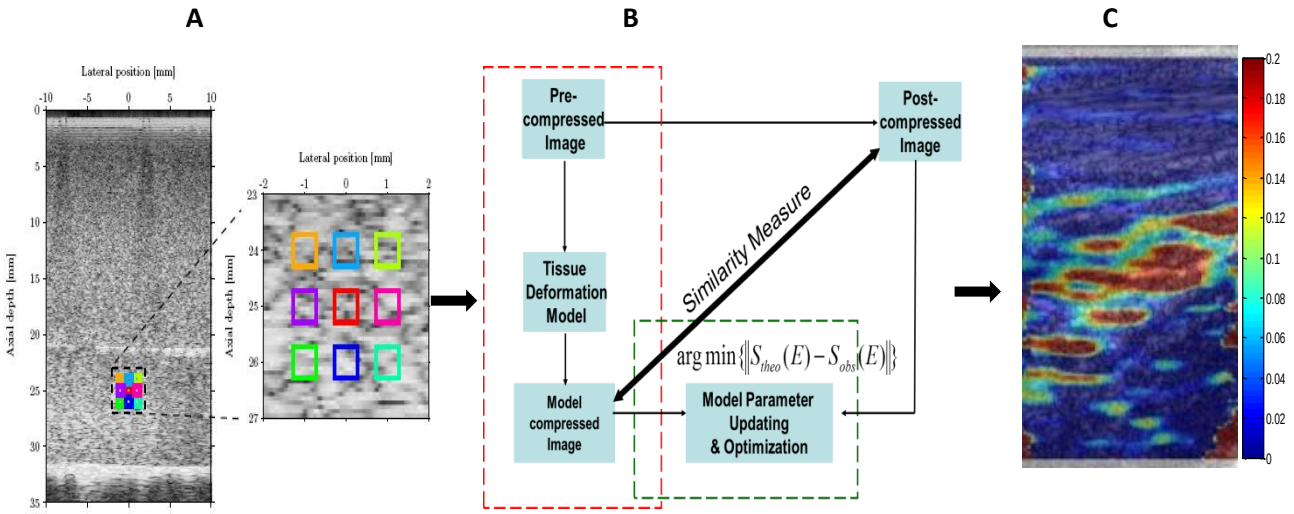


Figure 3.2. ***Details of a compression elastography method.*** *A)* ***non-overlapping regions in the B-mode image are tracked independently throughout the image sequence during stress application.*** *B)* ***The flowchart of the algorithm developed at the Institute of Biomedical Engineering, University of Oxford. The compression and decompression images are captured. The compressed images are modeled depending on the tissue deformation. The model is compared with post compression images and strain is calculated.*** *C)* ***The strain is plotted as a colour contour map and superimposed over the B-mode image to create an elastography image.***

3.1.2.1 Elastography of Tendon

Two major issues need to be addressed in order to provide localised tendon mechanical function estimation: firstly the tracking of the displacement along the tendon functional direction and secondly controlled and measured force application.

Compressional displacement within tendon tissues, which is stiffer than the surrounding soft tissues, is not easily produced without deforming the surrounding soft tissues beyond tracking threshold. Therefore a new algorithm to track deformation while the tendon is subjected to longitudinal stress is required to overcome this issue.

The aforementioned algorithm, which tracks displacement in the axial direction, may not produce optimal strain mapping images of the tendon. In collaboration with Phill Brown, a DPhil student in the BioMedIA and Mechanobiology groups at the Institute of Biomedical Engineering, we developed a new algorithm able to track displacement in the longitudinal axis of the tendon. The new technique is called the AutoQual Ultrasound elastography method (297) to track the displacement of the healing Achilles tendon.

Unlike compressional elasticity imaging, where the main force is axial, the tendons in this study were stressed in its functional direction by passively moving the foot and ankle into planter and dorsiflexion. The resulting strain was calculated in both probe axial (ε_y) and longitudinal (ε_x) directions (figure 3.3). Considering that axial loading using this method is minimal, the measurement will provide the longitudinal strain of the tendon. The novel method presented here, which applies the AutoQual algorithm to ultrasound captured together with a device for controlling and measuring ankle movement described below, is called Functional UltraSound Elastography (**FUSE**).

To avoid confusion, in this report the term "axial" will be used to refer to a direction parallel to the ultrasound probe axis, and "longitudinal" to the perpendicular direction in the imaged plane.

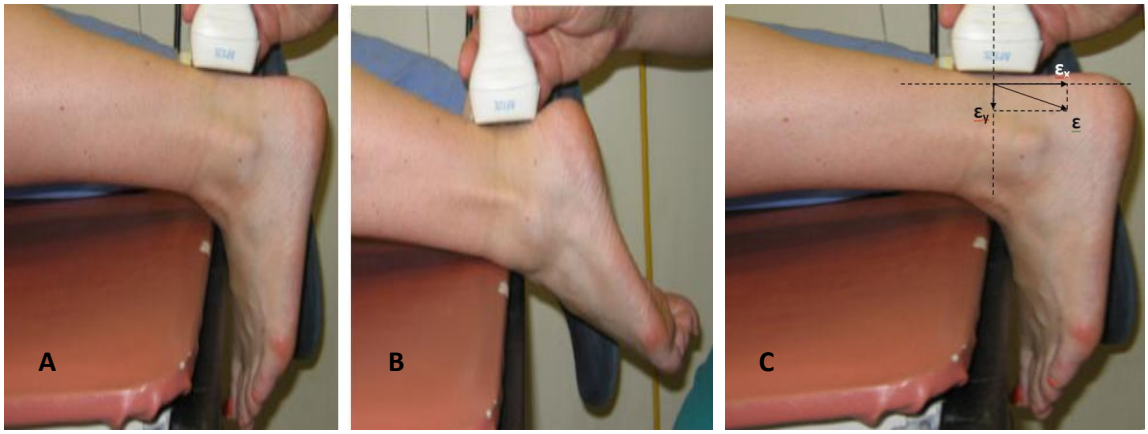


Figure 3.3. ***FUSE method and strain vector:*** *A* ***and*** *B****: applying stress on the tendon in its functional direction.*** *C****:Strain components: axial strain (****ε_y****) and longitudinal strain (****ε_x****).***

3.1.3 Developing Standardised Foot and Ankle Movement Device

Compressional elasticity imaging relies on freehand ultrasound acquisitions (296). Freehand elasticity imaging systems rely on the operator to depress the probe over the region of interest. The compressions need to be small and smoothly applied to maximize the quality of the resultant estimation. In addition, the transducer needs to remain in contact with the skin, and the maximum applied pressure should be such to avoid pain. As a result, this method is intrinsically limited by the operator's freehand ability (298). Poorly controlled movements will corrupt the performance of the

algorithm performance and ultimately reduces the elasticity image quality. Even with algorithmic error correcting measures, the results obtained are only as good as the quality of freehand data obtainable by the operator (294). Although compressional elasticity is replaced with longitudinal strain estimation elastography in FUSE methods, the freehand passive movement of the foot and ankle by the operator may have similar detrimental effects. A computer-controlled foot and ankle moving device was therefore designed by this thesis author to deliver increased precision and control to elasticity imaging of the tendon while maintaining the freehand operation familiar to radiologists. Figure 3.4 shows the devices and its components, which was designed by this thesis author. The Oxford Foot and Ankle Moving device (OFAM) design incorporates mechanical and electronic mechanisms to assure: 1) Controlled movement 2) Measurable force and 3) Protection of the tendon.

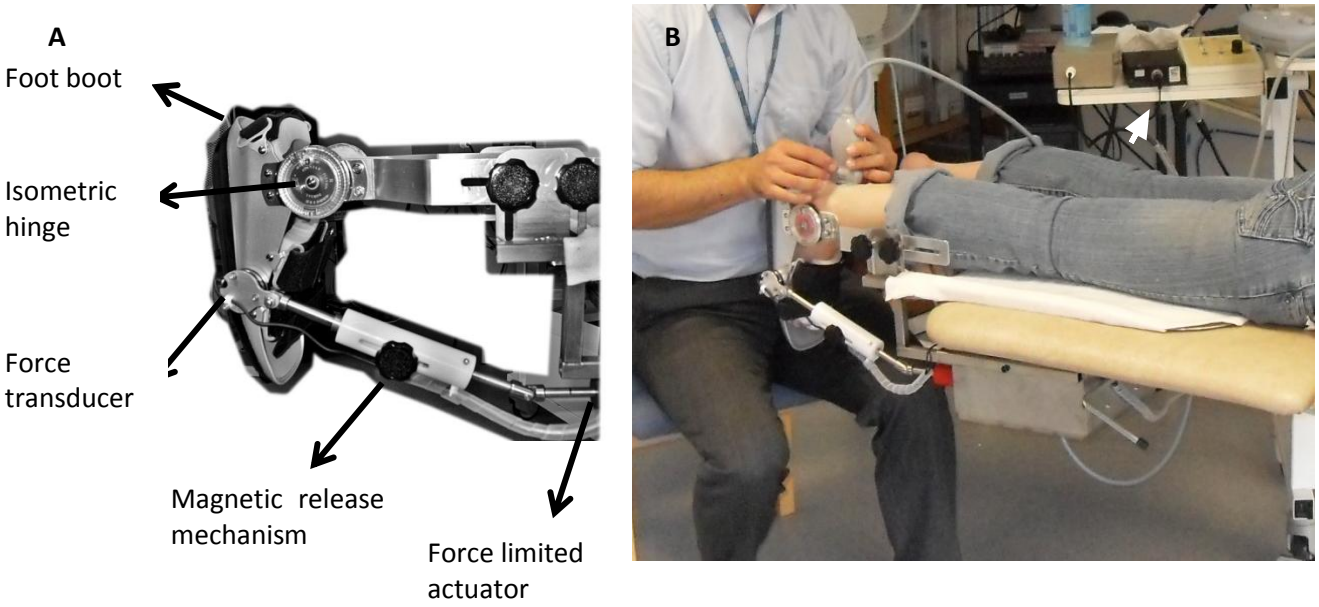


Figure 3.4. ***The Oxford Foot and Ankle Moving device (OFAM). A. shows the device components: the foot boot, which is provided with protective pads, straps, and hinges around the ankle to allow dorsi/planter flexion. A force transducer measures the force and allows the release of the protective mechanism and stops the actuating motor if maximum allowed force is exceeded. B: the device is clamped at the end of examination couch to allow comfortable fitting of the foot in the boot while patient is lying prone and facilitate access for ultrasound probe. White arrow shows the computer interface unit, which relays the computer commands to control the mechanical and electronic parts of the device.***

The device is controlled via a purposely designed computer-control unit to ensure smooth movement of the actuator motor at 10mm per second. This translates to approximately 1 mm per

second displacement at the tendon level. The unit measures the forces using ATI Mini 40-E transducer (ATI Industrial Automation, USA). To protect the tendon, a magnetic release mechanism, which connects the actuator motor to the foot boot, allows automated release of the foot and ankle if the force exceeded 10 N. The device fits at the end of examination couch and does not cover any area of the tendon to facilitate good exposure of the tendon to the ultrasound examiner. The control unit is connected to the same computer that is collecting the RF data from the ultrasound machine allowing precise synchronization of the signals. A bespoke MatLab software allows simultaneous RF data collection and labeling when the OFAM device is moving the foot. Data was labeled according to the direction of foot movement: DF (dorsal flexion) and PF (planter flexion). Compressional data was collected using the same software but with OFAM device disabled electronically.

3.1.4 Functional Ultrasound Elastography of Achilles Tendon Studies

To be effective, Elastography technique must deliver increased precision and control to elasticity imaging of Achilles tendon. This means constraining and controlling deformations more accurately than freehand compressional scanning. Constraining deformation implies minimizing out-of-plane motion, whereas controlling deformations implies an increased correspondence between actual and intended deformation within acquisition (298). Laboratory experiments to validate this method were carried out by a collaborating team at the Institute of Biomedical Engineering (IBME) (294, 297, 298). To translate this into relevant clinical setting, I designed and conducted two studies:

1. **FUSE Volunteers Study**

   To investigate the feasibility of this technique in scanning Achilles tendon elastography *in vivo, a healthy-volunteers study* was conducted to test the system performance and to identify the mechanical properties of healthy Achilles tendon in healthy volunteers.

2. **FUSE Patients Study**

   This was followed by a study in patients with Achilles tendon rupture to investigate the changes in healing tendon mechanical properties as part of PATH trial (chapter 5).

The methods of both studies are presented in this chapter along with results of the volunteer study and initial testing results in patients study. The full results of the patient study are presented in Chapter 5.

3.1.5 FUSE Volunteers Study

The aim of this study was to evaluate the use of Functional Ultra Sound Elastography (FUSE) to assess strain mapping of normal Achilles tendon in healthy volunteers and the feasibility to use this method as an outcome measure in Achilles tendon injury. The objectives of this study were:

1. To investigate whether functional ultra sound elastography (FUSE) can provide an accurate measurement of strain along the Achilles tendon and produce strain gradient colour images of the tendon and surrounding tissues.
2. To study the appearance of the Achilles tendon on strain colour gradient image in healthy subjects.
3. To assess the use of functional ultra sound elastography as an outcome measure for Achilles tendon injury.

3.1.6 Volunteers Study Design and Protocol

FUSE is a quantitative observational healthy volunteers study. Participants were recruited from the general public under a study approved by the Oxfordshire ethics committee B (OxREC reference 09/H0605/79). The study was conducted at the Kadoorie Research Centre at John Radcliffe Hospital in full conformity with the current revision of the Declaration of Helsinki (last amended October 2000, with additional footnotes added 2002 and 2004). It was conducted according to the following protocol:

1. **Inclusion criteria**: participants are 18-55 year of age, able to give informed consent for participation in the study and able (in the Investigators opinion) and willing to comply with all study requirements.
2. **Exclusion criteria**: The participant may not enter the study if ANY of the following apply: Any Participant with a VISA-A score <90%, previous tendon or foot and ankle injury, participant is known to have a psychological, developmental, physical and emotional or social disorder that may interfere with compliance with study requirements.
3. Potential participants were given a participant information sheet and the study is explained to them and informed consent is obtained by the chief investigator (J Alsousou).
4. Participants were asked to complete the Victorian Institute of Sports Assessment- Achilles tendon (VISA-A) questionnaire prior to the study (appendix 5.6).
5. Each participant underwent an ultrasound scan of both Achilles tendons using clinically available US scan machine and probe. The scans were performed by Dr E McNally (Musculoskeletal radiologist) and J Alsousou (chief investigator). All images were saved to the ultrasound machine in DICOM and RF format.
6. Each tendon was studied in three sections at full probe width (figure 3.5):
    a. Proximal Third (musculotendinous junction)
    b. Middle third (2-6 cm above insertion)
    c. Distal third (insertion at the calcaneus)



Figure 3.5.
Tendon sections

7. Each tendon was scanned using 6 different elastography methods using the same ultrasound machine:
    a. Freehand B-mode US scan in transverse and longitudinal planes
    b. Freehand Compression/decompression Elastography scan
    c. Freehand Dorsal Flexion (DF)/Planter flexion (PF) elastography scan
    d. Controlled FUSE with OFAM device
    e. Real-time Elastography scan (manufacturer's built-in elastography)

The scans were selected to compare standard elastography technique (b) and commercial real-time elastography (e) with the new method using manual FUSE technique (c) and controlled FUSE (d).

8. Each scan was repeated 3 times for each tendon third. During elastography scanning the B-mode was displayed on a screen and assessed for adequacy and out-of-plane motion. The 3 best-fit B-mode sequences were then selected and saved for analysis.
9. DICOM and RF data were analysed at the Institute of BioMedical Engineering (IBME) using the aforementioned elastography algorithm (Appendix 3.1).

3.1.6.1 Data Acquisition Method

Radio Frequency (RF) data was captured using Zonare z.one© (ZONARE Medical Systems Inc, Mountain View, CA) with a L14-5 linear array transducer with a central frequency of 12MHz. The probe was applied in the longitudinal direction with its ultrasound transducers parallel to the tendon. Data was captured using the protocol in Appendix 3.1. RF data was transferred to the Institute of Biomedical Engineering (IBME) were it was processed to generate displacement and strain images using the algorithm described earlier in this chapter. Strain mapping images for each tendon third were presented in semiquantative colour gradient (red: compliant to blue: stiff). Strain images were overlaid over the related B-mode image. Displacement was also calculated in mm and presented in colour gradient for all tendons (Appendix 3.1). Average strain measurements in the tendon and fat pad were determined by using a MatLab code, also developed at the IBME, to draw boundaries of regions of interest on the B-mode elastography overlay. The code then calculated the average strain in the selected tissue area.

3.1.6.2 Average Strain and Strain Index

Assuming that when the Achilles tendon is injured, the injury is contained within the paratenon and the mechanical properties of Kager's fat pad do not change substantially (299, 300), it is possible to use the fat pad strain measurement to monitor the progress of the healing tendon. Therefore, a strain index, obtained by dividing the strain of the tendon by that of the fat pad, was calculated for all tendons in this study.

In each of the three elastograms of each tendon the Achilles tendon average strain (A) and Kager's fat (B) strain were measured using the Matlab algorithm. This allowed the investigator to draw shapes at the area of interest (tendon or fat pad), which included as much of the tendon and fat pad respectively. The strain index (SI) was then calculated for each image as the ratio between the tendon strain (A) and the fat-pad strain (B) respectively (SI = A/B). All measurements were performed by a single investigator (JA).

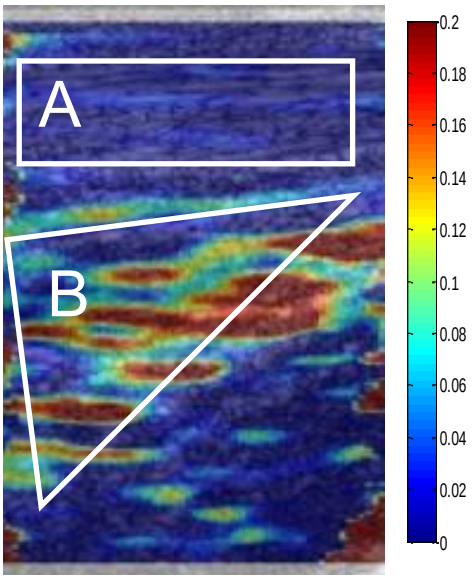


Figure 3.6. ***Strain index measurement. (A) Achilles tendon, (B) Fat pad.***

3.1.6.3 Statistical Methods

The elastographic images were qualitatively reviewed by visual inspection for tendon visibility and for determining the elastographic pattern. Descriptive statistics (number of participants, age mean, and standard deviation) are reported. VISA-A pre-screening score was reported as mean and standard deviation. Elastography results were described in terms of visual appearance of the tendon and anatomical structures in the area. Tendon axial and longitudinal strain was reported, tested for normality and compared between elastography techniques using ANOVA (for normally distributed data) or Kruskal-Wallis tests (for non-parametric data). The difference between tendon and fat pad strain means is performed using paired t-test. Significance level was set at 0.05. All statistical parameters were calculated using Statistical Package for the Social Sciences (SPSS PAWS 18.0 for Windows, Chicago, IL, USA). Graphical presentation of the data was performed using Prism Graph Pad (Version 5.03, Graphpad Inc, La Jolla, USA).

3.1.7 Volunteers Study Results

3.1.7.1 Recruitment

40 Achilles tendons in 20 healthy participants (10 male and 10 female) were studied. The average age was 34.1 ± 10.5 years old. There was no report of any symptoms related to the Achilles tendon prior to recruitment. VISA-A score was 98.1 ± 1.0, which indicates that the tendons were healthy. No adverse effect was reported after all scans. All participants reported that OFAM device did not cause any discomfort while moving during scans.

3.1.7.2 B-Mode Ultrasound

The Achilles tendons were clearly visualised on the grey scale b-mode images in both transverse and longitudinal scans (figure 3.6). Other anatomical structures such as Kager's fat pad, flexor Hallucis Longus (FHL) and plantaris tendons were clearly visible. No abnormality was detected in any of the tendons. The average Achilles tendon thickness measured on longitudinal scans was 5.4 ± 2.1 mm.

3.1.7.3 Elastography of Achilles tendon Images

The elastographic images were qualitatively reviewed by visual inspection for tendon visibility and for determining the elastographic pattern in each scan type. The Achilles tendons were clearly visualised in all DF, PF and controlled elastography techniques. Compression/decompression elastography images were affected by movement artefact and lack of displacement in the tendon tissues. Real-time elastography, which is the built-in elastography technique, failed to show clear structures in all the images (figure 3.7). This may be because this technique was designed and validated for bigger softer organs such as breast, liver and spleen.

Using controlled FUSE techniques with OFAM device, the colour pattern of the Achilles tendon was consistent between consecutive images of the same tendon. In all cases the tendon appeared blue (hard stiff tissues) with no evidence of softening or red areas in the middle of the scan area. Sharp artefacts on the either sides of the images were present in most images as expected and explained earlier in this chapter. The artefacts did not affect tendon visualisation in most images. The deeper

tissue strain varied between tendon, muscles and fat. The peri-Achilles Kager's fat-pad appeared in a mix of red/yellow (soft) representing the varied pliability of the fatty tissues. Muscles appeared in a mosaic of blue and red, which reflected muscle fibres contraction variability. Other tendons such as flexor hallucis longus (FHL) were also visible in blue.

Several compressional images were invalid due to the loss of displacement in the tendon tissues. All had edge artefact due to loss of compression with the contour of the probe edges. In the majority of compressional images in the distal third were invalid due to the difficulty in applying compression over the insertion into the calcaneum. A similar problem was also evident over the musculotendinous junction where the variability in the tissue compliance meant the equal application of compression was not possible resulting in artefacts. Compared with freehand and controlled motion images, the controlled motion offered sharper images with better quality strain mapping and fewer artefacts around the peripheries or inside the image. It was clear on the b-mode movies that compression results in displacement of the fat pad over the posterior aspect of the tibia bone, which may have caused the tissues to move laterally. There was difficulty in assessing tendon displacement on b-mode image sequence. The hard tendon tissues transferred the compressional forces directly to the very soft fat pad underneath. There was no difference between compression and decompression elastography visual appearance. Figure 3.7 shows representative images of each scan type.

Considering the visual appearance in b-mode and elastography images, strain measurement and strain index calculations was only performed in Freehand DF/PF and Controlled FUSE images.

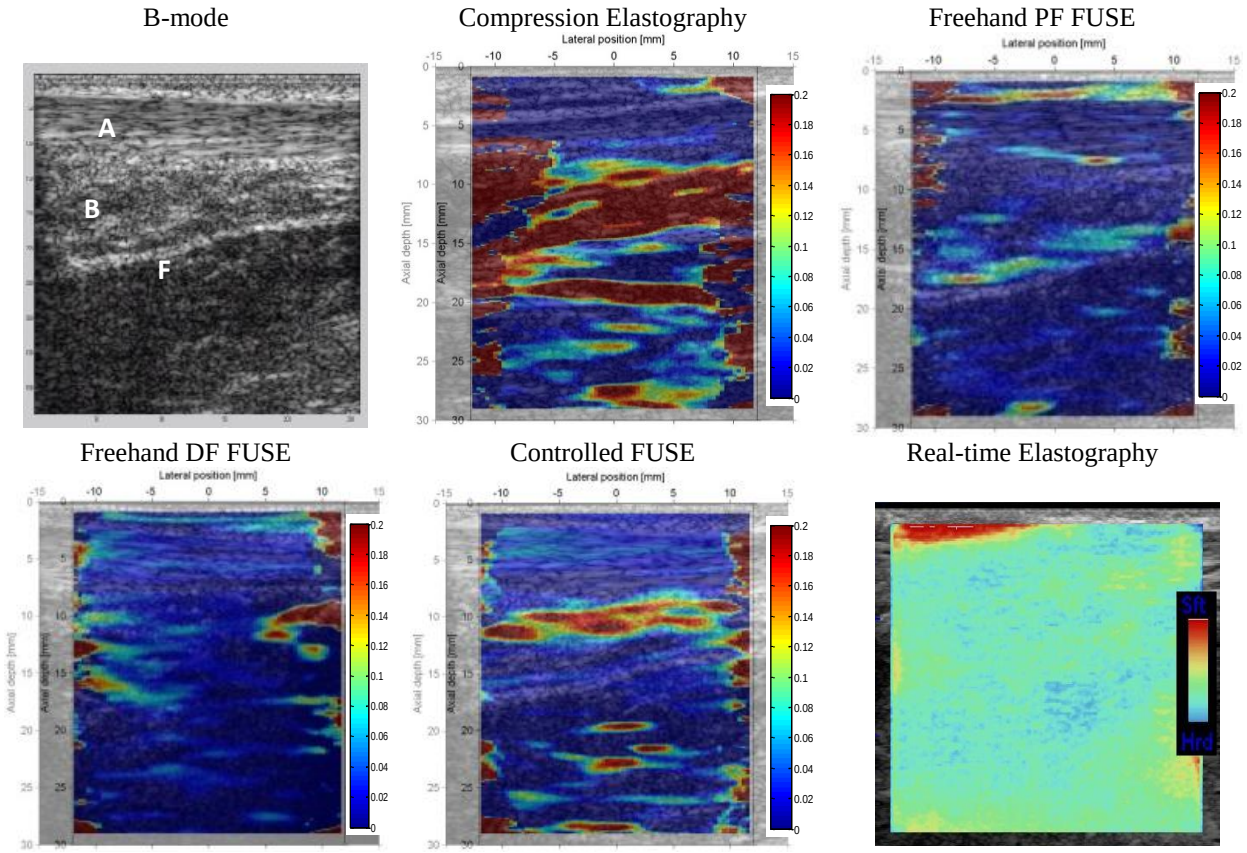


Figure 3.7. ***Examples of scan images of the same tendon using B-mode grey scale image, compression elastography, freehand planter flexion (PF) FUSE, Freehand dorsal flexion (DF) FUSE, Controlled motion FUSE with OFAM device and RT- elastography. (A) Achilles tendon, (B) Kegar's fat Pad and (F) flexor hallucis longus.***

3.1.7.4 Strain Measurement

Average strains in the tendon and fat-pad areas were measured using freehand compression/decompression, freehand and controlled FUSE elastography images of the 40 healthy tendons in both axial and longitudinal directions (figure 3.3). Strain measurement was not possible using real-time elastography. The results are presented in figure 3.8.

Using controlled FUSE technique; the tendon median strain was εx 3.2 ± 1.81 % and εy 2.485 ± 1.90 % in axial and longitudinal directions respectively. As expected the fat pad had higher strain mean (εx 6.171 ± 3.343 % and εy 9.076 ± 5.23 % in axial and longitudinal directions respectively) with wider data range. This appearance was also evident using freehand FUSE technique. The median tendon axial strain was εx 2.318 ± 2.39% and longitudinal strain was εy 3.459 ± 3.736%. The

fat pad responded to the stress with higher strain in both directions (ε_x 5.571 ± 3.503% and ε_y 11.66 ± 5.068%).

D'Agostino-Pearson normality test of all the data confirmed that the data is not normally distributed (P value <0.05). Therefore, nonparametric Kruskal-Wallis test with Dun's post-test were used to analyse the data.

Using the controlled FUSE scans there was no significant difference between the axial and longitudinal strains in tendon (p value 0.45). There was significant difference between fat pad axial and longitudinal strain (p 0.022). When comparing tendon and fat pad strain, tendon strain was significantly less than fat pad strain in both directions (p <0.0001) (Figure 3.8).

Using freehand FUSE technique, the visual difference between the tendon and the fat pad was not confirmed statistically (P >0.05). The difference between fat pad longitudinal and axial strain was not significant (P 0.389). There was no difference between the axial and longitudinal strain of the tendon (P 0.207).

Comparing freehand and controlled FUSE techniques, a Kruskal-Wallis test showed that strain differed across all the scans (P <0.0001). Dun's post test showed that there was no difference between controlled and freehand in measuring fat pad strain (P>0.05). However there was a significant difference between the two in measuring tendon strain (P 0.0001).

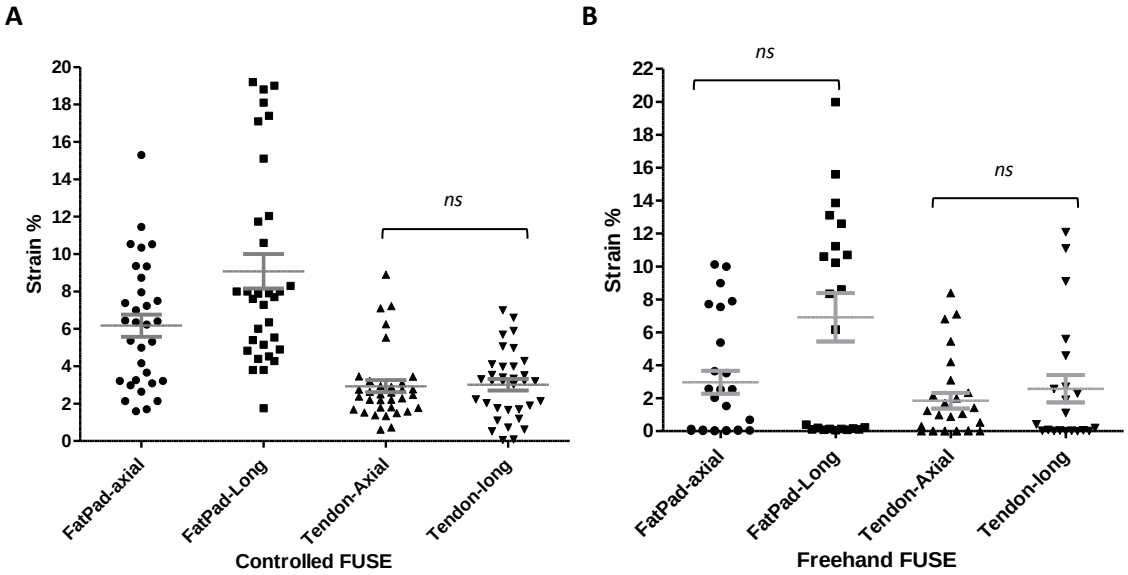


Figure 3.8. ***Average stain measurements for the Achilles tendon and fat pad in both axial and longitudinal directions. (A) The results of controlled motion FUSE technique using OFAM device. (B) Average strain of tendon and fat pad with freehand movement FUSE. (ns) refer to statistically nonsignificant difference between the marked scans.***

3.1.7.5 Strain Index

Strain index was calculated using the aforementioned method and is presented in figure 3.9. There was no difference between axial and longitudinal strain index in each of the controlled and freehand techniques (P value 0.069 and 0.356 respectively). There was an overall difference between the control and freehand strain index (P 0.029) (figure 3.9).

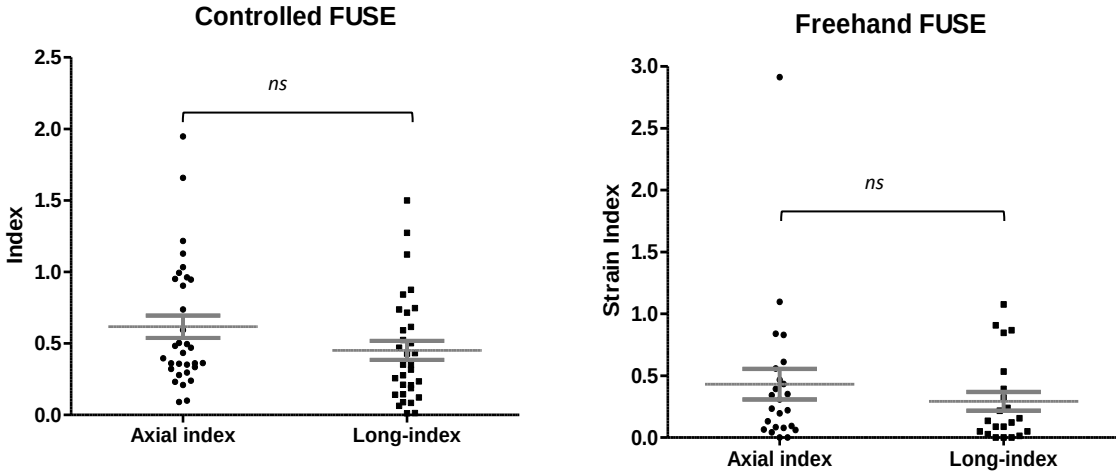


Figure 3.9. ***The results of strain index measurement of controlled and freehand FUSE.***

3.1.7.6 Displacement Imaging

Localised displacement was calculated using the aforementioned algorithm and converted to a 2D colour gradient image. Visual assessment of displacement images showed clearly unified movement of the tendon when moving the tendon in its functional loading directions (plantar flexion and dorsal flexion. In compressional methods the displacement of the tendon appeared in dark blue reflecting minimal movement or inability to detect the movement. Deeper tissues seemed to move slightly more with this method and displaced in light blue colour. An example of the results is displayed in figure 3.10. Freehand PF, DF and controlled FUSE showed the displacement range in yellow which is approximately 1.5-2 mm displacement. Real-time elastography did not produce displacement images and RF data for this was not retrievable. Tracking the displacement image may be useful in the diagnosis of acute or chronic tendon rupture where the tendon ends may move paradoxically to each other producing different colours within the tendon.

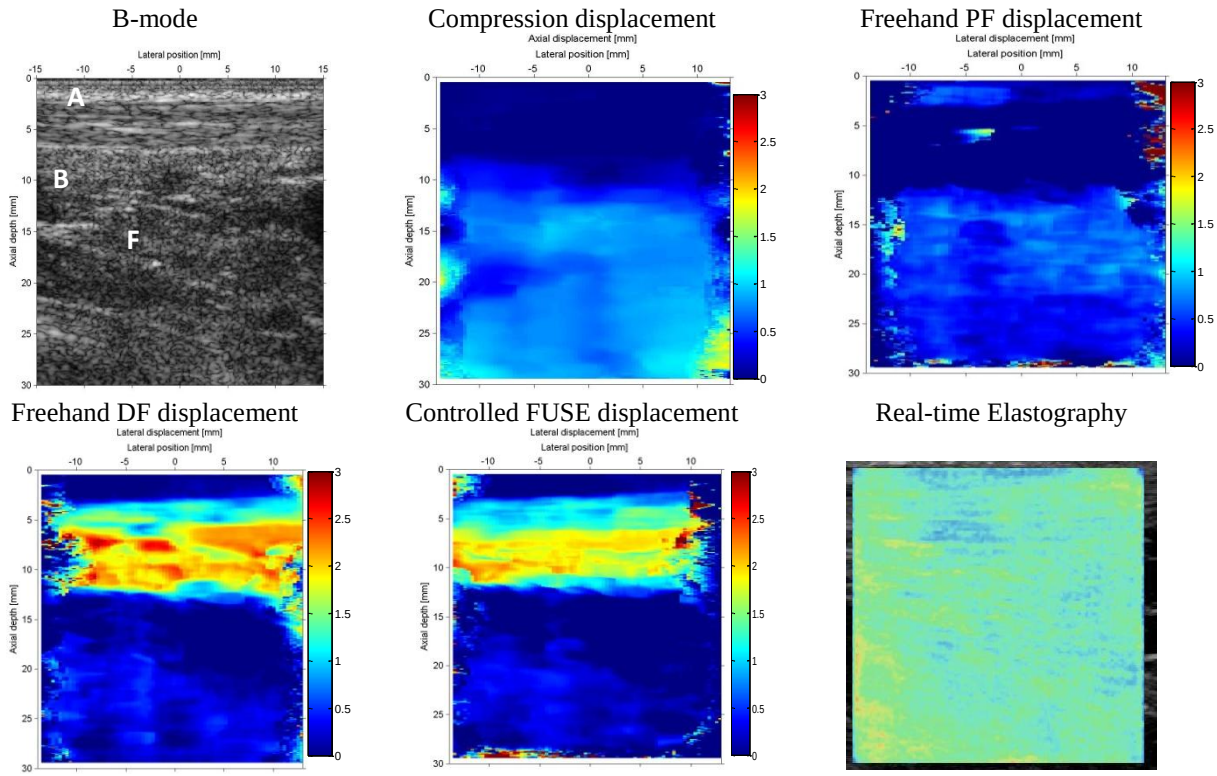


Figure 3.10. ***Examples of displacement images of the same tendon, using B-mode grey scale image, compression elastography, freehand planter flexion (PF) FUSE, Freehand dorsal flexion (DF) FUSE, Controlled motion FUSE with OFAM device and RT- elastography. (A) Achilles tendon, (B)Kegar's fat Pad and (F) flexor halluces longus. The displacement is measured in mm.***

3.1.8 FUSE Patients study

This study was conducted to investigate the feasibility of FUSE methods in patients with Achilles tendon rupture and to investigate the changes in healing tissue mechanical properties. This study was conducted as part of Platelet Rich Plasma in Achilles Tendon Healing (PATH) trial (chapter 5). In the current Chapter, the method of elastography imaging is described and initial scans results are reported. Full results will be statistically analysed and reported in Chapter 5 alongside the outcome measures of the trials.

3.1.8.1 FUSE Patients Study Methods

Full Ethics committee approval was obtained from Oxfordshire Ethics Committee B (reference 09/H0605/78) for the clinical trial including this elastography study. Acute Achilles tendon rupture patients were recruited into the trial as described in chapter 5. All patients underwent B-mode dynamic USS to confirm the diagnosis. Once informed consent was obtained patients underwent Functional Ultra Sound Elastography (FUSE) scan as described earlier in this chapter at baseline and then at week 1, 3, 6, 8, 12 and 24 post treatment. The patient was positioned prone on a couch with their injured leg in the OFAM device to protect the tendon. Each tendon was scanned using B-mode scan, compressional scan and controlled FUSE scan. Radio Frequency (RF) data was captured using Zonare z.one© (ZONARE Medical Systems Inc, Mountain View, CA) with a L14-5 linear array transducer with a central frequency of 12MHz. The probe was applied in the longitudinal direction with its ultrasound transducers parallel to the tendon. Data was captured using the protocol in appendix 3.1.

Average tendon and fat pad strain were measured and strain index was calculated using the same MatLab code that was used in the volunteers study for every follow-up week. Cumulative follow up data was analysed using linear regression analysis and compared to clinical outcome measures.

3.1.8.2 FUSE Patients Study Results

20 patients were recruited in the trial (Chapter 5). All had baseline elastography scans and week 1-24 follow-up scans. There was no report of any adverse event resulting from FUSE scans. There was no report of discomfort or pain during OFAM device movement. Most patients reported that the OFAM device boot offered better support during scanning when compared with freehand dynamic scanning. The results of B-mode imaging is reported in chapter 5.

Ruptured Achilles strain Imaging

In the acute stage (week 0), the longitudinal strain plots showed the rupture gap clearly in red (compliant) between the tendon ends (figure 3.11). The tendon edges were in blue colour representing the stiff tendon tissues. Axial strain did not show the gap as clearly, which remained in blue in several cases. The longitudinal displacement image at this stage showed the paradoxical movement of the tendon ends at the rupture site with tendon ends moving in different direction (different colours) (figure 3.11). Axial displacement images showed uniformly distributed displacement. There was no visualisation of the paradoxical movement or the rupture gap.

During the follow-up period, the improvement in tendon appearance on B-mode scans (figure 5.14) was reflected in improvement of the longitudinal displacement images. The tendon displacement gradually became uniform and the tendon started moving as one from week 3 onwards. This was reflected in changes in the elastography images. In the longitudinal strain images the red gap appeared to gradually become blue over the follow up period to reach normal strain colour (blue) at week 24. This improvement was not as obvious in axial strain imaging or axial displacement imaging.

In comparison, the commercial real time elastography failed to pick up the changes at acute presentation and throughout the follow up period. There was no change in appearance over time and the image remained undistinguishable (figure 5.15).

The results of FUSE imaging and data analysis are presented in chapter 5 alongside clinical trial methodology and clinical outcome measures.

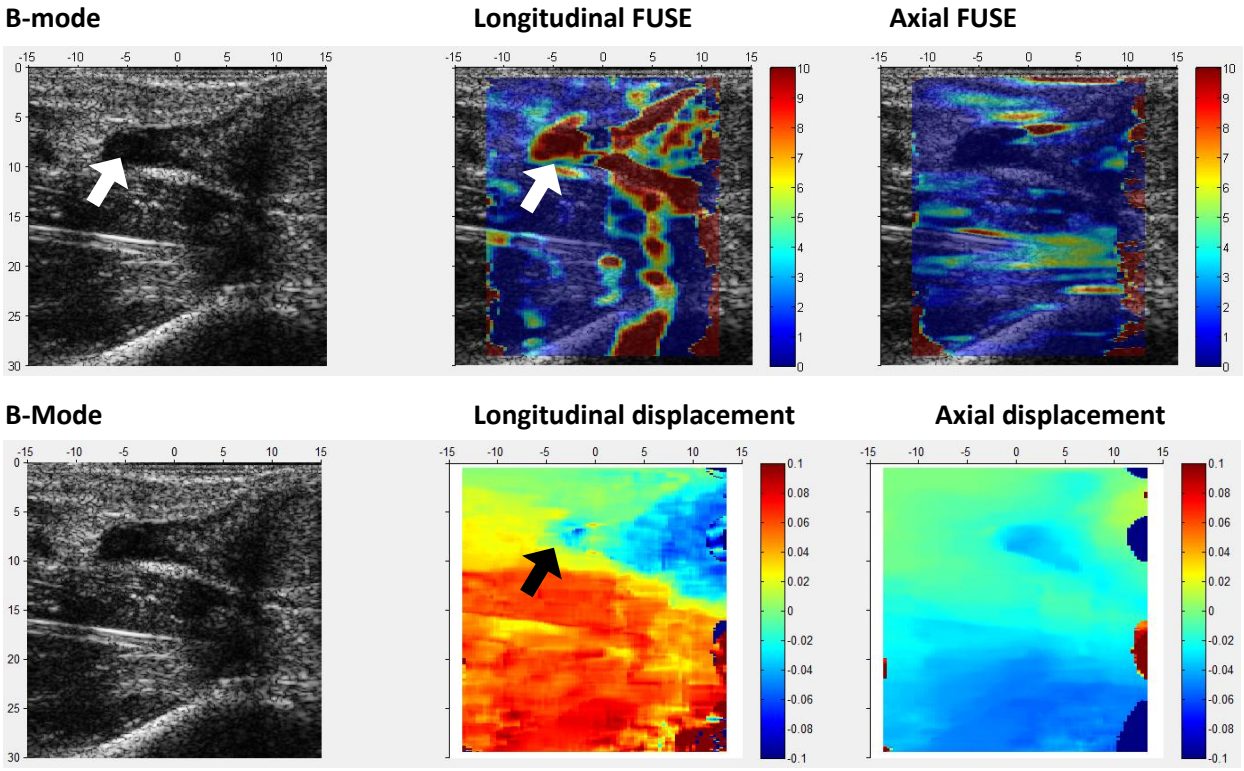


Figure 3.11. ***An example of acutely ruptured Achilles tendon FUSE scan. B-mode image shows the discontinuity of the tendon (arrow). Longitudinal strain FUSE elastography image shows the rupture area appearing in red (soft) and spreading between the two tendon ends. The corresponding displacement image shows paradoxical movement of the tendon ends (arrow). Axial strain mapping failed to show the same result in both strain and displacement images.***

3.2 Chapter conclusion

The study of the mechanical properties of the tendon has been so far employed either in an *in-vitro* studies using excised tendons or *in-vivo* using invasive techniques. In this chapter, a novel non-invasive method to measure strain and displacement of the tendon and display it in a colour image is introduced. The advantage of OFAM controlled FUSE was statistically significant, with both increased precision and control provided for elasticity imaging. FUSE technique can increase the clinical utility of ultrasound in the diagnosis and follow-up of Achilles tendon pathology.

The volunteer study confirmed that this method is feasible using clinically applicable ultrasound scan machine and method. The improved algorithm allowed investigators to measure localised strain within the studied tissues. This measurement was normalised using the tendon fat pad to create a

strain index. This technique also allowed the visualisation of tendon displacement as it was subjected to load in its functional role. The results show that current real-time elastography methods do not show tendon and localised musculoskeletal tissue strain. Further, longitudinal strain imaging (FUSE) is better than the traditional compressional elastography. Both free-hand and controlled FUSE technique showed the strain in the anatomical structures. However, controlled FUSE was better in measuring tendon strain and showed crisper more accurate images. This study demonstrated that controlled FUSE was successful in delivering sufficient acquisition quality for effective tendon elasticity imaging.

This method was piloted in patients with acute Achilles tendon rupture as part of a clinical trial (chapter 5). FUSE elastography images interrelated with the finding of the grey-scale US images. The controlled elastography method allowed the identification of rupture gap and quantification of the healing tendon throughout the follow-up. A final analysis made on the results of FUSE in patients with acute Achilles tendon is presented in chapter 5.

There are, to our knowledge, no other literature reports on similar experiments for measuring strain in healthy or ruptured tendons. Further work still needs to be performed to improve the ability to measure forces and thereby estimate material properties of the tendon such as young modulus.

Chapter 4 PRP Biological Contents, Viability and Function

4.1 Chapter Introduction

Clinically relevant PRP is prepared using various methods that result in a wide range of PRP products with varying biological components [Table 2.3]. Most of these products have varying concentration of blood cells (platelet, leukocytes and erythrocytes) and bioactive factors. Along with platelet concentration, Ehernfest et al (21) identified two components that may play important role in PRP biological properties: Leukocytes and fibrin. While Mishra et al (280), categorised PRP according to Leukocytes presence and activation. In chapter 2 of this thesis, a new classification system that takes into account: platelet critical concentration, leukocytes, fibrin content, activation, and preparation technique was suggested. The ability to identify PRP product characteristics and correlate it to clinical findings, offer the opportunity to detect the effective parameters of various PRP products and the ability to manipulate future products to maximise efficacy.

The effect of PRP on tissue healing is likely to be a function of many variables, which include: PRP biological characteristics, tissue injury type and extent, existing tissue condition prior to injury and the overall medical condition of the patient. PRP properties are measurable and can be altered to improve the outcome. Therefore identifying the biological properties of PRP and understanding its correlation to clinical outcomes is crucial when studying PRP in clinical trials (6).

The biological properties of PRP are based on the properties of the biological contents of PRP. These include cells (platelets, leukocytes and erythrocytes), proteins (fibrin and plasma proteins) and other bioactive factors (chemokines and cytokines, interleukins, clotting factors, complement) [table 2.1 and 2.2]. The mechanism of PRP action has been attributed to the release of multiple growth factors from platelets alpha and dense granules upon activation (7). However, Leukocytes play a crucial role in tissue repair and regeneration especially in the inflammatory stage of tendon healing and their role may extend to the repair stage (39). Direct cellular interaction between platelets, leukocytes and tenocytes is still largely unknown. In addition, fibrin forms scaffolding networks that supports

both platelet and leukocytes at the start of the healing process (165). Therefore, platelet concentration, leukocyte concentration and growth factor levels in PRP are important PRP parameters to monitor when studying PRP clinical effects.

Moreover, Platelets are delicate anucleated cells that go through biochemical, morphological and functional changes when prepared or stored in inadequate conditions. Those changes lead to platelet senescence and eventual death, which is characterised by loss of functional responsiveness to agonists (thrombin or collagen), loss of plasma membrane integrity, degranulation, loss of aggregation and lack of survival upon implantation into recipients (301). Hence, PRP preparation techniques need to be gentle to avoid destroying platelets yet powerful enough to increase platelet concentration. The assessment of platelet viability in PRP in both resting and activated states is vital to ascertain the efficacy of PRP products. This is achieved by studying platelet activation function, aggregation and degranulation. Platelet activation is a measurement of the population of platelets that can be activated by a stimulus (i.e. thrombin or collagen). Aggregation is a measurement of the platelets' ability to adhere together and form a clot (302). Platelet degranulation occurs upon activation and leads to the release of growth factors stored in their alpha and dense granules [chapter 2], which can be calculated indirectly by measuring growth factors concentration in PRP.

In the current chapter, the aforementioned vital properties of the autologous PRP, which is used in the clinical trial [chapter 5] and the linked *in-vitro* biological experiments [chapter 7], are investigated. Details of Platelets and leukocytes count, Platelet viability, Platelet aggregation and growth factors concentration assays are discussed in the methods section. The results are used to classify PRP according to the three classification systems: Ehrenfest, Mishra and Alsousou et al. Later on in this thesis, the current chapter results are linked to the *in vivo* and *in vitro* studies and potential improvements to the product are discussed further in the discussion section.

4.2 Methods

Autologous whole blood was obtained from Achilles tendon rupture patients recruited in Platelet rich plasma in Accelerated Tendo-Achilles Healing (PATH) trial [chapter 5]. In Tenocyte cell culture studies, whole blood was collected from consented healthy volunteers. All blood and tissue samples were processed in full compliance with HTA (Health Technology Assessment), Oxfordshire Ethics Committee approval (reference: OxREC 09/H0605/78) and with Helsinki Declaration of 1975, as revised on 1983. In this section, the methodology of blood collection and processing techniques and PRP analysis assays (cell count, aggregation, GF concentration and viability assays) are presented in detail.

4.2.1 Whole Blood Collection and PRP Preparation Technique

After obtaining informed consent, 52 ml of whole blood was withdrawn from the anticubital vein of each participant in PATH trial using sterile MDK300 Magellan® disposable blood withdrawal kit (17 gauge large bore butterfly cannula, 60 ml syringe primed with 8ml ACD-A anticoagulant) [Appendix 4.1]. The blood was withdrawn at a rate of 1ml per second to avoid damaging cells or activating platelets. The syringe was labelled then inverted several times to insure adequate mixing of the blood and anticoagulant.

The blood was processed immediately in the outpatient clinic or theatre to obtain PRP. Magellan ® Autologous Platelet Separator System and COS320 autologous thrombin kit (Arteriocyte ltd, USA) were used to prepare PRP [appendix 4.1]. This table-top automated device uses two centrifuging cycles to separate blood into three layers (RBC, buffy coat and plasma). In the first cycle, 160g centrifuging force is used to separate red blood cells from blood. The device uses an infrared sensor to detect the layers after centrifugation and the red blood cells layer is removed from the centrifuging chamber back into the 60-ml syringe. A second centrifugation cycle up to 300g follows and separates the blood into two layers: buffy coat and plasma layers. 8ml of the buffy coat and plasma (PRP) is automatically aspirated into a 10-ml sterile syringe [figure 4.1]



Figure 4 .1 PRP preparation using Magellan autologous platelet separator system (A). The large syringe contains whole blood (white arrow), which is being injected into the centrifugation chamber. Once it is ready PRP is aspirated into the small syringe (yellow arrow). The pictures on the right show the sequence of preparation in the chamber. B1: whole blood is spinning at 160g. B2: Red blood cells are centrifuged to the peripheries of the chamber. B3: RBC are discarded from the chamber. B4: further centrifusion cycle at 300g results in separating the buffy coat (Platelet, Leukocytes and small amount of plasma) from Platelet-poor plasma. The buffy coat (black arrow) is then automatically aspirated into the small syringe.

The resulting 8ml PRP was allocated to four portions:

- 1ml for autologous thrombin preparation
- 3ml to Inject in the tendon as per PATH trial protocol [chapter 5]
- 1ml to prepare culture medium in the *in vitro* studies [chapter 7]
- 3ml for count, aggregation, viability and growth Factors concentration ELISA assays

Autologous thrombin was prepared using Magellan® autologous thrombin disposable kit (Areteriocyte ltd, USA). Briefly, 1 ml of PRP was transferred to a sterile syringe containing glass fibre and calcium chloride and shaken gently for 5 minutes until a clot is formed. This is then transferred into 1ml syringe via selective 20µm filter to remove all the cells and clot. The autologous thrombin syringe and the remaining 3ml PRP syringe are attached to a dual applicator and used in the clinical trial [figure 4.6].

4.2.2 Blood Cells count assay

Platelets, leukocytes and erythrocytes were counted in each whole blood sample and subsequent PRP preparation using a KX-21N impedance counter (Sysmex UK, UK). This fully automated system uses only 50µl to analyse 18 parameters of the samples including histograms for cells. Haematocrit and leukocytes distribution were also measured in whole blood and correlated PRP samples.

4.2.3 Growth Factors Concentration

Samples were prepared for growth factors concentration analysis using the protocol in Appendix 4.1. In brief, 0.5ml autologous thrombin was added to 1.5ml of PRP in a test tube and shaken gently. The sample was incubated for 30 minutes at 37°c to allow clot formation, platelet activation and degranulation. After incubation, all samples formed a visible clot, which were then centrifuged at 2500rpm for 20 minutes to separate serum from the clot. The serum was aspirated and aliquoted into small vials, labelled and saved in -80°c freezer until the day of analysis.

Growth factors concentration was determined in each patient sample using specific Enzyme-Linked Immunosorbent assays (ELISA) for the following growth factors: IGF-1, PDGF-AB, TGF-β1 and VEGF. The Quantikine ELISA kits were obtained from R&D Systems Inc, UK and carried out according to the manufacturers' instructions [Appendix 4.3-4.6]. In principle, the ELISA assay employs the quantitative sandwich enzyme immunoassay technique. A monoclonal antibody specific for each growth factor has been pre-coated onto a microplate. Standards, controls and samples are pipetted into the wells and any growth factor present is bound by the immobilized antibody. After washing away any unbound substances, an enzyme-linked polyclonal antibody specific for each growth factor is added to the wells to sandwich the growth factor immobilized during the first incubation. Following a wash to remove any unbound antibody-enzyme reagent, a substrate solution is added to the wells and colour develops in proportion to the amount of growth factors bound in the initial step. The colour development is stopped and the intensity of the colour is measured using microplate reader (APCTRAmax Plus, Molecular devices ltd) set at the specified wavelength.

4.2.4 Aggregation analysis

Platelet aggregation, the process by which platelets adhere to each other at sites of injury, has long been recognized as critical for haemostatic plug formation and thrombosis. Until relatively recently, platelet aggregation was considered a straightforward process involving the bridging of integrin αIIbβ3 receptors on the platelet surface by the dimeric adhesive protein fibrinogen. However, with recent technical advances enabling real-time analysis of platelet aggregation *in vivo*, it has become apparent that this process is much more complex and dynamic than previously anticipated (22). Over the last decade, it has become clear that platelet aggregation represents a multistep adhesion process involving distinct receptors and adhesive ligands (GPIb-V-IX, GPIIb/IIIa, fibronectin, vitronectin, thrombospondin, vWF and GPVI) and can occur independently of platelet activation and integrin $\alpha_{IIb}\beta_3$ engagement (303). Activated platelets adhere, via glycoprotein (GP) Ia, to the collagen that is exposed by endothelial damage. Myosin and actin filaments in platelets are stimulated to contract during aggregation, further reinforcing the plug. An aggregation test is a measure of platelet viability and reflects the function of the aforementioned factors.

This assay investigates the aggregation function of platelets in PRP, which is prepared using the automated platelet separator system, after exposure to autologous thrombin and compares it to control (normal saline). In addition, the ability of collagen to aggregate platelet in PRP is studied using soluble collagen I and compared to thrombin and control. This assay was performed on all PRP samples using a Multiplate® Electrode Aggregometer (MEA), Verum Diagnostica ltd, Germany. This sensitive reliable method is based on the impedance aggregometry principle (304), which measures the increase in electrical resistance following platelets aggregation on platinum electrodes. Each multiplate test cell incorporates two independent impedance sensor units for quality control. The increase of electrical impedance due to the attachment of platelets to the electrodes is detected for each sensor unit separately and transformed to arbitrary aggregation units (AU) that are plotted against time (305). Three cells were used for each PRP sample: collagen, control and Thrombin cells [appendix 4.7].

4.2.5 Platelet Function Assay: CD62p marker expression

To determine platelet activation and resting status in the prepared PRP before and after applying autologous thrombin, CD62P (P-Selectin, GMP-140) expression was measured using Flowcytometery. P-Selectin (CD62P) was identified as a glycoprotein antigen expressed on the surface of activated platelets (13). It is constitutively expressed in megakaryocytes, where it is packaged into the membranes of α-granules of circulating platelets. Within minutes following activation of platelets P-selectin is expressed on the cell surface because of fusion of the intracellular storage membranes of α-granules with the plasma membrane (306). The expression of CD62P on the platelet surface reflects the degranulation of platelets and thus serves as a sensitive marker for the activation status of platelets in vitro and in vivo [figure 4.2]. During preparation (blood collection, centrifugation, pooling, and/or filtration) of PRP, platelets may become gradually become activated and partially lose their membrane integrity, which leads to platelet senescence (biological aging resulting in cell death). Therefore, it is important to establish the viability and functional status of platelets in PRP product.

In this assay, CD62p expression on the surface of platelets was used to study platelet degranulation immediately after preparation and after activation with autologous thrombin. The protocol of this assay is detailed in appendix 4.7. In principle, this assay employs flowcytometric technology to detect CD62P at the surface of a platelet using fluorescent-labelled non-blocking monoclonal mouse anti-human CD62P antibody (BD Biosciences, USA) [figure 4.2] (22, 307, 308). In brief, 150 µl PRP was mixed with 50 µl Gly-Pro-Arg-Pro (GPRP) to inhibit platelet aggregation. 100 µl of autologous thrombin was added to the mix and incubated for 10 minutes at 37°c. Subsequently, 5 µl of mouse anti-human CD62P antibody was added to test tubes. Negative control antibody (Mouse IgG1 Isotype control, BD biosciences, USA) was used to quantify non-specific binding and added to control tubes. The solution in all tubes was diluted to a total of 50 µl with Isoton and incubated for 10-15 minutes. Calibrated BD FACSCalibur flowcytometer (BD biosciences, USA) was used to capture light

scatter of gated platelets. To our knowledge this is the first analysis of platelet function in PRP using specific CD62P marker expression.

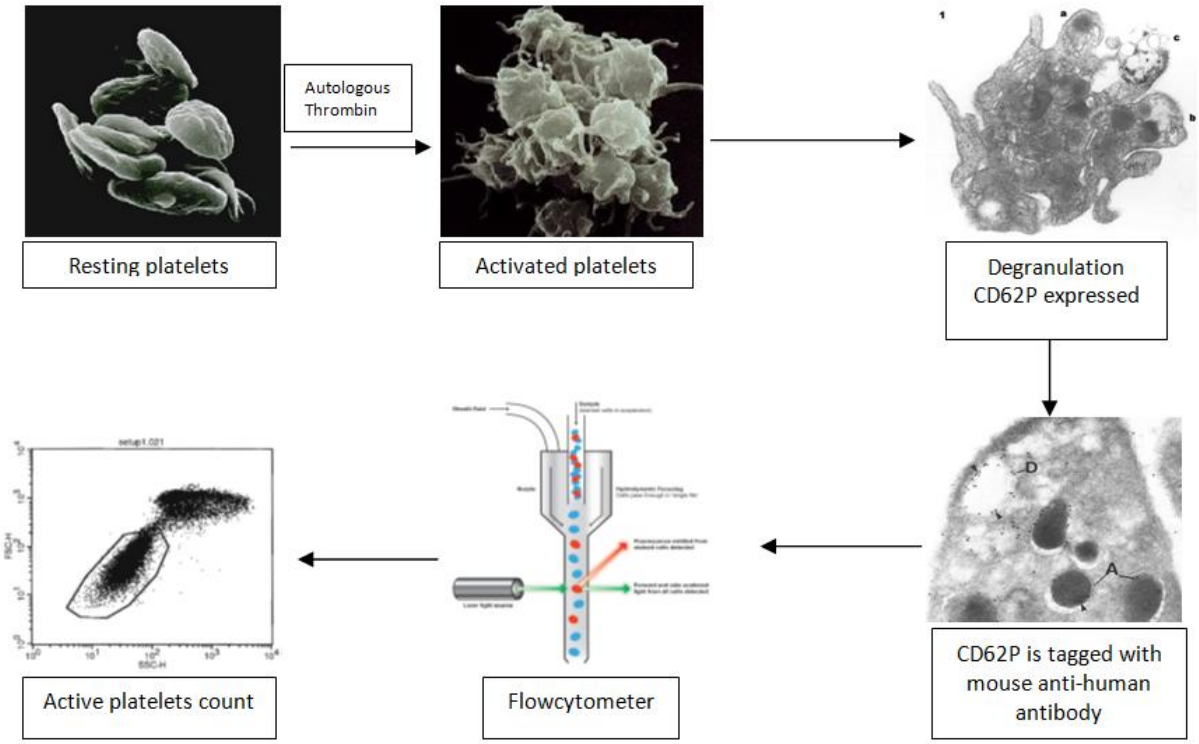


Figure 4 .2 Illustration of CD62p expression flowcytometry assay. When platelets are active, alpha-granules migrated to the surface and degranulate releasing their content and expressing CD62P. This is labelled with specific florescent antibodies, which allow CD62P counting using flowcytometer.

4.3 Results

4.3.1 Blood Cells count

The average platelet count in PRP increased by 4.74±0.73 fold compared to the original whole blood platelet count, taking into account the dilution factor of the ACD-A. Erythrocytes were also present in PRP but at a very low concentration (0.74±0.2 x10^6/µl) compared to the original whole blood (5.36 ± 2.1 x10^6/µl). The corresponding haematocrit dropped from 32.87±2.95% in whole blood to 5.91±1.09% in PRP [table 4.1 and figure 4.3].

There was also an increase in leukocyte count by 2.16±0.9 fold. Interestingly, there was a reverse of lymphocytes/neutrophils ratio in PRP when compared with original whole blood. Lymphocytes population in PRP exceeded that of neutrophils. [Table 4.1 and figure 4.3].

Table 4.1: The average cell count in PRP and initial whole blood. Yield is the result of cell count in PRP divided by cell count in initial blood. Data represent mean ± SD. (% is for percentage of cells out of that group total number, i.e Lymphocytes percentage out of total white cells).

	Whole Blood (60ml)	**PRP (8ml)**	**Yield**
Platelet (x1000/µl)	231.03 ± 45.81	1044.89 ± 302.00	4.74 ± 0.73
WBC (x1000/µl)	5.78 ± 2.34	11.9 ± 7.01	2.16 ± 0.90
RBC (x10^6/ µl)	5.35 ± 1.36	0.54 ± 0.12	0.1 ± 0.03
Hct (%)	32.87 ± 2.95	5.91 ± 1.09	N/A
Lymphocytes (x1000/µl)	2.0 ± 0.5	8.6 ± 1.45	4.3 ± 0.9
(%)	29.7%	61.4%	
Neutrophil ((x1000/µl)	3 ± 1.01	4.3 ± 2.08	1.43 ± 2.05
(%)	63.4%	21.4%	

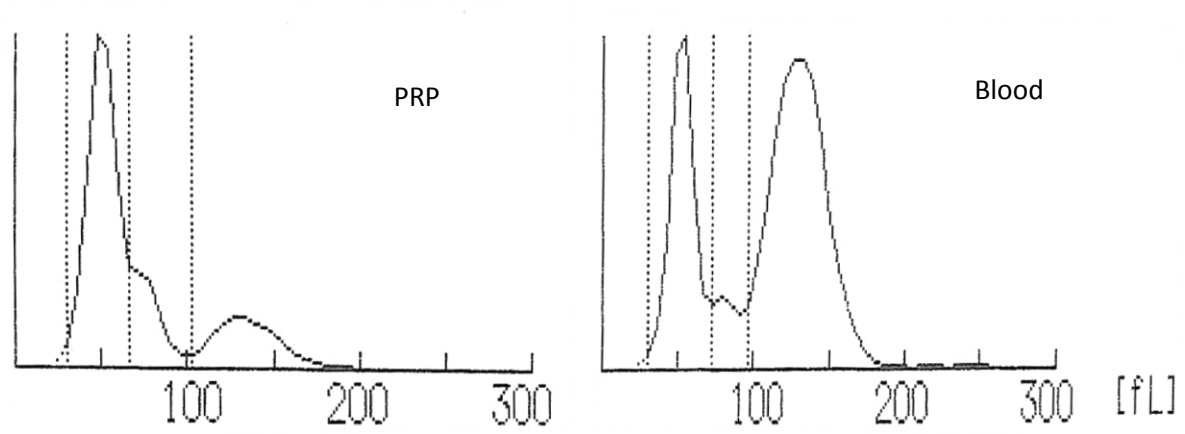


Figure 4 .3 Examples of histogram analysis of PRP (left) and whole blood (right). Vertical axis is for number of readings and horizontal axis is for volume of particles in FL. Whole blood histogram shows the typical two peaks appearance of RBC and PLT. In contrast, PRP histogram shows clear large peak at platelet range and a small one at RBC range and a small trough at WBC range.

4.3.2 Growth Factors Concentration

The concentration of TGF-B1, PDGF-AB, IGF-1 and VEGF in PRP that is measured using ELISA technique is shown in Table 4.2. The known published whole blood concentration of the same growth factors in healthy adults is used as a comparator.

The concentration of all growth factors was significantly higher in PRP samples when compared with their concentration in whole blood. The PDGF-AB level was 69.2 fold higher in PRP when compared with published whole blood concentration. TGF-ß1 and VEGF concentrations increased approximately at the same rate (9.73 and 9.06 fold respectively). Remarkably, IGF-1 was slightly higher in PRP than the published concentration in whole blood although this falls within the standard deviation and is unlikely to be significant.

Table 4.2: The concentration of growth factors in whole blood and PRP. The far right column shows the ratio between growth factor concentrations seen in PRP and whole blood.

Growth Factor	**Whole Blood Concentration (published)**	**PRP Concentration**	**PRP/Whole Blood**
TGF-ß1	4.1 ± 2 ng/ml (309)	39.9 ± 12.2 ng/ml	9.73
PDGF-AB	470 ± 320 pg/ml (144)	32529 ±15.2 pg/ml	69.2
VEGF	76 ± 8.5 pg/ml (134)	688.6 ± 51.4 pg/ml	9.06
IGF-1	84.2 ± 23.6 (134)	136.5 ± 45.7 ng/ml	1.62

4.3.3 Aggregation analysis

This assay was performed using all PRP samples to study the aggregation effect of both autologous thrombin and collagen. Normal saline was used as a control. The increase of electric impedance due to the attachment of platelets to the electrodes is detected for each sensor unit separately and transformed to arbitrary aggregation units (AU) that are plotted against time. Figure 4.4 shows examples of the aggregation graphs for the three comparators.

Kruskal-Wallis statistical test of this non-parametric data confirmed no difference between collagen and Thrombin in aggregating the platelets (p 0.4). Both thrombin and collagen significantly aggregated platelets in PRP when compared with control (P 0.003). Although thrombin aggregation time was significantly less than collagen (p 0.009), the overall aggregation effect of collagen was similar to that of thrombin (p 0.23) [table 4.3].

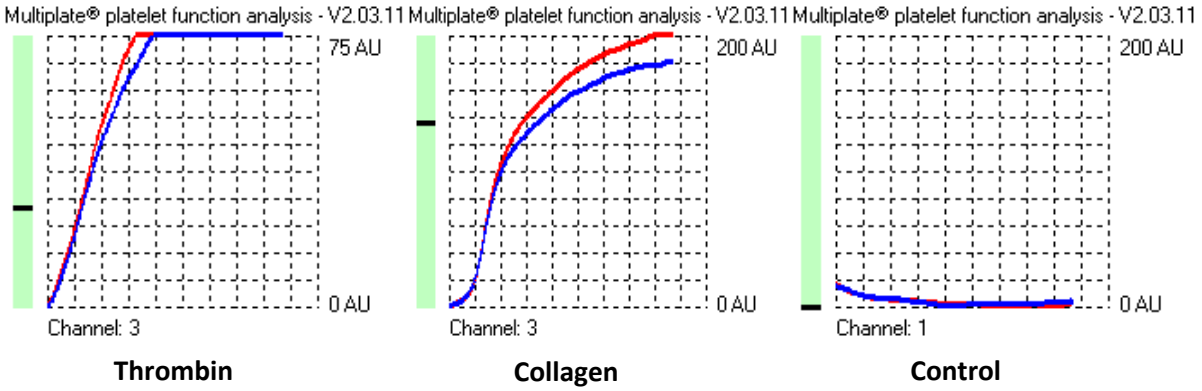


Figure 4 .4 Three examples of electrical impedance graphs, which plot arbitrary aggregation units against time of both cells (red and blue lines). Autologous thrombin reaches the maximum aggregation effect within 3 minutes. Collagen is slower to achieve maximum aggregation (6 minutes), but it reaches higher AU values than thrombin. The control (normal saline) fails to aggregate platelets.

Table 4.3: The mean aggregation units and standard deviation of thrombin, collagen and control in PRP.

n = 11	**Collagen**	**Thrombin**	**Control**
Mean AU±SD	175.13±27.02	186 ± 13.6	1.38±3.3
Time to max AU minutes	4.2±1.8	1.8±0.7	n/a

4.3.4 Platelet Function Assay: CD62p marker expression

Active platelets expressed CD62P as shown in figure 4.5. The percentage of activated and resting platelets in PRP immediately after preparation and post activation with thrombin is shown in table 4.4. The results reveal that the PRP preparation method used in the trial did not cause premature activation of the platelets. The majority of platelets (92.57%) were in a viable resting phase despite going through two cycles of centrifugation. The preparation technique (aspiration, centrifugation, mounting in syringe), and handling caused minor platelet activation which could be considered within normal range for *in vivo* blood (22). The majority of the platelet population (68.42%) in PRP

also retained their function and became active after adding autologous thrombin. This confirms the high percentage of viable platelets being injected back into the patient after the preparation stages.

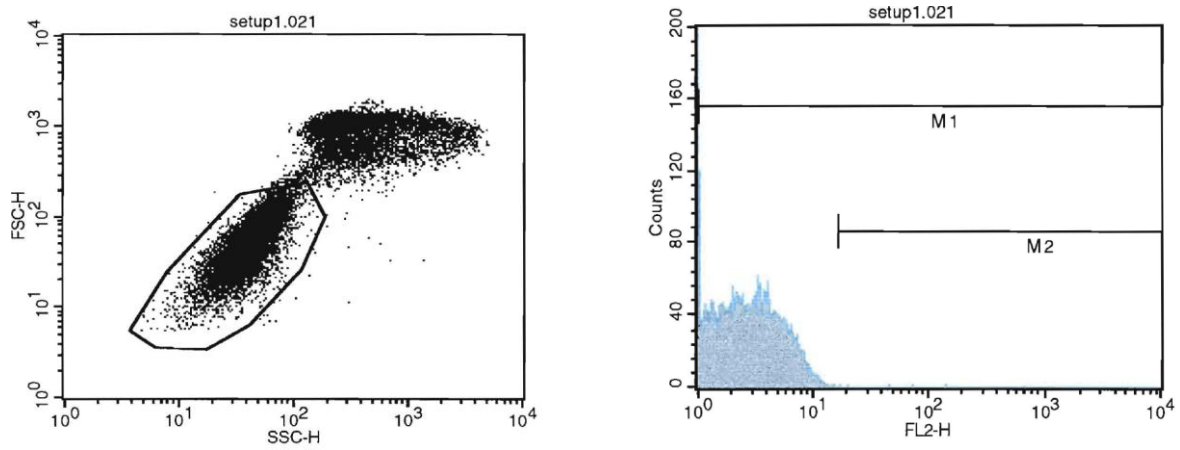


Figure 4 .5 An example of PRP function analysis using flowcytometry. Left graph shows active platelets population (circled). The right graph shows gating of platelets expressing CD62P to exclude non-specific binding of antibody (M1 and M2).

Table 4.4: The results of platelet function assay in PRP. P value was calculated using Mann-Whitney statistical test

n 11	**Before Thrombin (Mean ± SD)**	**After Thrombin (Mean ± SD)**	**P value**
Activated Platelets %	7.43±6.5	68.42 ± 4.52	0.001
Resting Platelets %	92.57±4.1	31.58±3.82	0.001

4.4 Chapter Discussion

The work in this chapter was to determine the biological properties and viability of the Platelet rich plasma product, which will be used in the clinical trial and the linked *in vitro* biological experiments. The results confirmed the high percentage of viable platelets in PRP and offered information on the biological content of the PRP.

The PRP, which was produced using a clinically-relevant commercial preparation system, has a very high concentration of platelets when compared with whole blood platelets count. Interestingly, this technique did not just increase the platelet count by 4.74 fold but also more than doubled the count of leukocytes with reversal of the lymphocyte neutrophils ratio. The average neutrophils count

remained higher than that of blood. This indicates that large number of the neutrophils population (being large cells) may have been centrifuged to the buffy coat layer, which was automatically removed. This ratio reversal has not been reported before and its effect is yet to be explored. In addition, despite the double centrifugation cycles, a small amount of erythrocytes remained in PRP making it red in colour [figure 4.6]. Although RBCs are present in the haematoma that ensues following an injury, the role of low erythrocytes concentration in PRP is currently unknown. In Chapter 7, the overall *in vitro* effect of this PRP product on tenocytes is studied but more experiments are needed to investigate whether altering cell ratios results in differing outcome.

Growth factors analysis revealed high concentrations of PDGF-AB, TGF-β1 and VEGF in activated PRP. Remarkably, IGF-1 concentration was only mildly above its concentration in whole blood. Weibrich et al found similar results with regards to IGF-1 level in PRP (134). The interpretation of IGF-1 levels is complicated by the wide normal ranges, and variations by age, sex, and pubertal stage (310). Although PRP effect is likely to be a complex process, these highly concentrated growth factors may kick start the regenerative pathways of the targeted tissues (7, 12).

Collagen and thrombin influence on platelet aggregation in PRP was studied using normal saline as a passive control. The results revealed that platelets in PRP retained the complex aggregation function. It also confirmed that collagen is an active agonist that causes platelet aggregation in PRP that matches the thrombin aggregation effect. In the clinical trial of the current thesis, we used autologous thrombin activation during injection [figure 4.6]. However, autologous thrombin production is costly and time consuming. Considering that collagen is abundant in the injured tendon, therefore it is possible that PRP may be injected directly into the injury site without the need of thrombin.

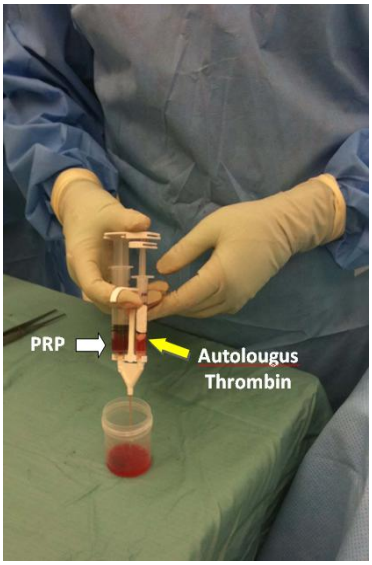


Figure 4 .6 PRP is mounted in a dual syringe ready for clinical application. The white arrow points to the PRP, which was produced from autologous blood using Magellan device and disposable kit. The yellow arrow refers to autologous thrombin, which is obtained using Magellan Autologous thrombin disposable kit.

Finally, in a novel study, platelet function and viability in PRP was studied using CD62P expression. The results confirmed that the majority of platelets in PRP were viable in resting state after preparation. The platelets became active after adding thrombin and expressed CD62P, which indicates degranulation and release of alpha granules contents.

The information provided by the assays in this chapter allows the authors to classify this PRP. The high leukocytes and mild fibrin contents makes this L-PRP class according to Ehrenfest classification. Considering that the average leukocyte count was less than 5 and thrombin was used to activate PRP, this correlates with type 2B according to Mishra classification. Using the centrifuging preparation technique locates it as L-PRP IB1 using the classification in table 2.6.

4.5 Chapter Conclusion

The experiments in this chapter, which investigated the viability and biological properties of PRP, confirmed that PRP is a viable autologous blood product rich in growth factors. The results also confirmed that leukocytes and platelets are present in very high concentration with reversal of lymphocyte neutrophil ratio. The combination of supraphysiological levels of bioactive factors and cellular contents may play a role in kick starting the repair process of injured tendon. In the following three chapters, the clinical, histological and biological effect of this PRP is explored in purposely designed studies.

Chapter 5 Platelet Rich Plasma in Accelerated Tendo-Achilles Healing (PATH) Trial

5.1 Introduction

In the previous chapter, the viability of PRP and biological components were established. In the current chapter, this PRP will be trialled in a randomised controlled trial pilot study to detect its potential clinical effects, establish the feasibility of its use clinically and obtain the statistical parameters to set up an appropriately powered multi-centre randomised controlled trial. The newly developed functional ultrasound elastography (FUSE) is used to study mechanical properties changes in the healing Achilles tendon throughout the healing stages. This will be compared to the data obtained from healthy volunteers in chapter 3. All clinical and imaging results are reported in this chapter, but any relationship of the findings from this clinical trial with the linked *in vitro* experiments in chapter 7 and histopathological findings in chapter 6 is discussed in the general discussion chapter.

5.2 BACKGROUND AND RATIONALE

5.2.1 Achilles tendon Rupture

Tendon injuries are common and incapacitating for months in the aging but physically active population. Achilles tendon is the most commonly injured tendon in the human body, it accounts for 20% of all tendon ruptures. The prevalence of ATR is 12-18 /10000/year and it is on the increase due to upsurge in recreational sport (78) in patients engaged in sedentary or professional occupation.

Although tendons have the ability to heal after injury, the process is slow and mechanical and biological properties of healed tendons never appear to match those of intact tendons leading to higher risk of further injury (65). This limited healing capacity of tendons appears to be caused by poor vascularisation, changes to the matrix structure and alteration in the mechanical environment of this connective tissue (32, 69, 127, 128). Therefore, even with the best available clinical

management, tendon injuries give rise to substantial morbidity that may last for several months and pose a considerable challenge for clinicians(3).

A Cochrane review reported mean rehabilitation and work absence of 63-108 days leading to huge NHS and societal costs (311). The current treatment strategies has been mechanical augmentation with suture or immobilization in cast, both of which do not alter the existing biological regenerative pathway of the tendon leading to long rehabilitation, reduced function and high rerupture risk (5-15%) (311). On average the rehabilitation programme last a minimum of 12 weeks and patients are not allowed to run or get involved in sporting activities for 18 weeks (114). Therapies are currently dominated by the conflicting priorities of rapid rehabilitation and a return to work versus the risk of re-rupture and/or surgery. New cost-effective treatments that reduce both the risk of re-rupture and time to functional healing are needed to address this challenge.

5.2.2 Platelet Rich Plasma

Platelets have evolved over millennia to deliver a combinatorial wound healing cocktail that comprises over 1100 active soluble and membrane bound components, delivered sequentially over a timeframe from minutes to the lifespan of the platelets.(6, 12) This ordered sequence of release is optimized to recruit a diverse range of cell types, acting on the injured tendon and disrupted blood vessels as well as promoting chemotaxis and homing of distant white blood cells and local or circulating stem cells.

In acute tendon rupture; platelets immediately form a clot formation in the resulting haematoma. Stem cells and surviving tenocytes are recruited by chemotaxis and motogenic stimulation into the ruptured area, followed by proliferation to start the healing process. The active growth factors in PRP act as both motogenic and chemotaxis agents for tenocytes. Tenocyte monolayers subjected to scratch assay fill in the wound area 2 days ahead of controls, through a combination of mitosis and migration. When tenocytes are placed in a transwell suspended above a clot of PRP, tenocytes move avidly through the membrane towards the PRP while control cells do not cross it. While PRP contains

many active growth factors and chemokines we found that a key effect is the stimulation of tenocytes to begin their own production of these growth factors (5). Thus the cells which are attracted by PRP rapidly begin to contribute to the tendon healing cocktail. Similarly invading WBC will add their agents to the milieu.

Although in-vitro and animal studies demonstrate the synergetic effect of PRP on tendon healing, clinical evidence is lacking (6).

5.2.3 Achilles tendon Rupture and PRP

A thorough literature search of the application of PRP in Achilles tendon rupture in both animal and human studies was conducted. Nine studies present results for the use of platelets in Achilles tendon rupture treatment, seven from animal experiments and two from human trials (162, 163). Six of the animal studies used a rat model, and one used an ovine model. All animal studies, using biomechanical and histological assessments, are in agreement showing a beneficial effect of platelets. Only two human studies have tested the effect of platelets on the treatment of Achilles tendon rupture based on imaging techniques and clinical results [table1].

Sanchez et al (14) found positive effects in a group of 12 athletes treated with PRP suture repair at 32 months in a case-control study. There was less tendon thickening, higher concentrations of TFG-beta and other growth factors and patients regained range of motion faster and returned to gentle running earlier. In a randomised study of 30 patients, Schepull et al (162) found no effect of platelets on radioisometrical tendon contraction. Both of these under powered clinical studies used PRP as an adjunct to open surgical repair and this may have obscured any effect of PRP on healing.

There are three other studies that report on the use of platelets in human Achilles tendinopathy however we cannot infer the results of these trials on Achilles tendon rupture, which has a very different pathology, regenerative properties and treatment pathways. Therefore there is only one underpowered RCT that has assessed PRP in Achilles tendon rupture (274). The authors recognised a

limitation in their platelet preparation technique and storage (of up to 20 hours) resulted in only a 20% release of growth factors from the platelets. In our 20-patient pilot study we achieved 69% activation (312).

Recently published systematic reviews (275, 276) have concluded that there are encouraging signs that PRP could be developed as an effective tendon therapy. Sadoghi et al (275) concluded that there is evidence in support of a positive effect of platelet concentrates in the treatment of Achilles tendon ruptures in vivo in animal models and human application, consistent with a medium to large sized effect this effect is most likely attributed to fastened accelerated and enhanced scar tissue maturation. In another systematic review, Taylor et al (276) concluded that PRP use in tendon and ligament injuries has several potential advantages, including faster recovery and, possibly, a reduction in recurrence, with no adverse reactions described. Both reviews emphasised the need for an adequately-powered RCT to establish PRP efficacy with disease-specific outcome measures.

In this chapter, PRP use in Achilles tendon ruptures as an adjunct therapy to standard treatment was studied in a pilot phase on a small group of patients.

5.3 Hypothesis

PRP application as an adjunct therapy to standard treatment in acute Achilles tendon Rupture (ATR) in adults is feasible to apply in clinical sitting and it may lead to accelerated tendon functional recovery as measured using a validated patient reported outcome measure.

5.4 Methods

5.4.1 Aims and Objectives

The aim of this study is:

1. Evaluate the feasibility of Platelet Rich Plasma (PRP) application as an adjunct therapy to standard treatment in Acute Achilles tendon.
2. Detect the efficacy signal in a pilot study using validated patient reported outcome measures.
3. Explore the potential use of Functional Ultrasound Elastography as an outcome measure tool in Achilles tendon rupture and study.
4. Provide PRP and tissue samples for PRP quality testing (chapter 4), immunohistochemistry analysis of tissue response to PRP (chapter 6) and *in-vitro* studies of PRP effect on the injured tendon (chapter 7).

5.4.1.1 Primary Objectives

To investigate in a pilot study whether the use of PRP local injection into the Achilles tendon rupture gap leads to accelerated healing and faster return to normal function than standard cast immobilisation treatment or operative repair.

5.4.1.2 Secondary Objectives

To assess the feasibility of Platelet Rich Plasma injection use to enhance Achilles tendon healing in both conservative and operative treatment groups.

To assess whether the use of platelet rich plasma in conjunction with the standard Achilles tendon treatment (conservative or operative) reduces the risk of re-rupture.

To further develop and validate the novel US functional imaging tool (Elastography) for tendon outcome measurement.

5.4.2 PATH Trial

5.4.2.1 Ethics

Full Ethics committee approval was obtained from Oxfordshire Ethics Committee B (reference 09/H0605/78). The PRP product and its methods of application in the clinical settings of this trial was discussed with MHRA (E/2009/0819), which confirmed that MHRA approval was not required considering that this is not a clinical trial of an investigational medicinal product (IMP). This trial was conducted in full conformity with the current revision of the Declaration of Helsinki (last amended October 2000, with additional footnotes added 2002 and 2004) and with relevant regulations and with the ICH Guidelines for Good Clinical Practice (CPMP/ICH/135/95) July 1996.

5.4.2.2 Trial Design

PATH was the pilot phase of a parallel, patient-blinded, individually randomised controlled efficacy trial of PRP in conservatively and operatively treated Achilles tendon ruptures. The trial was conducted as part of the work for this thesis and to obtain the information required to design and power a large confirmative trial. The pilot trial design is shown in the flow chart (figure 5.1). 20 patients were recruited at The John Radcliffe Hospital, Oxford, which is a major NHS acute hospital. Patients followed a conservative or operative pathway according to the established protocol (appendix 5.2). This was determined depending on the TA rupture gap size measured by USS. Patients in the operative and conservative pathways were then randomised into one of two groups (PRP or Control) using computer generated randomisation. The allocation to treatment was as follows:

Conservative treatment (rupture gap < 5mm)

1. Standard Cast immobilisation group
2. Platelet Rich Plasma (PRP) and Standard Cast immobilisation group

Operative treatment (rupture gap > 5mm)

3. Standard surgical repair group
4. Platelet Rich Plasma (PRP) and Standard surgical repair group

Patients in each treatment arm followed the same rehabilitation protocol. Patients in all groups were asked to complete Achilles Tendon Rupture score (ATRS) questionnaire and other outcome measures questionnaire in the follow up outpatient clinic. In addition, a Functional UltraSound Elastography (FUSE) Scan was performed to determine the mechanical properties of the healing tendon in all groups at each visit. Histological biopsies were obtained from the healing tendon at week 6 using needle biopsy under ultrasound guidance. The histological and immunohistochemical response to PRP was compared to control and is presented in Chapter 6. Blood and PRP samples were analysed as presented in Chapter 4.

5.4.3 Study Population

All patients with acute complete closed Achilles tendon rupture, aged 18 to 55 years, and attending within 72 hours of sustaining an injury due to sport activity or low energy hyper dorsal flexion of the foot were eligible for recruitment.

5.4.3.1 Inclusion Criteria

- Participant is willing and able to give informed consent for participation in the study.
- Male or Female, aged 18 years – 55 years.
- Diagnosed with acute Achilles tendon rupture
- Presenting within 72 hours post injury
- Able (in the Investigators opinion) and willing to comply with all study requirements.

5.4.3.2 Exclusion Criteria

The participant did not enter the study if ANY of the following apply:

- Previous Achilles tendon injury
- History of Diabetes Mellitus (insulin dependent?)
- Platelet abnormality or platelets count < $100x10^9$ /l
- Haematological disorder

- Use of systemic steroids
- Use of any anticoagulant
- Evidence of gangrene/ ulcers or peripheral vascular disease
- History of hepatic or renal impairment or dialysis
- Patient is known to have a psychological, developmental, physical, emotional or social disorder that may interfere with compliance with study requirements
- History of Alcohol or drug abuse
- Patient has a religious or cultural conflict with the use of platelet gel treatment or blood products
- Patient is currently receiving or has received radiation or chemotherapy within the last 3 months prior to the study
- Patient has evidence of Charcot foot / ankle joint
- Female participants who are pregnant, lactating or planning pregnancy during the course of the study.

5.4.4 Outcome Measures

5.4.4.1 Primary Outcome Measures

The Achilles Tendon Total Rupture Score (ATRS) is a patient reported outcome measure incorporating questions relating to muscle strength and fatigue, pain, lower limb function and disability (313).

A systematic review of disease-specific outcome measures for Achilles tendon rupture identified the ATRS as the only tool to have undergone appropriate validation (314). An additional study has recently reported positively on the internal consistency, convergent validity and responsiveness of the ATRS, strengthening the evidence-base for use of this tool as an outcome measure for trials evaluating interventions for this injury (315). The progression of ATRS score during the follow up period is the primary outcome measure.

5.4.4.2 Secondary Outcome Measures

1. **Functional Ultrasound Elastography (FUSE)**: this method is presented in chapter 3. FUSE was performed at each follow up visit to study the mechanical properties of the healing tendon
2. **Victorian Institute for Sport Assessments- Achilles score (VISA-A)**(316) is a reliable Achilles tendon function measurement tool when assessing patients with Achilles tendinopathy based on Iversen et al systematic review (317). VISA-A score was developed as an index of AT clinical symptoms and their effect on physical activity. This scale was used to assess Achilles tendon rupture prior to the development of ATRS (318).
3. **Foot and Ankle Outcome Score (FAOS)** is a patient-reported outcome scale developed for variety of foot and ankle-related problems. FAOS has been used in patients with ankle instability, Achilles tendinosis and plantar fasciitis (319). FAOS consists of 5 subscales: Pain, Symptoms, Adult Daily living, Sport and foot and ankle related quality of life (QoL). Although this score is not validated for Achilles tendon rupture, it was used to validate ATRS, therefore it is used in this study.
4. **Maximal bilateral and unilateral heel raise at 24 weeks:** A standardised protocol of clinical assessments was used to obtain clinical physical objective measures for the function of the triceps surae muscle complex. The participant was asked to lift themselves on tip toe and the distance between both heels and the floor was measured in centimetres (84).
5. **Maximum ROM at 12 and 24 weeks:** This is an assessment of stiffness following Achilles tendon rupture treatment
6. **Time to return to normal activities:** number of weeks to return to work or sport activity
7. **Calf Girth:** A measure of calf girth of both sides at every visit to assess calf muscle wasting following treatment.
8. **SF-36 questionnaire:** measures functional health and well-being from the patient's point of view. It is a practical, reliable, and valid measure of physical and mental health in a wide range of conditions. (320)

5.4.5 Trial Flow Chart

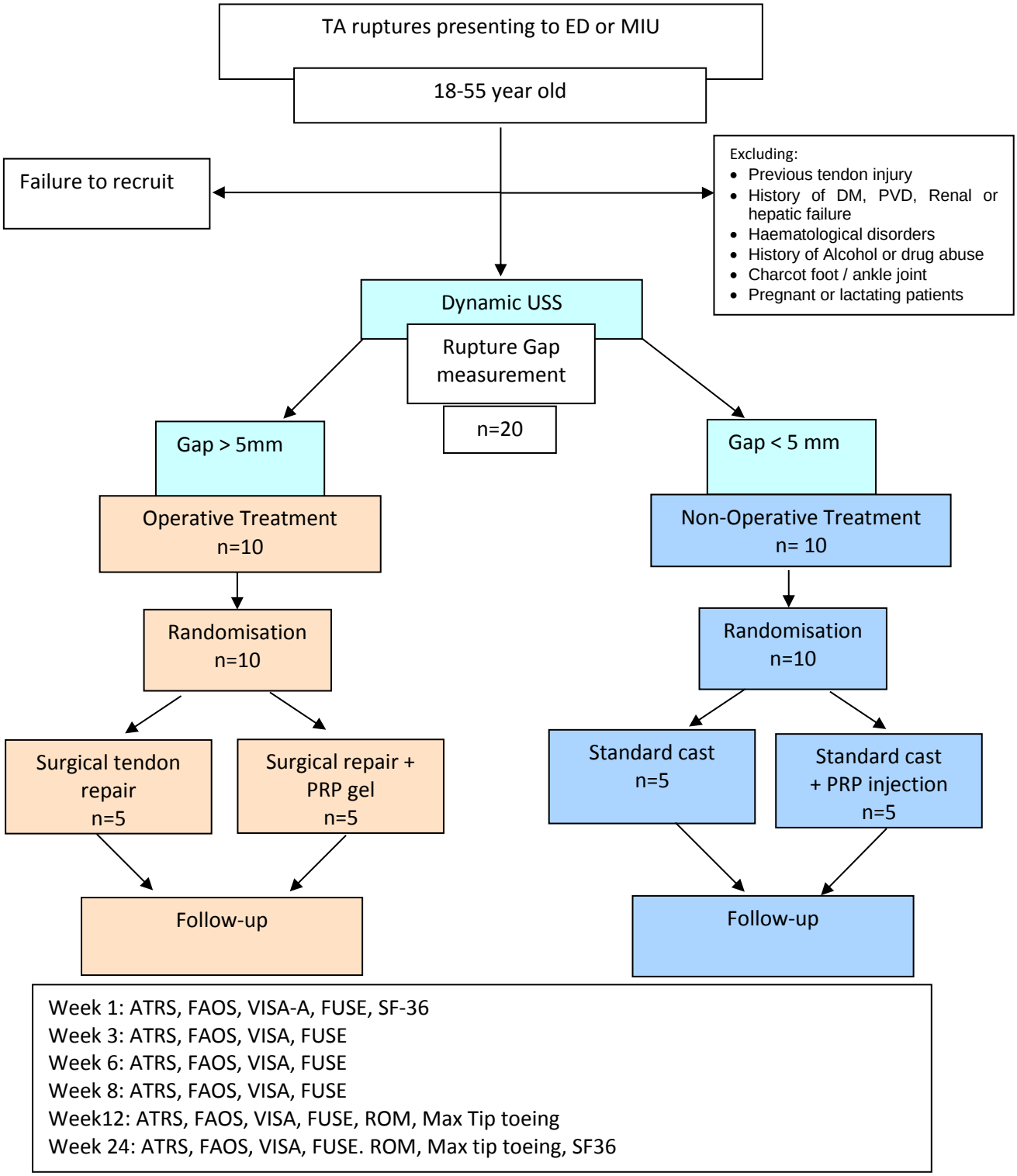


Figure 5 .1 CONSORT Flow chart: patients were identified in ED and Dynamic Ultrasound scan was booked. Once the diagnosis of complete rupture was confirmed, they followed operative or conservative treatment pathway depending on the gap size. Within each pathway, participants were randomised to receive PRP or control. All patients followed standardised rehabilitation protocol and followed up for 24 weeks.

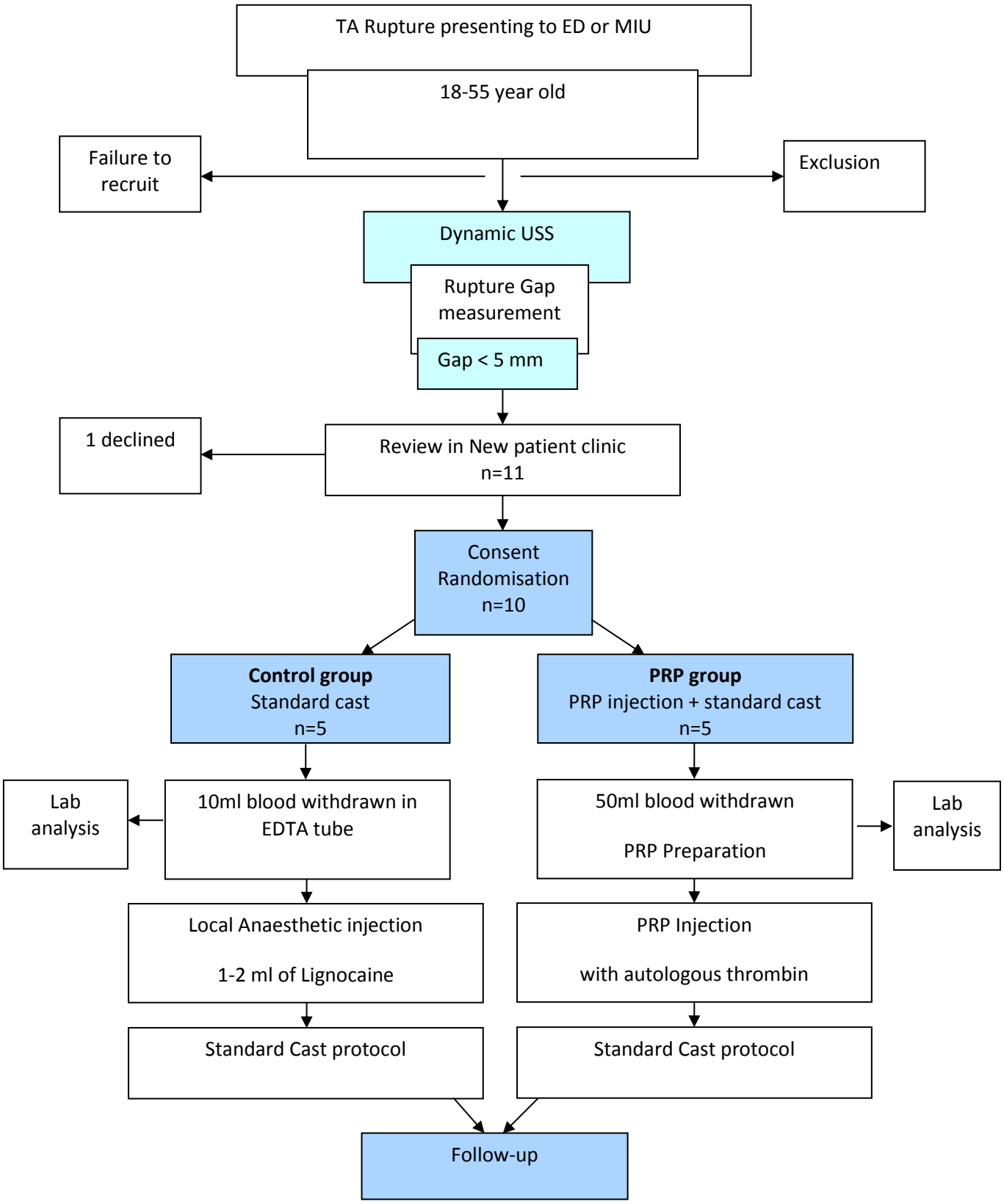


Figure 5 .2 Flow chart of the non-operative leg of the trial. All patients with rupture gap less than 5 mm were included and randomised to control injection and standard cast or PRP injection and standard cast. All patients followed the Oxford rehabilitation protocol.

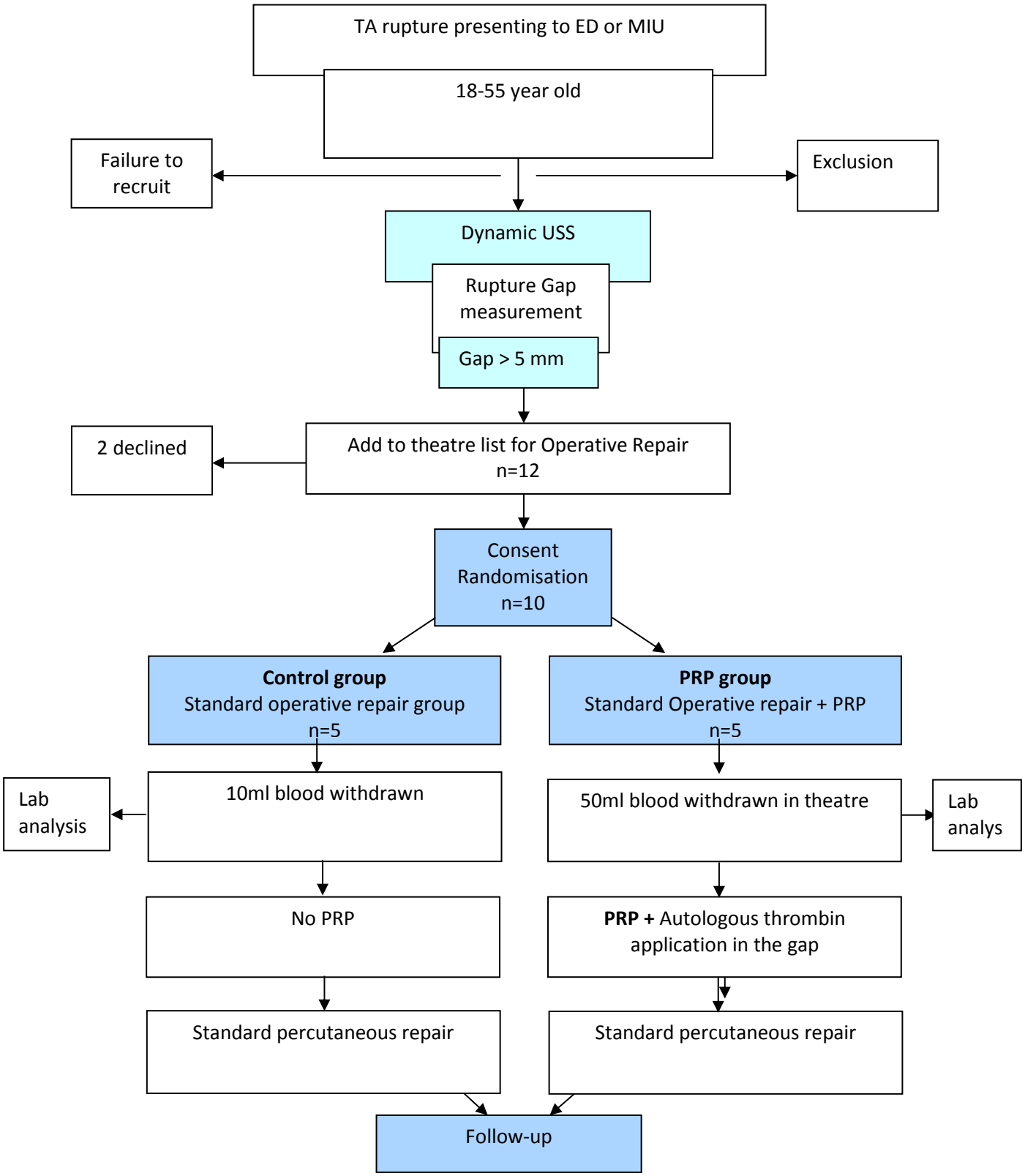


Figure 5 .3 Flow chart of the operative leg of the trial. All patients with rupture gap more than 5 mm were included and randomised to control and standard surgical repair or PRP and standard surgical repair. All patients followed the Oxford percutaneous repair rehabilitation protocol.

5.4.5.2 Trial Protocol

a) Potential participants with suspected Achilles tendon rupture were identified by staff in the emergency department and patient information sheet was given to them. (Appendix 5.1)

b) Patients had Dynamic USS of the affected leg by a musculoskeletal radiologist (appendix 5.2)

C) The current established Oxford Achilles Tendon Rupture protocol was followed (see appendix 5.2). Briefly, Dynamic USS is performed on all patients and the tendon gap area is marked while the foot in equinus. The size of the gap determined the treatment pathway. If the gap is > 5mm, operative repair was indicated, while tendons with gap <5mm received conservative treatment (101).

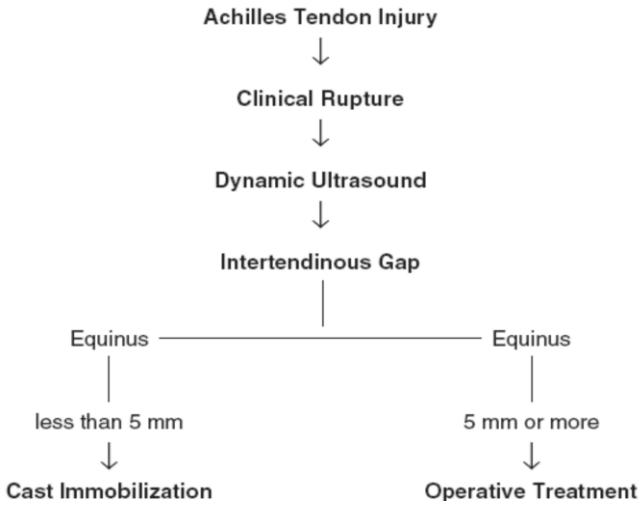


Figure 5 .4 The Oxford Achilles Tendon Rupture treatment selection pathway.

D) Patients were reviewed in the outpatient clinic immediately following the scan by the research fellow (JA). Patient's eligibility to participate in the trial was assessed using the aforementioned inclusion and exclusion criteria and patients were categorised to:

I. Eligible to participate and recruited to take part in the trial

II. Eligible to participate but fail to take part in the trial:

- Not interested in participating
- Does not live locally, so will be followed up outside the area
- Due to go away/abroad so cannot be followed up

III. Excluded: (see exclusion criteria)

E) Informed consent was obtained by the research fellow and documented in patients' medical notes and a copy was kept in the trial master file.

F) Patients were allocated to treatment pathway, blinded and followed trial procedures in each pathway as follow:

G) Conservative treatment

Tendons with a rupture gap ≤ 5 mm on Dynamic USS were treated conservatively. Participants were randomly assigned to intervention or control using computer generated concealed allocation. The groups were:

1. Control group: Standard immobilisation protocol group

A blood sample was taken for laboratory analysis (see appendix 4.1). The participant was placed prone on an examination couch in the clinic. The foot and ankle were placed slightly off the end of the couch. To assure blinding the patient to the treatment option, a curtain was drawn so patient was not able to see the procedure (Figure 5.5). The participant received an injection of subcutaneous local anaesthetic (2ml Lignocaine 1%) over the rupture site as a mock injection of the intervention. All participants in this group received standard immobilisation cast applied according to the established protocol (appendix 5.3: Sheffield regime Protocol for Achilles tendon rupture).

2. Treatment group: PRP injection and immobilisation protocol group

In this group; 52 ml of venous blood was withdrawn from participant's anti cubital fossa vein using large bore butterfly needle and a syringed primed with 8ml ACD-A anticoagulant. PRP is prepared within 20 min using Medtronic Magellan© Autologous Platelet Separator Device (figure 4.1). Autologous thrombin was generated as per manufacturer protocol (Chapter 4: PRP preparation). PRP and autologous thrombin were injected in the tendon gap using a dual syringe. All participants in this group received standard immobilisation cast according to the established protocol (appendix 5.4: Sheffield regime Protocol for Achilles tendon rupture).



Figure 5 .5 Patient blinding method. Patient is lying prone on examination couch with both legs of the end of the couch. The affected leg is placed in the foot and ankle device for comfort. The procedure is performed as described above. In this picture: the Zonare ultrasound system is visible and was used to capture elastography data (Chapter 3).

H) Operative treatment arm

Participants with Achilles tendon rupture gap > 5 mm on Dynamic USS were treated operatively. Participants were randomly assigned to intervention or control. Randomly generated and concealed allocation was assured via computer-generated randomisation system, using permuted blocks of random size. The randomisation groups were:

3. Control group: Standard TA percutaneous surgical repair group

This group had percutaneous surgical repair and cast immobilisation applied according to the established protocol (Appendix 5.3) and followed up in the outpatient clinic.

4. Treatment group: PRP application and percutaneous surgical repair group.

Blood was obtained prior to surgery. 52 ml of venous blood was drawn from participant's anti-cubital fossa vein using large bore butterfly needle and a syringe which was primed with 8ml ACD-A anticoagulant. PRP was prepared within 20 min using Medtronic Magellan© Autologous Platelet Separator Device in theatre (figure 4.1). Autologous thrombin was generated as per manufacturer protocol (Chapter 4: PRP preparation). PRP and autologous thrombin were mixed in a sterile pot to generate PRP clot (figure 5.6). The tendon was repaired using percutaneous technique as described by Webb et al and recently modified by Carmont et al (104, 321) (figure 5.6).The PRP clot was applied in the tendon gap and the paratenon was sutured over it using absorbable suture. Skin was sutured using 3'0 Monocryl and steristrips. The wound was covered with non-adherent dressing and Cast immobilisation was applied according to the established protocol (appendix 5.4).

During the operative repair, tendon trimmings from the ruptured area were placed in sterile DMEM-F12 medium. The tissues were used in the tissue and cell *in vitro* studies (Chapter 7).

I) All groups followed standardised rehabilitation protocol (appendix 5.3 and 5.4). The conservative treatment patients followed the Oxford modified Sheffield regiment as detailed in appendix 5.3. The operative treatment participants followed the Oxford percutaneous Achilles tendon repair rehabilitation protocol as detailed in appendix 5.4.

J) Follow up assessments were carried out at baseline and 1, 3, 6, 8, 12 and 24 weeks post treatment using the following outcome measures:

- ATRS (Achilles Tendon Total Rupture Score): appendix 5.5
- VISA-A (Victorian Institute for Sport Assessments- Achilles) score: Appendix 5.6
- FAOS-UK (Foot and Ankle Outcome Score): Appendix 5.7
- Functional UltraSound Elastography (FUSE): Appendix 5.8
- Maximal heel raise at 6months
- Maximum ROM at 6 months
- Time to return to normal activities
- calf girth ratio
- SF-36 questionnaire (Appendix 5.9)

5.4.6 Interventions

5.4.6.1 Conservative control mock procedure

The participant was placed prone on an examination couch as shown in Figure 5.5. 1ml of 1% Lignocaine local anaesthetic was injected to the skin in the conservative control arm. The injection was over the rupture gap area and caution was taken not to penetrate deeper than the subcutaneous tissues. The mock PRP injection procedure was carried out to make sure that patient remained blinded to treatment allocation. The area was covered with dressing and leg was placed in cast as per protocol.

5.4.6.2 PRP injection in conservative arm

PRP and autologous thrombin were mounted in a dual syringe applicator. Local anaesthetic injection was used to anaesthetise the skin over the tendon rupture gap. A small scalpel was used to make small 2mm incision in the skin. The dual applicator was introduced to the tendon rupture gap and 3 ml of PRP was injected in the rupture gap. The area was covered with dressing and leg was placed in cast as per protocol.

5.4.6.3 Percutaneous Achilles tendon Repair

The torn Achilles tendon was repaired using modified Webb suture technique under local anaesthetics. In brief, patient is positioned prone on theatre table and tourniquet is applied at mid-calf and kept deflated unless required. Preparation to the skin was performed using non-alcoholic iodine solution. 20ml of 1% Lignocaine was injected around the planned skin incisions and deeper tissues including the tendon (figure 5.6). Stab incisions to the skin were performed proximal and distal to the rupture. At rupture site a transverse 2 cm incision was made slightly medial to avoid damaging the sural nerve. The incision was deepened to the paratenon and the ruptured tendon ends were exposed to obtain tissue trimming from the ruptured tendon. The suture was passed proximally and distally as per Carmont at al technique (321). In the PRP group; 3ml of PRP clot was placed in the tendon gap and the suture was tightened with foot in equinus to approximate the

tendon ends. The paratenon was closed over the repair with absorbable suture. The stab incisions were closed with steristreps and covered with mepore dressing. The foot and ankle were placed in equinus plaster of Paris backslab (figure 5.6). Patients were discharged home the same day with follow up appointments as above.



Figure 5 .6 Percutaneous surgical TA repair. A: Local anaesthetic injection in the skin and tendon. The middle skin mark is the location of the rupture gap as identified using dynamic ultrasound scan. B: skin incisions are made slightly medially to mid line to avoid the sural nerve. C: The tendon ends were delivered through the middle transverse incision to obtain tissue samples. D: Webb suture is passed proximally using Maffulli technique. E: the suture in place ready to be tightened. F: in PRP group, PRP clot was applied in the tendon gap before tightening the suture in G. H: the incisions following closure with Monocryl. I: The incisions at 1 week follow up.

5.4.7 PRP Preparation Technique

In conservative arm, PRP was prepared in the outpatient fracture clinic. In the operative arm, blood was obtained in the anaesthetic room and PRP was prepared in the operating theatre. PRP was prepared using the technique described in chapter 4, whole blood collection and PRP preparation technique and appendix 4.1 (figure 4.6). In conservative treatment participants, PRP and autologous thrombin were injected in the tendon simultaneously using the dual applicator. In the operative arm, PRP was mixed with thrombin in a sterile pot to form a clot that was applied in the tendon rupture gap during repair.

5.4.8 Follow-up assessments

Each participant was assessed in the outpatient clinic at baseline and 1, 3, 6, 8, 12 weeks and 24weeks. These are key points in the rehabilitation pathway. During each visit the following assessments was carried out:

- Baseline: ATRS, VISA-A, FAOS, SF-36, and Functional US Elastography scan
- Week 1: wound review, ATRS, VISA-A, FAOS, Functional US Elastography scan.
- Week 3: wound review, ATRS, VISA-A, FAOS, Functional US Elastography scan.
- Week 6: wound review, ATRS, VISA-A, FAOS, Functional US Elastography scan and ROM
- Weeks 8: ATRS, VISA-A, FAOS, Functional US Elastography scan and ROM
- Week 12: ATRS, VISA-A, FAOS, Functional US Elastography scan and ROM
- Week 24: ATRS, VISA-A, FAOS, Functional US Elastography, ROM, Maximum Heel raise, and SF-36.

In addition, calf girth in both legs was recorded at each follow-up in all groups. Participants' compliance with the established rehabilitation protocol is checked and advice for the next step was given (see appendix 5.3 and 5.4). Time to return to normal activity was checked at each visit and recorded accordingly. All serious, suspected and unexpected adverse events were documented and reported to the ethics committee.

5.4.9 Statistical Analysis

5.4.9.1 Descriptive Statistics

Participants' demographics and rupture characteristics were reported for all patients. Descriptive statistics (number of patients, means and standard deviation) were reported for each treatment group, within the operative and non-operative arm for the primary and secondary outcome measures at baseline and at each follow-up time point. Statistical analysis was performed using SPSS PASW version 18.0 statistical package. Graphs were generated using Graphpad Prism version 5.03. The significance level was chosen at 0.05 for all statistical tests.

5.4.9.2 Primary Outcome (ATRS) Analysis

This was a longitudinal study; patients were assessed repeatedly over time. Although it would be possible to compare the treatment groups at each time point, there is a risk of reaching significant difference between groups by chance due to multiple testing. A better approach is that of linear mixed models. This method is particularly useful when there are missing observations either due to a missed visit or a patient leaving the study. They can be used when patients are not all assessed at exactly the same time point as the exact time for each observation is used in the analysis. All available data are used in the analysis. The change in ATRS is calculated for each individual with an intercept and gradient (the rate of change with time). Adjustment for baseline characteristics is achieved by adding these to the model.

5.4.9.3 Time to return to normal activities analysis

The time to return to normal activities measured from the time the injury occurred was analysed using Mann-Whitney U test was used to compare the difference between PRP and control groups means.

5.5 Results

20 patients (10 in each pathway) were recruited in total to this pilot trial with mean age 39.6 ± 7.95 (11 males and 9 females). 10 in the operative treatment group were randomised to receive PRP (5 patients) or control (5 Patients). On the conservative side 5 patients received PRP and 5 had control injection. Description of the recruited patients is displayed in table 5.1.

Table 5.1: Patients' recruitment summary

	Operative arm	**Conservative arm**
Screened	12	11
Declined	1 (lives too far to attend f/u)	0
Ineligible	1 (Diabetes) 1 (> 2 weeks injury)	1 (neglected injury)
Recruited	10	10
PRP group	5	5
Control group	5	5
Age (mean ± SD)	37.5 ± 8.8	41.7±7.1
Sex	5 males 5 females	6 males 4 females
Average Rerupture gap measurment	12.4mm	3.2mm
Rupture location	4.8cm	4.1cm
SAE	1 DVT (control)	1 partial-rerupture (control)

18 patients (90%) sustained the injury whilst involved in recreational sport activities. 6 were sustained during football, 5 squash, 2 volleyball, 2 tennis, 1 netball, 1 running, 1 jumping. Two patients (10%) sustained the injury in non-sport activity. One when jumping from the back of a lorry at work and the other when climbing stairs.

All patients reported nearly the same symptoms: “sharp pain at the back of the heel as if someone kicked me”. Patients were unable to weight bear on the injured leg and described bruising and swelling around the area. No patient reported any previous symptoms at the Achilles tendon area.

Patients were seen in the Emergency department and provided with Plaster of Paris (POP) backslab in equinus. All patients had dynamic ultrasound scan to confirm the diagnosis and decide the treatment pathway before they were recruited in the trial. The mean rupture location was 4.8cm from the tendon insertion at the calcaneum. All tendons appeared thickened with mean thickness of 16mm measured at the rupture site. The paratenon appeared thickened and plantaris tendon was reported intact in all 20 patients. Measuring the tendon gap in equinus revealed an average gap of 12.4mm in operatively treated patients and 3.2mm in the conservatively treated patients. Functional ultrasound elastography finding at baseline is reported in Chapter 3.

5.5.1 ATRS

The results of the linear regression analysis of the primary outcome measure ATRS is displayed in figure 5.7. The analysis of the 20 participants data revealed that PRP group had significantly better ATRS score progression as evident by the liner regression slope elevation from week 3 till week 24 ($P < 0.00510$). This analysis included both operative and non-operative patients because the outcome at this stage has been reported to be similar (114). Further analysis of each treatment pathway is shown in figure 5.8.

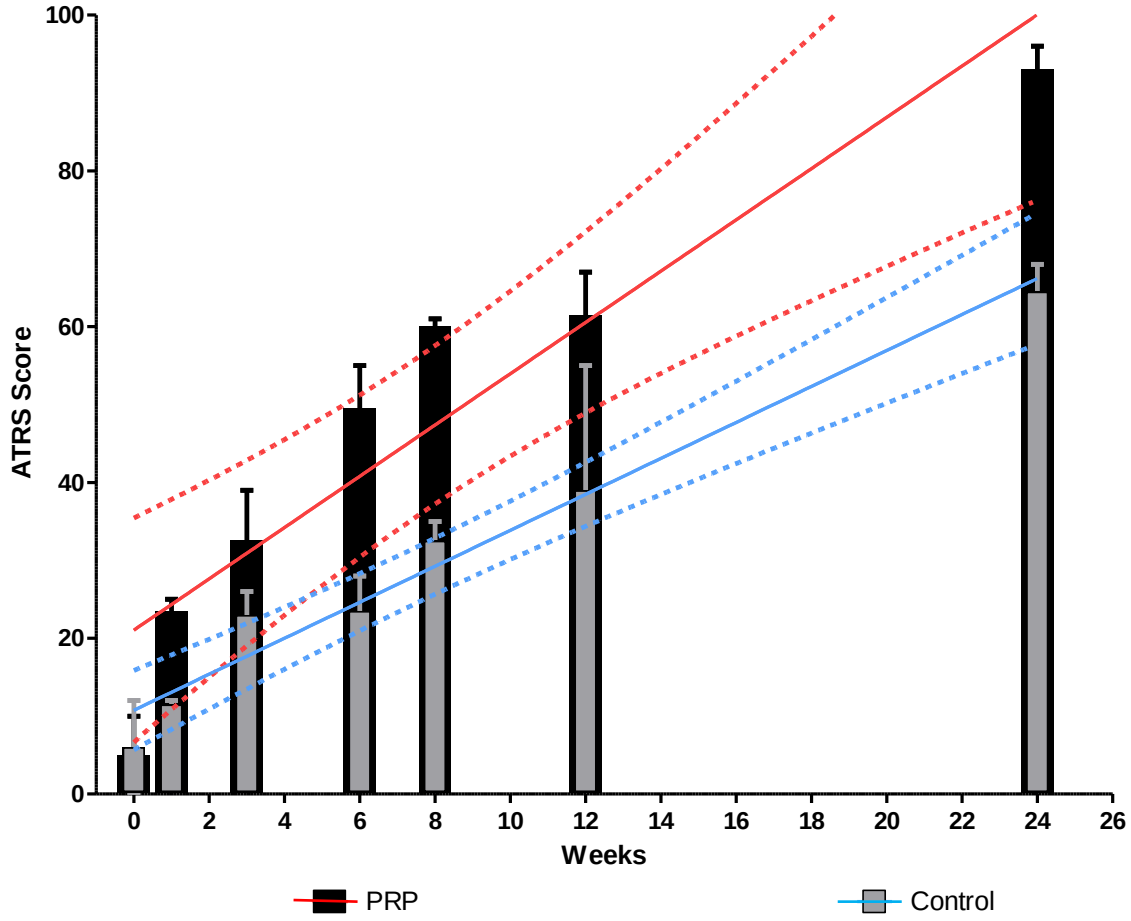


Figure 5 .7 ATRS linear regression analysis for all treatment pathways. R square value for each linear slope is 0.9196 for PRP and 0.9375 for the control group. The slopes are significantly different (P 0.049). The elevations of the two slopes are significantly different (p 0.0051). The dotted lines show the 95% confidence intervals.

The analysis of ATRS in the operative group (n =10) is shown in figure 5.8 (left). This reveals there is no difference between PRP and control group (PRP line R^2 is 0.833, Control line R^2 is 0.819, slope P value 0.891 and elevation p value 0.137).

The analysis of ATRS in the conservative treatment pathway (n = 10) is shown in figure 5.8 (right). This reveals there is significant difference between PRP and control group (PRP line R^2 is 0.7292, Control line R^2 is 0.8317, slope P value 0.05 and elevation p value 0.0006). PRP group had better outcome starting from week 6 in this group.

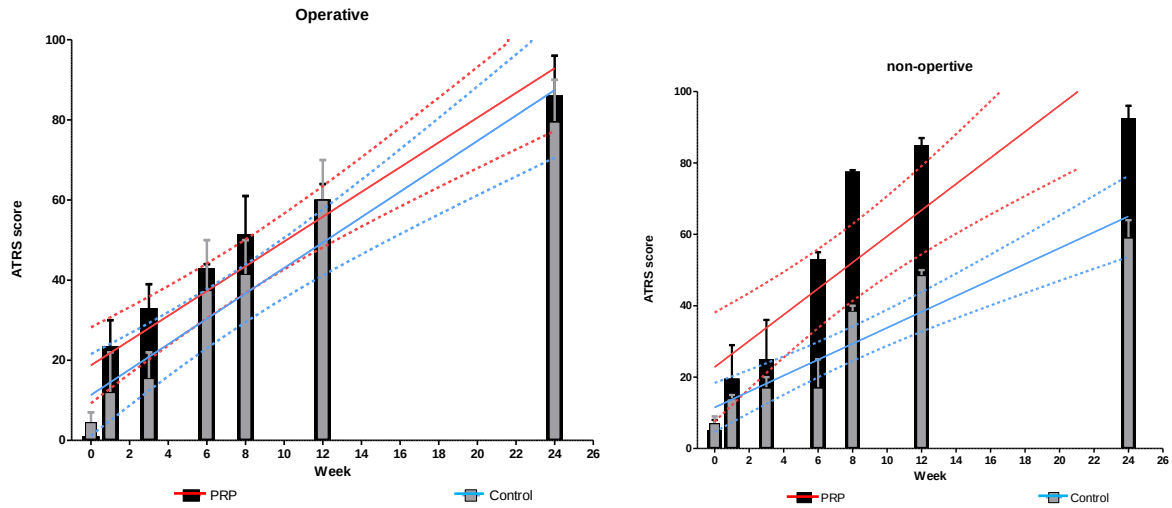


Figure 5 .8 ATRS linear regression analysis for operative treatment pathway (left). R square value for each linear slope is 0.833 for PRP and 0.0.819 for the control group. The slopes are not significantly different (P 0.891). (right) ATRS linear regression analysis for conservative treatment pathway. The lines are significantly different in terms of slope (p 0.05) and elevation (p 0.0006). The dotted lines show the 95% confidence intervals.

5.5.2 VISA-A

The results of the linear regression analysis of the secondary outcome measure VISA-A score for operative and conservative treatment pathways (n=20) is displayed in figure 5.9. The analysis revealed that PRP group had significantly better VISA-A score progression as evident by the regression line slope and elevation (P 0.045). Further analysis of each treatment pathway is shown in figure 5.10.

Further analysis of the operative and conservative treatment pathways is displayed in figure 5.10. The analysis of VISA-A outcome measure in the operative treatment pathway (n =10) revealed that there is no difference between PRP and control group (PRP line R^2 is 0.0772, Control line R^2 is 0.823, slope P value 0.818 and elevation p value 0.106).

In the conservative treatment patients, the linear regression analysis conformed that PRP group progression was significantly better than control group (R PRP line R^2 is 0.75, Control line R^2 is 0.697, p = 0.0278). In these patients, the positive effect of PRP started to differ from week 6 onwards as shown in the diagram. The progression of VISA-A score throughout the 24 weeks follow up resembles that of ATRS score progression. The critical time for remarkable improvement seems to

start on week 6 and thereafter, this may be explained by the fact that the cast is removed at this time according to the rehabilitation protocol. This allows patients to start moving and notice the improvement in healing.

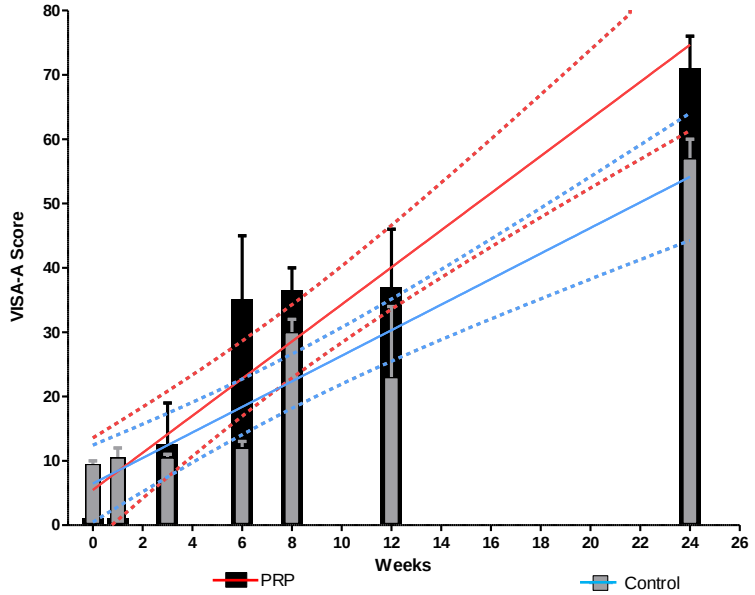


Figure 5 .9 VISA-A linear regression analysis. R2 is 0.8566 and 0.838 for PRP and control groups respectively. The overall slopes are significantly different (p 0.045). The dotted lines are the 95% confidence intervals.

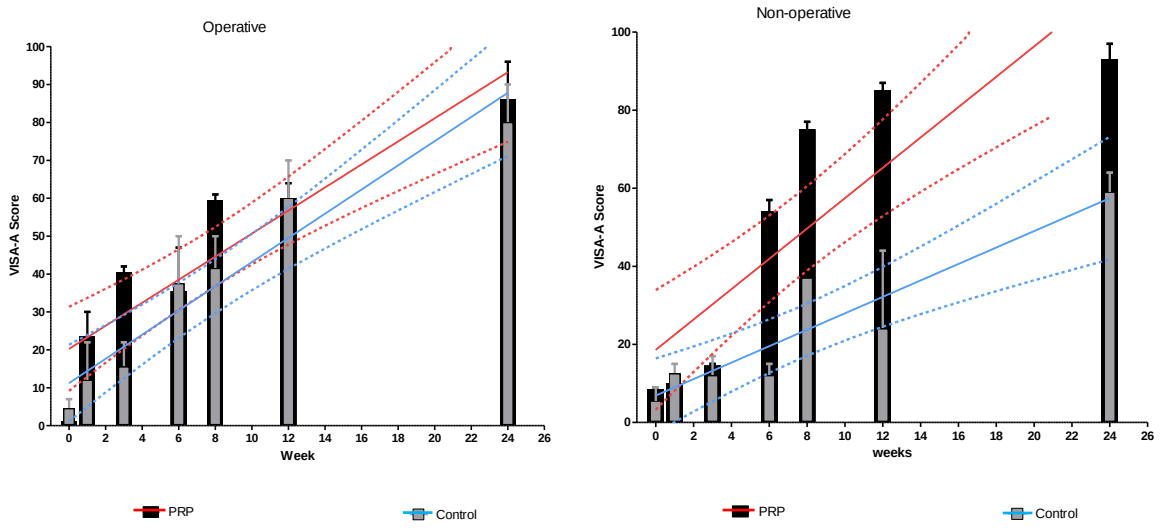


Figure 5 .10 Shows the analysis of VISA-A progression in the operative treatment pathway (left). There is no difference between PRP and control groups (p 0.818). (Right): Linear regression analysis of VISA-A score in the conservative treatment pathway. The two lines are significantly different in slope and elevation (P 0.0278).

5.5.3 Foot and Ankle Outcome Score (FAOS)

This is a patient-reported outcome scale developed for variety of foot and ankle-related problems (319). FAOS consists of 5 subscales: Pain, Symptoms, Activities of Daily Living (ADL), Sport and foot and ankle related quality of life (QoL). Each of the subscales is analysed and presented separately in this section.

5.5.3.1 FAOS –Pain

Linear regression analysis of FAOS pain score showed significant difference between the two groups progression during the 24-week follow up period (p 0.004). The score between the two groups started to differ from week 3 onwards. Further analysis of the conservative and operative pathways did not reveal any significance between PRP treated patients and controls (p 0.20 and 0.54 respectively).

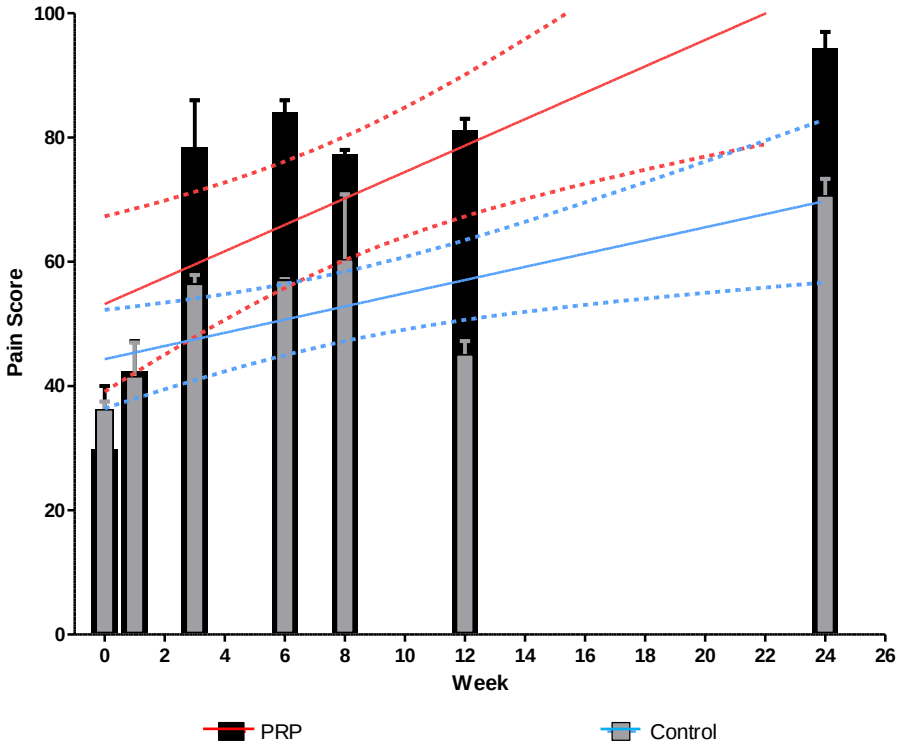


Figure 5 .11 The analysis of FOAS- Pain score. The two lines are significantly different (PRP group R^2 is 0.515, Control group R^2 is 0.456, p 0.004).

5.5.3.2 FAOS- ADL

Analysis of FAOS-ADL sub score showed no significant difference between the PRP and control groups progression during the 24-week follow up (p 0.20). Further analysis of the conservative and operative pathways did not reveal any significance between PRP treated patients and controls (p 0.640 and 0.079 respectively).

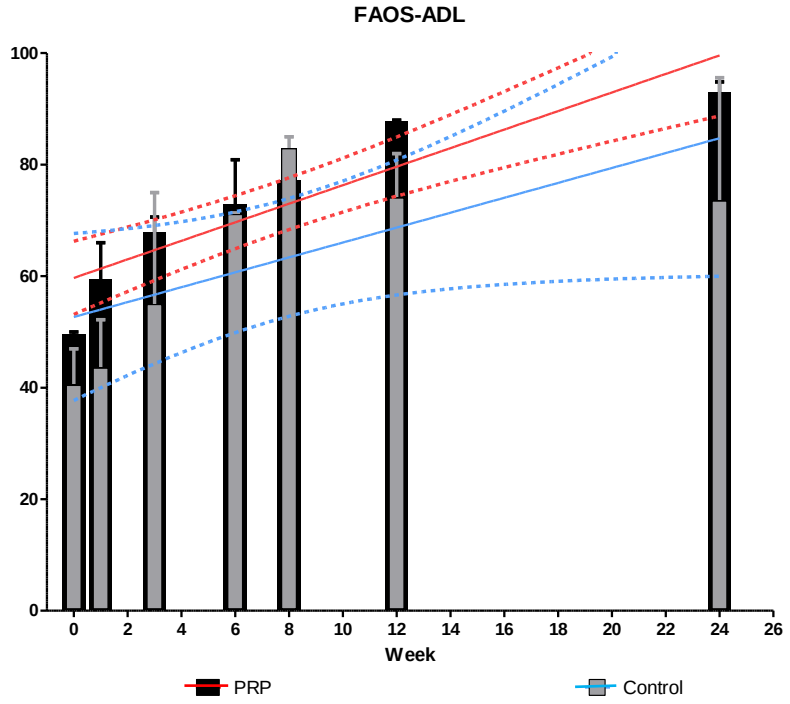


Figure 5 .12 The analysis of FOAS- ADL score (PRP group R2 is 0.75, Control group R2 is 0.272, p 0.2).

5.5.4 FAOS – Sport

Analysis of FAOS-Sport sub score showed no significant difference between the PRP and control groups progression during the 24-week follow up (p 0.991) (figure 5.13). Further analysis of the conservative and operative pathways did not reveal any significance between PRP treated patients and controls (p 0.20 and 0.971 respectively).

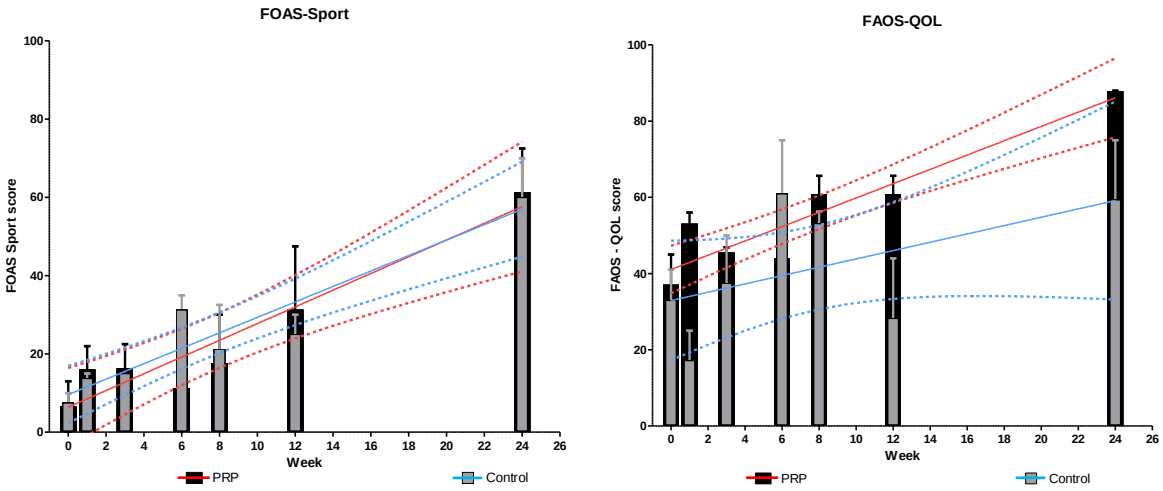


Figure 5 .13 The analysis of FAOS- sport score (PRP group R2 is 1.519 x10-21, Control group R2 is 6.374 x10-019) (left). The two lines are almost identical. Right: Quality of Life FAOS subscore analysis (PRP group R2 is 0.808, Control group R2 is 0.185). The slopes of the two lines are not different (p 0.281). However the elevation of the PRP line is significantly higher than Control (p 0.0161).

5.5.5 FAOS- QOL

The quality of life sub score analysis revealed that there is no difference between the PRP and control lines slope (figure 5.13: right). However there was significant difference with line elevation that may suggest that PRP improved the outcome and sustained it throughout the follow up period. The confidence interval however interacts widely between the two lines as a reflection of the small sample size in this pilot trial. Further analysis of PRP versus Control groups in the operative and conservative treatment pathways did not reveal statistically significant difference (P 0.917 and 0.977 respectively.

5.5.6 Functional Ultrasound Elastography

The proof of concept and trial of validity of the FUSE technique was discussed in Chapter 3. The application of this technique in Achilles tendon rupture patients and procedures to protect the healing tendon was also discussed in the Chapter 3.

5.5.6.1 Ultrasound Images

Grey scale B-mode images were of a consistent and of good quality with the tendon, fat, muscles, ruptured area and other tear features usually very clearly visible. The ruptured gap was identified at presentation by using dynamic ultrasound scanning technique (appendix 3.1). The typical features of ruptured tendon included: swelling of the tendon, intratendon haematoma, paradoxical movement of tendon ends, fibre arrangement disruption and gap between the ruptured tendon ends (figure 5.14). B-mode images at each follow-up showed the progression of the healing tissue from fluid haematoma at week 0 to organised tendon fibres at week 24. All patients showed satisfactory progression in tendon healing although this was not quantified at each visit due to the lack of validated scoring system. The tendon was considered healed when the tendon fibres moved uniformly during plantar and dorsi-flexion of the ankle. There was reduction in the thickness of the tendon and restoration of fibre arrangement.

In the conservative cases there was a shadow caused by the blood clot at initial presentation and this gradually disappeared to allow better visualisation of the deeper structures at week 1 onwards. In operative cases there were significant shadows caused by the knot of surgical suture. The sutures themselves were identifiable as bright speckles in the proximal and the distal tendon ends (figure 5.14). In a few cases (<1%) there was poor contact with the skin or obvious large amounts of de-correlation of the speckle pattern. In cases where this caused artefacts in the displacement and strain images, the analysis was discarded.

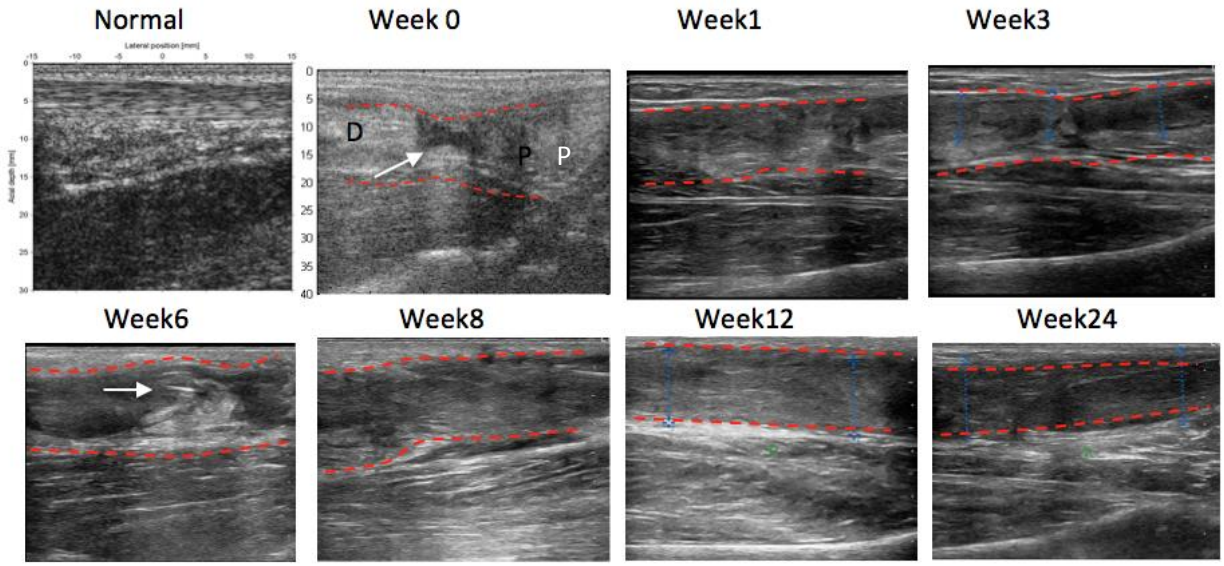


Figure 5 .14 Example of B-mode longitudinal images output for ruptured Achilles tendon throughout the follow-up period between rupture diagnosis at week 0 to final scan at week 24. Normal: is a scan of the same area in the normal tendon of the contralateral side. The tendon is between 5-8mm in thickness and located under the subcutaneous tissues. The tendon fibres appear well organised and move uniformly during foot plantar or dorsal flexion. Week 0: the Achilles tendon outlines are marked with dashed red line. The tendon rupture gap is visible as dark area in the middle of the tendon (white arrow). The proximal (P) and distal (D) ends of the ruptured tendon move paradoxically during dynamic scanning. Week 1-24: Show the appearance of the healing tendon at each follow up appointment. Tendon swelling gradually reduces and tendon callus appears at week 6 as hyper-echoic areas at the site of the rupture gap (white arrow). The repair suture is also visible as high-density white line. Tendon fibres gradually replace the callus and the tendon appearance normalises gradually between week 8 and week 24. The tendon remains thicker and lacks the highly organised tendon fibre appearance when compared to the normal tendon.

5.5.6.2 Real-time Elastography

The Zonare Real-time elastography imaging using manual compression-decompression method according to manufacturer recommendation did not show any relationship with clinical appearance. The tendon and surrounding structures strain images were indistinguishable in most cases. The images were mainly blue-green colour of all the anatomical structures in the area: tendons, fat pad, muscles and bone. This method failed to pick up the acute tendon rupture changes at presentation, although the rupture gap and the haematoma represent the most severe changes in the mechanical properties of the tissue (figure 5.15). Subsequently, there was no change in strain imaging during follow-up. The may be explained by the fact that real-time elastography algorithm was not specifically developed for musculoskeletal application.

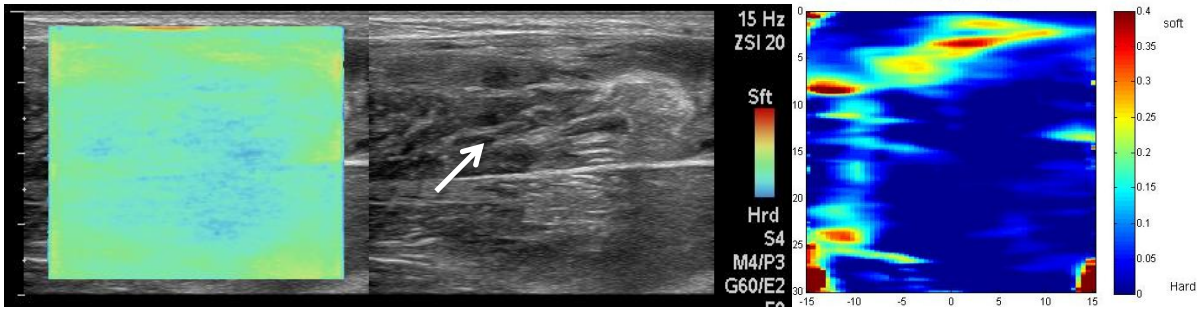


Figure 5 .15 (left) Zonare real-time elastography scanning of a PATH trial patient at the time of acute diagnosis (week 0), superimposed over the B-mode image. The rupture gap and haematoma do not show different strain colour. (middle) B-mode grey scale image of the ruptured tendon shows the rupture (arrow).. Right: Functional UltraSound Elstography (FUSE) image using the algorithm in chapter 3. The haematoma and rupture gap is visible as very soft red and yellow area.

5.5.6.3 Functional Ultrasound Elastography Results

The various techniques of functional elastography were discussed in chapter 3. Examples of FUSE images of the healing tendon progression throughout the follow up period are displayed in figure 5.16. Manual compression-decompression method did not show any relationship with clinical scores. The images resulting of this technique showed poor strain mapping of the different structures in the area (figure 5.15). While functional elastography in dorsal and plantar motion (DF and PF) showed good imaging of strain in the affected area at acute presentation and during the follow-up scans. The ability to measure average strain over the affected area of the tendon allowed us to monitor the progression of healing tissue strain during follow-up.

For each motion type the average strain was plotted over time as shown in figure 5.17. This was visually compared with clinical outcome measures. PF motion showed no real correlation, but the average scores of the DF fit much better. DF Lateral motion results showed a good general trend match of mean patient group strain values (Fig. 5.17) to the mean of the inverse of the ATRS and VISA-A clinical scores for all patients.

The computer controlled lateral motions in DF also had substantially lower variation between repeat measurements of the same patient at the same week and lower patient to patient variability as measured by the R^2 value when fitted to an exponential healing model.

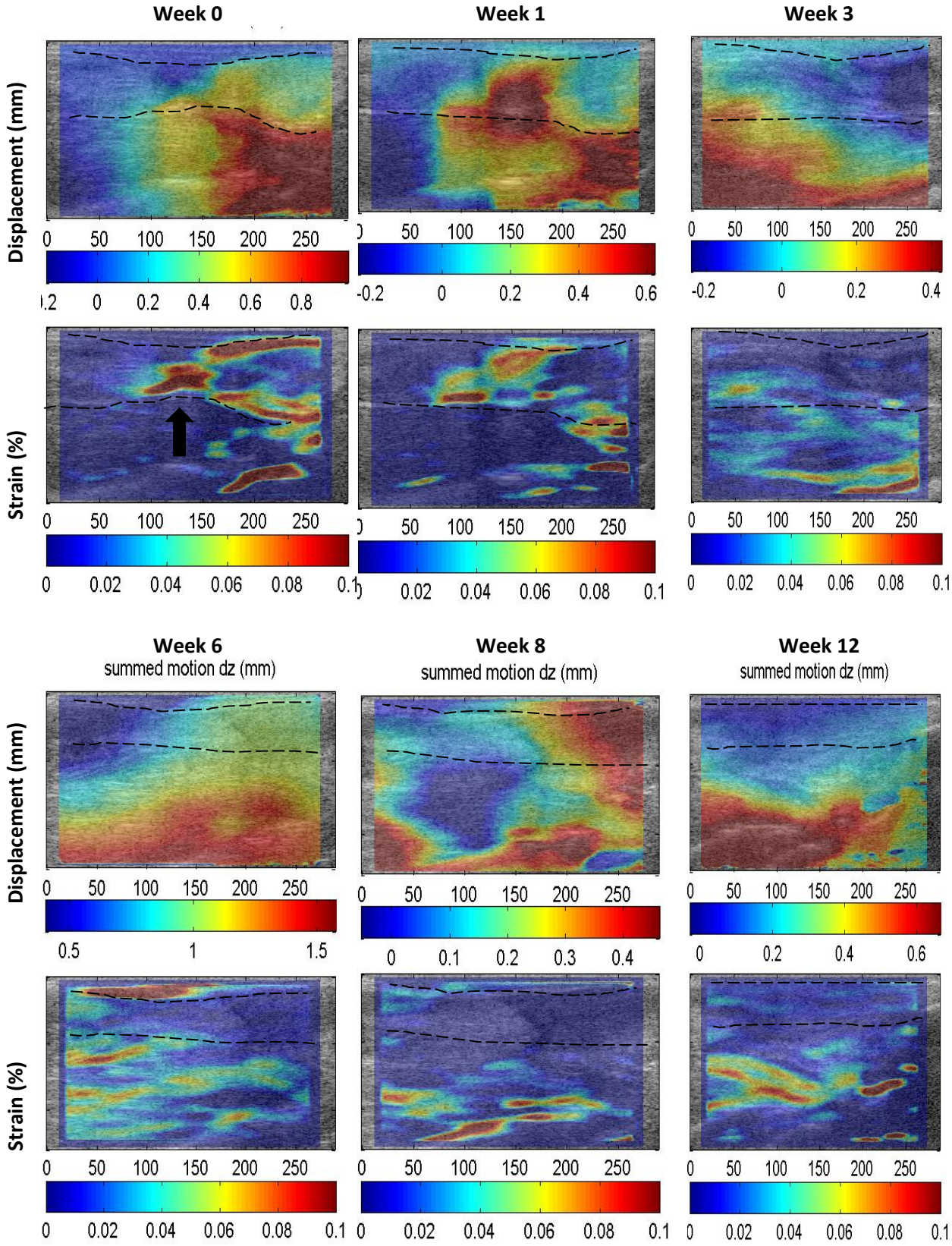


Figure 5 .16 The progression of the ruptured tendon from acute presentation at week0 to healing at week 12. Displacement images is displayed in mm while strain image scale is in %. The dotted lines represent tendon borders. At week 0, white arrow shows the ruptured gap, which corresponds with paradoxical movement of the tendon in the displacement image. As the tendon heals, displacement becomes more uniform and the tendon becomes harder (blue).

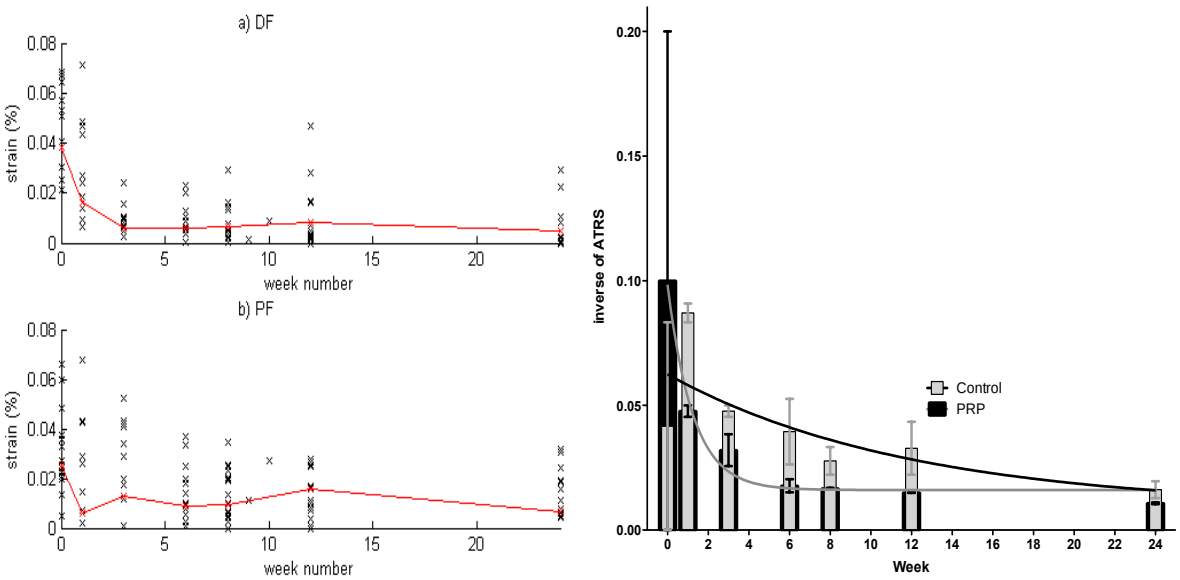


Figure 5 .17 The results of elastography strain compared to clinical outcome. Left a) the average strain of all patients. Left a): Dorsal Flexion average strain plotted for all patients over treatment period. The red line shows the mean. Left b): Plantar Flexion average strain plotted for all patients over treatment period. Right: Average patient 1/ATRS scores. (ATRS is a score of positive ability; so 1/ ATRS is presented here to show similarity to strain pattern).(322)

Strain Index

The strain index of Achilles tendon was introduced in chapter 3 and it makes use of the fat pad average strain to normalize the average strain measurement of the tendon. The fat pad strain is assumed to stay the same during the healing period, while the tendon injured area start as soft haematoma and gradually becomes stiffer tendon tissues as the tendon goes through the healing phases to restore its normal function and structure. This index allows the monitoring of the change in the healing tendon average strain during the healing phase. The fat pad is normally softer than the tendon therefore the index is small, while in injured tendon the presence of haematoma and oedema makes the tendon softer and the strain index higher. The index gradually decreases to reach normal values prior to injury as the tendon heals. The acutely ruptured tendon average strain was high in both longitudinal and axial components (ε_x 4% and ε_y 5.79%). The fat-pad average strain remained approximately the same as in normal tendons (ε_x 9.6% and ε_y 6.2%) (figure 5.17). The index progression at follow-up was analysed using regression analysis, which showed better normalization of the index in the PRP group from week 8 onwards (PRP R^2 = 0.569, Control R^2 = 0.5125, PRP F=15.8, control F = 12.62, overall P= 0.589 and from week 8 onwards p =0.0313).

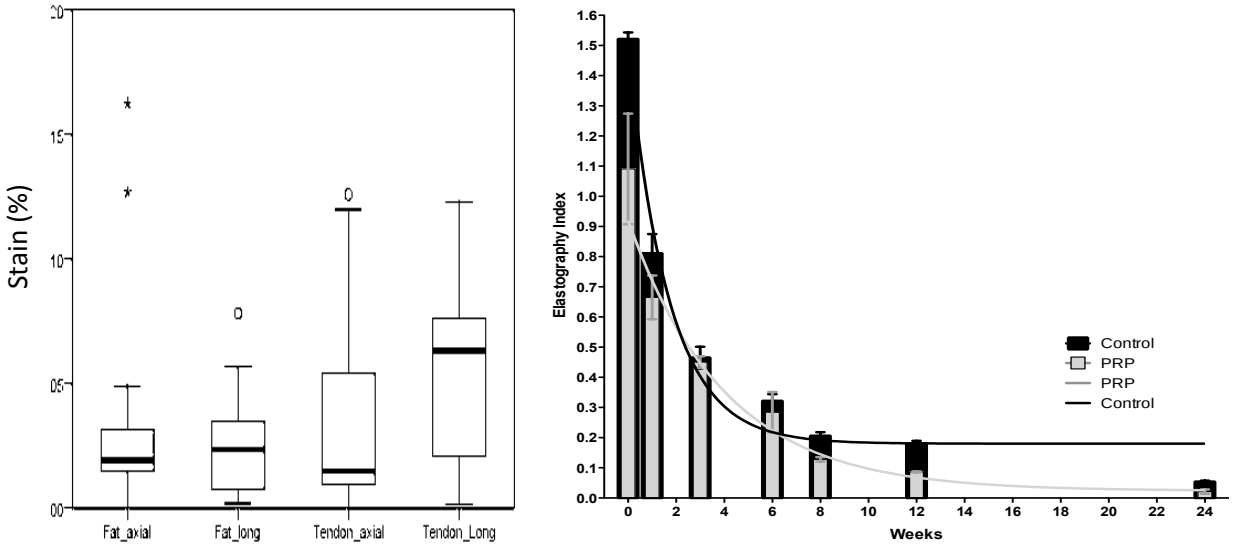


Figure 5 .18 Average strain measurement using FUSE algorithm and Elastography index progression throughout tendon healing. Left: average strain measurements at diagnosis. The tendon shows significantly higher strain than the fat pad. Right: the strain index plotted over the follow up weeks. There is decrease in the index in both PRP and control (no-PRP) groups. The PRP group showed better progression of the index from week 8 onwards.

5.5.7 Maximum Heel Raise at 6 months

The maximum heel-raise was measured as percentage of the maximum heel-raise on the affected side over the maximum heel-raise on the normal side. PRP group average heel raise was 88.73% ± 10.29 and control group (no-PRP) average was 85.45%±9.08 (figure 5.19). Mann-Whitney U test analysis showed no significant difference between PRP and control at 24 weeks follow-up (Mann-Whitney U 36.50, Sum of ranks 118.5 and 91.5, P value 0.325).

5.5.8 Time to return to Work and sport

The number of days to return to work was compared between the two groups. The results are shown in figure 5.19. The average number of days in the PRP group was 54.4±49.9 days while in the control group it was 72.8±48. 3 days. Mann-Whitney U test showed no difference between the two groups (Mann-Whitney U 31.5, Sum of ranks 86.5 and 123.5, P value 0.173). The majority of patients in both groups were sedentary workers who were able to return to work on part-time basis shortly. Few patients in both groups were manual workers and needed long time to return to work. One patient in each group had not returned to work at the time of final follow up.

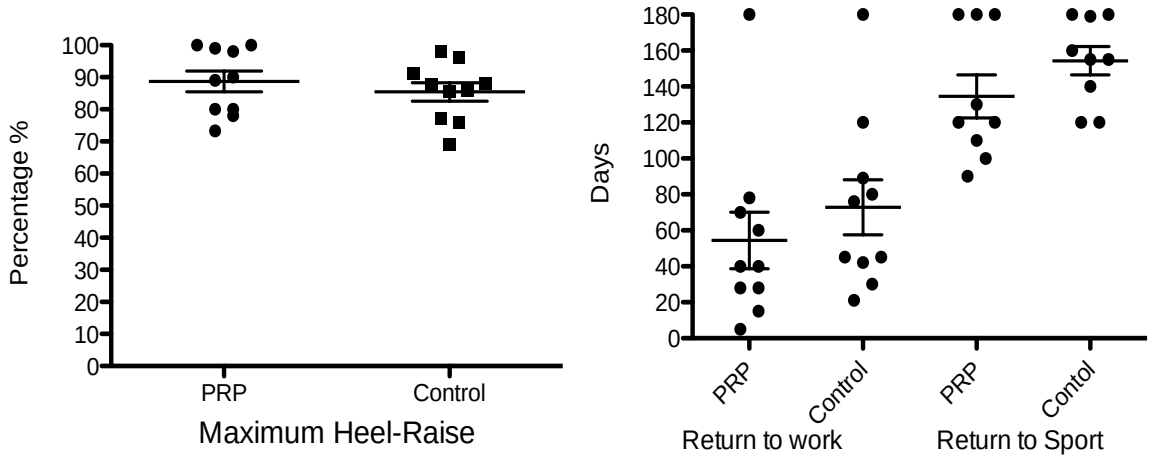


Figure 5 .19 The results of Maximum heel-raise test in PRP and control groups (left). There was no difference between the two groups. Right: The results of Return to work and return to sport analysis.

5.5.9 Calf Girth ratio

The calf girth ratio was measured to assess calf muscle atrophy in the affected leg during treatment. The results are shown in figure 5.20. In both groups the muscles on the injured side lost volume gradually over the period of immobilisation. Muscle atrophy was at its worse in week 8. The muscles gradually recovered after starting mobilisation and nearly returned to their volume prior to injury at week 24. Linear regression analysis revealed significant difference between the PRP and control (PRP R^2 0.045, control R^2 0508, F= 6.97, P value 0.014).

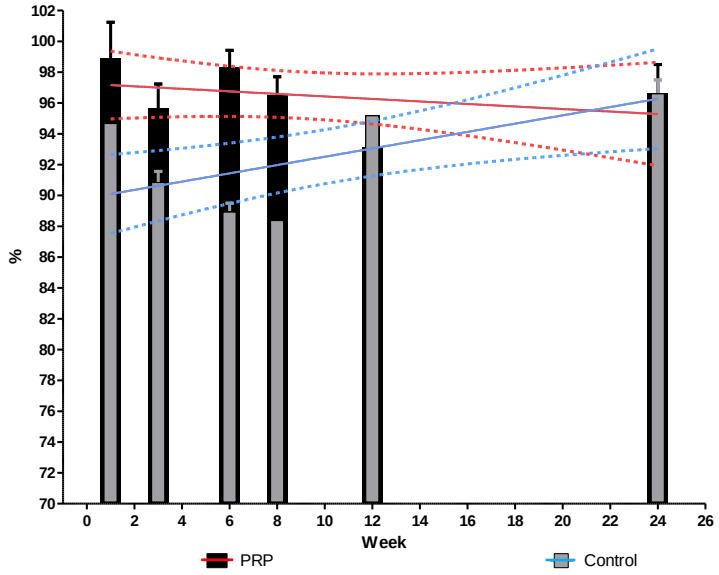


Figure 5 .20 Calf girth ratio analysis. The curved lines show the trend over the follow up period. The dashed lines represent linear regression analysis.

5.5.10 SF-36

SF-36™ is a generic health survey that asks 36 questions to measure functional health and well-being from the patient's point of view. The survey scans eight health domains (Physical Functioning, Role-Physical, Bodily Pain, General Health, Vitality, Social Functioning, Role-Emotional and Mental Health) and provides psychometrically-based physical component summary (PCS) and mental component summary (MCS) scores. Scores are calibrated so that 50 (with standard deviation of 10) is the average score or norm. PCS and MCS are the most useful SF-36 scores (323), therefore they are used in this study.

In the current study, SF-36 PCS statistical analysis using ANOVA test revealed no significant difference between the groups at baseline (PRP mean 31.74 ±7.3, Control mean 29.12 ± 12.47, P value 0.307) and at final follow-up in week 24 (PRP mean 45.24 ±6.4, Control mean 44.28 ± 5.9, P 0.596). However, there was significant improvement of both groups at week 24 when compared with week 0 (P value 0.001). The average was below the norm at week 0 and it rose to become within the normal range of SF-36 PCS score at week 24 (figure 5.21).

SF-36 MCS scores analysis using ANOVA test showed no significant difference between PRP and control at baseline (PRP mean 63.3 ± 6.39, Control mean 60.08 ± 4.8, P value 0.92) and at final follow-up (PRP mean 59.1 ± 5.88, Control mean 60.14 ± 6.7, P value 0.436). In addition, there was no difference between the baseline and week 24 scores for both PRP and control ($P > 0.05$) (figure 5.20). The mental health score in this group of patients remained within the norm regardless of the treatment pathway or the trial intervention at baseline and at final follow-up. This may be a reflection of the Achilles tendon patients who are usually fit and healthy and sustain the injury during sport activity. The sample size in this pilot trial is small and a larger sample is required to confirm these findings.

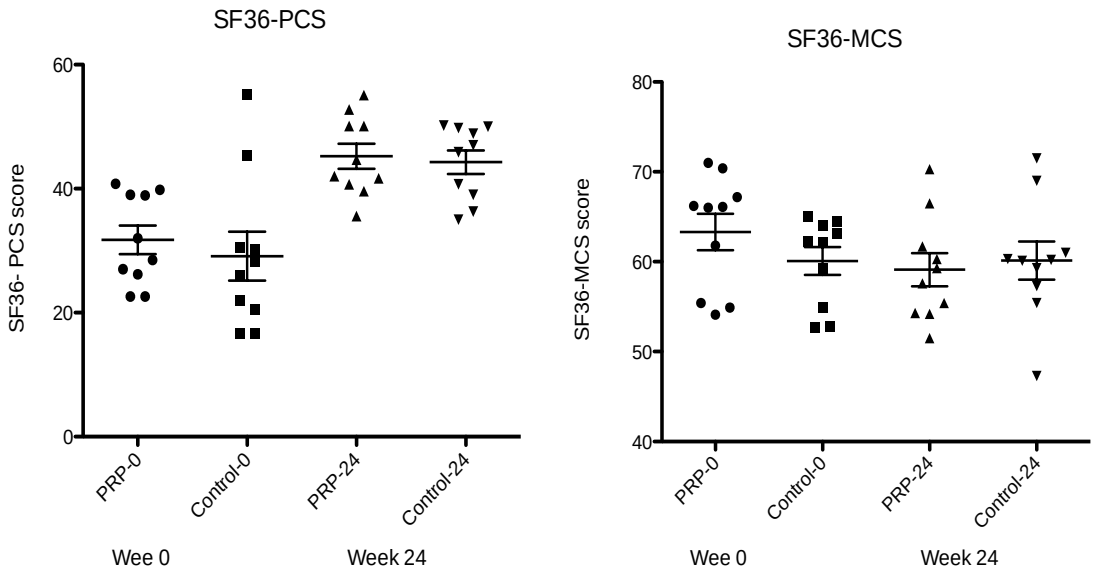


Figure 5 .21 SF-36 scores plot at baseline and at 24 week follow up. Left) PCS component of SF-36 scores plot for baseline and final follow up at week 24. No difference between groups at baseline or week 24. There is significant improvement of the score for both groups at final follow up when compared to baseline. Right) MSC component of SF36 Score. It shows o difference between groups at baseline or week 24. There is no change in the score at final follow up.

5.5.11 Adverse Events

Two adverse events were reported during this pilot study. One was partial deep vein thrombosis, which occurred one-week post treatment in an operative treatment control-group patient. This patient required hospital admission for shortness of breath resulting from subsequent pulmonary embolus in the right lung. He was treated with heparin and warfarin and made full recovery. He returned to work as a painter 6 weeks later. The second adverse was partial re-rupture occurred in a conservatively treated patient from the control group. The event occurred at week 8 post treatment when this patient ran upstairs to catch a plane in an airport. He was wearing Samson boot with wedges as per Sheffield protocol. He presented to our research team a week later with pain around the tendon. An ultrasound scan confirmed the diagnosis of partial re-rupture. He was treated non-operatively with further period of immobilisation. He made a good recovery and was able to return to full function following treatment.

5.6 Chapter conclusion

The aim of this pilot was to assess the feasibility of applying PRP in operative and non-operative treatment of Achilles tendon rupture. The method employed was found to be easy to use in both outpatient and operating theatres. Furthermore, platelets in PRP were viable and produced high concentration of growth factors upon activation. Patients position for treatment in the outpatient clinic or in theatre facilitated intervention blinding and imaging of the tendon.

The number of recruited patients in this pilot study limits its power and results can not be extrapolated to Acute Achilles tendon treatment in pragmatic settings. Therefore the results are indicative but not conclusive. The results in this chapter will be linked to the results in Chapter 4, 6 and 7 and discussed further in Chapter 8. To achieve the desired statistical power in pragmatic settings, a multicentre randomised controlled trial is recommended. This will be discussed further in Chapter 8.

The findings of this pilot trial suggest that PRP application in Achilles tendon acute rupture may lead to faster regeneration, improved pain and faster return to function as supported by a combination of objective and subjective outcome measures.

Chapter 6 The Achilles Tendon Histological Response to PRP: In Vivo Human Study

6.1 Chapter Introduction

The histological and immunohistochemical response of human Achilles tendon tissue *in-vivo* to PRP application has never been studied. Here we present the first study of its kind to investigate the injured human Achilles tendon *in-vivo* response to PRP application and compare it to a control using histological and immunohistochemical markers of key tendon healing milestones. These markers were identified in *in-vitro* and animal *in-vivo* studies as possible targets of PRP and their cocktail of bioactive proteins. They include: matrix collagen deposition, tenocytes proliferation, GAG content, angiogenesis and leukocytes infiltration.

In the first stage of tendon healing, inflammatory cells such as neutrophils are recruited to the injury site, along with erythrocytes. Monocytes and macrophages are recruited within the first 24 hours, and phagocytosis of necrotic materials at the injury site occurs. This stage lasts 3 days and the repair or proliferation stage then begins and lasts for about six weeks. During this stage tenocytes are involved in the synthesis of large amounts of collagen and proteoglycans at the site of injury, and the levels of GAG and water are high.(121)

It appears that optimal tendon repair requires high expression of collagen type I (324). As healing progresses, there is a switch from collagen type III, which is expressed early in the healing process, to collagen type I, which provides greater mechanical strength (324). It has been reported that TGF-β1 induces the expression of collagen type I and fibronectin mRNA in experiments in tissue culture (325). Upregulation of mRNAs expressing the α-chains of type I and III collagens has been reported to occur in tenocytes isolated from sheep cultured with and without autologous serum (326). Therefore investigating the ratio of collagen I and III may provide information on PRP influence on the maturation of the collagen matrix.

The positive effect of PRP on tenocytes proliferation is discussed in chapter two. In this thesis, the proliferative and migratory effect of PRP on tenocytes obtained from the injured tendon is presented in chapter 7. To study the proliferative effect of PRP on healing human ruptured Achilles tendon *in-vivo*, Ki-67 expression is studied. The Ki-67 protein (or MKI67) is a cellular marker strictly associated with proliferation (327) . Ki-67 is present during all active phases of the cell cycle (G_1, S, G_2, and mitosis), but is absent from resting cells (G_0). During interphase, the Ki-67 antigen can be exclusively detected within the cell nucleus, whereas in mitosis most of the protein is relocated to the surface of the chromosomes (327).

The infiltration of leukocytes during the initial stage of repair may last throughout the inflammatory and proliferation stage. Inflammatory cells such as neutrophils, monocytes and macrophages are recruited within the first 24 hours, and phagocytosis of necrotic materials at the injury site occurs. These cells also release growth factors and cytokines to start the repair process and regulate it (Chapter 1: Tendon Healing stages). The combination of growth factors and cytokines produced by platelets in PRP may increase leukocyte chemoattraction to the injury site, which may last throughout the first two stages of repair (140). CD45 (Protein tyrosine phosphatase, receptor type, C) is known as the leukocyte common antigen present on most human leukocytes but absent from erythrocytes and platelets. Quantifying CD45 expression indicates leukocytes infiltration in the target tissues.

The release of angiogenesis bioactive factors such as VEGF leading to new vessels formation in the injured area has been observed in several *in-vitro* and animal studies (161, 222, 328-330). Neoangiogenesis play important role in the repair and remodelling stages of healing. CD34 protein is a member of a family of single-pass transmembrane sialomucin proteins that show expression on early hematopoietic and vascular-associated tissue.(209) In this study CD34 marker will help identify and quantify vessels in the samples. All the aforementioned possible effects of PRP will be explored in the current study.

6.2 Methods

6.2.1 Patient Groups

The clinical trial ethics committee application was amended to include the needle biopsy and full approval was granted (Oxfordshire ethics committee C, reference 09/H0605/78). The demographics, patients groups, randomisation and interventions/control were presented in Chapter 5. Briefly, 20 patients were randomised to receive PRP or control (standard treatment) in both conservative and operative treatment pathways. 10 patients were recruited in this study (5 PRP and 5 controls). The biopsy was performed at week 6 post treatment.

6.2.2 Biopsy Procedure

On the affected side, biopsy specimens were obtained under ultrasound guidance using a 14G Automated Temno Evolution needle biopsy (Carefusion ltd, Waukegan, Illinois, USA). This is a disposable lightweight adjustable biopsy needle system. The gun needle moves in one stage when fired capturing the tissues in the needle notch. The sample diameter is 1.2 mm and is 10-20 mm long. This percutaneous biopsy technique has been used safely and effectively to sample Achilles, rotator cuff and patellar tendons (331-333) (Figure 6.1). Local anaesthesia (2ml of 2% Lignocaine) was given subcutaneously and in the paratenon. Through a small incision, a core needle biopsy specimen was obtained from each tendon. Each core biopsy specimen was placed separately in a coded, formalin-filled tube. Patients followed standardised rehabilitation protocol as discussed in Chapter 5.

6.2.3 Samples processing

All the tendon samples were placed in 20 ml of sterile 10% formalin in a universal container for transportation to the Pathology laboratory at the Nuffield Department for orthopaedic Rheumatology and Musculoskeletal Sciences (NDORMS). The samples were fixed in 10% neutral-buffered formalin for 24 to 48 hours and processed to paraffin wax. Samples were sectioned at 5-µm in longitudinal direction in-line with tendon fibres. Sections were then mounted onto 3-aminopropyltriethoxysilane-coated slides and dried at 37°C overnight.

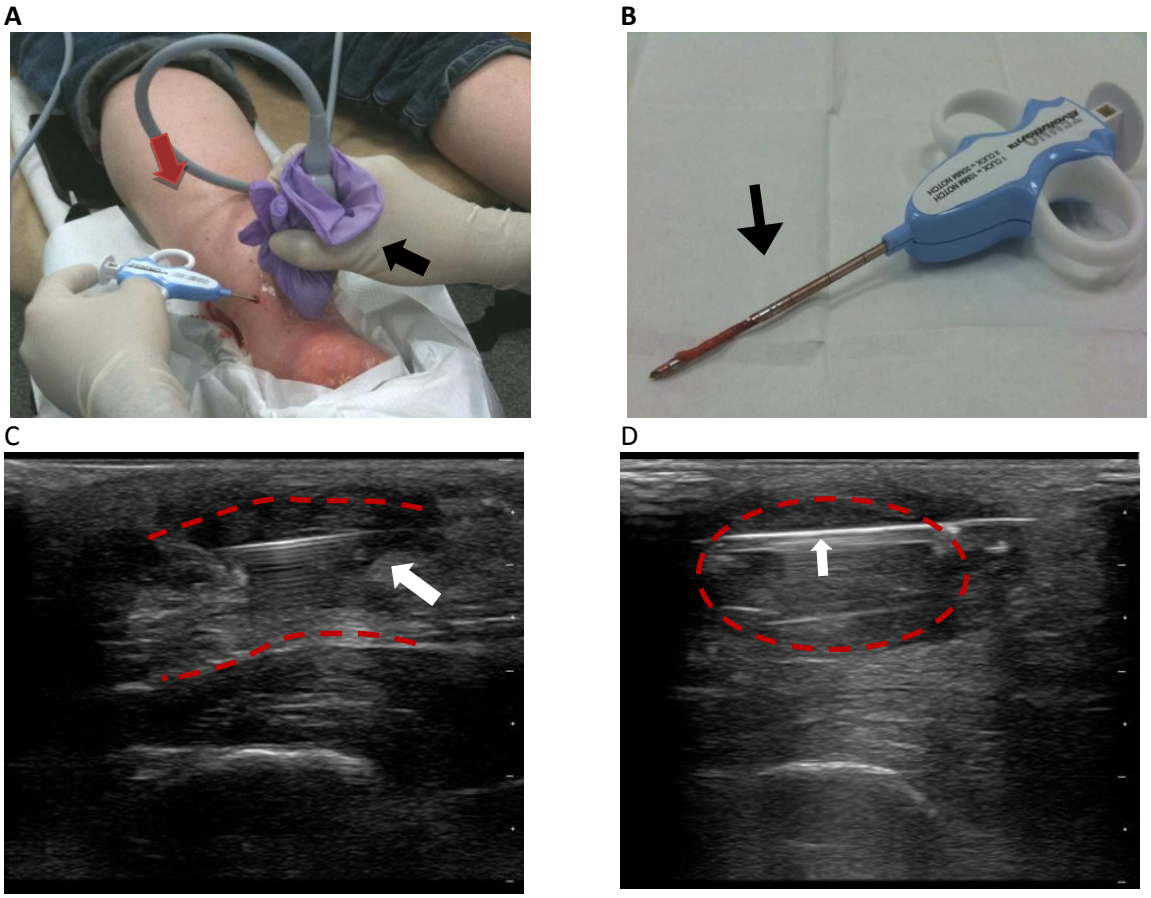


Figure 6 .1 The percutaneous US guided needle biopsy. A) Temno Evolution 14G biopsy needle (red arro) is inserted into the tendon at 45° under US guidance(black arrow) to maximize tissue capturing from the healing rupture area and to prevent transverse dissection of the tendon. B) Tissue sample in the needle notch. C) Longitudinal USS of the tendon during sampling shows the needle in the middle of the affected area. E) transverse scan confirming the position of the needle in the middle of the tendon.

6.2.4 Histological stains

6.2.4.1 H&E stain

Sections were dewaxed in two 10-minute changes of xylene, followed by one change in absolute alcohol, 95% alcohol and 70% alcohol, for 5 minutes each to rehydrate the sections. The sections were then rinsed with distilled water. Sections were stained using Harris haematoxylin solution for 8 minutes then washed in water for 5 minutes and differentiated with 0.3% acid alcohol. Then slides were counterstained in eosin solution for 30 second to 1 minute. The tissue was dehydrated with two changes of 95% ethyl alcohol and absolute alcohol for 5 minutes each. Slides were cleared with two changes of xylene, and mounted with coverslips using Permount mounting media. This stain protocol results in colouring the nuclei blue and cytoplasm pink to red (Appendix 6.1). (334)

6.2.4.2 Alcian blue Stain

Tissue sections were deparaffinised, hydrated and rinsed in distilled water as previously described. They were then incubated in 3% acetic acid for 3 minutes. The tissue sections were then incubated with Alcian blue stain for 1 hour at room temperature (0.1% Alcian blue 8GX in 3% acetic acid, pH 2.5). After rinsing in water for 10 minutes the sections were briefly counterstained in Eosin for 3 minutes and again rinsed in tap water. The tissue was dehydrated with two changes of 95% ethyl alcohol, absolute alcohol, cleared with two changes of xylene and coverslipped with Permount media (see Appendix 6.2). (335) Alcian blue stains acid mucosubstances and acetic mucins (Glycosaminoglycan GAG). Strongly acidic mucosubstances will be stained blue, nuclei will be stained pink to red, and cytoplasm will be stained pale pink.

6.2.4.3 Histology Scoring Systems

There are two scoring systems that can be used for classification of the histological findings in treated tendons: the Movin score (336) and its validated modifications (299, 337) and the Bonar score (338). The variables included in the Movin scale are 1) fibre structure; 2) fibre arrangement; 3) rounding of the nuclei; 4) regional variations in cellularity; 5) increased vascularity; 6) decreased collagen stainability; 7) hyalinization; and 8) GAG content. Each variable is scored between 0 and 3, with 0 being normal, 1 slightly abnormal, 2 abnormal, and 3 markedly abnormal [Table 6.1]. The total semiquantitative histologic score for a given sample could vary between 0 (normal tendon) and 24 (the most severe abnormality detectable).

The variables included in the Bonar scale are 1) tenocytes; 2) ground substance; 3) collagen; and 4) vascularity. A four-point scoring system is used, where 0 indicates a normal appearance and 3 a markedly abnormal appearance (Table 1). Overall, the total score for a given slide could vary between 0 (normal tendon) and 12 (most severe abnormality detectable) [table 6.1].

Maffulli et al studied both scoring systems and found that they assess the same characteristics in tendon histology.(339) The two scales have a high correlation and essentially assess the same

characteristics and variables of tendon histology. A minor difference between these two scoring systems is the grading and definition of hyalinization. Hyalinization is assigned as Grade 0 to 3 in the Movin system, and it is not present in the Bonar score. Maffulli suggested removal of hyalinization score as it is seldom present, and it is a poorly reproducible histopathological criterion. Kartus et al (340) modified Bonar score to suite the application of immunohistochemistry techniques and automated quantification methods (e.g. cell count).

For the aforementioned reasons, the analysis of the histological samples in this study is performed using the modified Bonar score as presented in table 6.2 (340). Fibre structure is evaluated using H&E stain images. Cellularity grading is determined via cell count in each microscopic field using automated cell counting technique. Vascularity is assessed in CD34 IHC images, which increases the confidence of identifying the vessels in the tendon tissues. GAGs are analysed using Alcian blue stain and the percentage of GAGs-rich areas using quantitative image analysis. Collagen III presence is evaluated using a specific collagen III marker antibody stain.

Table 6.1: The modified Bonar scoring system, which is based on Bonar scoring system, is used to classify the histopathological findings of tissue samples in both PRP treated tendons and controls (338, 340).

Histologic Classification Based on a Semiquantitative Four-Point Scoring System

Variable	Grade			
	0	1	2	3
Fiber structure	Straight, parallel, packed fibers, with slight waviness	Slight separation of fibers, increased waviness	Separation of fibers, deterioration of fibers	Complete loss of fiber structure and presence of hyalinization
Cellularity	<100 cells/high-power field (HPF)	100–199 cells/HPF	200–299 cells/HPF	>300 cells/HPF
Vascularity	Vessels run parallel to the collagen fiber bundles in the septa	Slight increase in vessels, including transverse vessels in the tendon tissue	Moderate increase in vessels within the tendon tissue	Markedly increased vascularity with clusters of vessels
Glycosaminoglycans	No alcianophilia[a]	Slight alcianophilia between the collagen fibers	Moderate increase in alcianophilia	Markedly increased alcianophilia forming blue lakes
Type III collagen	No positive staining	Slight positive staining	Moderate positive staining	Intensive positive staining

[a] Blue staining using Alcian blue (pH 2.5)/periodic acid-Schiff.

6.2.5 Immunohistochemistry stains

IHC staining was performed as shown in the diagram in figure 6.2 and described in appendix 6.3. In brief, paraffin fixed samples were baked at 60°C for 1 hour, dewaxed using Clearene and dehydrated with 100% Alcohol. Sections were quenched with 3% H_2O_2 in methanol for 10 min and transferred to warm 10 mmol/liter citrate buffer solution (pH 6) for 10 min. Appropriate pre-treatment to unmask the antigen was carried out according to the manufacturer's instructions. After two changes in wash buffer, the sections were incubated with blocking serum for 20 minutes. The sections were incubated with primary antibody in a humid chamber at 4°C overnight. The primary antibodies and the dilution used are listed in Table 6.2. After 3 changes in wash buffer for 5 minutes each, the sections were incubated with a secondary antibody, which is biotinylated anti-mouse/ rabbit IgG for 20 minutes. The classic antibody-binding complex method was used to amplify the specific binding signal using ABC kit (ABC system, Vector laboratories, USA). Finally, 3,3'-diaminobenzidine tetrahydrochloride (DAB) was used to colour the sections in the presence of H_2O_2. The sections were rinsed in distilled water and immersed in copper sulphate for 4 minutes to develop the colour. Counterstaining was performed using haematoxylin stain for 30 seconds then differentiated in acid alcohol. All sections were dehydrated through graded alcohol to xylene, and mounted with p-xylene-bis-pyridinium bromide (DPX) permount (Sigma-Aldrich, USA).

Table 6.2: Antibodies used for immunohistochemistry

Antibody	Specificity	Host	Monoclonal/ polyclonal	Concentration	Dilution	Source
Collagen I	Collagen I	Rabbit	Polyclonal IgG	0.4 mg/ml	1/10	AbD serotec, Oxford, UK
Collagen III	Collagen III	Rabbit	Polyclonal IgG	0.1 mg/ml	1/10	AbD serotec, Oxford, UK
KI-67	Proliferation	Rabbit	Monoclonal IgG	0.6-1 mg/ml	1/100	Vector Laboratories, CA, USA
CD-45	Leukocytes	Mouse	Monoclonal IgG	250µg/ml	1/100	Vector Laboratories, CA, USA
CD-34	Vessels	Mouse	Monoclonal IgG	250µg/ml	1/50	Vector Laboratories, CA, USA

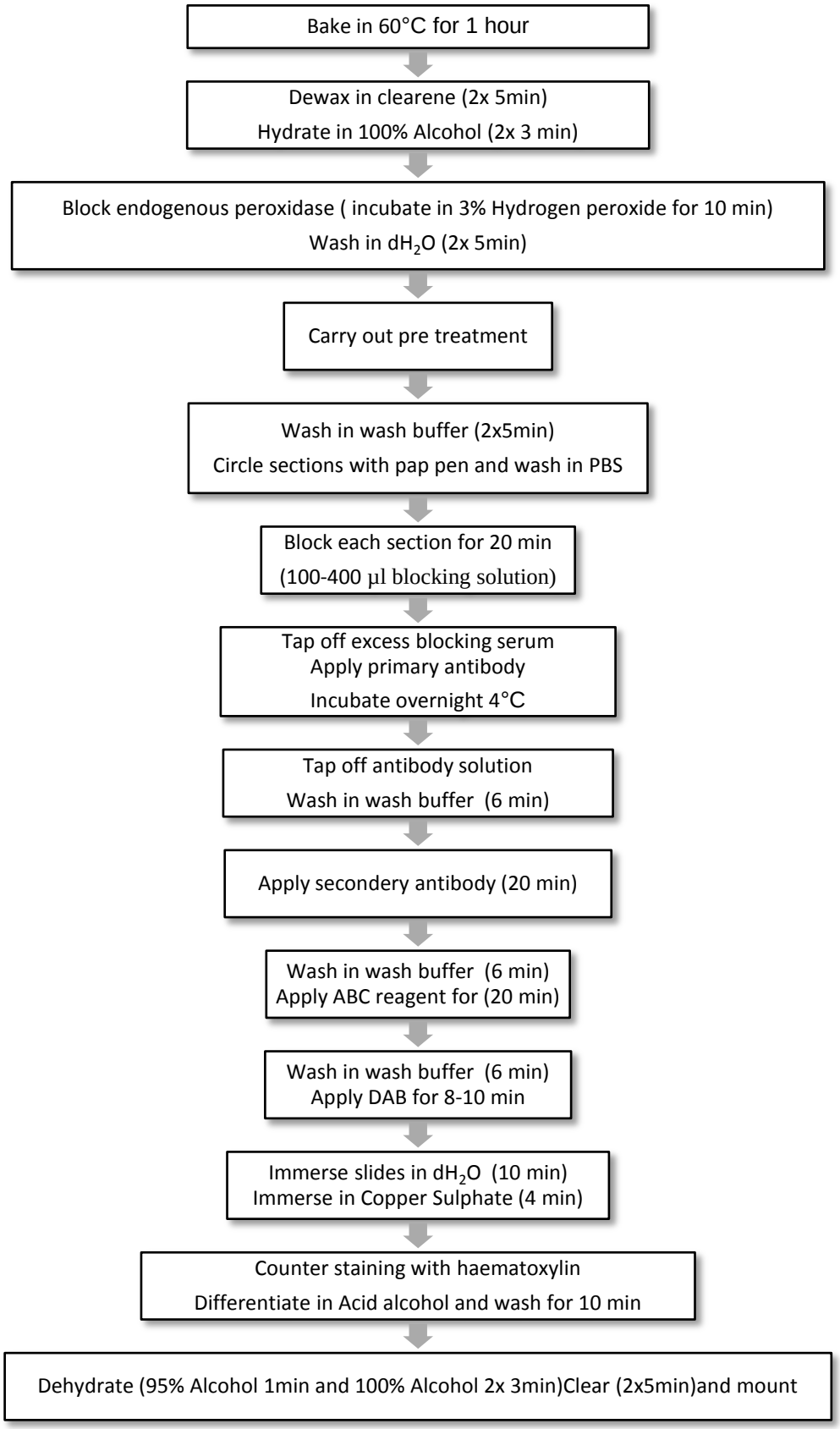


Figure 6 .2 General Immunohistochemistry (IHC) protocol outline. Pre-treatment and antibodies were used as per manufacturer recommendations. ABC is Avidin-Biotin Complex. DAB is 3,3'-Diaminobenzidine.

6.2.6 Imaging and Analysis

Image analysis was performed using a light microscope (Zeiss AXIO Imager M1 microscope, Carl Zeiss LLC, New York, USA) equipped with a high resolution microscopy digital camera (Axiocam HRC). Under 40x magnifications, samples were systematically digitally imaged to include the entire sample and avoid allocation bias. All images were blinded using Image J software (Image J v1.48c, Wayne Rasband, National Institute of Health, USA). The blinding code assigned images into random files prior to any analysis. The examiner was blinded to the sample allocation. The code was broken and files were allocated to each treatment group after all images were analysed.

H&E and Alcian blue slides were studied by the author and scored according to the modified Bonar score. The number of cells was calculated in 40x magnification field using Image J software (341).

Alcian blue images were further studied under confocal light using X-Cite® 120Q excitation light source (Lumen Dynamics Group Inc, Ontario, Canada) and digitally imaged. To quantify the proteoglycans in the tissue; Intensity of the staining was analysed using Image J software as described by Wei et al (342). After subtracting background to remove unevenly distributed back ground noise; colour deconvolution was set at Alcian Bule & H with threshold 49-143. The numbers of pixels in the region of interest (ROI) for each of 255 shades of blue were counted. The sum of these intensity values was then divided by the total number of pixels in the region, giving a (unit-less) semi-quantitative measure of Alcian blue stain for each sample.

The immunohistochemistry digital images were blinded and analysed using Image J software with varying parameters depending on the stain. Quantifying collagen I and III stained areas was performed according to Ashish et al technique using Image J software (343). In brief, the scale was changed to micrometres, colour deconvolution was set to H DAB and brown stained collagen was segmented using threshold at 44-157. The thresholded area was measured as described above. Collagen I and III % staining in each sample was calculated and col I/col III ratio was generated and compared between the groups.

KI-67, CD34 and CD45 markers count was performed using Image J technique as described by Libano et al (344). Briefly, the colour images were converted into greyscale. Background was subtracted and threshold was adjusted to highlight the cells with positive marker. Using analyse particles function, the number of positive cells was automatically calculated for all sections. This was divided by the total number of cells to obtain KI-67 index which was compared between the two groups. The average number of CD45 and CD34 cells for each tissue sample was calculated and compared between the two groups.

6.2.7 Statistical Analysis

Except when the mean± SD value is indicated, median (and range) values are presented. Assessment of normality was carried out using Shapiro-Wilk normality test and data was found to be non-parametric. Significant differences between the PRP and control groups were evaluated using non-parametric Mann-Whitney U two-tailed test. The modified Bonar score components were presented in each related section. The final score was tabulated and Kruskal-Wallis statistical test was used to analyse the component of Bonar score. A difference of $P<0.05$ was considered to be statistically significant using SPSS statistical package (SPSS 18,SPSS Inc., Chicago, IL, USA).

6.3 Results

6.3.1 Histological stains

6.3.1.1 Haematoxylin Eosin Stain

Cellularity of the tendon samples was significantly increased in the control group compared with the PRP group tendon samples six weeks post intervention. PRP samples cell count was 92 per microscopic field (range 10-316) and control samples count was 164 per microscopic field (range 27-583). The results are displayed in figure 6.3.

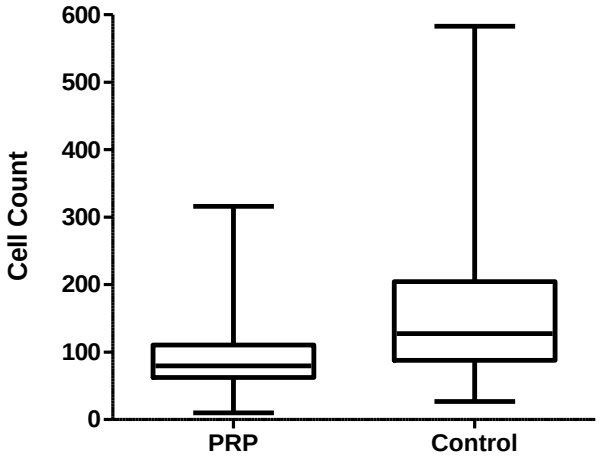


Figure 6 .3 H&E stained samples cell count in PRP and control group tendon tissues.

Fiber structure of the tissue was significantly better in the PRP group compared with control tissue (P <0.001) (figure 6.4) as measured by the modified Bonar score criteria. The overall appearance showed mostly dense collagen fibres with good stainability. The wavy configuration of the collagen fibres was apparent in all samples. However, separation and deterioration of fibres, fibrosis, hyalinization, or some combination of the three were observed in some specimens (figure 6.5).

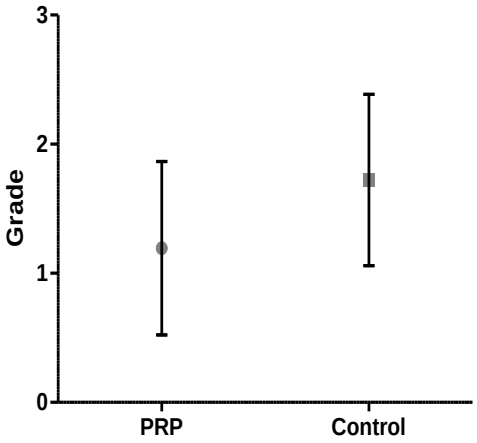


Figure 6 .4 H&E stain grading of fibre structure represented as mean ±SD.

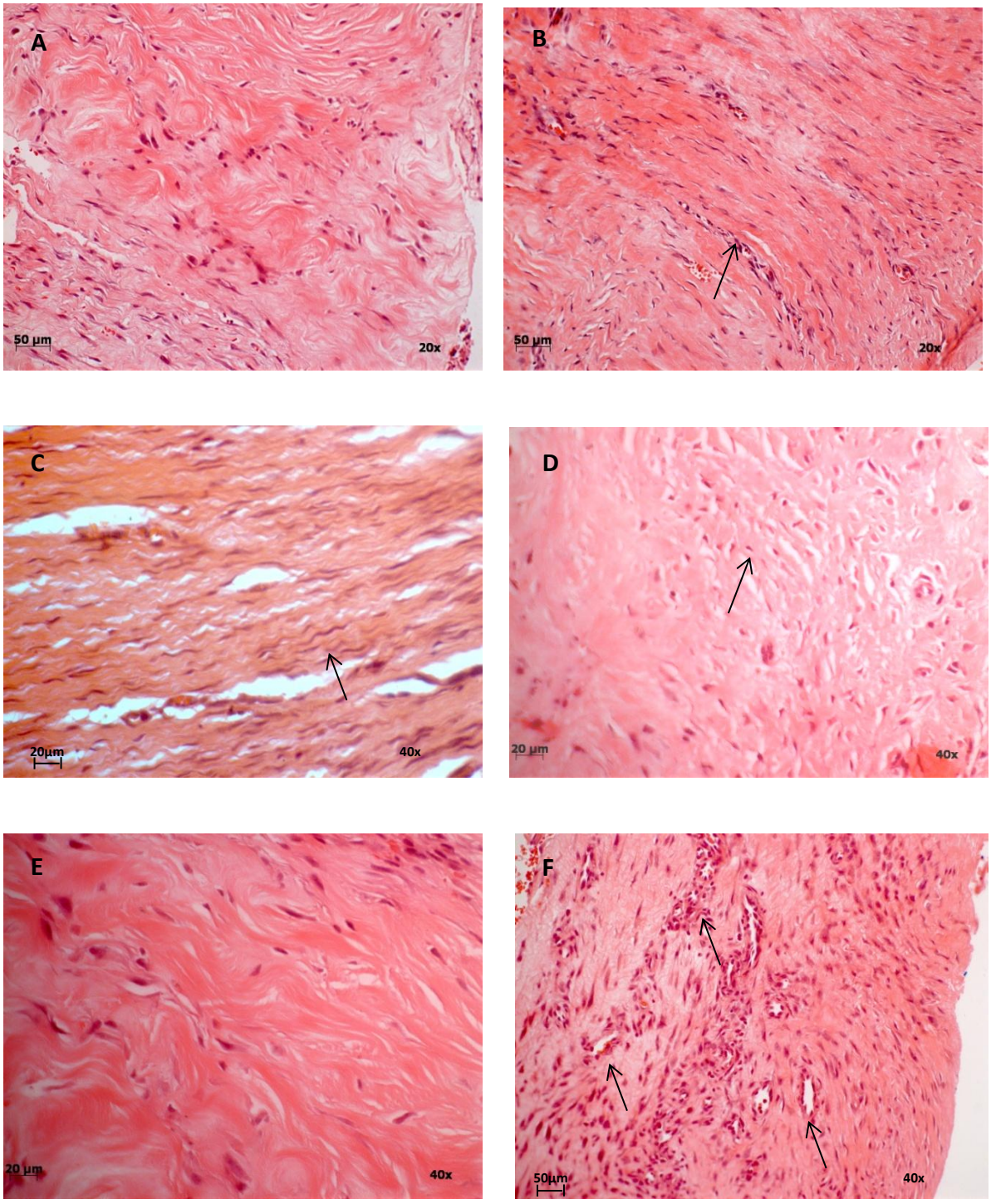


Figure 6 .5 H&E stain light microscopy examples: A) fibres arrangement in a control sample showing tight dense collagen fibres but with inter-waviness and loss of unified structural arrangement. B) tight collagen fibres, which are straight and parallel with minimum waviness in PRP treated tendon. Vessels run parallel to the fibres (arrow) C) high magnification (40x) of the collagen fibres in B showing the parallel fibres with typical collagen waves. There is some slight separation between fibres. The tenocytes located between the fibres and have flattened appearance (arrow). D) a typical appearance of disorganized fibres in control sample. The cells are round, small and dense (arrow). E) 40x magnification of an area with loose of fibre arrangement. F) and area with markedly high density of vessels with clusters of vessels(Vascularity grade 3).

6.3.1.2 Alcian blue Stain

Generally the sections were rich in blue stain indicating large GAG content. The blue stain appeared to run parallel to the collagen fibres. Using Image J software, areas stained blue (GAG-rich areas) and red (collagen) were measured in the whole microscopic field area (figure 6.6). The estimation of the alcian blue stained sections for GAGs area was significantly higher in PRP treated tendons (P< 0.0001) (figure 6.7).

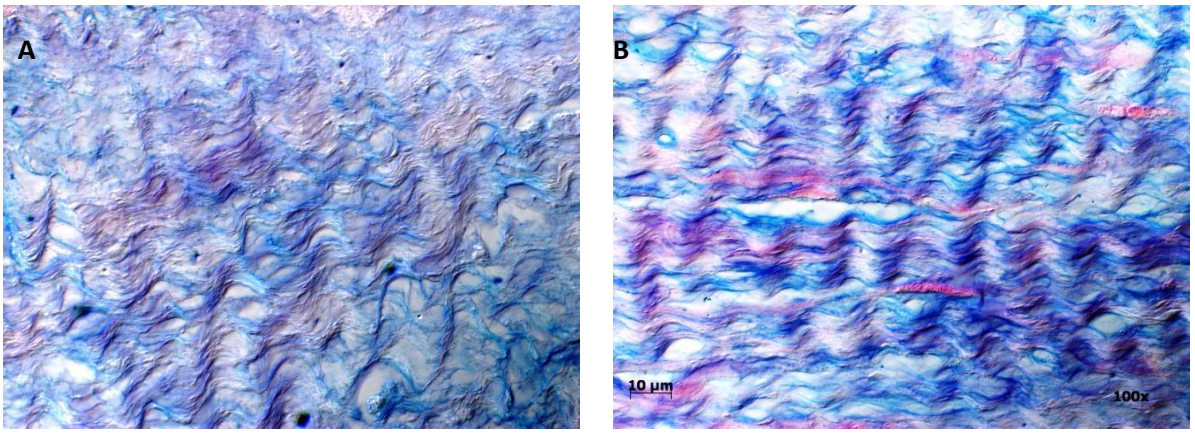


Figure 6 .6 Achilles tendon tissue Alcian blue stain (x100 magnification). GAG-rich areas stained in blue separating the red-stained tendon fibres. More GAG-rich stain was observed in PRP samples (A) when compared with control (B).

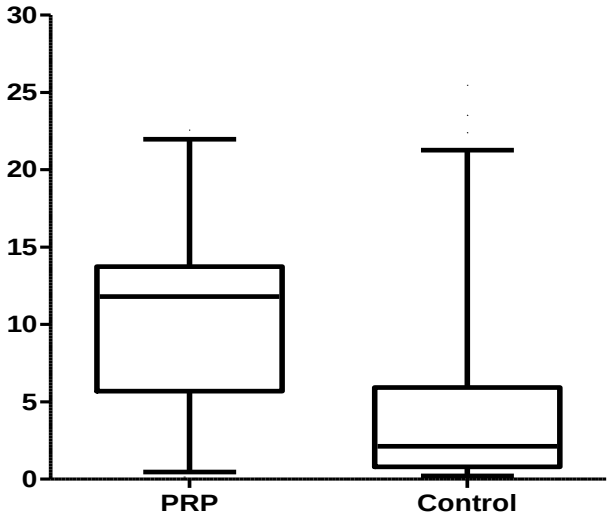


Figure 6 .7 The results of Alcian Blue stain: PRP treated tendons showed significantly more GAGs-rich areas than control (mean 11.81±9.67% and 5.11±7.67% for PRP and control respectively).

6.3.2 Immunohistochemistry stains

6.3.2.1 Collagen I

All samples showed heavy staining of collagen I antibody, which made the sample look brown in colour (DAB stain) (figure 6.8). Although both groups showed high collagen I staining, there was significantly higher content of collagen I in PRP when compared with control (PRP 55.32± 8.59% vs control 29.06 ±7.76, p = 0.0079) (figure 6.9).

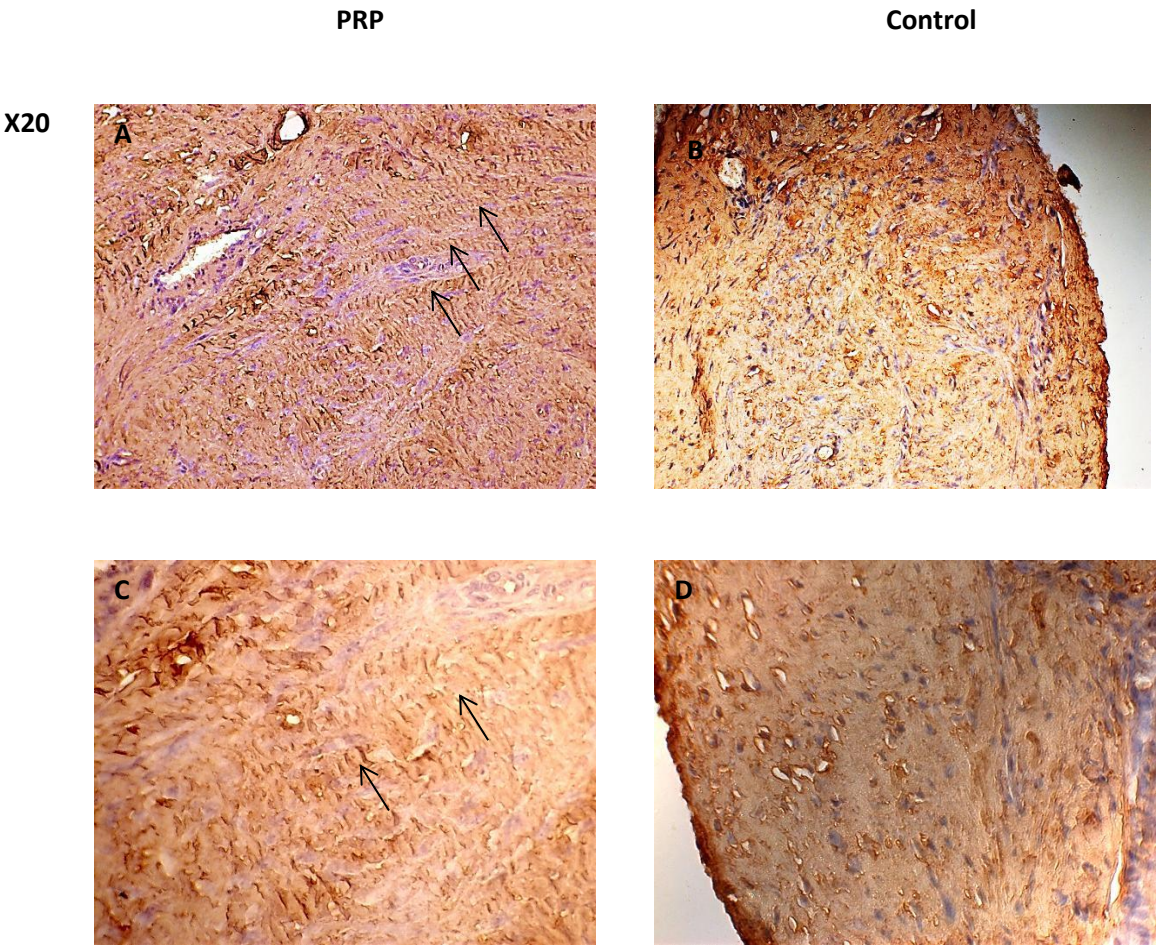


Figure 6 .8 Collagen I immunohistochemistry staining examples. A&B) The low magnification images show heavily stained tendon tissues, which reflect the high collagen content in the samples. C&E) PRP samples showing the organized collagen structure with typical wavy appearance (arrows). D&F) show control samples collagen IHC images: there is less collagen I stain and less organization.

6.3.2.2 Collagen III

Under light microscopy, all samples appeared in brown with high uptake of collagen III IHC staining (figure 6.9). There was no significant difference of collagen III content between PRP and control samples (PRP 19.58 ± 2.84 vs control 20.89±7.46, p = 1.00) (figure 6.10).

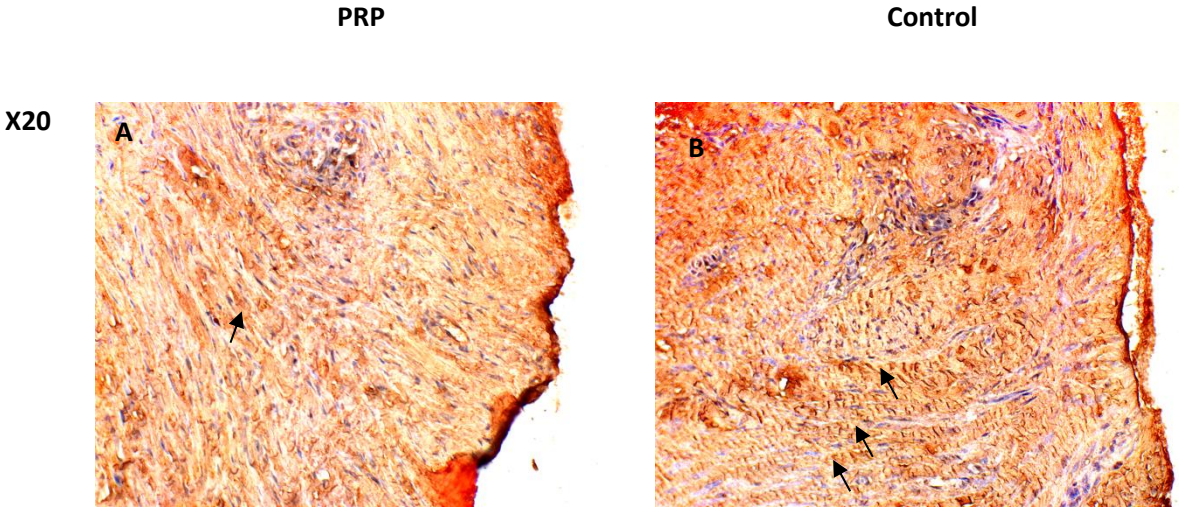


Figure 6 .9 Collagen III immunohistochemistry staining examples. The 20x magnification images show heavily stained tendon tissues, which reflect the high collagen content in the samples. A) PRP samples showing collagen III staining along the collagen fibres (arrow) (B) Collagen III stain is associated with the wavy configuration of the fibres.

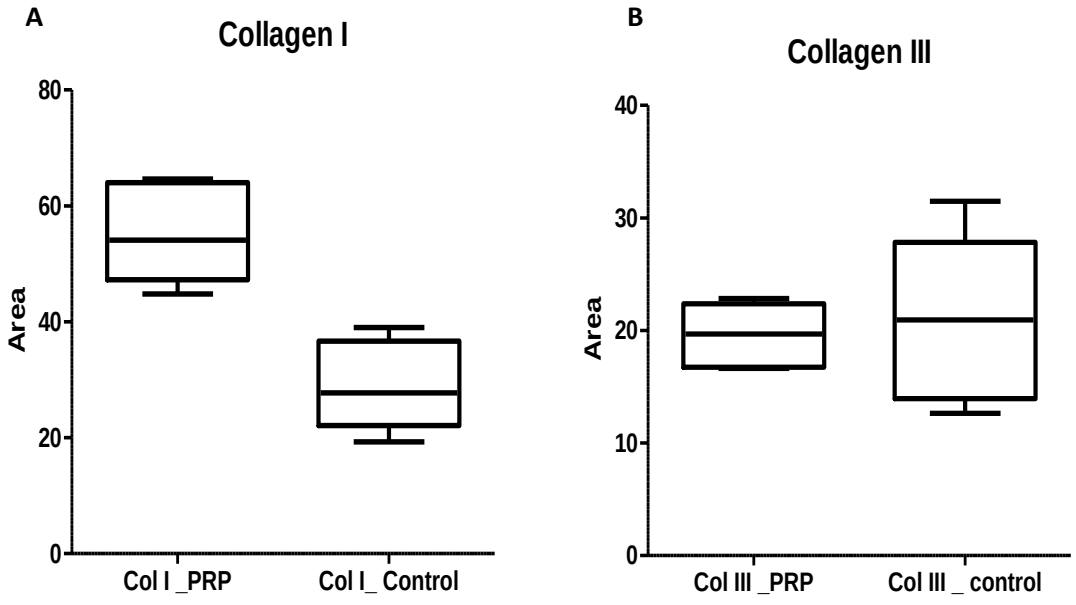


Figure 6 .10 The results of collagen I and III immune stain. A) Measurement of collagen I stain in PRP and control samples. Collagen I was significantly higher in PRP samples than in control (p = 0.007). B) Shows no difference in collagen III content between the groups (p = 1.0).

Collagen III / I Ratio

The ratio of collagen III over collagen I was significantly lower in PRP samples compared to control (PRP ratio 0.35 ± 0.03 vs control 0.77±0.37, p = 0.0079) (figure 6.11). It is noticeable that in PRP samples collagen ratio had tighter range in comparison to control. This may represent the varying degree of collagen maturity in the control samples or that PRP allow tissue to heal more uniformly.

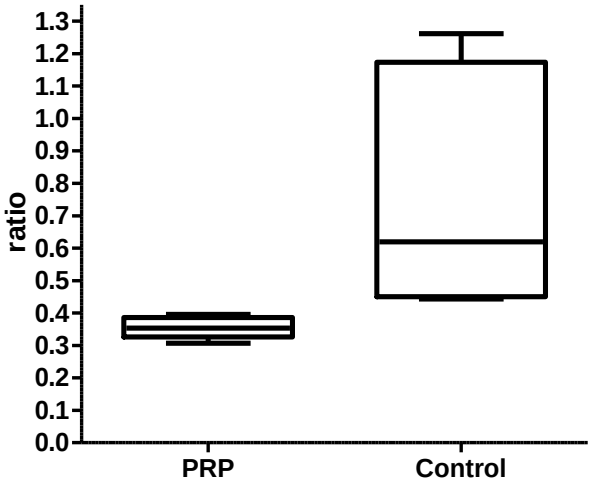


Figure 6 .11 The ratio of collagen III / collagen I in both groups.

6.3.2.3 KI67 – Proliferation Marker

Representative images of Ki67 staining are displayed in figure 6.12. Under light microscopy, both group showed small proportion of cell with positive KI-67 staining. A small number of these cells were not tenocytes but other invading cells such as leukocytes or vascular endothelial cells, and were located around the infiltrating vessels.

The proliferation index was calculated by counting the number of Ki-67 positive cells/total cells counterstained with haematoxylin (345). There was no difference in KI-67 index at 6 weeks between PRP and control samples (control KI index 0.338 ± 0.249 vs PRP Ki-67 index 0.288 ± 0.21, p value = 0.69) (figure 6.13).

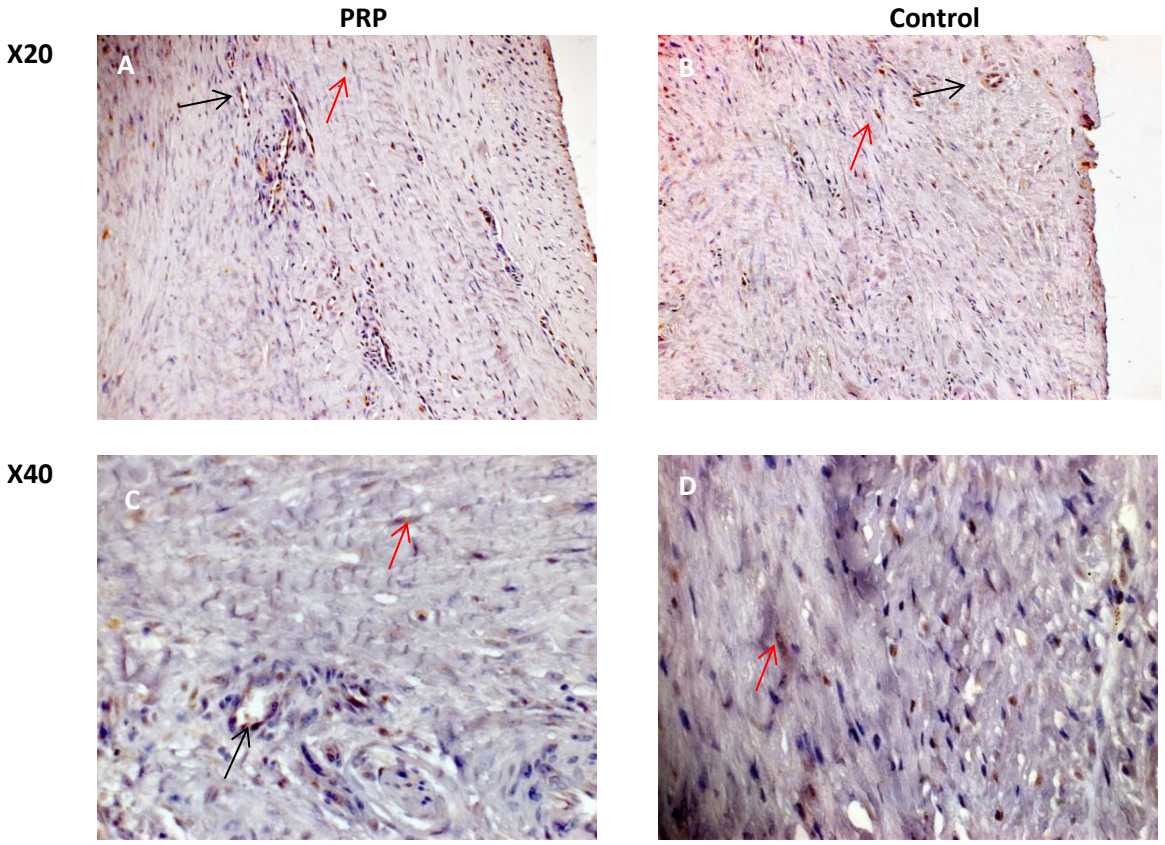


Figure 6 .12 IHC staining with KI-67. A) PRP sample with high number of KI67+ cells in the tendon intima (red arrow) and around blood vessels (black arrow). B) Control sample with KI67+ cells (red arrow) and endothelial KI67+ cells (black arrow) . C) Higher magnification showing the KI67+ tenocytes (black arrow) and endothelial cells (red arrow). D) Higher magnification of control sample showing KI-67+ tenocytes.

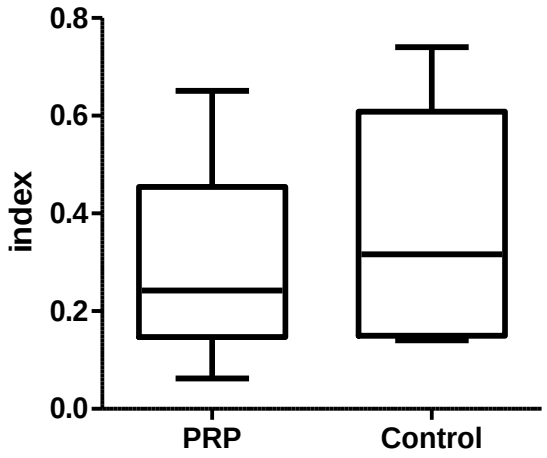


Figure 6 .13 Proliferation index: the number of KI67+cells/ all cells in the PRP and control groups. There is no significant difference between the two groups.

6.3.2.4 CD45 – leukocytes marker

The majority of leukocytes were scattered throughout the samples in between collagen fibres and the largest numbers were seen near blood vessels (figure 6.14). There were fewer leukocytes present in those specimens which contained mature fibrous tissue with low fibroblast cellularity. Some leukocytes were found in the paratenon lining in those specimens which contained this structure. There was no significant difference in CD45 marker between PRP and control group at this time point (P = 0.33) (figure 6.15).

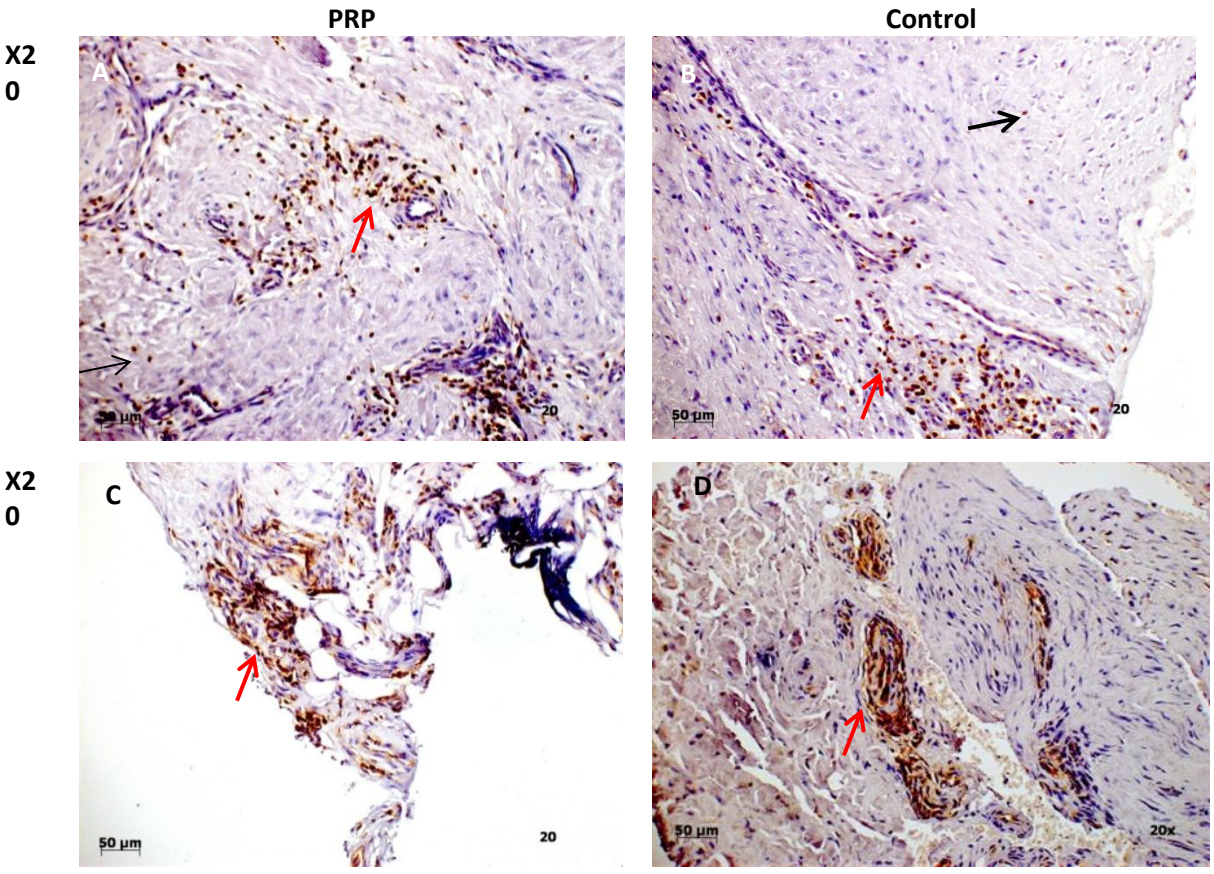


Figure 6 .14 CD 45 stain of the tendon samples. A) PRP sample with large number of leukocytes in the tendon intima (black arrow), which is highly cellular. There is high concentration of leukocytes around blood vessels (red arrow). B). Control sample with CD45+ leukocytes in the tendon intima (black arrow) and around blood vessels (red arrow). C &D) high infiltration of leukocytes in tendon edge and in the areolar tissues of the paratenon in both PRP and control samples.

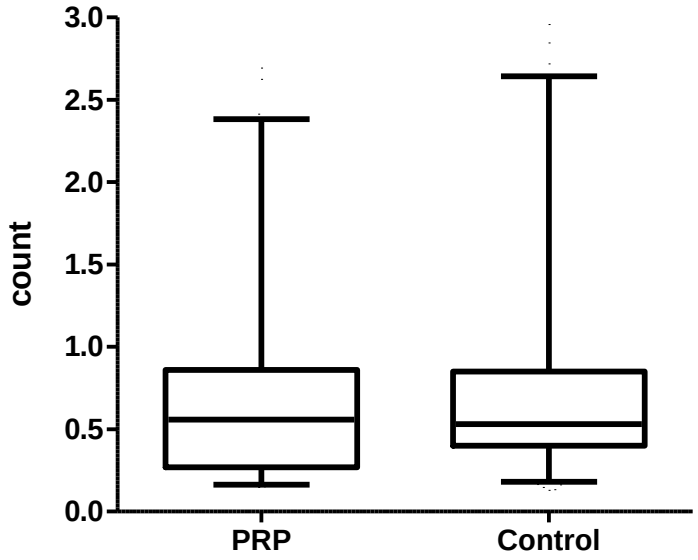


Figure 6 .15 A plot of CD 45 positive cells in the tendon samples of both groups.

6.3.2.5 CD34 – Vessels marker

CD34-positive vessels were abundant in most specimens. The vessels appeared inside the tendon tissues in most images (figure 6.16). In some images the vessels were located in the paratenon or on the peripheries of the tendon.

The count of CD34 cells measured using Image J software in both groups is displayed in figure 6.17. PRP had fewer CD34 positive cells than control (PRP mean 1.24±1.72, control mean 1.44±1.3, P = 0.023). The modified BONAR grade for vascularity variable was lower in PRP than in control (PRP mean 1.13±0.71, control mean 1.37±0.92, P = 0.024).

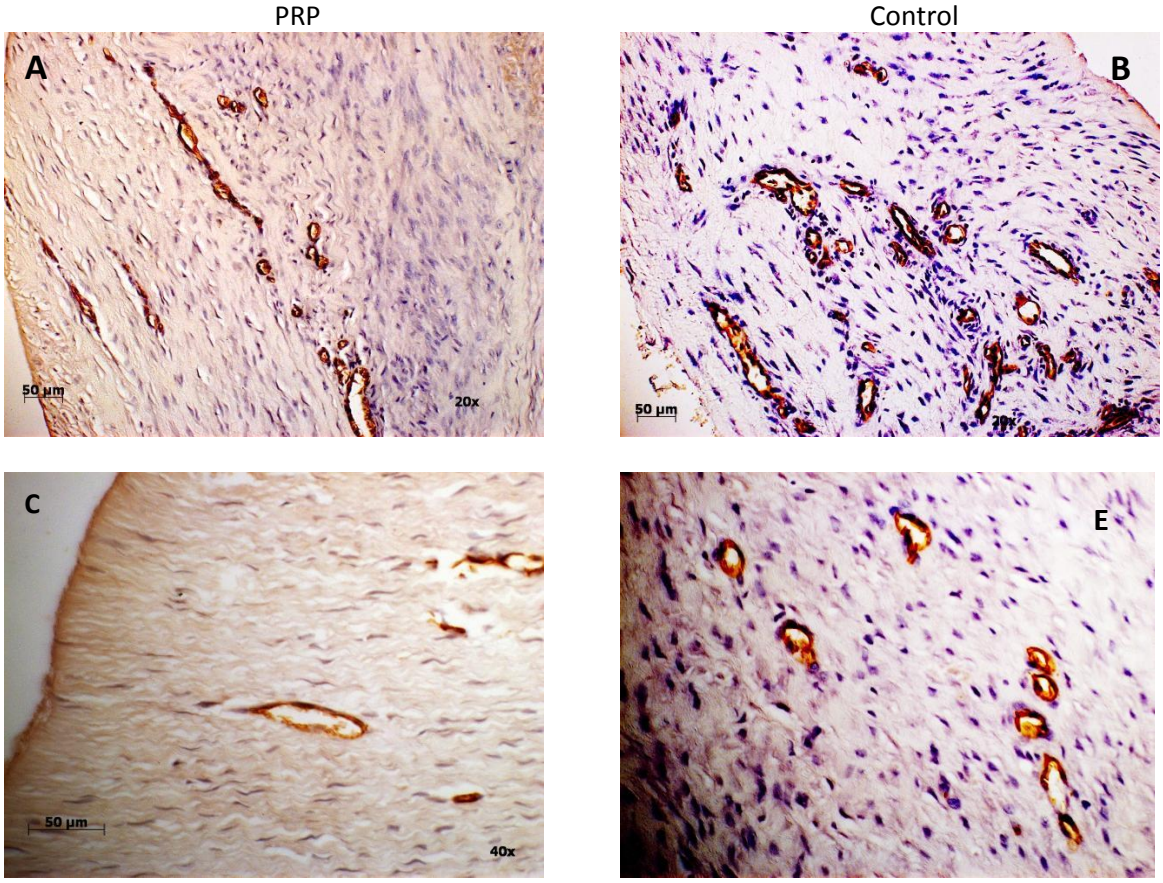


Figure 6 .16 CD 34 IHC stain of the tendon samples. A) PRP sample showing near mature collagen fibre structure with vessels running parallel to fibres. B) highly vascular control sample with vessels clustered in the tendon intima. Some vessels appear to run transverse to tendon fibres. C) Higher microscopic magnification of PRP sample showing the vessel parallel to tendon fibres. D) Transverse vessel cluster in control sample.

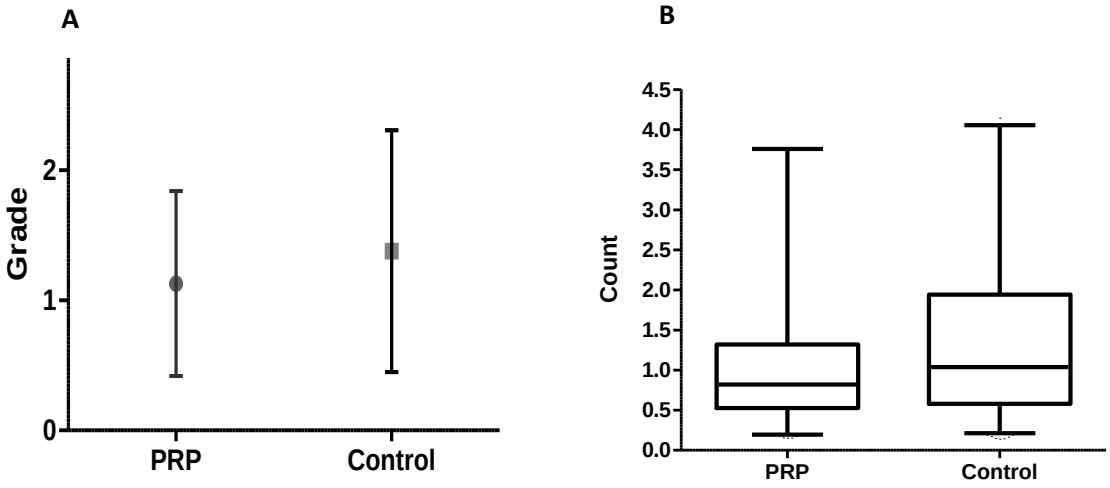


Figure 6 .17 Shows the vascularity grade as defined by the modified Bonar score. B) a plot of CD34 positive cell count in both groups.

6.3.3 Modified Bonar Score results

The modified Bonar score results in table 6.3 confirm the above findings that cellularity and vascularity were significantly lower in PRP samples compared with control specimens at 6 weeks post intervention (figure 6.3 and 6.17). Fibre structure was more mature and organised in PRP samples when compared to control (figure 6.4). GAG content was higher in PRP treated tendon than in control. With regards to collagen III presence, No significant difference was found between biopsy specimens obtained from PRP treated tendons and control. The overall modified Bonar score of PRP samples was significantly lower than control (table 6.3), which indicate better quality tendon tissues in those samples.

Table 6.3 summarises Bonar score results in each category. * Significant difference

	PRP (range)	**Control (range)**	***P vale***	***Significance***
Fibre structure	1 (0-3)	2 (0-3)	<0.0001*	s
Vascularity	1 (0-3)	1 (0-3)	0.024*	s
Ground substance (GAGs)	2 (0-3)	1 (0-3)	<0.0001*	s
Collagen	2 (0-3)	2 (0-3)	0.334	ns
Cellularity	0 (0-3)	1 (0-3)	<0.0001*	s
Total score	6 (0-15)	7 (0-15)	<0.0001*	s

6.4 Chapter discussion

The findings of the histology and immunohistochemistry studies of specimens obtained at 6 weeks post intervention confirmed that PRP may have accelerated the maturation of the healing ruptured tendon. This was evident in lower cellularity and vascularity of the healing tendons that were treated with PRP compared with control. Additionally, the collagen fibre structures were more organised with higher collagen I content and better collagen III/ collagen I ratio. Higher GAGs content was also observed in tendons exposed to PRP six weeks earlier. Interestingly, there was less cellular proliferation in PRP specimens at this stage, which correlates with the finding of fewer cells in those samples. The overall modified Bonar score was also better in PRP samples. This may be explained with earlier maturity of the healing tendon tissues and rapid progression towards a collagen rich matrix with low cell ratio.

To our knowledge, this study is the first of its kind to study *in-vivo* human ruptured Achilles tendon immunohistochemistry response to PRP. Several authors have attempted to study tendon tissue response to PRP in animal models. Majewski et al (346) studied PRP *in-vivo* biomechanical and histologic effect in rat Achilles tendon injury model. The author found that PRP treated tendons increased collagen I to a greater degree than that of collagen III, which is consistent with our finding. This was attributed to PRP markedly increasing the expression of mRNA coding for collagen I. (346) Stimulation of type I collagen mRNA expression by TGF-β1 was also documented by the studies in tissue culture of Ignotz et al (325). We speculate that the significant increase in collagen I and decrease of Collagen III/ Collagen I ratio in PRP samples in the current study is a result of the similar effect of PRP on the expression of col I gene. It is quite possible that the elevated concentration of TGF-β1 in PRP may have mediated part of the observed effects on tendon healing. This cytokine has pleiotropic effects on fibroblasts and has emerged as a pivotal mediator in tissue repair (347).

The quantitative evaluation of collagen I and III showed a reduced level of this collagen III/I ratio at in PRP-treated tendons compared with controls. This finding is in agreement with the reports of Aspenberg (220) and Virchenko (348), who also documented a beneficial effect of platelet concentrate administration on the histologic appearance of the healing tendon in rats, with a concomitant increased tendon callus strength and stiffness by about 30%.

The effect of PRP on leukocytes infiltration and angiogenesis at week 6 in this study may be explained by Xiong et al (349) and Kajikawa et al (184) studies in a rat tendon rupture models. Although at an early stage (between week 1 and 3) Xiong et al study showed an increase in leukocytes and angiogenesis in PRP treated tendons compared with control, this gradually decreased from week 4 onwards post intervention (349). In another *in-vivo* rat tendon study (184), the number of circulation-derived cells that infiltrated into the area was significantly increased in the PRP group, and the cells were more proliferative than in control group at 3 and 7 days after injury. However, 14 days after injury, the number of circulation-derived cells markedly decreased in both groups (184).

Inferring those results on the current study indicates that PRP tendons may have been progressing to maturity quicker with more collagen I and less cells.

The biopsy was performed at 6 weeks considering that at this stage there is significant clinical improvement. Patients are expected to discard the cast and start wearing splint/boot with minimal wedges and to be able to perform range of motion exercises. The biopsy confirmed that tissues are healing with good deposition of collagen; however this is still haphazard and lacks the normal order of tendon structure. This is not expected to normalise until the end of the remodelling stage which can take up to a year.

This chapter's findings help explain the improvement in clinical outcome scores presented in chapter 5 in patients treated with PRP. The larger collagen content and maturity of the tissues in PRP treated tendons compared with control may explain the mechanical improvement in the clinical outcome scores.

A limitation of the present study is that testing for mechanical properties of the healed tendon specimens was not performed. This may offer information to augment the histological findings. In addition, this was a single time point biopsy analysis (week 6 post intervention). A better model to assess the progression of the treatment would be to take multiple time-point biopsies and longitudinal analysis of the IHC markers especially proliferation and collagen laying activities.

6.5 Chapter conclusion

Locally applied PRP in Achilles tendon rupture enhance the maturity of the healing tendon tissues by promoting better collagen I deposition, improved Collagen III/Collagen I ratio, reduced cellularity, better vascular structure and higher GAGs content when compared with control. The finding may explain the clinical improvement observed in these patients at week 6 post-intervention onwards.

Chapter 7 PRP in vitro Effect on tissue and tenocyte cultures

7.1 Introduction

In chapter 5 of this thesis, Platelet Rich Plasma (PRP) showed a positive efficacy signal in accelerating the healing of ruptured Achilles tendon in the clinical pilot study. The biological mechanism of the observed PRP action is still under investigation. This may be the result of the combined effect of multiple growth factors stored in the platelet alpha and dense granules (chapter 2). However, PRP also contains leukocytes and fibrin which may play role in the repair. The *in vitro* effect of PRP conditioned medium on animal and human tenocytes has been studied by numerous authors as described fully in chapter 2. These studies suggest that the growth factors released into the plasma by activated platelets act positively upon cells, in ways which would improve initiation and continuation of healing.

Primary cell culture studies provide a platform for elucidating the effects of PRP at cellular and molecular level, however they deliver a reductionist paradigm and data should be interpreted within that context (211). Within the literature there are numerous methods of preparing PRP conditioned medium. This solution contains high concentration of growth factors and other bioactive proteins that are released during clot formation and upon platelet activation and degranulation (chapter 4) (18, 173, 207). However, this solution does not contain any cells nor it contains as high concentration of bioactive proteins as the original PRP. Although, this pragmatic approach is helpful to study the direct effect of growth factors on cells, it does not take into account the direct interaction between cells found in PRP (platelets, white cells and red cells) (136) and tenocytes, nor does it assess the effect of continuing growth factor production at a very high concentration for the remainder of the platelet life span. Finally it discounts the likely differences between *in vitro* model tissues and actual human tendon in injured patients under challenging cell-damaging environments.

As discussed in chapter 2, clinically prepared PRP is in fact a term that includes a wide range of products that have varying biological components (21). Most of these products have varying concentration of blood cells (platelets, white cells and red blood cells) (21). The effect of PRP preparations may vary according to their biological contents. Additionally, it is important when studying PRP effect on cells or tissues to use preparation methods that are identical to clinical preparation techniques and to identify the resultant product viability and biological components. To our knowledge, there is no published human tendon culture study that addresses all the above points.

This chapter aims to investigate, *in-vitro,* some of the possible biological processes that influence the clinically observed improvement in healing. This is achieved by investigating the effect of clinically prepared PRP, along with its cellular components, on tendon tissue and cells viability, tenocytes proliferation and mitogenic activities. The study also aims to study the effect of various PRP products over prolonged incubation periods. The hypothesis is that whole PRP with its cellular components will maintain human tendon tissue and cell viability, increase mitogenic DNA activities and enhance cellular proliferation when compared with controls.

7.2 Methods

Autologous whole blood and tendon tissues were obtained from Achilles tendon rupture patients recruited in Platelet rich plasma in Accelerated Tendo-Achilles Healing (PATH) trial (chapter 5). Whole blood was collected from consented healthy volunteers. All blood and tissue samples were processed in full compliance with HTA (Health Technology Assessment), Oxfordshire Ethics Committee approval (reference: OxREC 09/H0605/78) and with Helsinki Declaration of 1975, as revised on 1983.

The methods here describe the techniques used in obtaining and culturing tendon tissues, tissue and tenocytes experiments and PRP analyses.

7.2.1 Tissue culture

Tendon samples were obtained from patients undergoing Achilles tendon percutaneous repair after obtaining informed consent and recruiting them into PATH trial (as detailed in chapter 5). All patients sustained the rupture during sporting activity and they were asymptomatic prior to rupture. The samples were collected at time of surgery and placed into sterile bicarbonate-buffered Dulbecco's Modified Eagle Medium (DMEM: F12) solution (Lonza, Slough, United Kingdom) and processed immediately after collection according to previously described methods (Appendix 7.1) (350). Samples were carefully cut into approximately 1-3mm^3 sections using a scalpel, under sterile conditions. The sections were transferred to a 6-well cell culture plate and one of the following media was added to each well:

1. 100% PRP (whole autologous PRP with its cellular components)

2. 50% PRP (50:50 whole PRP with its cellular components and DMEM:F12)

3. 50% FCS (50:50 heat-inactivated fetal calf serum and DMEM:F12)

A 50µl drop of 1, 2 or 3 media was applied to each tendon piece, and the media type was consistent for each well. All tendon explants were incubated in a humidified incubator at 37°c in 5% CO_2 and atmospheric Oxygen for 48 hours, after which time cell counts and viability assays were performed (figure 7.1).

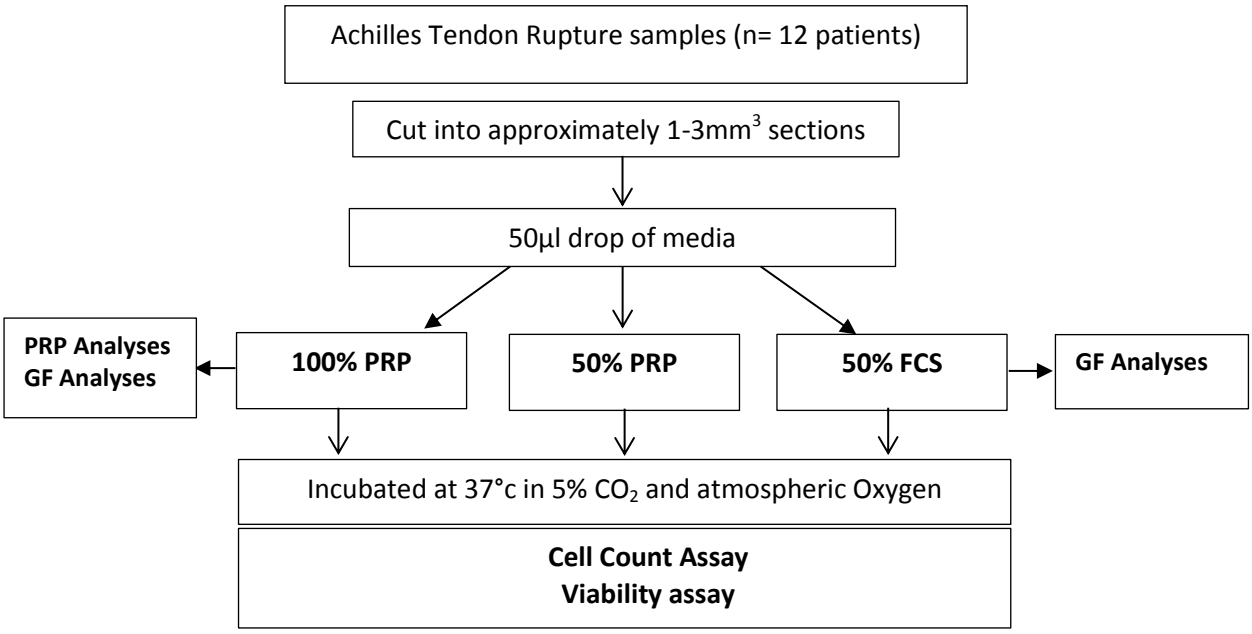


Figure 7 .1 Flowchart of tendon tissue cultures using the three medium types

7.2.2 Tendon cell culture

Tendon explanted pieces, derived from the PATH trial patients, which were not used in the above experiments, were cultured in 50% foetal calf serum (FCS, Biosera,UK) with DMEM: F12 (1:1) and 1% penicillin/streptomycin (Sigma, Poole, UK). After 48 hours of incubation in a humidified incubator at 37°c in 5% CO_2 and atmospheric Oxygen, 1ml of warm medium (DMEM F12 with 50%FBS and 1%penicillin/ streptomycin) was added gently to each well and plates returned to the incubator. Medium exchange and top up was performed every 2-3 days according to the protocol in appendix 7.1. When sufficient number of cells had migrated out from the tendon pieces, normally after 2 weeks, the tendon sections were removed and cells were cultured in DMEM: F12/10% FCS with 1% penicillin/streptomycin. Once the tenocytes reached 70-80% confluence the cells in each well were re-plated in a 10cm petri-dish and were fed with DMEM: F12/10% FCS with 1% penicillin/streptomycin until 70-80% confluent. Cells were then frozen in 10% dimethylsulfoxide DSMO (Sigma, Poole, UK)/ 90% FCS and placed in liquid nitrogen until they are used in this study experiments (Appendix 7.1).

This method of passaging of tenocytes has been well characterized previously, with no phenotypic drift of major tenocyte markers, collagen I, aggrecan and scleraxis until after passage 5 identified within our institute (351). Tenomodulin expression levels are low; typical of tenocytes in monolayer culture, and collagen II is completely absent (351). It has also been demonstrated by other groups that major tenocyte markers such as cell shape, total collagen, the ratio of collagen type I to type III, and decorin expression changes significantly after passage 5 (352). Cells up to passage 3 were used in this chapter experiments. The cells were seeded in the wells of 96-well plates with various medium types applied to each well as explained in each assay below.

7.2.3 PRP preparation

Platelet Rich Plasma was generated from fresh autologous whole blood collected from the same patients at the time of tendon repair (as detailed in chapter 4 and chapter 5). Briefly, Fifty-five millilitres of blood was processed using Magellan® centrifuging device. This clinically used system

automatically harvests PRP after two cycles of centrifuging using an infrared beam to collect the buffy coat (chapter 4). Four ml of the resulting 8 ml of PRP was used clinically and 3 ml were used to produce the abovementioned culture media in tissue culture experiments (figure 7.1). The remaining 1 ml of fresh PRP was immediately sent to the Oxford Haemophilia Centre, Churchill Hospital, for platelet and blood cell counts, platelet function and growth factors concentration assays (chapter 4).

For the tenocyte culture experiments, Platelet Rich Plasma was generated from 55ml of fresh whole blood collected from consented healthy volunteers (age range 25-38) using the same aforementioned preparation method. The resultant 8ml of sterile PRP was used to produce the culture mediums for tenocytes culture experiments [table 7.1]. One ml of this PRP was immediately sent to the Oxford Haemophilia Centre, Churchill Hospital, for platelet and blood cell counts, platelet function and growth factors concentration assays using the methods described in chapter 4.

7.3 Preparation of medium for Tenocyte culture Assays

To study the effect of various components of PRP and culture medium on tenocytes in the study experiments, eight different solutions were prepared. Table 7.1 shows culture medium types and their components. While the 96-well plate layout in each experiment is shown in Figure 7.2.

Whole PRP with its cellular components (platelets, white cells and red cells) was used in the first column of each 96-well plate. In the second column 10%PRP, this also contained blood cells but at a 10% dilution, was applied to cells. Those two column solutions were not activated with thrombin. The third column was used to study the effect of 10%FCS medium. While DMEM:F12 alone was added to the cells in the fourth column as a control medium. To study the effect of non-cellular component of PRP, a 20µm micro filter was used to remove all cells (platelets, white cells and red cells) from whole PRP. This produced PRP releasate, which we used at 10% concentration and 100% concentration in column five and six respectively. In column 7, which did not contain tenocytes, 100% PRP was added to study the background effect of cells in PRP in each experimental assay.

Thrombin is used to activate platelets in laboratory and clinical sittings. The potent effect of Thrombin on platelet leads to fast activation of platelets and release of the granular contents. It also activates the clotting cascade leading to forming fibrin clot. To our knowledge, the proliferative effect of thrombin activated PRP on tenocytes has never been compared to the effect of PRP without thrombin. We studied this by adding thrombin activated whole PRP to wells in column eight.

Tendon tissues are rich in collagen, which has the ability to activate platelets. Following binding of collagen to the receptors, arachidonic acid is released, which is the substrate of the platelet enzyme cyclooxygenase. Cyclooxygenase transforms arachidonic acid into thromboxane A2, a potent platelet activator (353). This was also confirmed in the aggregation experiment in chapter 4. The effect of collagen aggregated platelets in PRP was studied by adding COLtest (Dynabyte GmbH, Germany) to whole PRP and allowing it to clot before applying it to cells in column 6 wells. The last column did not have any cells and DMEM:F12 medium was added to subtract the background signal of this solution in each of the assays.

Table 7.1 shows the culture medium used in our experiments.

	Culture Medium	**Preparation**
1	**100%PRP**	whole PRP with its cellular components
2	**10%PRP**	10% dilution of whole PRP with DMEM:F12
3	**100% F-PRP**	filtered 100%PRP: micro filter was used to remove cells
4	**10% F-PRP:**	10% dilution of the 100% F-PRP with DMEM:F12
5	**10% T-PRP**	10% PPR which is activated using bovine thrombin and calcium chloride
6	**10% C-PRP:**	10% PRP which is activated using COLtest
7	**10% FCS**	10% FCS and 90% DMEM:F12
8	**C**	Dulbecco's Modified Eagle Medium (DMEM: F12)

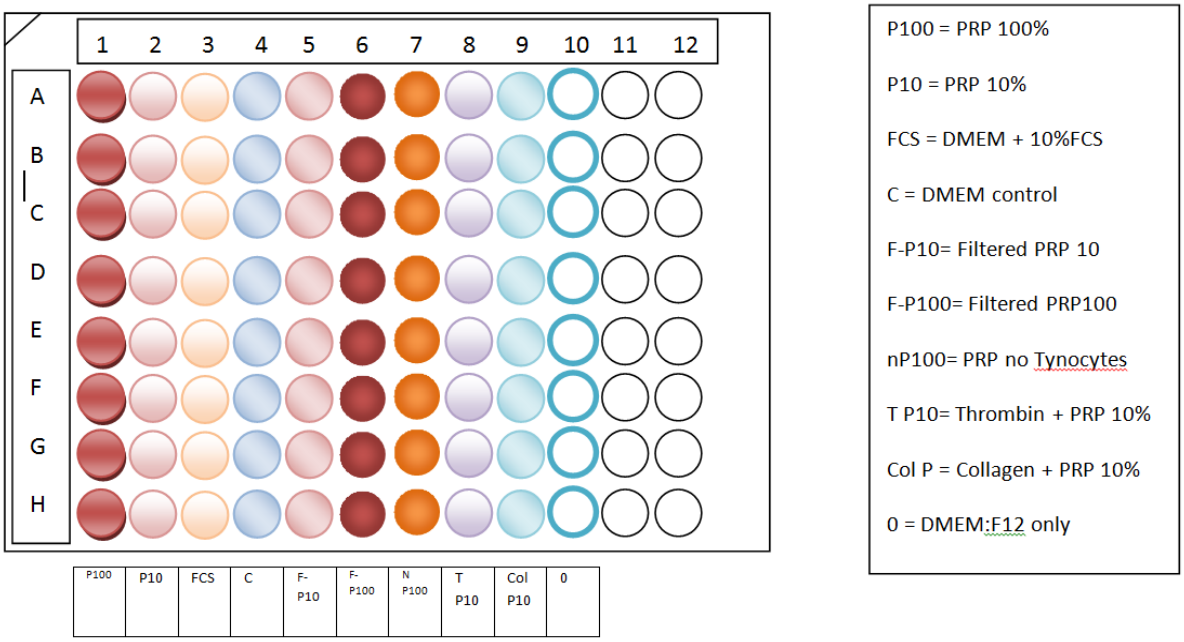


Figure 7 .2 The layout of the 96-well plate used in tenocyte culture experiments with different type of medium in each column. The last two columns are empty. The 7th column did not contain any tenocytes and was used to measure the background of PRP cells in each experiment. Similarly the 10th column did not contain any tenocytes. Tenocytes were cultured in all the wells in remaining columns.

7.3.2 PRP Function assay

Platelets, leukocytes and erythrocytes were counted in each whole blood sample and subsequent PRP preparation using a KX-21N impedance counter (Sysmex UK, Milton Keynes, UK). Platelet viability was studied using the method described in Chapter 4.

7.3.3 Growth Factors Concentration Assay

The growth factor concentration in patients' 100%PRP and 50%FCS was studied immediately after obtaining PRP using specific Enzyme-linked Immunosorbent Assays (ELISA) to quantify the following growth factors: IGF-1, PDGF-AB, TGF-β1 and VEGF. The Quantikine ELISA kits were obtained from R&D Systems Inc, Abingdon, UK, and carried out according to the manufacturers' instructions. ELISA protocol to measure GF concentration is explained in details in Chapter 4 and Appendix 2.5.

7.3.4 Tissue Culture Cell Counting Assay

Each tendon explant was imaged using a Nikon TE300 microscope with Retiga CCD camera. Tenocytes around each explant were counted at 48 hours post initial explantation. A semi-quantitative score was used to calculate the number of tendon cells around each explant in each media solution [Table 7.2 and figure 7.3].

Table 7.2 The semi-quantative score used to quantify cell count around each explant.

Score	Description
0	No cells present around the imaged explant
1	Few scattered cells are present in the microscopic field
2	More than a score of 1 and less than 3: plentiful tenocytes but not confluent
3	Confluent cells covering the whole microscopic field around the explant

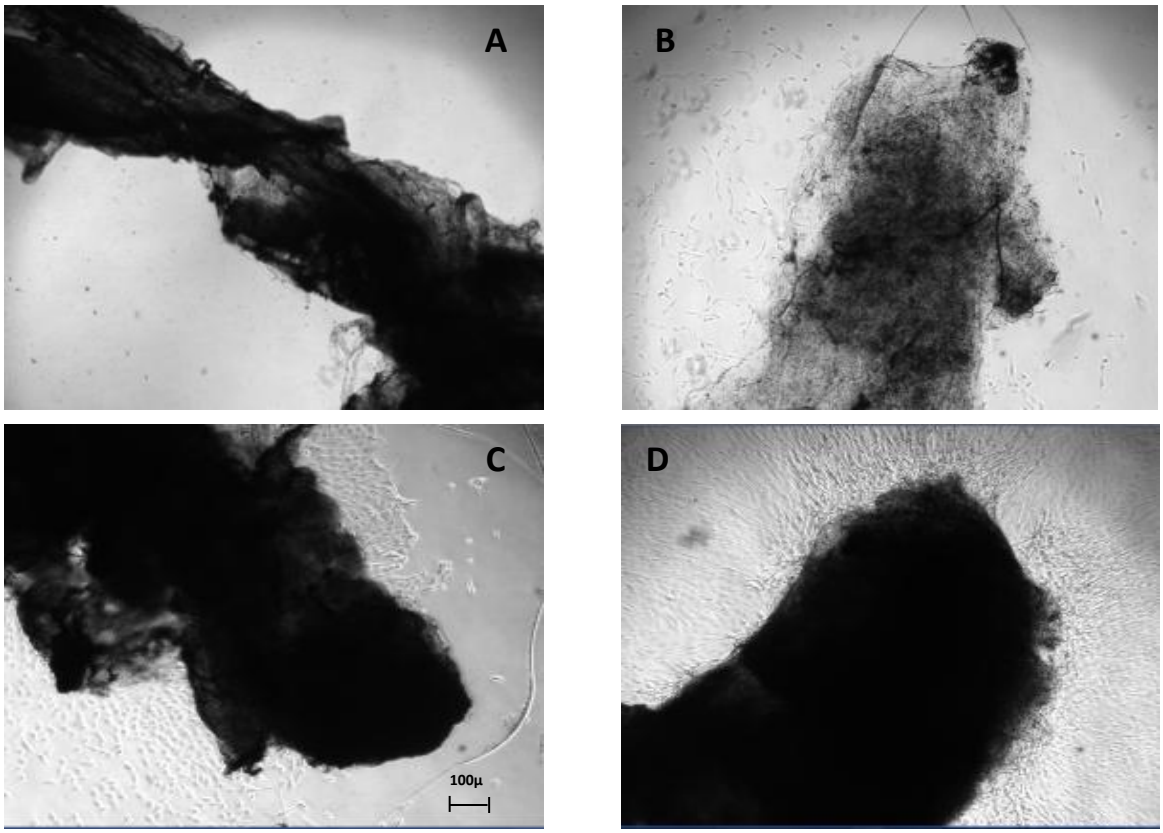


Figure 7 .3 Photomicrographs demonstrating the semi-quantitative scoring system. Figure A represents an explant with score 0, Figure B represents an explant score of 1, figure C demonstrates an explant score of 2, and figure D is a representative image of an explant with score 3.

The total number of cells around each explant determined the score. A score of 0 was determined when there were no discernible cells around the explants (fig 2a). When there were few cells around the explant it was given score of 1 (fig 2b). The highest score of 3 was given to fully confluent cells covering the microscopic field (fig 2d). A score of 2 was given to explants with a cell count between score 1 and 3 (fig 2c). The total number of explants was 349 (100%PRP media n=116, 50%PRP media n=116 and 50%FCS media n=117).

7.3.5 Tissue Viability Assay

The viability of each tendon explant was investigated after 48 hours incubation in the one of the three specific culture media (100%PRP, 50%PRP and 50%FCS). A Live & Dead stain (Invitrogen, Paisley, UK) was used according to the manufacturer's instructions and imaged using a Nikon TE300 microscope with Retiga CCD camera.

This assay is based on the simultaneous determination of live and dead cells with two probes that measure recognized parameters of cell viability—intracellular esterase activity and plasma membrane integrity(354-356). Live cells are distinguished by the presence of ubiquitous intracellular esterase activity, determined by the enzymatic conversion of the virtually nonfluorescent cell-permeant Calcein AM to the intensely fluorescent Calcein.(357) The polyanionic dye Calcein is well retained within live cells, producing an intense uniform green fluorescence in live cells (ex/em ~495 nm/~515 nm). While EthD-1 enters cells with damaged membranes and undergoes a 40-fold enhancement of fluorescence upon binding to nucleic acids, thereby producing a bright red fluorescence in dead cells (ex/em ~495 nm/~635 nm). EthD-1 is excluded by the intact plasma membrane of live cells. (358) The determination of cell viability depends on these physical and biochemical properties of cells. Background fluorescence levels are inherently low with this assay technique because the dyes are virtually non-fluorescent before interacting with cells.

The staining dye was prepared by adding 1 µl of Calcein AM and 1 µl EthD-1 to 1000 µl of PBS. Cultured tendon explants were washed twice in PBS to remove culture media which could interfere with staining. This was followed by adding 200 µl of staining mixture to each tendon explant in the

culture wells and incubated in complete darkness at room temperature for 30 minutes. Afterwards, tendon explants were washed PBS and transferred to glass slides. All explants were imaged and Live/Dead cell ratio was calculated for each tendon explant and compared for all three media types

7.3.6 Alamar Blue Assay- Tenocyte count

Tenocytes at passage 3 were cultured in 96-well plates with the aforementioned 8 media types. Viable cell number in each culture medium was determined using the Alamar Blue® assay at 48 and 96 hours incubation.

The Alamar Blue assay is a sensitive homogeneous fluorometric study of cell viability. It is based on the fact that when cells are metabolising they maintain a reducing environment within their cytosol. The reducing environment in the alamarBlue® assay is measured through the conversion of Resazurin (oxidised form) to Resorufin (reduced form). This results in colorimetric (absorbance) and fluorescence changes. Resazurin is blue and non-fluorescent whereas Resorufin is red and highly fluorescent. This change can be measured spectrophotometrically (359).

Alamar Blue® **(**Abd serotec, Kidlington, UK) was added at 1:10 dilution in DMEM:F12 to the cultures according to the protocol in appendix 7.3. The plate was then incubated for 3 hours. The REDOX state of Alamar blue was measured using a Spectramax Gemini XS microplate reader (Molecular Devices, Sunnyvale, CA, USA) at an excitation wavelength of 530 nm, and emission wavelength of 590 nm, with a 570 nm cut-off.

7.3.7 DNA Content in Tenocytes Assay

Double-stranded DNA (dsDNA) in the tenocytes was measured using Quant-iT™ PicoGreen® dsDNA quantitative kit (Invertrogen Molecular Probes Inc, Paisley, UK) according to the protocol in appendix 7.4.

PicoGreen is an ultrasensitive florescent nucleic acid stain for quantitating double-stranded DNA in solutions (360). In principle, PicoGreen binds to dsDNA and forms a highly luminescent complex when compared to the free dye in solution.

Six different concentration of λdsDNA stock were prepared for the standard curve. Tenocytes cultures were sonicated for 15 seconds each. 10 µl of samples were loaded into the 96-well plate in triplicates. 100 µl of 1 X TE buffer and 100 µl of Picogreen dsDNA quantitation reagent were added to the wells containing standards and samples and left at room temperature in the dark on a plate shaker for 30 minutes. The fluorescence was measured at excitation 490 nm, emission 540 nm and cut off 530 nm with the Spectramax Gemini microplate spectrofluorimeter.

7.3.8 Tenocytes Proliferation Assay

Four types of medium (100% PRP, 100% filtered PRP, FCS and control) were studied in this assay. Considering the high sensitivity of this assay only the above 4 types of media were used. The media were added to the cultured tenocytes in 96-well plates as described above. After 48 hrs incubation a Ziva™ ultrasensitive proliferation assay (Jaden Bioscience Inc, san Diego, USA) was performed according to the protocol in appendix 7.5.

Ziva™ proliferation assay is a non-isotopic ELISA ultrasensitive BrdU Cell Proliferation assay. The assay detects the incorporation of BromodeoxyUridine (BrdU), a DNA precursor, into cell DNA by using a labelled anti-BrdU antibody and detection substrate, in an ELISA format. Ziva™ can be performed in less than 1 hour and is approximately 200-500 times more sensitive than the 3H-thymidine method.

Briefly, after culturing the cells in the aforementioned mediums, BrdU label was added to the wells and left for 2 hours. The samples were centrifuged then rinsed with preparation solution. After adding fixing and stringency solution, anti-BrdU antibodies were added and left for 20 minutes in darkness. The chemiluminescence was measured using SpectraMax Plus 384 Microplate reader

(Molecular Devices Inc, Sunnyvale, USA) in each assay well in terms of Relative Light Units/second (RLU/sec). Each experiment was repeated independently three times for each patient's sample, with each treatment being performed in triplicate wells.

7.4 Results

7.4.1 PRP Function assay

The results of cell count is presented in chapter 4, table 4.1. The results of CD62p platelets viability assay is presented in Chapter 4, table 4.4.

7.4.2 Growth Factors concentration Assay

The concentration of TGF-B1, PDGF-AB, IGF-1 and VEGF in both 100% PRP and 50% FCS is shown in Table 3. The concentration of all growth factors was significantly higher in PRP samples when compared with their concentration in 50%FCS. The PDGF-AB level was 57.1 fold higher in PRP when compared with 50%FCS. The VEGF concentration reached 22 fold the concentration within 50%FCS. The other two growth factors IGF-1 and TGF- ß1 were 5.42 and 7.5 folds higher in PRP respectively.

Table 7.3 The concentration of growth factors in 100% PRP and 50% FCS . The far right column shows the ratio between growth factor concentrations seen in 100% PRP and 50% FCS.

Growth Factor	**PRP**	**50% FCS**	**PRP/FCS**	**P value**
IGF-1	136.5 ± 45.7 ng/ml	25.16 ± 3.6 ng/ml	5.42	< 0.0001
PDGF-AB	32.5 ±15.2 pg/ml	0.56 ± 0.21 pg/ml	57.1	< 0.0001
TGF-ß1	39.9 ± 12.2 pg/ml	5.32 ± 0.11 pg/ml	7.5	< 0.001
VEGF	688.6 ± 51.4 pg/nl	31.3± 2.5 pg/ml	22	< 0.0001

7.4.3 Cell Count Assay

The 352 tendon explants from the 12 participants were analysed using the aforementioned semi-quantative scoring system [table 7.3]. The cell count score in 100% PRP, 50% PRP and 50% FCS media was analysed using Kruskal-Wallis statistical analysis test. Explants cultured in 50% FCS had average cell count score of 1.48, while 100% PRP and 50% PRP average score were 2.14 and 1.9 respectively. 100% PRP and 50% PRP cultures have significantly higher number of cells when compared with 50%FCS cultures (p value was 0.002 and 0.028 respectively). The concentration of PRP also had a significant effect on cell count. Tendon explants cultured in 100% PRP showed significantly higher cell count when compared with 50% PRP (P = 0.018) (Figure 7.4).

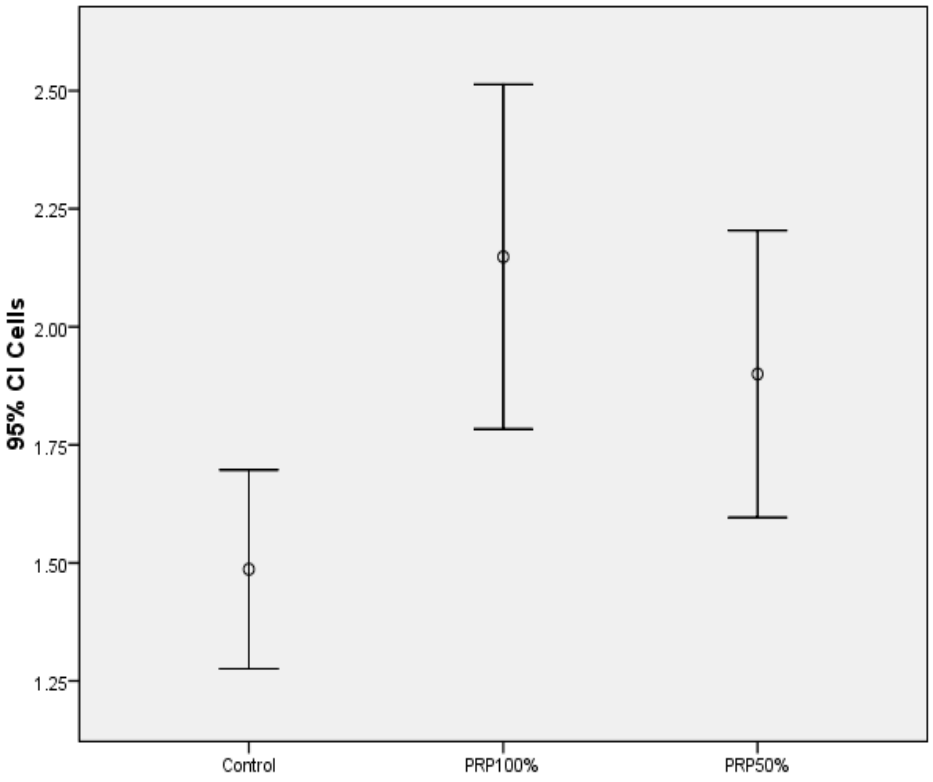


Figure 7 .4 The cell count average score in the three types of culture media: 100% PRP, 50% PRP and control (50% FCS DMEM-F12).

7.4.4 Tendon Tissue Viability Assay

At 48 hours, Tendon explants from the injured tendon cultured in PRP had a higher Live/Dead cell index when compared to explants cultured in 50% FCS (figure 7.5). 92% of cells were viable in those cultures exposed to 100% PRP, 81% were viable after exposure to 50% PRP, and 72% were viable in explants exposed to 50% FCS. Chi-square statistical analyses revealed that 100% PRP is significantly better than 50%PRP and 50%FCS in maintaining viability of tissues (P= 0.018 and 0.0001 respectively). Interestingly there was no significant statistical difference between 50% PRP and 50% FCS Live/Dead cell index (p = 0.07) (Figure 7.6).

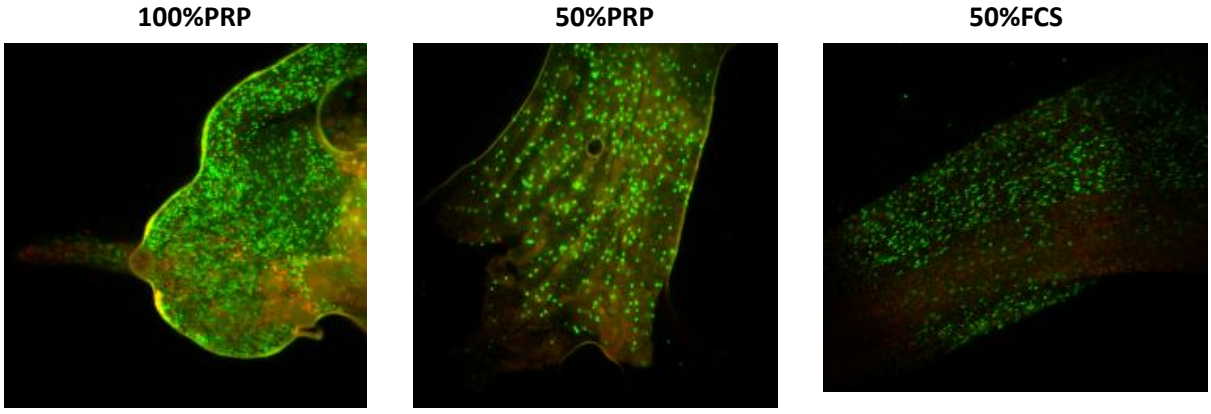


Figure 7 .5 Live & Dead staining in three samples cultured in the three media types. Florescent green cells are viable cells while red stained cells are non-viable.

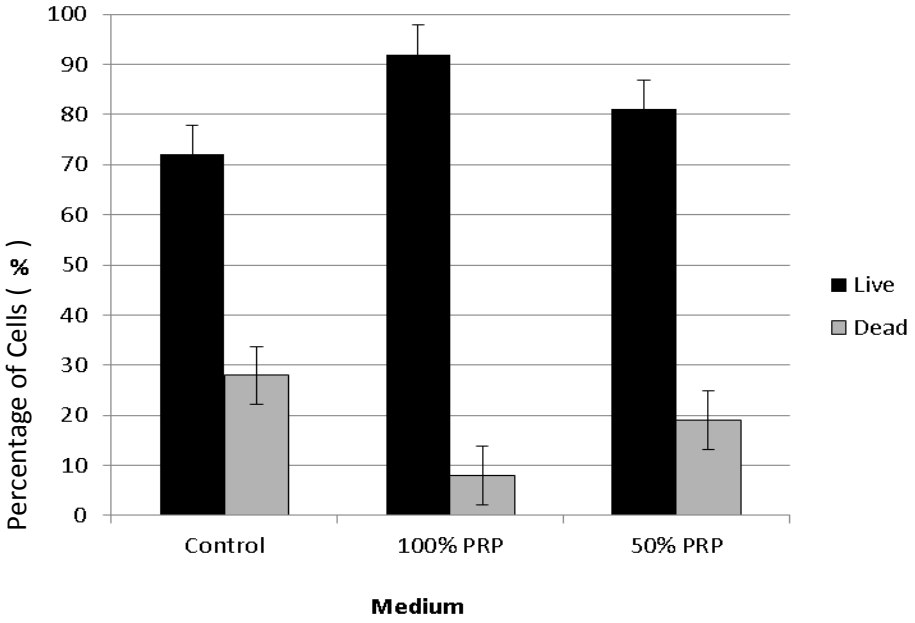


Figure 7 .6 Live dead cell tissue index in the three culture media types 100% PRP, 50% PRP and control (50% FCS DMEM-F12).

7.4.5 Alamar Blue Assay- Tenocyte count

Our experiments were performed over a wide range of PRP media and controls as shown in table 7.1. Alamar Blue fluorescence was measured as a reflection of metabolic activity and viability of tenocytes. The results for 48-hour and 96-hour incubation with all media types are shown in figure7.7. All media showed remarkable increase in florescence at 96-hours when compared with 48-hour incubation.

One way ANOVA statistical tests showed that the effect of PRP100% exceeded that of any other media type at both 48 and 96 hours ($p < 0.001$). At 48 hours there was no difference between Thrombin, collagen, 10%fPRP and FCS media effects on tenocytes viability. However, those media effects were significantly higher than 10%PRP (p 0.031). This difference levelled at 96 hours making the effect of Thrombin, Collagen, 10%PRP, 10%fPRP and FCS the same. Interestingly, cellular 100%PRP effect on maintained cells viability continued to significantly exceed that of filtered 100%PRP at both time points (p 0.025 and 0.018 respectively). The effect of cellular 10%PRP was similar non-cellular 10%fPRP at both time lines. It is also worth noting that the effect of 100%PRP nearly doubled at 96 hours when compared with 48 hour culture (P 0.031).

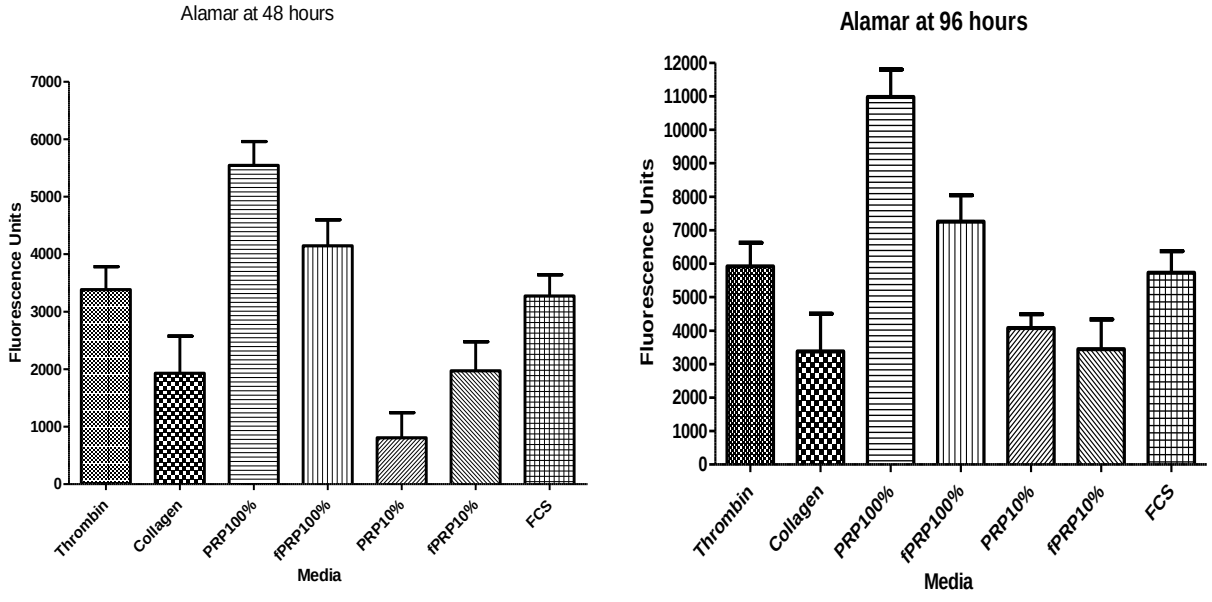


Figure 7 .7 Alamar Blue assay results after 48 hours incubation with culture medias (on the left). The result of this assay at 96-hour incubation is on the right.

7.4.6 DNA Content in Tenocytes Assay

The double strand DNA content of tenocytes was analysed at 48 and 96 hour culture in each of the media types. At 48 hour there was no difference between 100%PRP and 100%fPRP. The average dsDNA content in tenocytes cultured in cellular and non-cellular 100%PRP was approximatly 1.59, 2 and 10.6 folds higher than 10%PRP, FCS and 10%fPRP respectively (P <0.001). Double stranded DNA content was also higher in tenocytes subjected to thrombin activated PRP compared to collagen activated PRP (figure 7.8).

The dsDNA content continued to increase in the 100%PRP media and became significantly higher than 100%fPRP after 96 hour incubation (P 0.037). The effect of the other media types on dsDNA content reached similar levels at this time point (P >0.05). The effect of 100%PRP also increase significantly at 96 hour when compared with 48 hour incubation period (p value) (figure 7.8).

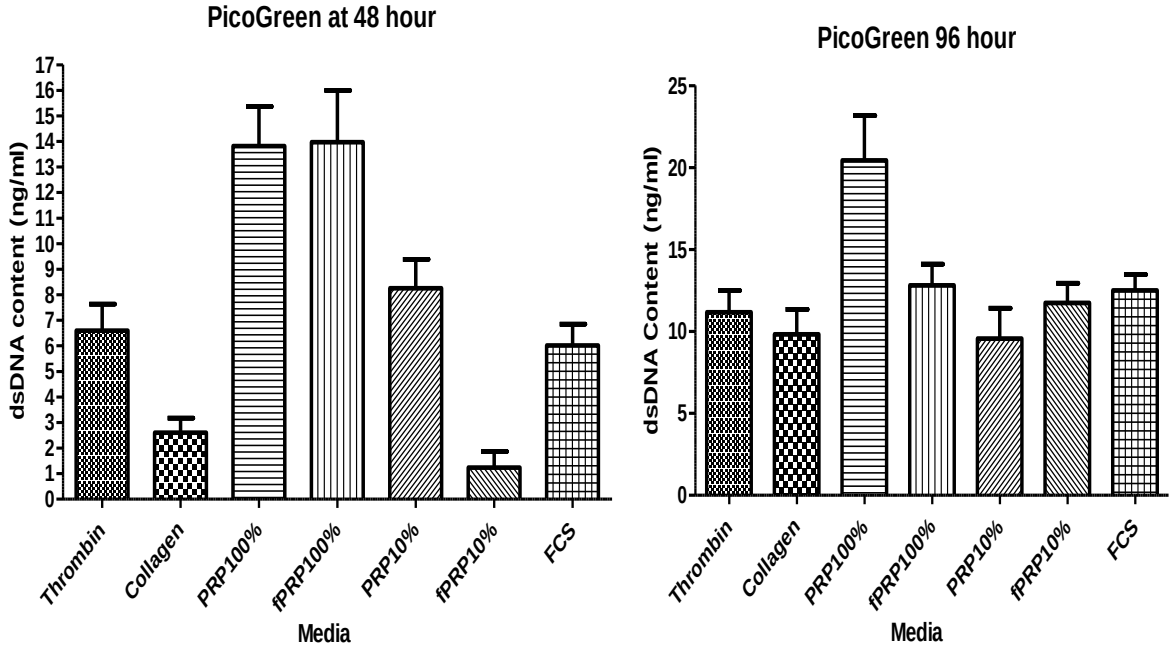


Figure 7 .8 The effect of media on dsDNA content of tenocytes after 48-hour (left) and 96-hour (right) incubation.

7.4.7 Tenocytes Proliferation Assay

After 48 hour of incubation with 100%PRP, fPRP100%, 50%FCS and control, tenocytes proliferation significantly increased in the presence of 100%PRP compared to filtered non-cellular media (fPRP100%), FCS and control [figure 7.9] (One way ANOVA test P<0.001, Tukey's post-hoc test P<0.05, P<0.001 and P<0.001 respectively). There was also significant increase in proliferation with fPRP100% when compared with 50%FCS and control (P 0.046 and 0.026 respectively). There was no difference between FCS and control.

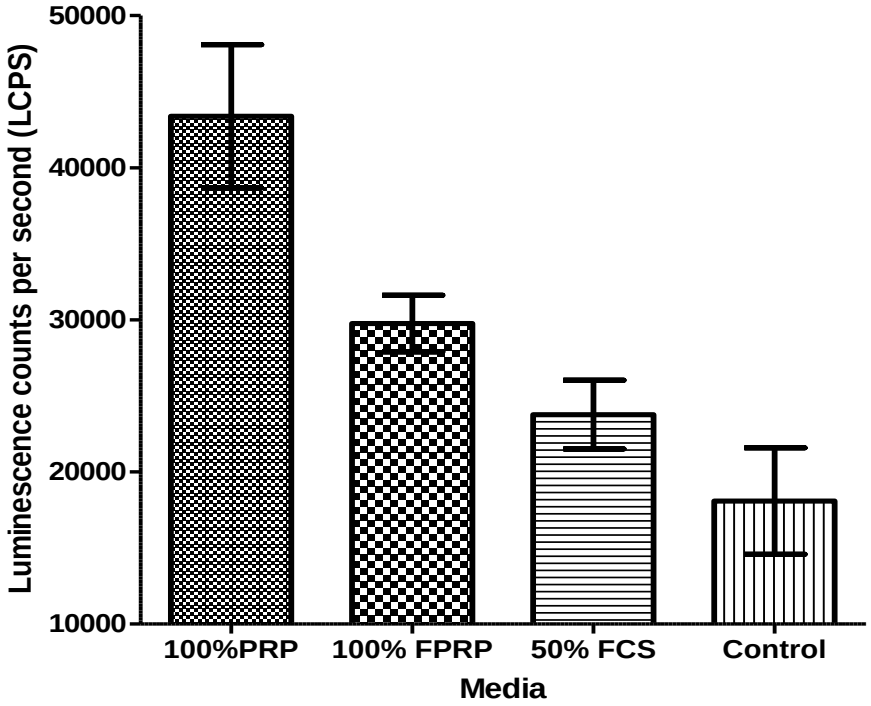


Figure 7 .9 The results of cell proliferation assay after 48 hour incubation.

7.5 Chapter Discussion

There are four important factors that need to be addressed when trying to study PRP biological effect on tenocytes: firstly the PRP preparation method and its resemblance to clinical preparation techniques, secondly the actual biological component of platelet concentrates, thirdly the viability of platelets within the PRP preparation and fourthly the use of autologous products. To our knowledge, there is no published human tissue culture study that addresses all the above mentioned points.

In the current study, steps were incorporated in our experiments to address each of the above points. The preparation technique is one of the commercially available pieces of clinical equipment, which is widely used in clinical practice in both operative and non-operative treatment.(12) This preparation method was used in the linked clinical trial (PATH) to assess PRP use in acute Achilles tendon rupture.

Highly concentrated viable autologous PRP with its entire cellular component was used in this chapter to investigate its potential proliferative and migratory effect on human tendon tissues. Moreover, the ability of PRP to maintain tissue viability in culture environment that resembles the post injury local environment was also studied. Quantifying tenocytes viability, dsDNA content and proliferation, which are key factors in tendon regeneration, after exposure to various concentrations of PRP was performed using cells cultured from ruptured tendons.

The results data showed that PRP significantly increased the number of tenocytes in the medium around each tendon tissue piece. This implies that PRP may have attracted cells to migrate from the targeted tendon tissue via the chemotactic effect of growth factors such as: PDGF-AB (151), IGF-1 (157), PF-4(160). Tenocytes migration to the injury site plays an important role in the repair process and lying of collagen matrix. The proliferative effect of PRP on migrating cells was also evident in our experiment. This effect may be caused by the proliferative influence of PDGF (1, 150, 151), TGF-β (146, 151, 361) and IGF-1 (1, 203, 204) on tenocytes. This effect forms a keystone in tendon regeneration and matrix production by tenocytes (362). Furthermore, cellular PRP increased the mitogenic activities of tenocytes leading to increase dsDNA content to a much higher level than other media types. Although the effect of both PRP100% and fPRP100% was similar at 48 hours, DNA content at longer incubation period showed the continuing effect of cellular PRP. This effect was also confirmed using ultrasensitive proliferation assay, which showed that tenocytes proliferation was significantly better with the presence of PRP cells.

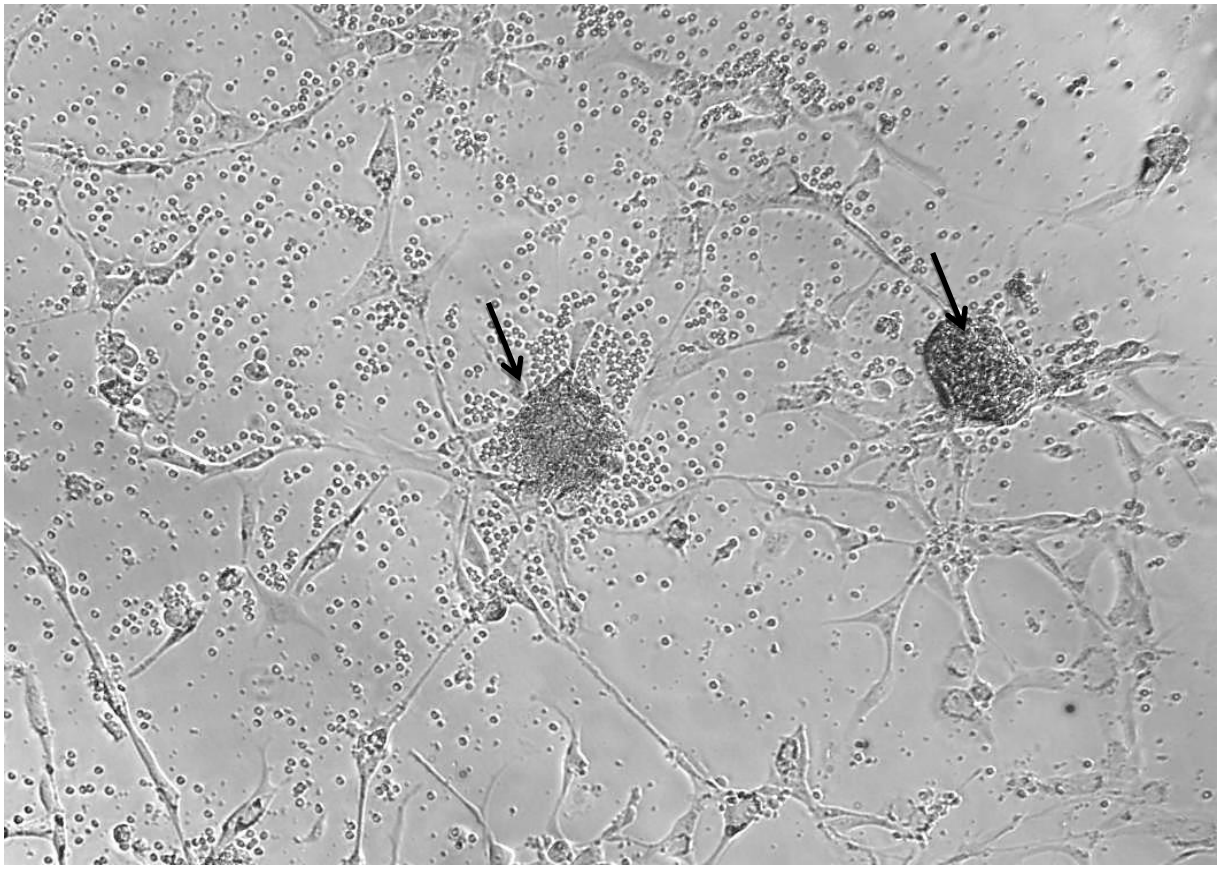


Figure 7 .10 Light microscopy image of tenocytes cultured with PRP in this study. Platelet clots or aggregations (arrows) seem to attract congregations of tenocytes around it. This may indicate intracellular interaction.

PRP also contains high concentration of leukocytes (L-PRP IB1). The effect of PRP components on tenocytes is a complex process that may involve growth factors and cytokines produced by both platelets and leukocytes. The direct cellular interaction between platelets, leukocytes and tenocytes is still largely unknown [figure 7.10]. Currently, it is well established that the initial binding of the platelets to the injured endothelium at the tissue injury site is mainly mediated by binding platelet GP Ibα to endothelial vWF, exposed collagen as well as binding to the endothelial adhesion molecule P-selectin (363). Polymorphonuclear leukocyte (PMN) adhesion to activated platelets is important for the recruitment of PMN at sites of tissue damage. The binding of activated platelets to PMN involves P-selectin and the activated β_2-integrin CD11b/CD18. (141)

The results suggest that PRP effectively protects against the loss of viability of tenocytes induced by both hypoxia and acidosis that ensues in the acute post tendon rupture time frame or immediately

following surgery (364, 365). The results of the Alamar blue assay showed that cellular 100%PRP is significantly better than any other media type at maintaining tenocyte viability. This effect exceeded that of non-cellular PRP (fPRP100%) and less concentrated solutions. Interestingly this effect significantly increased after 96 hours incubation, which may indicate that PRP cells (platelets and leukocytes) continued to produce bioactive proteins and that there may be direct cellular interaction with target cells.

However the mechanism by which PRP protects tenocytes from the adverse effects of the harmful environment and maintains tissue viability has yet to be investigated. The interaction between platelet-produced growth factors and cytokines with hypoxia-inducible factor-1 (HIF-1) has been suggested. (366) Hypoxia-inducible factor-1 (HIF-1) is a key regulator responsible for the induction of genes that facilitate adaptation and survival of cells and the whole organism from normoxia (~21% O_2) to hypoxia (~1% O_2) (367, 368). Cytokines and growth factors, as well as hypoxia in some cell types, can activate signalling pathways MAPK and PI3K, which promote cell proliferation/survival as well as contribute to HIF-1 activity. (369).

7.5.2 Limitations of the in-vitro studies

The experiments presented in this chapter have a few limitations. Firstly; cell culture studies did not include mechanical loading of tenocytes, which has been shown to regulate tenocytes proliferation and differentiation in a loading-magnitude dependent manner (370). However, physiological loading of tendons is best studied in an *in-vivo* animal or human studies. In chapter 3 of this thesis, we presented a novel technique to quantify mechanical properties of Achilles tendon and in chapter 5 this method was used in Achilles tendon rupture patients to study the progression of mechanical healing of the tendon.

Secondly; it is not possible to include other tissues that exist at the site of tendon injury such as paratenon and blood vessels in cell culture studies. This may only be possible with *in vivo* human or animal studies. This has been factored in the clinical trial and the immunohistological response to

PRP, including angiogenesis, is presented in chapter 6. Thirdly; the effect of dilution that may occur in the tissues is assessed by using low PRP concentration (10%). However the exact percentage of dilution and its extent is not known. The results of the experiments showed that the low 10% PRP concentration had positive effect on tenocytes although it didn't match that of whole PRP.

Further; the in vitro studies were carried out in normoxic conditions. It would be more desirable to use a hypoxic incubator to better replicate the in vivo injury site of the Achilles.

7.6 Chapter Conclusion

In conclusion, the *in-vitro* studies showed that autologous PRP with its cellular components, which include platelets, leukocytes and erythrocytes, has the ability to stimulate tendon cell migration to the injury site and stimulate proliferation in clinically relevant injured human tendon. Additionally, it may maintain tissue viability in the hypoxic environment that follows tendon injury. Promoting migration and proliferation of cells and maintain tissue viability may play an important role to accelerate tendon healing.

Chapter 8 General Discussion and Future Work

The story of this project has been built around a multi-dimensional approach (laboratory, mechanical and clinical studies) to determine the mechanobiological interactions and clinical applications of PRP in Achilles tendon rupture. The rational for this approach was introduced in Chapter 1 and summarised in figure 1.10. Tendon healing occurs at various stages of biological repair that result in significant changes at various levels in tendon structure, mechanical properties and clinical progress.

In order to establish the biological and clinical efficacy of PRP this project included experiments that allowed the exploration of the aforementioned healing levels as well as exploring the biological properties of PRP. The human cellular and tissue laboratory experiments, which are linked to *in vivo* mechanical and clinical studies formed the backbone of this research project. The tissue and cellular studies included assays that provided information on potential PRP mechanism in the targeted injured tendon tissues. In addition the clinical pilot trail provided a platform to detect efficacy signal using a combination of objective and subjective outcome measures. While FUSE tool offered information on the progression of the mechanical maturity of the healing tendon tissues.

In this chapter, the findings of each chapter's experiments are discussed in the light of the overall aim of this thesis.

8.1 Platelets Rich Plasma Biological properties

The effect of PRP on tissue healing is likely to be a function of many variables, which include: PRP biological characteristics, tissue injury type and extent, existing tissue condition prior to injury and the overall medical condition of the patient. PRP properties are measurable and can be altered to improve the outcome. Therefore, identifying the biological properties of PRP and understanding its correlation to clinical outcomes is crucial when studying PRP in clinical trials (6). With wide range of PRP products available commercially, the link between each product and clinical effect is crucial.

In this project, PRP preparation system was chosen from a list of commercial systems available for clinical application (table 2.3). This system was used to prepare autologous PRP for the clinical trial and laboratory experiments, which allowed the interpretation of clinical findings. Exploring the components of this product confirmed both the viability of platelets post centrifuging and the high concentration of growth factors and cells.

8.1.1 PRP potential bioactive componenets

This clinically applicable PRP had very high concentration of platelets when compared with whole blood platelets count. Interestingly, this technique did not just increase the platelet count by 4.74 fold but also more than doubled the count of leukocytes with reversal of the lymphocyte neutrophils ratio (class L-PRP 1B). This ratio reversal has not been reported before and its effect is yet to be explored.

High autologous leukocytes concentration may play a role in the inflammatory phase of tendon healing (39) but the relation between the concentration and tendon regeneration has never been studied before. Most published *in-vitro* PRP studies tend to focus on the role of platelets and their bioactive proteins and ignore the role of leukocytes. It is known that leukocytes move to the injury site and start producing cytokines and interleukins, which may pave the way for the inflammatory response that follows (39). The interaction between platelets, leukocytes and local cells still largely unidentified. Currently, it is well established that the initial binding of platelets to the injured endothelium at the tissue injury site is mainly mediated by binding platelet GP Ibα to endothelial vWF and exposed collagen as well as binding to the endothelial adhesion molecule P-selectin (363). Polymorphonuclear leukocyte (PMN) adhesion to activated platelets is important for the recruitment of PMN at sites of tissue damage. The binding of activated platelets to PMN involves P-selectin and the activated β_2-integrin CD11b/CD18 (141). The mechanism of platelets and leukocytes interaction with tenocytes in the tendon tissues needs to be further explored in purposely-designed experiments.

In addition, despite the double centrifugation cycles, a small amount of erythrocytes remained in PRP making it red in colour. Although erythrocytes are present in the haematoma that ensue following the injury, their role in tissue repair remains unclear.

Bioactive proteins in PRP are largely produced by platelet dense granules, however leukocytes may also contribute to the cocktail of growth factors, cytokines and interleukins. In this project, the concentration of relevant growth factors was remarkably higher than that of whole blood (table 4.2). VEGF, PDGF-AB and TGF-β1 concentrations were remarkably higher than IGF. Weibrich et al found similar results with regards to IGF-1 level in PRP (134). The interpretation of IGF-1 levels is complicated by the wide normal ranges, and variations by age, sex, and pubertal stage (310). Although PRP effect is likely to be a complex process, these highly concentrated growth factors may kick start the regenerative pathways of the targeted tissues (7, 12).

Further, tencocytes and fibroblasts may also boost the level of growth factors by producing growth factors such as VEGF and HGF (207). This may play role in local fibroblast response to injury and leukocytes regulation (361).

8.1.2 Platelets viability

Platelets are delicate anucleated cells that go through biochemical, morphological and functional changes when prepared or stored in inadequate conditions. Those changes lead to platelet senescence and eventual death, which is characterised by loss of functional responsiveness to agonists (thrombin or collagen), loss of plasma membrane integrity, degranulation, loss of aggregation and lack of survival upon implantation into recipients (301). Hence, PRP preparation techniques need to be gentle to avoid destroying platelets yet powerful enough to increase platelet concentration. The assessment of platelet viability in PRP in both resting and activated states is vital to ascertain the efficacy of PRP products.

In a novel study, platelet function and viability in the PRP used in this thesis studies was studied using CD62P expression. The results confirmed that the majority of platelets in PRP were viable in resting state after preparation. The platelets became active after adding thrombin and expressed CD62P, which indicates degranulation and release of alpha granules contents (371).

8.1.3 PRP Activation

Platelet activation is a measurement of the population of platelets that can be activated by a stimulus. Platelet degranulation occurs upon activation and leads to the release of growth factors stored in their alpha and dense granules [chapter 2]. In a novel study, Collagen and thrombin influence on platelet aggregation in PRP was studied using normal saline as a passive control.

The results revealed that platelets in PRP retained the complex aggregation function. It also confirmed that collagen is an active agonist that causes platelet aggregation in PRP that matches the thrombin aggregation effect.

However, autologous thrombin production is costly and time consuming. Considering that collagen is abundant in the injured tendon, it is possible that PRP may be injected directly into the injury site without the need of thrombin. In this thesis the pilot trial was conducted and completed in order to provide PRP samples for this experiments therefore these finding was not applied. Future trials should consider injecting PRP without thrombin activation.

8.1.4 PRP classification

Not all available PRP products are actually compliant with PRP definition. Most platelets concentrate products are termed Platelet-Rich Plasma (PRP). Unfortunately, this term is very general and incomplete, leading to confusion in the scientific literature and misleading conclusions (table 2.3). Clinically prepared PRP is in fact a term that include of wide range of products that have varying biological components (21). Most of these products have varying concentration of blood cells (platelets, leukocytes and erythrocytes). Building on previous attempts by Ehrenfest (21) and Mishra

(280) to classify PRP products, A new classification system is recommended. This new system uses a combination of numeric and alphabetical characters to identify the class of PRP product. In addition to the identifiers in Ehernfest and Mishra classifications: Leukocytes, Fibrin, the new system will also include: activation, platelet concentration and preparation method categories (table 2.7). Determining PRP product class in clinical trials will help establish the link between efficacy of each PRP product in the condition under study.

8.2 Functional Ultrasound Elstography: An outcome tool

8.2.1 FUSE use in ATR

The study of the mechanical properties of the tendon has been so far employed either in an *in-vitro* studies using excised tendons or *in-vivo* using invasive techniques. In this thesis, a novel non-invasive method to measure strain and displacement of the tendon and display it in a colour image is introduced. The volunteer study confirmed that this method is feasible using clinically applicable ultrasound scan machine and method. The novel algorithm allowed investigators to visualize tendon displacement and measure localised strain within the studied tissues. Controlled FUSE was better in measuring tendon strain and showed crisper and more accurate images than manual FUSE and commercial elastography. This study demonstrated that controlled FUSE was successful in delivering sufficient acquisition quality for effective tendon elasticity imaging. In Achilles tendon rupture, this tool was able to track the changes in local strain throughout follow-up (figure 5.16, page 137). The feasibility of this technique was demonstrated in the pilot trial even in the initial presentation at the acute phase. Interestingly, dorsiflexion movement allowed good visualisation of local strain, which also correlated with clinical outcome measures.

There are, to my knowledge, no other literature reports on similar experiments for measuring strain in healthy or ruptured tendons. Further work still needs to be performed to improve the ability to measure forces and thereby estimate material properties of the tendon. Purposely designed experiments too test the validity and repeatability of this technique is recommended.

8.3 Clinical efficacy of PRP in ATR: Pilot study

8.3.1 Feasibility assessment

The method employed was found to be easy to use in both outpatient and operating theatres. Furthermore, platelets in PRP were viable and produced high concentration of growth factors upon activation. Patient position for treatment in the outpatient clinic or in theatre facilitated intervention blinding and imaging of the tendon. The table top centrifuging device was easy to use in outpatient clinic and theatre. The automated PRP harvesting technique allowed surgeons to be free while PRP is prepared and eliminated variation in the sample that may result from manual preparation techniques. The two adverse events reported were not related to PRP treatment confirming the safety of this product.

8.3.2 PROMS signal

The results of the linear regression analysis of the primary outcome measure ATRS revealed that PRP group had significantly better ATRS score progression from week 3 till week 24 in operative and non-operative treatments. Further analysis of the subgroups showed no difference in operative treatment pathway and significant difference in the conservatively treated patients (figure 5.7 and 5.8). This was also confirmed when analysing VISA-A score. PRP groups had significantly better progression from week 6 onwards. There was no difference in operative treatment groups. Significant difference was found in conservatively treated groups. Foot and Ankle Outcome Score (FAOS) Linear regression analysis of FAOS showed that the only significance was in pain score ($p<0.05$). The other components of this score were not significantly different between PRP and control groups. This outcome measure is designed for chronic foot and ankle conditions and it has not been validated in acute Achilles tendon rupture. SF-36 showed improvement of PCs component between baseline and final follow-up but there was no difference between PRP and control.

8.3.3 Objective outcome measure

8.3.3.1 FUSE

Manual compression-decompression method did not show any relationship with clinical scores. The images resulting of this technique showed poor strain mapping of the different structures in the area (figure 5.15). While functional elastography in dorsal and plantar motion (DF and PF) showed good imaging of strain in the affected area at acute presentation and during the follow-up scans. There was visual correlation between the progression of strain measurement and PROMS trend. This shows the correlation between mechanical improvement in the tendon tissue and related outcome measure components.

Using the fat pad as a normalising structure, the strain index was calculated to allow monitoring of normal mechanical properties restoration. The index progression over the follow-up period showed that the index decreases to reflect the reinstatement of the tendon strain properties. PRP showed better progression of the index from week 8 post intervention onwards.

8.3.3.2 Maximum heel rise and Calf Girth ratio

PRP did not improve maximum heel rise at 24 weeks follow up. Although calf girth progressed better throughout the follow up period, there was no difference at the final follow-up point. This is likely to be due to the existing variation between patients and the small number recruited in this pilot study.

8.4 Tendon Immunohistochemical response to PRP

The findings of the histology and immunohistochemistry studies of specimens obtained at 6 weeks post intervention confirmed that PRP may have accelerated the maturation of the healing ruptured tendon. This was evident in lower cellularity and vascularity of the healing tendons that were treated with PRP compared with control. Additionally, the collagen fibre structures were more organised with higher collagen I content and better collagen III/ collagen I ratio. Higher GAGs content was also observed in tendons exposed to PRP six weeks earlier. To my knowledge, this study is the first of its kind to study *in-vivo* human ruptured Achilles tendon immunohistochemistry response to PRP.

This chapter's findings help explain the improvement in clinical outcome scores presented in chapter 5 in patients treated with PRP. The larger collagen content and maturity of the tissues in PRP treated tendons compared with control may explain the mechanical improvement in the clinical outcome scores.

8.5 In-vitro PRP effect on cells and tissues

8.5.1.1 Tissue response

In this novel study, highly concentrated viable autologous PRP with its entire cellular component was used in this chapter to investigate its potential proliferative and migratory effect on human tendon tissues obtained from ruptured Achilles tendons. The results showed that PRP significantly increased the number of tenocytes in the medium around each tendon tissue piece. This implies that PRP may have attracted cells to migrate from the targeted tendon tissue. Tenocytes migration to the injury site plays an important role in the repair process and lying of collagen matrix. The experiment also confirmed that PRP maintained tissue viability which exceeded that of positive control.

8.5.1.2 Cells response to PRP

PRP increased the mitogenic activities of tenocytes leading to increase dsDNA content when compared to positive and negative controls. Although the effect of both PRP100% and fPRP100% was similar at 48 hours, DNA content at longer incubation period showed the continuing effect of cellular PRP. This effect was also confirmed using ultrasensitive proliferation assay, which showed that tenocytes proliferation was significantly better with the presence of PRP cells.

8.6 The efficacy signal of PRP in ATR: in –vitro and in-vivo

The results of the above chapters confirmed the positive efficacy signal of PRP application in Achilles tendon rupture. The combination of linked *in-vitro* and *in-vivo* studies offered better understanding of the potential mechanism of PRP. The *in-vitro* signal was confirmative and showed that PRP with its cellular components enhanced tenocytes proliferation, migration and DNA content. The clinical

study results on the other hand were indicative of positive efficacy signal in tendon function progression to normality. To confirm this signal an appropriately powered randomised controlled trial is recommended. The data from this pilot study and from ATRS validation paper (2) allows the calculation of sample size and inform the methodology.

8.7 Limitations

8.7.1 Limitations of Elastography Studies

These studies have a number of limitations. Extensive testing of elastography validity in breast cancer was carried out at the University of Oxford. However, this algorithm musculoskeletal validity testing is on the way and data captured in the volunteer and patient studies will help refine and validate the protocol. A group of engineers collaborating with surgeons is now testing the validity of different algorithm protocols using *in-vitro* experiments. Capturing images and RF data was performed by this thesis author. Although this offered good data homogeneity, the measurements needed to be repeated at different times by the same observer to allow inter-observer measurement. This was not possible due to the acute nature of this injury and the changes in the healing tissues over time. Measurement of intra-observer error and repeatability assessment was not possible. A purposely designed study to assess inter- and intra-observer error is recommended.

Progression of strain index was compared to PROMS progression; however histological correlation of the findings was not possible as the biopsies were only done at one time point (week 6). Moreover, correlation with biomechanical parameters, such as the amount of physical activity, was not available.

Rigorous repeatability, reliability and responsiveness tests of FUSE technique needs to be carried out in purposely designed experiments. This work is now been carried out by a DPhil student at the Institute of Biomedical engineering in collaboration with this thesis author.

8.7.2 Limitations of PRP Biological Properties studies

There are several limitations related to these studies. First of all, the small number of blood and PRP samples obtained from patients did not allow correlation between cells and growth factors concentration and outcome measures. This correlation may inform the ongoing debate whether PRP concentration plays part in the clinical response. Similarly the correlation between cells concentration and growth factor concentration was not possible. It is assumed that the higher platelet and white cells concentration in the mix the higher the growth factors levels. However it is not possible to test this assumption with small number of samples.

Further, identifying growth factors producing cells was not possible in this project. Although most authors advocate that platelets produce most of the bioactive factors initially. The role of white cells in producing and regulating bioactive proteins synthesis and release is still unknown. Purposely designed studies to investigate the role of leukocytes in PRP are recommended.

8.7.3 Limitations of the clinical pilot study

The number of recruited patients in this pilot study limits its power and results can not be extrapolated to acute Achilles tendon treatment in pragmatic settings. Therefore, the results are indicative but not conclusive. In addition, the pilot study included patients from both operative and non-operative treatment pathways under the assumption that biological and clinical healing tendon healing is not different between the two. This assumption facilitated the analyses of PRP technique in both settings and allowed the detection of efficacy signal. Although Khan et al (114) meta-analysis showed no difference between operative and non-operative treatment in terms of functional outcome at 24 week, Surgical intervention may alter the biological environment and lead to varying effect of PRP. To detect the effect of PRP in each treatment, PRP efficacy trials need to be performed in one treatment pathway or adequately powered to allow adequate analysis of each pathway and comparison between the two.

The Achilles Tendon Total Rupture Score (ATRS) is a validated patient-reported outcome measure incorporating questions relating to muscle strength and fatigue, pain, lower limb function and disability (2, 372) but it does not contain objective components. This has been considered by an external reviewer of the future trial to be a limitation and the use of objective outcome measure was recommended. In PATH trial, objective outcome measures such as calf girth, FUSE, maximal heel raise and maximum ROM were used to support the primary outcome measure. However the small number of participants did not allow confirmative analysis. This informed the design of the future trial and sample size will allow analysis of primary objective outcome measure and secondary PROMs (see Future Work section).

8.7.4 Limitations of the histology studies

A limitation of the histological study is that testing mechanical properties of the healed tendon specimens was not performed. This may offer information to augment the histological findings. In addition, this was a single time point biopsy analysis (week 6 post intervention). A better model to assess the progression of the treatment would be to take multiple time-point biopsies and longitudinal analysis of the IHC markers especially proliferation and collagen laying activities.

The small size of the biopsy samples allowed the analysis of small number of selected IHC markers to identify important tendon tissues response to the intervention. Analysing more potential pathways will help to identify possible PRP effect mechanism that may be responsible for its effect. Using newly developed high throughput mRNA profiling bioinformatics platform techniques will allow analysing numerous numbers of markers and pathways from the small sample tissue. This will generate gene expression profiling and allow the comparison between the expression levels of many genes between sample groups. Understanding PRP bioactive proteins influence on genes expression will allow further manipulation or alteration of PRP components to target effective pathways.

8.7.5 Limitations of in-vitro cell and tissue studies

The experiments presented in this Chapter 7 have a few limitations. Firstly; cell culture studies did not include mechanical loading of tenocytes, which has been shown to regulate tenocytes proliferation and differentiation in a loading-magnitude dependent manner (370). However, physiological loading of tendons is best studied in an *in-vivo* animal or human studies. In-vivo mechanical assessment is challenging and so far non-invasive techniques are not available. Although FUSE presents a novel method to quantify some of the mechanical properties in living tissues, this will need rigorous validation tests.

Secondly; it is not possible to include other tissues that exist at the site of tendon injury such as paratenon and blood vessels in cell culture studies. However, studying those structures is best performed using *in-vivo* methods such as the analysis of histological samples, which is presented in Chapter 6.

Thirdly; the effect of dilution that may occur in the tissues is assessed by using low PRP concentration (10%). However the exact percentage of dilution and its extent is not known. The results of the experiments showed that the low 10% PRP concentration had positive effect on tenocytes although it didn't match that of whole PRP.

Further; the in vitro studies were carried out in normoxic conditions. It would be more desirable to use a hypoxic incubator to better replicate the in vivo injury site of the Achilles. However, this on its own does not resemble the post injury environment and would be considered as simplification of the complex changes that occur post injury. A better model may be *in-vivo* animal or human study to assess cells and tissue response to the changing environment post injury at various stages of healing.

8.8 Future Work

At the time of writing this thesis, funding to conduct a major randomised controlled trial was secured from the National Institute of Health Research (NIHR). The suture trial design and methodology is presented below. This is a phase II multi-centre UK-wide RCT to evaluate the efficacy and mechanism of PRP in patients with Achilles tendon rupture treated non-operatively. If proven efficacious then the next step is to explore the role of PRP as a biological adjunct or alternative therapy to costly surgical repair. This will be done in a randomised control trial comparing PRP in conservatively treated tendon with tendons treated surgically.

8.8.1 Multi-Centre Randomised Controlled Trial

8.8.1.1 Rational for the proposed study

Despite the lack of high-quality trial data, PRP administration remains an attractive strategy given its cost-effective and minimally invasive nature. The clinical evidence for PRP use in acute tendon injury is limited to small cohort studies. In Achilles tendon rupture, two under powered cohort studies showed conflicting results (14, 274). Two recent reviews concluded that the poor methodological quality of trials assessing PRP for tendon injury meant evidence for effectiveness is limited (275, 276). A systematic review/meta-analysis of PRP for orthopaedic conditions (373) stated the need for adequately powered studies using disease-specific and patient-important outcomes and to investigate the efficacy of PRP.

There has been a recent spike in PRP use for musculoskeletal conditions. It is estimated that PRP is used to treat 86000 tendons annually in the United States and a similar number in Europe.(374)

In the UK, there is evidence that PRP injections are starting to be used in NHS clinical practice, in addition to wider use in private sports medicine. We explored the use of PRP in NHS hospitals and found four NHS trusts offering PRP for tendon injuries. In addition a NICE review of PRP use (IP 549/2 [IPG 438]) states that some specialist advisors' noted that this was an established practice. It is of

concern that these techniques are being introduced without adequate investigation into their efficacy or standardisation of protocols. This exposes patients to an intervention that may require further clinical investigation. The NHS is also incurring extra treatment costs for a treatment with unproven clinical effects. Therefore, providing evidence for PRP effectiveness in improving Achilles tendon rupture outcome has potential major benefits for patients and the NHS. There is a pressing need to undertake this study before the use of PRP becomes widely adopted.

8.8.1.2 Hypothesis

PRP application as an adjunct to standard care will achieve improved musculotendinous function and patient recovery after acute Achilles tendon rupture (ATR) in adults

8.8.1.3 Trial objectives

The proposed research objectives are:

1. Evaluate the clinical efficacy of PRP in acute ATR in terms of mechanical muscle-tendon function
2. Evaluate the clinical efficacy of PRP in acute ATR in terms of patient reported functional recovery, pain and quality of life
3. Determine the key components of PRP that contribute to its mechanism of action
4. Further understand in a sub-study the mechanisms of PRP immunohistochemical effects, which may be account for its clinical efficacy. This includes tendon tissue regeneration, cell differentiation, collagen formation, tissue morphology and pain neuroreceptors count in the healing tendon.
5. Identify the histological pathways that PRP may alter to exert its effects. Using these results and that from the PRP biological component sub-study, to inform future targeted manipulation of PRP properties to maximise its efficacy in tendon healing.
6. Inform the design of a potential future major evaluative confirmatory clinical trial of optimal PRP therapy versus surgical repair for ATR in restoring patient function.

8.8.1.4 Research Design

A prospective multi-centre, double blinded, randomised, placebo-controlled trial.

Two sub-studies are embedded within the main study to understand the active PRP biological components distribution in the affected population and to study the immunohistochemical response which may explain its mechanism in healing tendons. This information combined with the objective and subjective clinical outcomes will ascertain PRP efficacy and primary mechanism.

The sub-studies are:

1) PRP components analysis (107 participants): measures cell concentrations, platelet activation and growth factor concentrations in PRP.

2) Tendon immunohistochemical response to PRP in comparison to control (16 participants): analysis of relevant tissue healing markers and pathways.

8.8.1.5 Allocation and Randomisation

15 NHS hospital orthopaedic units will participate to recruit 214 patients with acute ATR. Participants and assessors will be blinded to intervention allocation. Participants are blinded using the same method we used in our pilot study. Patients will be prone on an examination couch with the foot and ankle slightly off the edge of the bed. Participants will not be able to see the intervention on their tendon. Both treatment and control procedures are performed after local anaesthetic injection and with same size needles. Assessors are trained research nurses and physiotherapists, who will assess the participants outcome and they will not be informed of the intervention type. Randomisation is performed via remote computer-generated permuted blocks of random and undisclosed sizes stratified by site and age to minimise imbalance in mobility and tendon health between groups.

8.8.1.6 Study population

All patients with acute Achilles tendon rupture attending within 7 days of sustaining the injury will be eligible for inclusion in the trial. The same inclusion exclusion criteria used in the pilot trial will apply in this trial.

8.8.1.7 Planned interventions

Participants will be randomly assigned to intervention or control via remote computer-generated permuted blocks of random and undisclosed sizes stratified by site and age to minimise imbalance in mobility and tendon health between groups. Allocations: **PRP group**: local anaesthetic and PRP injection to the tendon rupture gap. **Control Group**: local anaesthetic injection to skin, then needle insertion into tendon. The control injection will mimic PRP injection. Same needle size and location is used. The needle is introduced via skin to the tendon tissue and withdrawn without injecting anything so the biological haematoma is not disturbed (312).

8.8.1.8 Proposed outcome measures

Primary outcome measure: Heel-rise endurance test (HRET)

To comply with funder feedback an objective outcome measure was chosen. The HRET is a commonly used clinical assessment of mechanical muscle-tendon function (375). The test involves repeated concentric-eccentric muscle activity in single leg stance. Instrumented measurements using a linear encoder (Ergotest technology, Norway) have been shown to provide optimal methods of assessment of muscle function when compared to simple counts or height of the heel-raises performed (376). The HRET has also been used in a clinical trial comparing surgical and non-surgical treatment of ATR and was found to be more sensitive to group differences than patient-reported outcomes at 6 months(372). Previous studies have established that the HRET is reliable in healthy and ATR groups (377, 378). Work performed during the test (in Joules) is calculated by calibrated instruments and software, and is then converted into a limb symmetry index (%), comparing injured and uninjured limbs to normalise each participant's performance (injured/uninjured*100). We

would standardise the test for this trial by developing SOPs and providing training to the blinded assessors. All outcome assessors will be physiotherapists who are familiar with such procedures and will be trained by the trial research physiotherapist. HRET has also been shown to have similar reliability to Isokinetic muscle testing (377).

8.8.1.9 Secondary Outcome Measures

Achilles Tendon Rupture Score (ATRS)

The ATRS is an injury specific patient-reported outcome measure incorporating questions relating to muscle strength, fatigue, pain and function. A systematic review of patient-reported outcome measures used to assess Achilles tendon rupture management identifies the ATRS as the only questionnaire that has literature supporting content and construct validity, internal consistency, reproducibility and responsiveness(379). The ten items are each scored on a 0 to 10 Likert scale and are summed to give a score between 0 and 100, with a higher score indicating less symptoms and better physical function(2). Validation studies have indicated the score has minimal ceiling effects and no floor effects(315). Originally developed in Sweden, a recent study from the UK has validated the English language version of the ATRS, reporting excellent same-day test-retest reliability at 3, 6 and 12 months post-rupture (overall ICC=0.99). The ATRS has been shown to correlate with the ability to perform a heel-raise at 12 weeks (an earlier indicator of muscle strength recovery) after rupture and also the degree of fear of movement (Tampa Scale for Kinesiophobia)(380). The ATRS has so been shown to significantly correlate with heel-rise endurance measurements at 6 months(376).

Other secondary outcome measures

1. Daily pain diary for 2 weeks (VAS): records pain in the early phase of healing
2. Patient Specific Functional Scale (PSFS): a PROM developed to be used with patients with varying levels of independence and recovery goals(381). The patient is asked to identify 5 activities they are having difficulty with or are unable to perform due to the injury, and rate

the current difficulty on an 11-point scale. The items are then rescored on follow-up to quantify changes in disability status specific to the patients goals(382).

3. SF-12: a health-related Quality of Life scale
4. PRP components analysis (sub-study 1): cells count, selected tendon active Growth Factors (TGF, VEGF, PDGF, IGF & FGF) concentrations and platelet activation status (CD62P expression)
5. Immunohistochemohistry analysis (sub-study 2) (16 participants: 8 in each arm): samples will be scored by a blinded histologist using validated histological score (Bonar and Movin). Proliferation(KI-67), Collagen I & III, neuroreceptors and hypoxia/reactive oxygen species Immunohistochemistry markers are scored using automated image analysis software

8.8.1.10 Assessment and follow up

Standardisation of post-intervention rehabilitation

There is heterogeneity in the rehabilitation protocols after Achilles rupture(383). We are in the process of conducting a two-stage survey of major trauma centres and existing research collaborators to assess what rehabilitation protocols they would find acceptable for non-operative Achilles tendon rupture within a clinical trial. The results from the first stage from 80 clinicians suggest consensus will be feasible in terms of the position and method of ankle immobilisation, and also guidelines on timescales for return to weight-bearing and dynamic activities such as running and jumping.

Assessment of efficacy/effectiveness

Outcomes will be assessed at key clinical points

1. Baseline: ATRS, PSFS, SF-12 A recall of pre injury function
2. 2 weeks: VAS daily record of pain
3. Week 4, 7 and 13: ATRS, PSFS and SF-12 will be recorded by a telephone call

4. Week 24: ATRS, PSFS, SF-12 and HRET are obtained in clinic by a trained blinded physiotherapist.
5. PRP component analysis (107 PRP samples from PRP group) is analysed using BCSH guidelines with automated cell counter and validated CD62p expression flowcytometry technique (9). Growth factors (TGF, VEGF, PDGF, FGF and IGF) will be analysed using ELISA/multiplex.
6. The histology substudy: a small needle tendon biopsy under ultrasound guidance (an outpatient local anaesthetic sterile technique) at week-6. Our pilot study demonstrated the safety and pragmatic use of this technique.

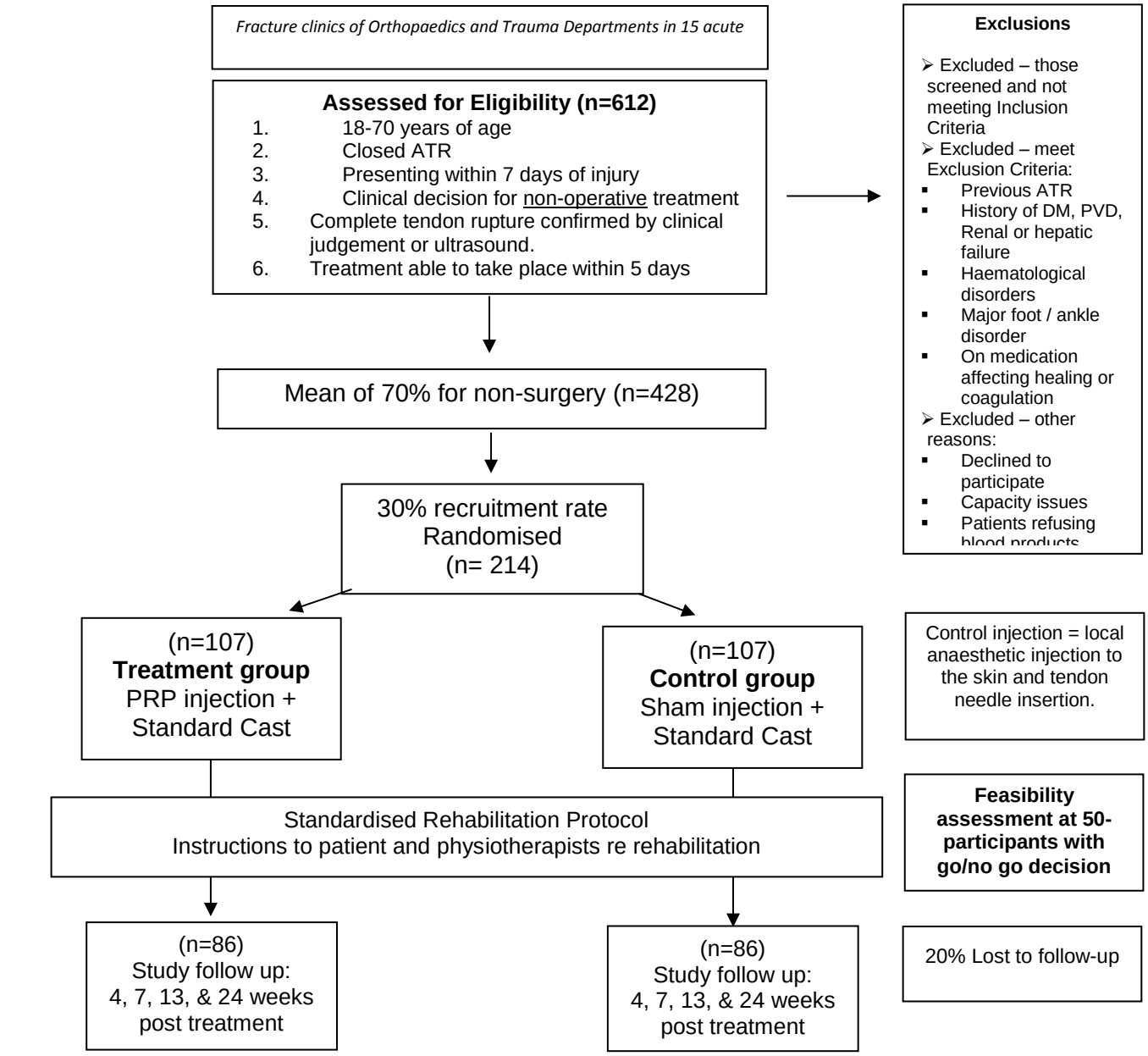
8.8.1.11 Proposed sample size

214 patients (107 per arm including 20% loss to follow-up) will be recruited to detect a standardised difference of 0.5 in the HRET work measured by the LSI at 24 weeks post randomisation and to give 90% power with 2-sided 5% significance level. Based on previous data (376) indicating a clinically important difference of 10% and SD of 20. This will also give the power to test an effect size of 0.5 in ATRS (patient reported outcome) which equates to a difference of 11 based on an SD of 21.4.

8.8.1.12 Statistical analysis

The primary outcome will be the HRET measured by the LSI at 24 weeks post randomisation. If the primary outcome is normally distributed then the two groups will be compared using a t-test, ANCOVA adjusting for stratification factors (primary analysis) and ANCOVA adjusting for additional prognostic factors in a multivariate framework. For all continuous outcomes if there are severe departures from normality the first approach will be transformation. If the data cannot be transformed to normality then the Mann-Whitney U test will be used and in this case no adjustment will be made. The analysis will be by intention to treat. Patterns of missing data will be explored (i.e missing at random or missing completely at random). We will use multiple imputation technique to test the sensitivity of our findings to missing data.

8.8.1.13 The future trial flow chart



Primary Outcome
Heel-Rise Endurance Test (HRET) at 24 weeks

Secondary Outcomes

At baseline, 4, 7 and 13 weeks by telephone and at week-24 hospital visit:

- **ATRS**
- **Patient Specific Functional Scale (PSFS)**
- **SF-12**
- **Adverse Events**
- **Pain diary** (Visual Analogue Scale over 2 weeks post intervention)

PRP components analysis

- Cell count analysis in PRP at baseline (107 samples)
- Platelet Activation Analysis (107 samples)
- Growth Factors Concentration in PRP (107 samples)

Subgroups - Evidence on PRP mechanism

16 participants in total (8+8 in each arm) in 1 or 2 recruiting sites with Research Fellow support

Subgroup study

Needle Biopsy at 6 weeks

Immunohistochemistry analysis for:

- Pain receptors
- Cell markers including angiogenesis
- Proliferation markers
- Collagen markers

8.9 Conclusion

The use of PRP as an adjunct to standard treatment in Achilles tendon rupture has been shown to improve the mechanobiological and clinical outcomes in both *in vitro* and *in vivo* studies.

The viability and growth factors releasing ability of PRP was confirmed in novel experiments. This viable clinically prepared PRP was then used in a series of *in* vitro experiments to investigate the effect or PRP on the injured Achilles tendon cells and tissues. The results confirmed that PRP maintained tenocytes and tissue viability, increased tenocytes migration and proliferation. The presence of cells in PRP (Platelets and leukocytes) led to sustained significantly improved effect when compared with control.

The clinical application of PRP in this debilitating injury showed a positive efficacy signal that PRP led to faster healing, improved pain and earlier restoration of function. The findings of this pilot trial were indicative and not confirmative. A large adequately powered multicentre study to determine clinical efficacy in pragmatic setting is recommended.

The findings of this project has informed the design of a phase II large multi-centre randomised controlled trial and helped secure major funding from the National Institute of Health Research (NIHR). This trial will offer key information for PRP use tendon treatment.

Bibliography

1. Molloy T, Wang Y, Murrell GAC. The Roles of Growth Factors in Tendon and Ligament Healing. Sports Medicine. 2003;33(5):381-94.
2. Nilsson-Helander K, Thomeé R, Grävare-Silbernagel K, Thomeé P, Faxén E, Eriksson BI, et al. The Achilles Tendon Total Rupture Score (ATRS). The American Journal of Sports Medicine. 2007 March 1, 2007;35(3):421-6.
3. Metz R, Kerkhoffs G, Verleisdonk E-J, van der Heijden G. Acute Achilles tendon rupture: minimally invasive surgery versus non operative treatment, with immediate full weight bearing. Design of a randomized controlled trial. BMC Musculoskeletal Disorders. 2007;8(1):108.
4. Rompe JD, Nafe B, Furia JP, Maffulli N. Eccentric Loading, Shock-Wave Treatment, or a Wait-and-See Policy for Tendinopathy of the Main Body of Tendo Achillis. The American Journal of Sports Medicine. 2007 March 1, 2007;35(3):374-83.
5. Alsousou J FS, Hulley P, Thompson M, McNally E, Willett K. The Effect of Platelet Rich Plasma (PRP) on Tendon Regeneration: An in vitro Tissue Culture Study. International Symposium on Ligament and Tendon XI; Jan University of California: ISL&T; 2010. p. 58.
6. Engebretsen L, Steffen K, Alsousou J, Anitua E, Bachl N, Devilee R, et al. IOC consensus paper on the use of platelet-rich plasma in sports medicine. Br J Sports Med. 2010 Dec;44(15):1072-81.
7. Anitua E, Andia I, Ardanza B, Nurden P, Nurden AT. Autologous platelets as a source of proteins for healing and tissue regeneration. Thromb Haemost. 2004 Jan;91(1):4-15.
8. Nurden A. Platelets, Inflammation and tissue regeneration. Thromb Haemost. 2011;105 (Suppl 1):S13-33.
9. Coppinger JA CG, Toomey S, et al. Charecterization of the protein released from activated platelets leads to localization of novel platelet proteins in human atherosclerotic lesions. Blood. 2004;103:2096-104.
10. Bucholz RW HJ, Court-Brown CM. Bone and joint healing: Lippincott Williams & Wilkins; 2006.
11. Marx RE. Platelet-rich plasma (PRP): what is PRP and what is not PRP? Implant Dent. 2001;10(4):225-8.
12. Alsousou J, Ali A, Willett K, Harrison P. The role of platelet-rich plasma in tissue regeneration. Platelets.0(0):1-10.
13. Alsousou J, Thompson M, Hulley P, Noble A, Willett K. The biology of platelet-rich plasma and its application in trauma and orthopaedic surgery: a review of the literature. J Bone Joint Surg Br. 2009 Aug;91(8):987-96.
14. Sanchez M, Anitua E, Azofra J, Andia I, Padilla S, Mujika I. Comparison of surgically repaired Achilles tendon tears using platelet-rich fibrin matrices. Am J Sports Med. 2007 Feb;35(2):245-51.
15. Anitua E, Andia I, Sanchez M, Azofra J, del Mar Zalduendo M, de la Fuente M, et al. Autologous preparations rich in growth factors promote proliferation and induce VEGF and HGF production by human tendon cells in culture. J Orthop Res. 2005 Mar;23(2):281-6.
16. Oprea WE, Karp JM, Hosseini MM, Davies JE. Effect of platelet releasate on bone cell migration and recruitment in vitro. J Craniofac Surg. 2003 May;14(3):292-300.
17. Tohidnezhad M, Varoga D, Wruck CJ, Brandenburg LO, Seekamp A, Shakibaei M, et al. Platelet-released growth factors can accelerate tenocyte proliferation and activate the anti-oxidant response element. Histochem Cell Biol. 2011 May;135(5):453-60.
18. Zargar Baboldashti N, Poulsen RC, Franklin SL, Thompson MS, Hulley PA. Platelet-Rich Plasma Protects Tenocytes From Adverse Side Effects of Dexamethasone and Ciprofloxacin. The American Journal of Sports Medicine. 2011 September 1, 2011;39(9):1929-35.
19. Fallouh L, Nakagawa K, Sasho T, Arai M, Kitahara S, Wada Y, et al. Effects of autologous platelet-rich plasma on cell viability and collagen synthesis in injured human anterior cruciate ligament. J Bone Joint Surg Am. 2010 Dec 15;92(18):2909-16.

20. Akeda K, An HS, Okuma M, Attawia M, Miyamoto K, Thonar EJ, et al. Platelet-rich plasma stimulates porcine articular chondrocyte proliferation and matrix biosynthesis. Osteoarthritis Cartilage. 2006 Dec;14(12):1272-80.
21. Dohan Ehrenfest DM, Rasmusson L, Albrektsson T. Classification of platelet concentrates: from pure platelet-rich plasma (P-PRP) to leucocyte- and platelet-rich fibrin (L-PRF). Trends Biotechnol. 2009 Mar;27(3):158-67.
22. Harrison P. Measuring platelet function? Hematol J. 2004;5 Suppl 3:S164-9.
23. Marx RE. Platelet-rich plasma: evidence to support its use. J Oral Maxillofac Surg. 2004 Apr;62(4):489-96.
24. Burgess J. The Death and Afterlife of Achilles. Baltimore: Johns Hopkins University Press p 9 ISBN 0-8018-9029-2 Retrieved 5 February 2010. 2009.
25. Cummins EJ AB, Carr BW, Wrigh RR. The structure of calcaneal tendon (of Achilles) in relation to orthopaedic surgery With additional observations on the plantaris muscle. Surg Gynecol Obstet. 1946;83:107–16.
26. O'Brien M. The Anatomy of the Achilles Tendon. Foot and Ankle Clinics of North America. 2005;10(2):225-38.
27. Doral M, Alam M, Bozkurt M, Turhan E, Atay O, Dönmez G, et al. Functional anatomy of the Achilles tendon. Knee Surgery, Sports Traumatology, Arthroscopy. 2010;18(5):638-43.
28. Jozsa L, Kannus P, Balint JB, Reffy A. Three-dimensional ultrastructure of human tendons. Acta Anat (Basel). 1991;142(4):306-12.
29. Frey C, Rosenberg Z, Shereff MJ, Kim H. The retrocalcaneal bursa: anatomy and bursography. Foot Ankle. 1992 May;13(4):203-7.
30. Szaro P, Witkowski G, Śmigielski R, Krajewski P, Ciszek B. Fascicles of the adult human Achilles tendon – An anatomical study. Annals of Anatomy - Anatomischer Anzeiger. 2009;191(6):586-93.
31. Lagergren C, Lindholm A. Vascular distribution in the Achilles tendons: an angiographic and micro-angiographic study. Acta Chir Scand. 1959;116(suppl):491 - 5.
32. Ahmed I, Lagopoulos M, McConnell P, Soames R, Sefton G. Blood supply of the Achilles tendon. J Orthop Res. 1998;16:591 - 6.
33. Kannus P. Structure of the tendon connective tissue. Scand J Med Sci Sports. 2000 Dec;10(6):312-20.
34. Gould N, Korson R. Stenosing tenosynovitis of the pseudosheath of the tendo Achilles. Foot Ankle. 1980 Nov;1(3):179-87.
35. Birk DE, Fitch JM, Babiarz JP, Doane KJ, Linsenmayer TF. Collagen fibrillogenesis in vitro: interaction of types I and V collagen regulates fibril diameter. J Cell Sci. 1990 Apr;95 (Pt 4):649-57.
36. Franchi M, Quaranta M, De Pasquale V, Macciocca M, Orsini E, Trire A, et al. Tendon crimps and peritendinous tissues responding to tensional forces. Eur J Histochem. 2007;51 Suppl 1:9-14.
37. Elliott DH. Structure and Function of Mammalian Tendon. Biol Rev Camb Philos Soc. 1965 Aug;40:392-421.
38. Jozsa L, Kannus P. Histopathological findings in spontaneous tendon ruptures. Scand J Med Sci Sports. 1997;7:113 - 8.
39. Lin TW, Cardenas L, Soslowsky LJ. Biomechanics of tendon injury and repair. Journal of Biomechanics. 2004;37(6):865-77.
40. Fukuta S, Oyama M, Kavalkovich K, Fu FH, Niyibizi C. Identification of types II, IX and X collagens at the insertion site of the bovine achilles tendon. Matrix Biology. 1998;17(1):65-73.
41. Butler DL, Grood ES, Noyes FR, Zernicke RF. Biomechanics of ligaments and tendons. Exerc Sport Sci Rev. 1978;6:125-81.
42. Carlstedt CA. Mechanical and chemical factors in tendon healing. Effects of indomethacin and surgery in the rabbit. Acta Orthop Scand Suppl. 1987;224:1-75.
43. Jozsa L, Balint JB, Reffy A, Demel Z. Histochemical and ultrastructural study of adult human tendon. Acta Histochem. 1979;65(2):250-7.

44. Zhang G, Ezura Y, Chervoneva I, Robinson PS, Beason DP, Carine ET, et al. Decorin regulates assembly of collagen fibrils and acquisition of biomechanical properties during tendon development. Journal of Cellular Biochemistry. 2006;98(6):1436-49.
45. Raspanti M, Congiu T, Guizzardi S. Structural aspects of the extracellular matrix of the tendon: an atomic force and scanning electron microscopy study. Arch Histol Cytol. 2002 Mar;65(1):37-43.
46. Jozsa L, Lehto M, Kvist M, Balint JB, Reffy A. Alterations in dry mass content of collagen fibers in degenerative tendinopathy and tendon-rupture. Matrix. 1989 Mar;9(2):140-6.
47. Jarvinen M, Jozsa L, Kannus P, Jarvinen T, Kvist M, Leadbetter W. Histopathological findings in chronic tendon disorders. Scand J Med Sci Sports. 1997;7:86 - 95.
48. Khan KM, Cook JL, Maffulli N, Kannus P. Where is the pain coming from in tendinopathy? It may be biochemical, not only structural, in origin. Br J Sports Med. 2000 Apr;34(2):81-3.
49. Chuen FS, Chuk CY, Ping WY, Nar WW, Kim HL, Ming CK. Immunohistochemical characterization of cells in adult human patellar tendons. J Histochem Cytochem. 2004 Sep;52(9):1151-7.
50. McNeilly CM, Banes AJ, Benjamin M, Ralphs JR. Tendon cells in vivo form a three dimensional network of cell processes linked by gap junctions. J Anat. 1996 Dec;189 (Pt 3):593-600.
51. Waggett AD, Benjamin M, Ralphs JR. Connexin 32 and 43 gap junctions differentially modulate tenocyte response to cyclic mechanical load. Eur J Cell Biol. 2006 Nov;85(11):1145-54.
52. Schweitzer R, Chyung JH, Murtaugh LC, Brent AE, Rosen V, Olson EN, et al. Analysis of the tendon cell fate using Scleraxis, a specific marker for tendons and ligaments. Development. 2001 Oct;128(19):3855-66.
53. Pauly S, Klatte F, Strobel C, Schmidmaier G, Greiner S, Scheibel M, et al. Characterization of tendon cell cultures of the human rotator cuff. Eur Cell Mater. 2010;20:84-97.
54. Kadler KE, Holmes DF, Trotter JA, Chapman JA. Collagen fibril formation. Biochem J. 1996 May 15, 1996;316(1):1-11.
55. Parry DAD, Craig AS. Collagen fibrils and elastic fibers in rat-tail tendon: An electron microscopic investigation. Biopolymers. 1978;17(4):843-55.
56. Benedict JV, Walker LB, Harris EH. Stress-strain characteristics and tensile strength of unembalmed human tendon. Journal of Biomechanics. 1968;1(1):53-6, IN11, 57-63.
57. Screen HRC, Lee DA, Bader DL, Shelton JC. An investigation into the effects of the hierarchical structure of tendon fascicles on micromechanical properties. Proceedings of the Institution of Mechanical Engineers, Part H: Journal of Engineering in Medicine. 2004 February 1, 2004;218(2):109-19.
58. Korhonen R, Saarakkala S. Biomechanics and Modeling of Skeletal Soft Tissues2011.
59. Cui L, Maas H, Perreault EJ, Sandercock TG. In situ estimation of tendon material properties: differences between muscles of the feline hindlimb. J Biomech. 2009 Apr 16;42(6):679-85.
60. Haut RC. Age-dependent influence of strain rate on the tensile failure of rat-tail tendon. J Biomech Eng. 1983 Aug;105(3):296-9.
61. W BTG. Basic sience of soft tissue: Muscle and tendon. In: DeLee J & Drez D (eds) Orthopaedic Sports Medicine, Philadelphia, WB Saunders 1–45. 1994.
62. Peltonen J, Cronin NJ, Avela J, Finni T. In vivo mechanical response of human Achilles tendon to a single bout of hopping exercise. J Exp Biol. 2010 April 15, 2010;213(8):1259-65.
63. Komi PV, Fukashiro S, Jarvinen M. Biomechanical loading of Achilles tendon during normal locomotion. Clin Sports Med. 1992 Jul;11(3):521-31.
64. Fukashiro S, Komi PV, Jarvinen M, Miyashita M. In vivo Achilles tendon loading during jumping in humans. Eur J Appl Physiol Occup Physiol. 1995;71(5):453-8.
65. Therman H FOBA. Biomechanical studies of human Achilles tendon rupture. Unfallchirurg. 1995; 98:570–575.
66. Koivunen-Niemelä T, Parkkola K. Anatomy of the Achilles tendon (tendo calcaneus) with respect to tendon thickness measurements. Surgical and Radiologic Anatomy. 1995;17(3):263-8.

67. Rosager S, Aagaard P, Dyhre-Poulsen P, Neergaard K, Kjaer M, Magnusson SP. Load-displacement properties of the human triceps surae aponeurosis and tendon in runners and non-runners. Scandinavian Journal of Medicine & Science in Sports. 2002;12(2):90-8.
68. Kannus P, Józsa L, Natri A, Järvinen M. Effects of training, immobilization and remobilization on tendons. Scandinavian Journal of Medicine & Science in Sports. 1997;7(2):67-71.
69. Kjaer M, Langberg H, Miller BF, Boushel R, Crameri R, Koskinen S, et al. Metabolic activity and collagen turnover in human tendon in response to physical activity. J Musculoskelet Neuronal Interact. 2005;5(1):41-52.
70. Oliveira Milani J, Matheus J, Gomide L, Volpon J, Shimano A. Biomechanical Effects of Immobilization and Rehabilitation on the Skeletal Muscle of Trained and Sedentary Rats. Annals of Biomedical Engineering. 2008;36(10):1641-8.
71. Woo SL, Ritter MA, Amiel D, Sanders TM, Gomez MA, Kuei SC, et al. The biomechanical and biochemical properties of swine tendons--long term effects of exercise on the digital extensors. Connect Tissue Res. 1980;7(3):177-83.
72. Finni T, Hodgson JA, Lai AM, Edgerton VR, Sinha S. Nonuniform strain of human soleus aponeurosis-tendon complex during submaximal voluntary contractions in vivo. Journal of Applied Physiology. 2003 August 1, 2003;95(2):829-37.
73. Lichtwark GA, Wilson AM. In vivo mechanical properties of the human Achilles tendon during one-legged hopping. Journal of Experimental Biology. 2005 December 15, 2005;208(24):4715-25.
74. Maganaris CN, Paul JP. Tensile properties of the in vivo human gastrocnemius tendon. J Biomech. 2002 Dec;35(12):1639-46.
75. Barfred T. Achilles tendon rupture. Aetiology and pathogenesis of subcutaneous rupture assessed on the basis of the literature and rupture experiments on rats. Acta Orthop Scand. 1973;152(suppl):3 - 126.
76. Nillius SA, Nilsson BE, Westlin NE. The incidence of Achilles tendon rupture. Acta Orthop Scand. 1976 Feb;47(1):118-21.
77. Leppilahti J, Forsman K, Puranen J, Orava S. Outcome and prognostic factors of Achilles rupture repair using a new scoring method. Clin Orthop. 1998;346:152 - 61.
78. Leppilahti J, Puranen J, Orava S. Incidence of Achilles tendon rupture. Acta Orthop Scand. 1996 Jun;67(3):277-9.
79. Levi N. The incidence of Achilles tendon rupture in Copenhagen. Injury. 1997;28(4):311-3.
80. MAFFULLI N. Current Concepts Review - Rupture of the Achilles Tendon. J Bone Joint Surg Am. 1999 July 1, 1999;81(7):1019-36.
81. Orava S, Hurme M, Leppilahti J. Bilateral Achilles tendon rupture: a report on two cases. Scand J Med Sci Sports. 1996 Oct;6(5):309-12.
82. Fox J, Blazina M, Jobe F, Kerlan R, Carter V, Shields-CL J, et al. Degeneration and rupture of the Achilles tendon. Clin Orthop. 1975;107:221 - 4.
83. Maffulli N. Rupture of the Achilles tendon. J Bone Joint Surg Am. 1999 Jul;81(7):1019-36.
84. Nestorson J, Movin T, Moller M, Karlsson J. Function after Achilles tendon rupture in the elderly: 25 patients older than 65 years followed for 3 years. Acta Orthop Scand. 2000 Feb;71(1):64-8.
85. Dilsher S, Darshan P, Martin D. High dose inhaled Corticosteroids can cause Achilles Tendonitis. 2009;2(1):15-7.
86. van der Linden PD, Sturkenboom MCJM, Herings RMC, Leufkens HGM, Stricker BHC. Fluoroquinolones and risk of Achilles tendon disorders: case-control study. BMJ. 2002 June 1, 2002;324(7349):1306-7.
87. Wilson AM, Goodship AE. Exercise-induced hyperthermia as a possible mechanism for tendon degeneration. Journal of Biomechanics. 1994;27(7):899-901, 3-5.
88. Carr AJ, Norris SH. The blood supply of the calcaneal tendon. J Bone Joint Surg Br. 1989 Jan;71(1):100-1.

89. Kannus P, Jozsa L. Histopathological changes preceding spontaneous rupture of a tendon. A controlled study of 891 patients. J Bone Joint Surg Am. 1991;73:1507 - 25.
90. Hess GW. Achilles Tendon Rupture. Foot & Ankle Specialist. 2010 February 1, 2010;3(1):29-32.
91. Arner O, Lindholm A. Subcutaneous rupture of the Achilles tendon: a study of 92 cases. Acta Chir Scand. 1959;239(suppl):1 - 51.
92. Davidsson L, Salo M. Pathogenesis of subcutaneous tendon ruptures. Acta Chir Scand. 1969;135:209 - 12.
93. Waterston SW. Histochemistry and biochemistry of Achilles tendon ruptures. [B.Med.Sc. dissertation]. 1997.
94. Barfred T. Histology of the rat Achilles tendon before and after tendon rupture. Acta Pathol Microbiol Scand A. 1971;79:287 - 92.
95. McMaster PETamrCaesotcalosrJBaJS, 15: 705-722, July 1933.
96. Bradley J, Tibone J. Percutaneous and open surgical repairs of Achilles tendon ruptures. A comparative study. Am J Sports Med. 1990;18:188 - 95.
97. Simmonds FA. The diagnosis of the ruptured Achilles tendon. Practitioner. 1957 Jul;179(1069):56-8.
98. Thompson TC, Doherty JH. Spontaneous rupture of tendon of Achilles: a new clinical diagnostic test. J Trauma. 1962 Mar;2:126-9.
99. Copeland SA. Rupture of the Achilles tendon: a new clinical test. Ann R Coll Surg Engl. 1990 Jul;72(4):270-1.
100. Kihiczak D, Colletti PM, Terk MR. MRI of Destructive Achilles Tendon Rupture Associated with Skin Ulceration. Journal of Computer Assisted Tomography. 2000;24(6):900-2.
101. Kotnis R, David S, Ostlere S, Willet K. THE USE OF DYNAMIC ULTRASOUND IN THE MANAGEMENT OF ACHILLES TENDON RUPTURE. J Bone Joint Surg Br. 2008 July 1, 2008;90-B(SUPP_II):232-a-.
102. Lim J, Dalal R, Waseem M. Percutaneous vs. open repair of the ruptured Achilles tendon. A prospective randomized controlled study. Foot & Ankle Int. 2001;22:559 - 68.
103. Kerkhoffs G, Struijs P, Raaymakers E, Marti R. Functional treatment after surgical repair of acute Achilles tendon rupture: wrap vs walking cast. Arch Orthop Trauma Surg. 2002;122:102 - 5.
104. Webb J, Bannister G. Percutaneous repair of the ruptured tendo Achilles. J Bone Joint Surg. 1999;81:877 - 80.
105. Maffulli N, Tallon C, Wong J, Lim K, Bleakney R. Early weightbearing and ankle mobilization after open repair of acute midsubstance tears of the achilles tendon. Am J Sports Med. 2003;31(5):692 - 700.
106. Mortensen NH, Saether J, Steinke MS, Staehr H, Mikkelsen SS. Separation of tendon ends after Achilles tendon repair: a prospective, randomized, multicenter study. Orthopedics. 1992 Aug;15(8):899-903.
107. Aktas S, Kocaoglu B, Nalbantoglu U, Seyhan M, Guven O. End-to-end versus augmented repair in the treatment of acute Achilles tendon ruptures. J Foot Ankle Surg. 2007 Sep-Oct;46(5):336-40.
108. Nistor L. Surgical and non-surgical treatment of Achilles tendon rupture. A prospective randomized study. J Bone Joint Surg (Am). 1981;63:394 - 9.
109. Soldatis JJ, Goodfellow DB, Wilber JH. End-to-end operative repair of Achilles tendon rupture. Am J Sports Med. 1997 Jan-Feb;25(1):90-5.
110. Aldam CH. Repair of calcaneal tendon ruptures. A safe technique. J Bone Joint Surg Br. 1989 May;71(3):486-8.
111. Cetti R, Hendriksen L, Jacobsen K. A new treatment of ruptured Achilles tendons. A prospective randomized study. Clin Orthop. 1994;308:155 - 65.
112. Carter TR, Fowler PJ, Blokker C. Functional postoperative treatment of Achilles tendon repair. Am J Sports Med. 1992 Jul-Aug;20(4):459-62.

113. Motta P, Errichiello C, Pontini I. Achilles tendon rupture. A new technique for easy surgical repair and immediate movement of the ankle and foot. Am J Sports Med. 1997 Mar-Apr;25(2):172-6.
114. Khan RJ, Fick D, Keogh A, Crawford J, Brammar T, Parker M. Treatment of acute achilles tendon ruptures. A meta-analysis of randomized, controlled trials. J Bone Joint Surg Am. 2005 Oct;87(10):2202-10.
115. Ma G, Griffith T. Percutaneous repair of acute closed ruptured Achilles tendon: a new technique. Clin Orthop. 1977;128:247 - 55.
116. Rowley D, Scotland T. Rupture of the Achilles tendon treated by a simple operative procedure. Injury. 1982;14:252 - 4.
117. Stein V, Laprell H, Tinnemeyer S, Petersen W. Quantitative assessment of intravascular volume of the human Achilles tendon. Acta Orthop Scand. 2000;71:60 - 3.
118. Lea RB, Smith L. Non-surgical treatment of tendo achillis rupture. J Bone Joint Surg Am. 1972 Oct;54(7):1398-407.
119. McComis G, Nawoczenski D, DeHaven K. Functional bracing for rupture of the Achilles tendon. J Bone Joint Surg Am. 1997;79(12):1799 - 808.
120. Sharma P, Maffulli N. Tendon Injury and Tendinopathy: Healing and Repair. The Journal of Bone & Joint Surgery. 2005;87(1):187-202.
121. Wang JHC. Mechanobiology of tendon. Journal of Biomechanics. 2006;39(9):1563-82.
122. Gelberman R. Flexor tendon physiology: tendon nutrition and cellular activity in injury and repair. Instr Course Lect. 1985;34:351 - 60.
123. Wang W, Tang X, Zhang J, Yan X, Ma Y. Complete stress shielding of the Achilles tendon: ultrastructure and level of interleukin-1 and TGF-beta. Orthopedics. 2010 Nov;33(11):810.
124. Manske PR. Flexor tendon healing. J Hand Surg Br. 1988 Aug;13(3):237-45.
125. Bruns J, Kampen J, Kahrs J, Plitz W. Achilles tendon rupture: experimental results on spontaneous repair in a sheep-model. Knee Surg Sports Traumatol Arthrosc. 2000;8(6):364-9.
126. Kannus P, Natri A. Etiology and pathophysiology of tendon ruptures in sports. Scand J Med Sci Sports. 1997;7:107 - 12.
127. Fenwick S, Hazleman B, Riley G. The vasculature and its role in the damaged and healing tendon. Arthritis Res. 2002;4(4):252 - 60.
128. Brockis J. The blood supply of the flexor and the extensor tendons of the fingers in man. J Bone Joint Surg Br. 1953;35B:131 - 8.
129. Gibble JW, Ness PM. Fibrin glue: the perfect operative sealant? Transfusion. 1990 Oct;30(8):741-7.
130. Sanchez AR, Sheridan PJ, Kupp LI. Is platelet-rich plasma the perfect enhancement factor? A current review. Int J Oral Maxillofac Implants. 2003 Jan-Feb;18(1):93-103.
131. Whitman DH, Berry RL, Green DM. Platelet gel: an autologous alternative to fibrin glue with applications in oral and maxillofacial surgery. J Oral Maxillofac Surg. 1997 Nov;55(11):1294-9.
132. Gentile P, Cervelli V. Autologous platelet-rich plasma: guidelines in plastic surgery. Plast Reconstr Surg. 2010 Nov;126(5):269e-70e.
133. Marx RE, Carlson ER, Eichstaedt RM, Schimmele SR, Strauss JE, Georgeff KR. Platelet-rich plasma: Growth factor enhancement for bone grafts. Oral Surg Oral Med Oral Pathol Oral Radiol Endod. 1998 Jun;85(6):638-46.
134. Weibrich G, Kleis WK, Hafner G, Hitzler WE. Growth factor levels in platelet-rich plasma and correlations with donor age, sex, and platelet count. J Craniomaxillofac Surg. 2002 Apr;30(2):97-102.
135. Dragica S BG, Dragoslav D, Primo R. Allogeneic Platelet Gel with Autologous Cancellous Bone Graft for the Treatment of a Large Bone Defect. European Surgical Research 2007;39(3):170-4.
136. Harrison P, Cramer EM. Platelet alpha-granules. Blood Rev. 1993 Mar;7(1):52-62.
137. Everts PA, Devilee RJ, Brown Mahoney C, van Erp A, Oosterbos CJ, Stellenboom M, et al. Exogenous application of platelet-leukocyte gel during open subacromial decompression contributes to improved patient outcome. A prospective randomized double-blind study. Eur Surg Res. 2008;40(2):203-10.

138. Polasek J, Richardson M, Moore MA, Blajchman MA. Evidence for an alternative mechanism of human platelet secretion involving peripheralization of secretory granules and formation of membrane-associated multivesicular structures. Thromb Res. 1987 Mar 15;45(6):771-82.
139. Kroll MH, Hellums JD, McIntire LV, Schafer AI, Moake JL. Platelets and shear stress. Blood. 1996 Sep 1;88(5):1525-41.
140. Bielecki T, Dohan Ehrenfest DM, Everts PA, Wiczkowski A. The role of leukocytes from L-PRP/L-PRF in wound healing and immune defense: new perspectives. Curr Pharm Biotechnol. 2012 Jun;13(7):1153-62.
141. Evangelista V, Manarini S, Sideri R, Rotondo S, Martelli N, Piccoli A, et al. Platelet/Polymorphonuclear Leukocyte Interaction: P-Selectin Triggers Protein-Tyrosine Phosphorylation–Dependent CD11b/CD18 Adhesion: Role of PSGL-1 as a Signaling Molecule. Blood. 1999 February 1, 1999;93(3):876-85.
142. Franklin S, Zargar N, Willett K, Hulley P, Thompson M. Human Tenocyte Cellular Signalling Response in the Presence of Platelet-Rich Concentrate Journal of Bone & Joint Surgery, British Volume. 2012 May 1, 2012;94-B(SUPP XVIII):6.
143. van den Dolder J, Mooren R, Vloon AP, Stoelinga PJ, Jansen JA. Platelet-rich plasma: quantification of growth factor levels and the effect on growth and differentiation of rat bone marrow cells. Tissue Eng. 2006 Nov;12(11):3067-73.
144. Eppley BL, Woodell JE, Higgins J. Platelet quantification and growth factor analysis from platelet-rich plasma: implications for wound healing. Plast Reconstr Surg. 2004 Nov;114(6):1502-8.
145. Antoniades HN. Human platelet-derived growth factor (PDGF): purification of PDGF-I and PDGF-II and separation of their reduced subunits. Proc Natl Acad Sci U S A. 1981 Dec;78(12):7314-7.
146. Rappolee DA, Mark D, Banda MJ, Werb Z. Wound macrophages express TGF-alpha and other growth factors in vivo: analysis by mRNA phenotyping. Science. 1988 Aug 5;241(4866):708-12.
147. Sitaras NM, Sariban E, Pantazis P, Zetter B, Antoniades HN. Human iliac artery endothelial cells express both genes encoding the chains of platelet-derived growth factor (PDGF) and synthesize PDGF-like mitogen. J Cell Physiol. 1987 Aug;132(2):376-80.
148. Hauschka PV, Mavrakos AE, Iafrati MD, Doleman SE, Klagsbrun M. Growth factors in bone matrix. Isolation of multiple types by affinity chromatography on heparin-Sepharose. J Biol Chem. 1986 Sep 25;261(27):12665-74.
149. Ross R, Raines EW, Bowen-Pope DF. The biology of platelet-derived growth factor. Cell. 1986 Jul 18;46(2):155-69.
150. Oates TW, Rouse CA, Cochran DL. Mitogenic effects of growth factors on human periodontal ligament cells in vitro. J Periodontol. 1993 Feb;64(2):142-8.
151. Matsuda N, Lin WL, Kumar NM, Cho MI, Genco RJ. Mitogenic, chemotactic, and synthetic responses of rat periodontal ligament fibroblastic cells to polypeptide growth factors in vitro. J Periodontol. 1992 Jun;63(6):515-25.
152. Yang D, Chen J, Jing Z, Jin D. Platelet-derived growth factor (PDGF)-AA: a self-imposed cytokine in the proliferation of human fetal osteoblasts. Cytokine. 2000 Aug;12(8):1271-4.
153. Celeste AJ, Iannazzi JA, Taylor RC, Hewick RM, Rosen V, Wang EA, et al. Identification of transforming growth factor beta family members present in bone-inductive protein purified from bovine bone. Proc Natl Acad Sci U S A. 1990 Dec;87(24):9843-7.
154. Cheifetz S, Massague J. Isoform-specific transforming growth factor-beta binding proteins with membrane attachments sensitive to phosphatidylinositol-specific phospholipase C. J Biol Chem. 1991 Nov 5;266(31):20767-72.
155. Wrana JL, Maeno M, Hawrylyshyn B, Yao KL, Domenicucci C, Sodek J. Differential effects of transforming growth factor-beta on the synthesis of extracellular matrix proteins by normal fetal rat calvarial bone cell populations. J Cell Biol. 1988 Mar;106(3):915-24.
156. Bonewald LF, Mundy GR. Role of transforming growth factor-beta in bone remodeling. Clin Orthop Relat Res. 1990 Jan(250):261-76.

157. Hock JM, Centrella M, Canalis E. Insulin-like growth factor I has independent effects on bone matrix formation and cell replication. Endocrinology. 1988 Jan;122(1):254-60.
158. Cohen S. Isolation of a mouse submaxillary gland protein accelerating incisor eruption and eyelid opening in the new-born animal. J Biol Chem. 1962 May;237:1555-62.
159. Einhorn TA. The science of fracture healing. J Orthop Trauma. 2005 Nov-Dec;19(10 Suppl):S4-6.
160. Maurer AM, Zhou B, Han ZC. Roles of platelet factor 4 in hematopoiesis and angiogenesis. Growth Factors. 2006 Dec;24(4):242-52.
161. Ferrara N. Role of vascular endothelial growth factor in regulation of physiological angiogenesis. Am J Physiol Cell Physiol. 2001 Jun;280(6):C1358-66.
162. Herbst RS. Review of epidermal growth factor receptor biology. Int J Radiat Oncol Biol Phys. 2004;59(2 Suppl):21-6.
163. Chen CH, Cao Y, Wu YF, Bais AJ, Gao JS, Tang JB. Tendon Healing In Vivo: Gene Expression and Production of Multiple Growth Factors in Early Tendon Healing Period. The Journal of Hand Surgery. 2008;33(10):1834-42.
164. Cao R, Brakenhielm E, Pawliuk R, Wariaro D, Post MJ, Wahlberg E, et al. Angiogenic synergism, vascular stability and improvement of hind-limb ischemia by a combination of PDGF-BB and FGF-2. Nat Med. 2003 May;9(5):604-13.
165. Nurden AT. Platelets, inflammation and tissue regeneration. Thromb Haemost. 2011 May;105 Suppl 1:S13-33.
166. Ljungqvist A SM, Bachl N, et al. International Olympic Committee consensus statement: molecular basis of connective tissue and muscle injuries in sport. Clin Sports Med. 2008;27:231-9.
167. Lyras DN, Kazakos K, Tryfonidis M, Agrogiannis G, Botaitis S, Kokka A, et al. Temporal and spatial expression of TGF-beta1 in an Achilles tendon section model after application of platelet-rich plasma. Foot Ankle Surg. 2010 Sep;16(3):137-41.
168. Volpi P, Quaglia A, Schoenhuber H, Melegati G, Corsi MM, Banfi G, et al. Growth factors in the management of sport-induced tendinopathies: results after 24 months from treatment. A pilot study. J Sports Med Phys Fitness. 2010 Dec;50(4):494-500.
169. Harrison P MI, Mumford A, Briggs C, Liesner R, Winter M, Machin S. BCSH guidelines for platelet function testing.

. British Journal of Haematology and BCSH website. 2011;155(1):30-44.
170. Kevy SV JM. Comparison of methods for point of care preparation of autologous platelet gel. The Journal of extra-corporeal technology. 2004;36(1):28-35.
171. Landesberg R RM, Glickman RS. Quantification of growth factors levels using a simplified method of platelet rich plasma gel preparation. J Oral Maxillofac Surg. 2000;58:297-300.
172. Apher C SDW, Williamson L H, Sheckler V L, Fitzgerald B P. Platelet Collection with the Autopheresis -C apheresis system. Vox Sang. 1990;58:100-4.
173. Knape PAECBMJJHJPSHABAvZJT. Platelet-rich plasma preparation using three devices: Implications for platelet activation and platelet growth factor release. Growth Factors. 2006 September;24(3):165-71.
174. Ho CH, Chan IH. The influence of time of storage, temperature of storage, platelet number in platelet-rich plasma, packed cell, mean platelet volume, hemoglobin concentration, age, and sex on platelet aggregation test. Ann Hematol. 1995 1995/09/01;71(3):129-33.
175. Sweeney J, Kouttab N, Holme S, Kurtis J, Cheves T, Nelson E. Storage of platelet-rich plasma–derived platelet concentrate pools in plasma and additive solution. Transfusion. 2006;46(5):835-40.
176. Landesberg R, Moses, M., and Karpatkin, M. Risks of using platelet rich plasma gel. J Oral Maxillofac Surg. 1998;56:1116-998.
177. Cmolik BL, Spero, J.A., and Magovern, G.J. Redo cardiac surgery: late bleeding complications from topical thrombin induced factor five deficiency. J Thorac Cardiovasc Surg. 1993;105:222-7.

178. Man D, Plosker H, Winland-Brown JE. The use of autologous platelet-rich plasma (platelet gel) and autologous platelet-poor plasma (fibrin glue) in cosmetic surgery. Plast Reconstr Surg. 2001 Jan;107(1):229-37; discussion 38-9.
179. Harrison S VP, Kevy S, Jackobson M, Zurakowski D, Murray M. Platelet Activation by Collagen Provides Sustained Relsease of Anabolic Cytokines. Am J Sports Med. 2011;39(4):729-34.
180. Fufa D, Shealy B, Jacobson M, Kevy S, Murray MM. Activation of platelet-rich plasma using soluble type I collagen. J Oral Maxillofac Surg. 2008 Apr;66(4):684-90.
181. Choi BH, Zhu SJ, Kim BY, Huh JY, Lee SH, Jung JH. Effect of platelet-rich plasma (PRP) concentration on the viability and proliferation of alveolar bone cells: an in vitro study. Int J Oral Maxillofac Surg. 2005 Jun;34(4):420-4.
182. Weibrich G, Kleis WK. Curasan PRP kit vs. PCCS PRP system. Collection efficiency and platelet counts of two different methods for the preparation of platelet-rich plasma. Clin Oral Implants Res. 2002 Aug;13(4):437-43.
183. Castelnovo L, Dosquet C, Gaudric A, Sahel J, Hicks D. Human platelet suspension stimulates porcine retinal glial proliferation and migration in vitro. Invest Ophthalmol Vis Sci. 2000 Feb;41(2):601-9.
184. Kajikawa Y, Morihara T, Sakamoto H, Matsuda K, Oshima Y, Yoshida A, et al. Platelet-rich plasma enhances the initial mobilization of circulation-derived cells for tendon healing. J Cell Physiol. 2008 Jun;215(3):837-45.
185. Bertrand-Duchesne MP, Grenier D, Gagnon G. Epidermal growth factor released from platelet-rich plasma promotes endothelial cell proliferation in vitro. J Periodontal Res. 2010 Feb;45(1):87-93.
186. Bertoldi C, Pinti M, Zaffe D, Cossarizza A, Consolo U, Ceccherelli GB. Morphologic, histochemical, and functional analysis of platelet-rich plasma activity on skeletal cultured cells. Transfusion. 2009 Aug;49(8):1728-37.
187. Ishida K, Kuroda R, Miwa M, Tabata Y, Hokugo A, Kawamoto T, et al. The regenerative effects of platelet-rich plasma on meniscal cells in vitro and its in vivo application with biodegradable gelatin hydrogel. Tissue Eng. 2007 May;13(5):1103-12.
188. Pantou AL, Markopoulou CE, Dereka XE, Vavouraki H, Mamalis A, Vrotsos IA. The effect of platelet-rich plasma (PRP) combined with a bone allograft on human periodontal ligament (PDL) cells. Cell Tissue Bank. 2010 Dec 1.
189. Feng Y, Sun Y, Jia W, Zhang C. Platelet-rich plasma and 1,25(OH)2 vitamin D3 synergistically stimulate osteogenic differentiation of adult human mesenchymal stem cells. Biotechnol Lett. 2010 May;32(5):635-42.
190. Huang S, Wang Z. Influence of platelet-rich plasma on proliferation and osteogenic differentiation of skeletal muscle satellite cells: an in vitro study. Oral Surg Oral Med Oral Pathol Oral Radiol Endod. 2010 Oct;110(4):453-62.
191. Lucarelli E, Fini M, Beccheroni A, Giavaresi G, Di Bella C, Aldini NN, et al. Stromal stem cells and platelet-rich plasma improve bone allograft integration. Clin Orthop Relat Res. 2005 Jun(435):62-8.
192. Lee JY, Nam H, Park YJ, Lee SJ, Chung CP, Han SB, et al. The effects of platelet-rich plasma derived from human umbilical cord blood on the osteogenic differentiation of human dental stem cells. In Vitro Cell Dev Biol Anim. 2011 Feb;47(2):157-64.
193. Arpornmaeklong P, Kochel M, Depprich R, Kubler NR, Wurzler KK. Influence of platelet-rich plasma (PRP) on osteogenic differentiation of rat bone marrow stromal cells. An in vitro study. Int J Oral Maxillofac Surg. 2004 Jan;33(1):60-70.
194. Soffer E, Ouhayoun JP, Dosquet C, Meunier A, Anagnostou F. Effects of platelet lysates on select bone cell functions. Clin Oral Implants Res. 2004 Oct;15(5):581-8.
195. Duan J, Kuang W, Tan J, Li H, Zhang Y, Hirotaka K, et al. Differential effects of platelet rich plasma and washed platelets on the proliferation of mouse MSC cells. Mol Biol Rep. 2011 Apr;38(4):2485-90.

196. Creeper F, Lichanska AM, Marshall RI, Seymour GJ, Ivanovski S. The effect of platelet-rich plasma on osteoblast and periodontal ligament cell migration, proliferation and differentiation. J Periodontal Res. 2009 Apr;44(2):258-65.
197. Weibrich G, Hansen T, Kleis W, Buch R, Hitzler WE. Effect of platelet concentration in platelet-rich plasma on peri-implant bone regeneration. Bone. 2004;34(4):665-71.
198. Cheng M, Wang H, Yoshida R, Murray MM. Platelets and plasma proteins are both required to stimulate collagen gene expression by anterior cruciate ligament cells in three-dimensional culture. Tissue Eng Part A. 2010 May;16(5):1479-89.
199. McCarrel T, Fortier L. Temporal growth factor release from platelet-rich plasma, trehalose lyophilized platelets, and bone marrow aspirate and their effect on tendon and ligament gene expression. J Orthop Res. 2009 Aug;27(8):1033-42.
200. Schnabel LV, Mohammed HO, Miller BJ, McDermott WG, Jacobson MS, Santangelo KS, et al. Platelet rich plasma (PRP) enhances anabolic gene expression patterns in flexor digitorum superficialis tendons. J Orthop Res. 2007 Feb;25(2):230-40.
201. Sanchez M, Anitua E, Azofra J, Prado R, Muruzabal F, Andia I. Ligamentization of tendon grafts treated with an endogenous preparation rich in growth factors: gross morphology and histology. Arthroscopy. 2010 Apr;26(4):470-80.
202. Morizaki Y, Zhao C, An KN, Amadio PC. The effects of platelet-rich plasma on bone marrow stromal cell transplants for tendon healing in vitro. J Hand Surg Am. 2010 Nov;35(11):1833-41.
203. Lyras DN, Kazakos K, Georgiadis G, Mazis G, Middleton R, Richards S, et al. Does a single application of PRP alter the expression of IGF-I in the early phase of tendon healing? J Foot Ankle Surg. 2011 May-Jun;50(3):276-82.
204. Lyras DN, Kazakos K, Agrogiannis G, Verettas D, Kokka A, Kiziridis G, et al. Experimental study of tendon healing early phase: Is IGF-1 expression influenced by platelet rich plasma gel? Orthopaedics & Traumatology: Surgery & Research. 2010;96(4):381-7.
205. Hu ZM, Peel SA, Ho SK, Sandor GK, Clokie CM. Comparison of platelet-rich plasma, bovine BMP, and rhBMP-4 on bone matrix protein expression in vitro. Growth Factors. 2009 Oct;27(5):280-8.
206. Tomoyasu A, Higashio K, Kanomata K, Goto M, Kodaira K, Serizawa H, et al. Platelet-rich plasma stimulates osteoblastic differentiation in the presence of BMPs. Biochem Biophys Res Commun. 2007 Sep 14;361(1):62-7.
207. Anitua E, Andí I, Sanchez M, Azofra J, del Mar Zalduendo M, de la Fuente M, et al. Autologous preparations rich in growth factors promote proliferation and induce VEGF and HGF production by human tendon cells in culture. Journal of Orthopaedic Research. 2005;23(2):281-6.
208. de Mos M, van der Windt AE, Jahr H, van Schie HTM, Weinans H, Verhaar JAN, et al. Can Platelet-Rich Plasma Enhance Tendon Repair? The American Journal of Sports Medicine. 2008 June 1, 2008;36(6):1171-8.
209. Lyras D, Kazakos K, Verettas D, Polychronidis A, Simopoulos C, Botaitis S, et al. Immunohistochemical study of angiogenesis after local administration of platelet-rich plasma in a patellar tendon defect. Int Orthop. 2010 Feb;34(1):143-8.
210. Lyras DN, Kazakos K, Verettas D, Polychronidis A, Tryfonidis M, Botaitis S, et al. The influence of platelet-rich plasma on angiogenesis during the early phase of tendon healing. Foot Ankle Int. 2009 Nov;30(11):1101-6.
211. Slater M, Patava J, Kingham K, Mason RS. Involvement of platelets in stimulating osteogenic activity. J Orthop Res. 1995 Sep;13(5):655-63.
212. de Mos M, van der Windt AE, Jahr H, van Schie HT, Weinans H, Verhaar JA, et al. Can platelet-rich plasma enhance tendon repair? A cell culture study. Am J Sports Med. 2008 Jun;36(6):1171-8.
213. Mariano R, Messora M, de Morais A, Nagata M, Furlaneto F, Avelino C, et al. Bone healing in critical-size defects treated with platelet-rich plasma: a histologic and histometric study in the calvaria of diabetic rat. Oral Surg Oral Med Oral Pathol Oral Radiol Endod. 2010 Jan;109(1):72-8.

214. Pessoa RS, Oliveira SR, Menezes HH, de Magalhaes D. Effects of platelet-rich plasma on healing of alveolar socket: split-mouth histological and histometric evaluation in Cebus apella monkeys. Indian J Dent Res. 2009 Oct-Dec;20(4):442-7.
215. Jungbluth P, Wild M, Grassmann JP, Ar E, Sager M, Herten M, et al. Platelet-rich plasma on calcium phosphate granules promotes metaphyseal bone healing in mini-pigs. J Orthop Res. 2010 Nov;28(11):1448-55.
216. Fennis JP, Stoelinga PJ, Jansen JA. Mandibular reconstruction: a clinical and radiographic animal study on the use of autogenous scaffolds and platelet-rich plasma. Int J Oral Maxillofac Surg. 2002 Jun;31(3):281-6.
217. Kanthan SR, Kavitha G, Addi S, Choon DS, Kamarul T. Platelet-rich plasma (PRP) enhances bone healing in non-united critical-sized defects: A preliminary study involving rabbit models. Injury. 2011 Aug;42(8):782-9.
218. Giovanini AF, Gonzaga CC, Zielak JC, Deliberador TM, Kuczera J, Goringher I, et al. Platelet-rich plasma (PRP) impairs the craniofacial bone repair associated with its elevated TGF-beta levels and modulates the co-expression between collagen III and alpha-smooth muscle actin. J Orthop Res. 2011 Mar;29(3):457-63.
219. Broggini N, Hofstetter W, Hunziker E, Bosshardt DD, Bornstein MM, Seto I, et al. The influence of PRP on early bone formation in membrane protected defects. A histological and histomorphometric study in the rabbit calvaria. Clin Implant Dent Relat Res. 2011 Mar;13(1):1-12.
220. Aspenberg P, Virchenko O. Platelet concentrate injection improves Achilles tendon repair in rats. Acta Orthop Scand. 2004 Feb;75(1):93-9.
221. Bosch G, van Schie HT, de Groot MW, Cadby JA, van de Lest CH, Barneveld A, et al. Effects of platelet-rich plasma on the quality of repair of mechanically induced core lesions in equine superficial digital flexor tendons: A placebo-controlled experimental study. J Orthop Res. 2010 Feb;28(2):211-7.
222. Bosch G, Moleman M, Barneveld A, van Weeren PR, van Schie HT. The effect of platelet-rich plasma on the neovascularization of surgically created equine superficial digital flexor tendon lesions. Scand J Med Sci Sports. 2010 Mar 10.
223. Bir SC, Esaki J, Marui A, Sakaguchi H, Kevil CG, Ikeda T, et al. Therapeutic treatment with sustained-release platelet-rich plasma restores blood perfusion by augmenting ischemia-induced angiogenesis and arteriogenesis in diabetic mice. J Vasc Res. 2011;48(3):195-205.
224. Li NY, Yuan RT, Chen T, Chen LQ, Jin XM. Effect of platelet-rich plasma and latissimus dorsi muscle flap on osteogenesis and vascularization of tissue-engineered bone in dogs. J Oral Maxillofac Surg. 2009 Sep;67(9):1850-8.
225. Hadad I, Johnstone BH, Brabham JG, Blanton MW, Rogers PI, Fellers C, et al. Development of a porcine delayed wound-healing model and its use in testing a novel cell-based therapy. Int J Radiat Oncol Biol Phys. 2010 Nov 1;78(3):888-96.
226. Mishra A, Velotta J, Brinton TJ, Wang X, Chang S, Palmer O, et al. RevaTen platelet-rich plasma improves cardiac function after myocardial injury. Cardiovasc Revasc Med. 2011 May-Jun;12(3):158-63.
227. Nakamura S, Ishihara M, Takikawa M, Murakami K, Kishimoto S, Yanagibayashi S, et al. Platelet-rich plasma (PRP) promotes survival of fat-grafts in rats. Ann Plast Surg. 2010 Jul;65(1):101-6.
228. Milano G, Sanna Passino E, Deriu L, Careddu G, Manunta L, Manunta A, et al. The effect of platelet rich plasma combined with microfractures on the treatment of chondral defects: an experimental study in a sheep model. Osteoarthritis Cartilage. 2010 Jul;18(7):971-80.
229. DeRossi R, Coelho AC, Mello GS, Frazilio FO, Leal CR, Facco GG, et al. Effects of platelet-rich plasma gel on skin healing in surgical wound in horses. Acta Cir Bras. 2009 Jul-Aug;24(4):276-81.
230. Tanidir ST, Yuksel N, Altintas O, Yildiz DK, Sener E, Caglar Y. The effect of subconjunctival platelet-rich plasma on corneal epithelial wound healing. Cornea. 2010 Jun;29(6):664-9.

231. Matsuo R, Nakano Y, Ohkohchi N. Platelet administration via the portal vein promotes liver regeneration in rats after 70% hepatectomy. Ann Surg. 2011 Apr;253(4):759-63.
232. Yamaguchi R, Terashima H, Yoneyama S, Tadano S, Ohkohchi N. Effects of platelet-rich plasma on intestinal anastomotic healing in rats: PRP concentration is a key factor. J Surg Res. 2012 Apr;173(2):258-66.
233. Yu W, Wang J, Yin J. Platelet-rich plasma: a promising product for treatment of peripheral nerve regeneration after nerve injury. Int J Neurosci. 2011 Apr;121(4):176-80.
234. Sheth U, Simunovic N, Klein G, Fu F, Einhorn TA, Schemitsch E, et al. Efficacy of autologous platelet-rich plasma use for orthopaedic indications: a meta-analysis. The Journal of bone and joint surgery American volume. 2012;94(4):298-307.
235. Pietrzak W, Eppley BL. Platelet rich plasma: biology and new technology. Journal Craniofacial Surgery

Journal Craniofacial Surgery. 2005;16(6):1043-54.
236. Lowery GL, Kulkarni S, Pennisi AE. Use of autologous growth factors in lumbar spinal fusion. Bone. 1999 Aug;25(2 Suppl):47S-50S.
237. Hartmann EK, Heintel T, Morrison RH, Weckbach A. Influence of platelet-rich plasma on the anterior fusion in spinal injuries: a qualitative and quantitative analysis using computer tomography. Arch Orthop Trauma Surg. 2010 Jul;130(7):909-14.
238. Seijas R, Santana-Suarez RY, Garcia-Balletbo M, Cusco X, Ares O, Cugat R. Delayed union of the clavicle treated with plasma rich in growth factors. Acta Orthop Belg. 2010 Oct;76(5):689-93.
239. Rodrigues SV, Acharya AB, Thakur SL. An evaluation of platelet-rich plasma without thrombin activation with or without anorganic bone mineral in the treatment of human periodontal intrabony defects. Platelets. 2011;22(5):353-60.
240. Nagaveni NB, Praveen RB, Umashankar KV, Pranav B, Sreedevi R, Radhika NB. Efficacy of platelet-rich-plasma (PRP) in bone regeneration after cyst enucleation in pediatric patients--a clinical study. J Clin Pediatr Dent. 2010 Fall;35(1):81-7.
241. Scala M, Gipponi M, Mereu P, Strada P, Corvo R, Muraglia A, et al. Regeneration of mandibular osteoradionecrosis defect with platelet rich plasma gel. In Vivo. 2010 Nov-Dec;24(6):889-93.
242. Curi MM, Cossolin GS, Koga DH, Araujo SR, Feher O, dos Santos MO, et al. Treatment of avascular osteonecrosis of the mandible in cancer patients with a history of bisphosphonate therapy by combining bone resection and autologous platelet-rich plasma: Report of 3 cases. J Oral Maxillofac Surg. 2007 Feb;65(2):349-55.
243. Cenni E, Fotia C, Rustemi E, Yuasa K, Caltavuturo G, Giunti A, et al. Idiopathic and secondary osteonecrosis of the femoral head show different thrombophilic changes and normal or higher levels of platelet growth factors. Acta Orthop. 2011 Feb;82(1):42-9.
244. Gandhi A, Bibbo C, Pinzur M, Lin SS. The role of platelet-rich plasma in foot and ankle surgery. Foot Ankle Clin. 2005 Dec;10(4):621-37, viii.
245. Herouy Y, Mellios P, Bandemir E, Stetter C, Dichmann S, Idzko M, et al. Autologous platelet-derived wound healing factor promotes angiogenesis via alphavbeta3-integrin expression in chronic wounds. Int J Mol Med. 2000 Nov;6(5):515-9.
246. Lacci KM, Dardik A. Platelet-rich plasma: support for its use in wound healing. Yale J Biol Med. 2010 Mar;83(1):1-9.
247. Crovetti G, Martinelli G, Issi M, Barone M, Guizzardi M, Campanati B, et al. Platelet gel for healing cutaneous chronic wounds. Transfus Apher Sci. 2004 Apr;30(2):145-51.
248. O'Connell SM, Impeduglia T, Hessler K, Wang XJ, Carroll RJ, Dardik H. Autologous platelet-rich fibrin matrix as cell therapy in the healing of chronic lower-extremity ulcers. Wound Repair Regen. 2008 Nov-Dec;16(6):749-56.
249. Driver VR, Hanft J, Fylling CP, Beriou JM. A prospective, randomized, controlled trial of autologous platelet-rich plasma gel for the treatment of diabetic foot ulcers. Ostomy Wound Manage. 2006 Jun;52(6):68-70, 2, 4 passim.

250. Krupski WC, Reilly LM, Perez S, Moss KM, Crombleholme PA, Rapp JH. A prospective randomized trial of autologous platelet-derived wound healing factors for treatment of chronic nonhealing wounds: a preliminary report. J Vasc Surg. 1991 Oct;14(4):526-32; discussion 32-6.
251. Frykberg RG, Driver VR, Carman D, Lucero B, Borris-Hale C, Fylling CP, et al. Chronic wounds treated with a physiologically relevant concentration of platelet-rich plasma gel: a prospective case series. Ostomy Wound Manage. 2010 Jun;56(6):36-44.
252. Cervelli V, Gentile P, De Angelis B, Calabrese C, Di Stefani A, Scioli MG, et al. Application of enhanced stromal vascular fraction and fat grafting mixed with PRP in post-traumatic lower extremity ulcers. Stem Cell Res. 2011 Mar;6(2):103-11.
253. Cervelli V, Lucarini L, Spallone D, Palla L, Colicchia GM, Gentile P, et al. Use of platelet-rich plasma and hyaluronic acid in the loss of substance with bone exposure. Adv Skin Wound Care. 2011 Apr;24(4):176-81.
254. Cervelli V, Lucarini L, Spallone D, Brinci L, de Angelis B. Use of platelet rich plasma and hyaluronic acid on exposed tendons of the foot and ankle. J Wound Care. 2010 May;19(5):186, 8-90.
255. Balbo R, Avonto I, Marenchino D, Maddalena L, Menardi G, Peano G. Platelet gel for the treatment of traumatic loss of finger substance. Blood Transfus. 2010 Oct;8(4):255-9.
256. Cieslik-Bielecka A, Bielecki T, Gazdzik TS, Arendt J, Krol W, Szczepanski T. Autologous platelets and leukocytes can improve healing of infected high-energy soft tissue injury. Transfus Apher Sci. 2009 Aug;41(1):9-12.
257. Lawlor DK, Derose G, Harris KA, Lovell MB, Novick TV, Forbes TL. The role of platelet-rich plasma in inguinal wound healing in vascular surgery patients. Vasc Endovascular Surg. 2011 Apr;45(3):241-5.
258. Almdahl SM, Veel T, Halvorsen P, Vold MB, Molstad P. Randomized prospective trial of saphenous vein harvest site infection after wound closure with and without topical application of autologous platelet-rich plasma. Eur J Cardiothorac Surg. 2011 Jan;39(1):44-8.
259. Gaweda K, Tarczynska M, Krzyzanowski W. Treatment of Achilles tendinopathy with platelet-rich plasma. Int J Sports Med. 2010 Aug;31(8):577-83.
260. Kon E, Filardo G, Delcogliano M, Presti ML, Russo A, Bondi A, et al. Platelet-rich plasma: new clinical application: a pilot study for treatment of jumper's knee. Injury. 2009 Jun;40(6):598-603.
261. Gosens T, Peerbooms JC, van Laar W, den Oudsten BL. Ongoing Positive Effect of Platelet-Rich Plasma Versus Corticosteroid Injection in Lateral Epicondylitis: A Double-Blind Randomized Controlled Trial With 2-year Follow-up. Am J Sports Med. 2011 Jun;39(6):1200-8.
262. Creaney L, Wallace A, Curtis M, Connell D. Growth factor-based therapies provide additional benefit beyond physical therapy in resistant elbow tendinopathy: a prospective, single-blind, randomised trial of autologous blood injections versus platelet-rich plasma injections. Br J Sports Med. 2011 Mar 28.
263. de Vos RJ, Weir A, van Schie HTM, Bierma-Zeinstra SMA, Verhaar JAN, Weinans H, et al. Platelet-Rich Plasma Injection for Chronic Achilles Tendinopathy: A Randomized Controlled Trial. JAMA. 2010 January 13, 2010;303(2):144-9.
264. de Vos RJ, Weir A, Tol JL, Verhaar JA, Weinans H, van Schie HT. No effects of PRP on ultrasonographic tendon structure and neovascularisation in chronic midportion Achilles tendinopathy. Br J Sports Med. 2011 Apr;45(5):387-92.
265. Vogrin M, Rupreht M, Dinevski D, Haspl M, Kuhta M, Jevsek M, et al. Effects of a platelet gel on early graft revascularization after anterior cruciate ligament reconstruction: a prospective, randomized, double-blind, clinical trial. Eur Surg Res. 2010;45(2):77-85.
266. Radice F, Yánez R, Gutiérrez V, Rosales J, Pinedo M, Coda S. Comparison of Magnetic Resonance Imaging Findings in Anterior Cruciate Ligament Grafts With and Without Autologous Platelet-Derived Growth Factors. Arthroscopy: The Journal of Arthroscopic & Related Surgery. 2010;26(1):50-7.
267. Silva A, Sampaio R. Anatomic ACL reconstruction: does the platelet-rich plasma accelerate tendon healing? Knee Surg Sports Traumatol Arthrosc. 2009 Jun;17(6):676-82.

268. Vogrin M, Rupreht M, Crnjac A, Dinevski D, Krajnc Z, Recnik G. The effect of platelet-derived growth factors on knee stability after anterior cruciate ligament reconstruction: a prospective randomized clinical study. Wien Klin Wochenschr. 2010 May;122 Suppl 2:91-5.
269. Randelli PS, Arrigoni P, Cabitza P, Volpi P, Maffulli N. Autologous platelet rich plasma for arthroscopic rotator cuff repair. A pilot study. Disabil Rehabil. 2008;30(20-22):1584-9.
270. Castricini R, Longo UG, De Benedetto M, Panfoli N, Pirani P, Zini R, et al. Platelet-rich plasma augmentation for arthroscopic rotator cuff repair: a randomized controlled trial. Am J Sports Med. 2011 Feb;39(2):258-65.
271. Hamilton B, Knez W, Eirale C, Chalabi H. Platelet enriched plasma for acute muscle injury. Acta Orthop Belg. 2010 Aug;76(4):443-8.
272. de Vos RJ, van Veldhoven PL, Moen MH, Weir A, Tol JL, Maffulli N. Autologous growth factor injections in chronic tendinopathy: a systematic review. Br Med Bull. 2010;95:63-77.
273. Kampa RJ, Connell DA. Treatment of tendinopathy: is there a role for autologous whole blood and platelet rich plasma injection? Int J Clin Pract. 2010 Dec;64(13):1813-23.
274. Schepull T, Kvist J, Norrman H, Trinks M, Berlin G, Aspenberg P. Autologous platelets have no effect on the healing of human achilles tendon ruptures: a randomized single-blind study. Am J Sports Med. 2011 Jan;39(1):38-47.
275. Sadoghi P, Rosso C, Valderrabano V, Leithner A, Vavken P. The role of platelets in the treatment of Achilles tendon injuries. Journal of Orthopaedic Research. 2012:n/a-n/a.
276. Taylor DW, Petrera M, Hendry M, Theodoropoulos JS. A Systematic Review of the Use of Platelet-Rich Plasma in Sports Medicine as a New Treatment for Tendon and Ligament Injuries. Clinical Journal of Sport Medicine. 2011;21(4):344-52 10.1097/JSM.0b013e31821d0f65.
277. Marlovits S, Mousavi M, Gabler C, Erdos J, Vecsei V. A new simplified technique for producing platelet-rich plasma: a short technical note. Eur Spine J. 2004 Oct;13 Suppl 1:S102-6.
278. Maffulli N, Del Buono A. Platelet plasma rich products in musculoskeletal medicine: Any evidence? The Surgeon. 2012;10(3):148-50.
279. Dohan Ehrenfest DM, Bielecki T, Mishra A, Borzini P, Inchingolo F, Sammartino G, et al. In search of a consensus terminology in the field of platelet concentrates for surgical use: platelet-rich plasma (PRP), platelet-rich fibrin (PRF), fibrin gel polymerization and leukocytes. Curr Pharm Biotechnol. 2012 Jun;13(7):1131-7.
280. Mishra A, Harmon K, Woodall J, Vieira A. Sports medicine applications of platelet rich plasma. Curr Pharm Biotechnol. 2012 Jun;13(7):1185-95.
281. Maganaris CN, Paul JP. In vivo human tendon mechanical properties. J Physiol. 1999 Nov 15;521 Pt 1:307-13.
282. Fleming BC, Beynnon BD. In vivo measurement of ligament/tendon strains and forces: a review. Ann Biomed Eng. 2004 Mar;32(3):318-28.
283. Doyley MM, Bamber JC, Fuechsel F, Bush NL. A freehand elastographic imaging approach for clinical breast imaging: system development and performance evaluation. Ultrasound Med Biol. 2001 Oct;27(10):1347-57.
284. Taylor LS, Porter BC, Rubens DJ, Parker KJ. Three-dimensional sonoelastography: principles and practices. Phys Med Biol. 2000 Jun;45(6):1477-94.
285. Bercoff J, Chaffai S, Tanter M, Sandrin L, Catheline S, Fink M, et al. In vivo breast tumor detection using transient elastography. Ultrasound Med Biol. 2003 Oct;29(10):1387-96.
286. Hall TJ, Zhu Y, Spalding CS. In vivo real-time freehand palpation imaging. Ultrasound Med Biol. 2003 Mar;29(3):427-35.
287. Muthupillai R, Lomas DJ, Rossman PJ, Greenleaf JF, Manduca A, Ehman RL. Magnetic resonance elastography by direct visualization of propagating acoustic strain waves. Science. 1995 Sep 29;269(5232):1854-7.
288. Bishop J, Samani A, Sciarretta J, Plewes DB. Two-dimensional MR elastography with linear inversion reconstruction: methodology and noise analysis. Phys Med Biol. 2000 Aug;45(8):2081-91.

289. Ophir J, Céspedes I, Ponnekanti H, Yazdi Y, Li X. Elastography: A quantitative method for imaging the elasticity of biological tissues. Ultrasonic Imaging. 1991;13(2):111-34.
290. Pesavento A, Perrey C, Krueger M, Ermert H. A time-efficient and accurate strain estimation concept for ultrasonic elastography using iterative phase zero estimation. IEEE Trans Ultrason Ferroelectr Freq Control. 1999;46(5):1057-67.
291. Kadour MJ, Noble JA. Assisted-freehand ultrasound elasticity imaging. IEEE Trans Ultrason Ferroelectr Freq Control. 2009 Jan;56(1):36-43.
292. Inoue Y, Takahashi M, Arita J, Aoki T, Hasegawa K, Beck Y, et al. Intra-operative freehand real-time elastography for small focal liver lesions: "visual palpation" for non-palpable tumors. Surgery. 2010 Nov;148(5):1000-11.
293. Chernak LA, Thelen DG. Tendon motion and strain patterns evaluated with two-dimensional ultrasound elastography. Journal of Biomechanics. 2012;45(15):2618-23.
294. Kadour M. Assisted-Freehand Ultrasound Elastography Imaging of the Breast [D-Phil]. oxford: University of Oxford; 2007.
295. Drakonaki EE, Allen GM, Wilson DJ. Real-time ultrasound elastography of the normal Achilles tendon: reproducibility and pattern description. Clinical Radiology. [doi: DOI: 10.1016/j.crad.2009.08.006]. 2009;64(12):1196-202.
296. Ophir J, Cespedes I, Ponnekanti H, Yazdi Y, Li X. Elastography: a quantitative method for imaging the elasticity of biological tissues. Ultrason Imaging. 1991 Apr;13(2):111-34.
297. Brown PG AJ, Cooper A, Thompson M, Noble JA. The AutoQual ultrasound elastography method for quantitative assessment of post rupture Achilles tendons. Journal of Biomechanics. 2013(Submitted Manuscript).
298. Kadour M, Noble JA. Assisted-freehand ultrasound elasticity imaging. Ultrasonics, Ferroelectrics and Frequency Control, IEEE Transactions on. 2009;56(1):36-43.
299. Maffulli N, Barrass V, Ewen SWB. Light Microscopic Histology of Achilles Tendon Ruptures. The American Journal of Sports Medicine. 2001 November 2001;28(6):857-63.
300. Waterston SW, Maffulli N, Ewen SW. Subcutaneous rupture of the Achilles tendon: basic science and some aspects of clinical practice. Br J Sports Med. 1997 Dec;31(4):285-98.
301. Rinder HM, Smith BR. In vitro evaluation of stored platelets: is there hope for predicting posttransfusion platelet survival and function? Transfusion. 2003 Jan;43(1):2-6.
302. Michelson A. Flow cytometry: a clinical test of platelet function. Blood. 1996 June 15, 1996;87(12):4925-36.
303. Jackson SP. The growing complexity of platelet aggregation. Blood. 2007 June 15, 2007;109(12):5087-95.
304. Toth O, Calatzis A, Penz S, Losonczy H, Siess W. Multiple electrode aggregometry: a new device to measure platelet aggregation in whole blood. Thromb Haemost. 2006 Dec;96(6):781-8.
305. Baumgarten A, Wilhelmi M, Kalbantner K, Ganter M, Mischke R. Measurement of platelet aggregation in ovine blood using a new impedance aggregometer. Veterinary Clinical Pathology. 2010;39(2):149-56.
306. Johnston G, Pickett E, McEver R, George J. Heterogeneity of platelet secretion in response to thrombin demonstrated by fluorescence flow cytometry. Blood. 1987 May 1, 1987;69(5):1401-3.
307. Schmitz G, Rothe G, Ruf A, Barlage S, Tschope D, Clemetson KJ, et al. European Working Group on Clinical Cell Analysis: Consensus protocol for the flow cytometric characterisation of platelet function. Thromb Haemost. 1998 May;79(5):885-96.
308. Curvers J, De Wildt-Eggen J, Heeremans J, Scharenberg J, De Korte D, Van Der Meer PF. Flow cytometric measurement of CD62P (P-selectin) expression on platelets: a multicenter optimization and standardization effort. Transfusion. 2008;48(7):1439-46.
309. Wakefield LM, Letterio JJ, Chen T, Danielpour D, Allison RS, Pai LH, et al. Transforming growth factor-beta1 circulates in normal human plasma and is unchanged in advanced metastatic breast cancer. Clinical Cancer Research. 1995 January 1, 1995;1(1):129-36.

310. Friedrich N, Alte D, Völzke H, Spilcke-Liss E, Lüdemann J, Lerch MM, et al. Reference ranges of serum IGF-1 and IGFBP-3 levels in a general adult population: Results of the Study of Health in Pomerania (SHIP). Growth Hormone & IGF Research. 2008;18(3):228-37.
311. Khan R, Fick D, Brammar T, Crawford J, Parker M. Interventions for treating acute Achilles tendon ruptures. Cochrane Database Syst Rev. 2004;3:CD003674.
312. Alsousou J HP, Thompson M, Handley R, McNally E, Noble A, Willett K. Platelet Rich Plasma in Accelerated Tendo-Achilles Healing (PATH): Randomised Controlled Trial - Pilot PHase. BOA Congress; 05-09-2012; Manchester2012.
313. Nilsson-Helander K, Thomee R, Silbernagel KG, Thomee P, Faxen E, Eriksson BI, et al. The Achilles tendon Total Rupture Score (ATRS): development and validation. The American journal of sports medicine. 2007 Mar;35(3):421-6.
314. Kearney RS, Achten J, Lamb SE, Plant C, Costa ML. A systematic review of patient-reported outcome measures used to assess Achilles tendon rupture management: what's being used and should we be using it? Br J Sports Med. 2012 Dec;46(16):1102-9.
315. Kearney RS, Achten J, Lamb SE, Parsons N, Costa ML. The Achilles tendon total rupture score: a study of responsiveness, internal consistency and convergent validity on patients with acute Achilles tendon ruptures. Health Qual Life Outcomes. 2012;10:24.
316. Robinson JM, Cook JL, Purdam C, Visentini PJ, Ross J, Maffulli N, et al. The VISA-A questionnaire: a valid and reliable index of the clinical severity of Achilles tendinopathy. Br J Sports Med. 2001 Oct;35(5):335-41.
317. Iversen JV, Bartels EM, Langberg H. The victorian institute of sports assessment - achilles questionnaire (visa-a) - a reliable tool for measuring achilles tendinopathy. Int J Sports Phys Ther. 2012 Feb;7(1):76-84.
318. Schonberger TJ, Janzing HM, Morrenhof JW, de Visser AC, Muitjens P. Operative treatment of acute Achilles tendon rupture: Open end-to-end-reconstruction versus reconstruction with Mitek-anchors. Acta Chir Belg. 2008 Mar-Apr;108(2):236-9.
319. Roos EM, Brandsson S, Karlsson J. Validation of the foot and ankle outcome score for ankle ligament reconstruction. Foot Ankle Int. 2001 Oct;22(10):788-94.
320. Garratt AM, Ruta DA, Abdalla MI, Buckingham JK, Russell IT. The SF36 health survey questionnaire: an outcome measure suitable for routine use within the NHS? BMJ. 1993 1993-05-29 00:00:00;306(6890):1440-4.
321. Carmont MR, Maffulli N. Modified percutaneous repair of ruptured Achilles tendon. Knee Surg Sports Traumatol Arthrosc. 2008 Feb;16(2):199-203.
322. Brown P, Alsousou J, Thompson M, Noble A, editors. Controlled motion strain measurement using lateral speckle tracking in Achilles tendons during healing. Biomedical Imaging (ISBI), 2012 9th IEEE International Symposium on; 2012 2-5 May 2012.
323. Ware JE, Jr. SF-36 health survey update. Spine (Phila Pa 1976). 2000 Dec 15;25(24):3130-9.
324. Liu SH, Yang RS, al-Shaikh R, Lane JM. Collagen in tendon, ligament, and bone healing. A current review. Clin Orthop Relat Res. 1995 Sep(318):265-78.
325. Ignotz RA, Endo T, Massague J. Regulation of fibronectin and type I collagen mRNA levels by transforming growth factor-beta. J Biol Chem. 1987 May 15;262(14):6443-6.
326. Brink HE, Miller GJ, Beredjiklian PK, Nicoll SB. Serum-dependent effects on adult and fetal tendon fibroblast migration and collagen expression. Wound Repair and Regeneration. 2006;14(2):179-86.
327. Schonk DM, Kuijpers HJH, Drunen E, Dalen CH, Geurts van Kessel AHM, Verheijen R, et al. Assignment of the gene(s) involved in the expression of the proliferation-related Ki-67 antigen to human chromosome 10. Hum Genet. 1989 1989/10/01;83(3):297-9.
328. Ferrara N, Gerber HP. The role of vascular endothelial growth factor in angiogenesis. Acta Haematol. 2001;106(4):148-56.
329. Gelberman R, Chu C, Williams C, Seiler J, Amiel D. Angiogenesis in healing autogenous flexor-tendon grafts. J Bone Joint Surg Am. 1992;74:1207 - 16.

330. Shweiki D, Itin A, Soffer D, Keshet E. Vascular endothelial growth factor induced by hypoxia may mediate hypoxia-initiated angiogenesis. Nature. 1992;359:843 - 5.
331. Liden M, Movin T, Ejerhed L, Papadogiannakis N, Blomen E, Hultenby K, et al. A histological and ultrastructural evaluation of the patellar tendon 10 years after reharvesting its central third. Am J Sports Med. 2008 Apr;36(4):781-8.
332. Movin T, Guntner P, Gad A, Rolf C. Ultrasonography-guided percutaneous core biopsy in Achilles tendon disorder. Scandinavian Journal of Medicine & Science in Sports. 1997;7(4):244-8.
333. Shalabi A, Svensson L, Kristoffersen-Wiberg M, Aspelin P, Movin T. Tendon injury and repair after core biopsies in chronic Achilles tendinosis evaluated by serial magnetic resonance imaging. Br J Sports Med. 2004 Oct;38(5):606-12.
334. Kiernan JA. Histological and Histochemical Methods: Bloxham, UK: Scion; 2008.
335. Vogel KG, Peters JA. Histochemistry defines a proteoglycan-rich layer in bovine flexor tendon subjected to bending. J Musculoskelet Neuronal Interact. 2005 Mar;5(1):64-9.
336. Movin T, Gad A, Reinholt FP, Rolf C. Tendon pathology in long-standing achillodynia. Biopsy findings in 40 patients. Acta Orthop Scand. 1997 Apr;68(2):170-5.
337. Longo UG, Franceschi F, Ruzzini L, Rabitti C, Morini S, Maffulli N, et al. Light microscopic histology of supraspinatus tendon ruptures. Knee Surg Sports Traumatol Arthrosc. 2007 Nov;15(11):1390-4.
338. Cook JL, Feller JA, Bonar SF, Khan KM. Abnormal tenocyte morphology is more prevalent than collagen disruption in asymptomatic athletes' patellar tendons. Journal of Orthopaedic Research. 2004;22(2):334-8.
339. Maffulli N, Longo U, Franceschi F, Rabitti C, Denaro V. Movin and Bonar Scores Assess the Same Characteristics of Tendon Histology. Clinical Orthopaedics and Related Research®. [10.1007/s11999-008-0261-0]. 2008;466(7):1605-11.
340. Kartus J, Movin T, Papadogiannakis N, Christensen LR, Lindahl S, Karlsson J. A radiographic and histologic evaluation of the patellar tendon after harvesting its central third. Am J Sports Med. 2000 Mar-Apr;28(2):218-26.
341. J I. Two ways to count cells using Image J. [25.08.2013]; Available from: www.unige.ch/medecine/bioimaging/.../imagejtutorials/CellCounting.pdf.
342. Wei A, Williams LA, Bhargav D, Shen B, Kishen T, Duffy N, et al. BMP13 prevents the effects of annular injury in an ovine model. Int J Biol Sci. 2009;5(5):388-96.
343. N A. 2012 [10-06-2013]; Available from: http://rsbweb.nih.gov/ij/docs/examples/stained-sections/index.html.
344. Labno C. Two Ways to count Cells with Image J. University of Chicago2013 [04-09-2013]; Available from: www.unige.ch/medecine/bioimaging/.../imagejtutorials/CellCounting.pdf.
345. Tang LH, Gonen M, Hedvat C, Modlin IM, Klimstra DS. Objective quantification of the Ki67 proliferative index in neuroendocrine tumors of the gastroenteropancreatic system: a comparison of digital image analysis with manual methods. Am J Surg Pathol. 2012 Dec;36(12):1761-70.
346. Majewski M, Ochsner PE, Liu F, Flückiger R, Evans CH. Accelerated Healing of the Rat Achilles Tendon in Response to Autologous Conditioned Serum. The American Journal of Sports Medicine. 2009 November 2009;37(11):2117-25.
347. O'Kane S, Ferguson MW. Transforming growth factor beta s and wound healing. Int J Biochem Cell Biol. 1997 Jan;29(1):63-78.
348. Virchenko O, Aspenberg P. How can one platelet injection after tendon injury lead to a stronger tendon after 4 weeks? Interplay between early regeneration and mechanical stimulation. Acta Orthop. 2006 Oct;77(5):806-12.
349. Xiong X, Wu L, Xiang D, Ni G, Zhao P, Yu B. [Effect of platelet-rich plasma injection on early healing of Achilles tendon rupture in rats]. Zhongguo Xiu Fu Chong Jian Wai Ke Za Zhi. 2012 Apr;26(4):466-71.

350. Torricelli P, Fini M, Giavaresi G, Carpi A, Nicolini A, Giardino R. Effects of systemic glucocorticoid administration on tenocytes. Biomedicine & Pharmacotherapy. 2006;60(8):380-5.
351. Poulsen RC, Carr AJ, Hulley PA. Protection against glucocorticoid-induced damage in human tenocytes by modulation of ERK, Akt, and forkhead signaling. Endocrinology. 2011 Feb;152(2):503-14.
352. Yao L, Bestwick CS, Bestwick LA, Maffulli N, Aspden RM. Phenotypic drift in human tenocyte culture. Tissue Eng. 2006 Jul;12(7):1843-9.
353. Belcher PR, Muriithi EW, Day SP, Wheatley DJ. Platelet aggregatory responses to low-dose collagen are maintained in hirudin-anticoagulated whole blood for 24 h when stored at room temperature. Platelets. 2001 Feb;12(1):34-6.
354. Walum E, Clemedson C, Ekwall B. Principles for the validation of in vitro toxicology test methods. Toxicol In Vitro. 1994 Aug;8(4):807-12.
355. Papadopoulos NG, Dedoussis GVZ, Spanakos G, Gritzapis AD, Baxevanis CN, Papamichail M. An improved fluorescence assay for the determination of lymphocyte-mediated cytotoxicity using flow cytometry. Journal of Immunological Methods. 1994;177(1–2):101-11.
356. Kaneshiro ES, Wyder MA, Wu Y-P, Cushion MT. Reliability of calcein acetoxy methyl ester and ethidium homodimer or propidium iodide for viability assessment of microbes. Journal of Microbiological Methods. 1993;17(1):1-16.
357. J Cell Biol 133, 1041 (1996).
358. J Cell Biol 133, 1053 (1996);.
359. Nakayama GR, Caton MC, Nova MP, Parandoosh Z. Assessment of the Alamar Blue assay for cellular growth and viability in vitro. J Immunol Methods. 1997 May 26;204(2):205-8.
360. Rye HS, Dabora JM, Quesada MA, Mathies RA, Glazer AN. Fluorometric assay using dimeric dyes for double- and single-stranded DNA and RNA with picogram sensitivity. Anal Biochem. 1993 Jan;208(1):144-50.
361. Anitua E, Sánchez M, Zalduendo MM, De La Fuente M, Prado R, Orive G, et al. Fibroblastic response to treatment with different preparations rich in growth factors. Cell Proliferation. 2009;42(2):162-70.
362. Hee CK, Dines JS, Solchaga LA, Shah VR, Hollinger JO. Regenerative Tendon and Ligament Healing: Opportunities with Recombinant Human Platelet-Derived Growth Factor BB-Homodimer. Tissue Eng Part B Rev. 2012 Feb 2.
363. Massberg S, Brand K, Gruner S, Page S, Muller E, Muller I, et al. A critical role of platelet adhesion in the initiation of atherosclerotic lesion formation. J Exp Med. 2002 Oct 7;196(7):887-96.
364. Sharma P, Maffulli N. Tendinopathy and tendon injury: the future. Disabil Rehabil. 2008;30(20-22):1733-45.
365. Zargar Baboldashti N. PR, Franklin SL., Thompson MS., Hulley PA. The effect of PRP in Protection and Migration of Tenocytes (TERMIS) 2010. TERMIS; June; Ireland2012.
366. Feldser D, Agani F, Iyer NV, Pak B, Ferreira G, Semenza GL. Reciprocal Positive Regulation of Hypoxia-inducible Factor 1α and Insulin-like Growth Factor 2. Cancer Research. 1999 August 15, 1999;59(16):3915-8.
367. Wang GL, Jiang BH, Rue EA, Semenza GL. Hypoxia-inducible factor 1 is a basic-helix-loop-helix-PAS heterodimer regulated by cellular O2 tension. Proceedings of the National Academy of Sciences. 1995 June 6, 1995;92(12):5510-4.
368. Semenza GL. Hypoxia-inducible factor 1: master regulator of O2 homeostasis. Current Opinion in Genetics & Development. 1998;8(5):588-94.
369. Semenza GL. Targeting HIF-1 for cancer therapy. Nat Rev Cancer. [10.1038/nrc1187]. 2003;3(10):721-32.
370. Zhang J, Wang JH. Mechanobiological response of tendon stem cells: implications of tendon homeostasis and pathogenesis of tendinopathy. J Orthop Res. 2010 May;28(5):639-43.

371. Leytin V, Mody M, Semple JW, Garvey B, Freedman J. Flow Cytometric Parameters for Characterizing Platelet Activation by Measuring P-Selectin (CD62) Expression: Theoretical Consideration and Evaluation in Thrombin-Treated Platelet Populations. Biochemical and Biophysical Research Communications. 2000;269(1):85-90.
372. Nilsson-Helander K, Silbernagel KG, Thomee R, Faxen E, Olsson N, Eriksson BI, et al. Acute achilles tendon rupture: a randomized, controlled study comparing surgical and nonsurgical treatments using validated outcome measures. Am J Sports Med. 2010 Nov;38(11):2186-93.
373. Sheth U, Simunovic N, Klein G, Fu F, Einhorn TA, Schemitsch E, et al. Efficacy of autologous platelet-rich plasma use for orthopaedic indications: a meta-analysis. J Bone Joint Surg Am. 2012 Feb 15;94(4):298-307.
374. ErythroSave. ErythroSave. Snapshot of PRP markets (US). Available at: http://www.erythrosave.net/index.php?option=com_content&task=view&id=15&Itemid=29. . 2012 [28-8-2013].
375. Hebert-Losier K, Newsham-West RJ, Schneiders AG, Sullivan SJ. Raising the standards of the calf-raise test: a systematic review. J Sci Med Sport. 2009 Nov;12(6):594-602.
376. Silbernagel KG, Nilsson-Helander K, Thomee R, Eriksson BI, Karlsson J. A new measurement of heel-rise endurance with the ability to detect functional deficits in patients with Achilles tendon rupture. Knee Surg Sports Traumatol Arthrosc. 2010 Feb;18(2):258-64.
377. Moller M, Lind K, Styf J, Karlsson J. The reliability of isokinetic testing of the ankle joint and a heel-raise test for endurance. Knee surgery, sports traumatology, arthroscopy : official journal of the ESSKA. 2005 Jan;13(1):60-71.
378. Moller M, Movin T, Granhed H, Lind K, Faxen E, Karlsson J. Acute rupture of tendon Achillis. A prospective randomised study of comparison between surgical and non-surgical treatment. The Journal of bone and joint surgery British volume. 2001 Aug;83(6):843-8.
379. Kearney RS, Achten J, Lamb SE, Plant C, Costa ML. A systematic review of patient-reported outcome measures used to assess Achilles tendon rupture management: What's being used and should we be using it? Br J Sports Med. 2011 Nov 16.
380. Olsson N, Karlsson J, Eriksson BI, Brorsson A, Lundberg M, Silbernagel KG. Ability to perform a single heel-rise is significantly related to patient-reported outcome after Achilles tendon rupture. Scand J Med Sci Sports. 2012 Jun 21;In press.
381. Stratford P. Assessing Disability and Change on Individual Patients: A Report of a Patient Specific Measure. Physiotherapy Canada. 1995 01/01/;47(4):258-63.
382. Horn KK, Jennings S, Richardson G, Vliet DV, Hefford C, Abbott JH. The patient-specific functional scale: psychometrics, clinimetrics, and application as a clinical outcome measure. The Journal of orthopaedic and sports physical therapy. 2012 Jan;42(1):30-42.
383. Kearney RS, McGuinness KR, Achten J, Costa ML. A systematic review of early rehabilitation methods following a rupture of the Achilles tendon. Physiotherapy. 2012 Mar;98(1):24-32.

Appendices

Appendix 3.1 Achilles Tendon Study Data Management Protocols

System connection

1. When using the Zonare portable machine, first connect the only Zonare USB port to the 1-4 USB port splitter
2. Insert the external USB flash disk to one port of the USB splitter for US data storage
3. Connect the COM port of the external PC with one port of the USB splitter using the COM-to-USB cable for command control.
4. When using the Zonare docking system, there're two USB ports on the back of the system. Connect one port to the USB flash disk and the other port to the external PC.

Clinical data Acquisition

1. Turn on the Zonare
2. Select "Achilles Tendon" protocol in Zonare
3. Press "F1" button if you want to switch to Elastography mode on Zonare
4. Press "freeze" button to freeze current image and "freeze" again to unfreeze. Click "Store" to save the image (B mode or elastography) on Zonare hard drive
5. Turn on the external PC
6. Login with username: "at_study" password: "at_study"
7. Double click the "at_study" icon on the desktop and wait for GUI to boot.
8. Click "Init" button on the at_study GUI to initialize force transducer, motor and COM port
9. Wait for participant
10. In at_study GUI, enter participant number
11. Choose Left or Right Achilles Tendon
12. For PC controlled motion, click "PF" or "DF" for plantar flexion or dorsal flexion
13. For manual compression/decompression, click "Store" button right after scan was over
14. Wait till US data has been stored on external USB flash drive and image on Zonare has been unfreezed
15. The clinical US data should be stored on the External USB flash disk and the force data should be stored on the external PC under e:\at_study\. The US/Elastography images on Zonare could be exported to the flash disk by pressing "Achieve" and then "Export". Take the US data to Ying at IBME for further analysis

Data Analysis

Zonare© DATA preprocessing

1. The US data should have been brought back to IBME for Ying to process. On iris, the Zonare research package toolkits should have been properly installed. Check the Zonare research package User Guide for installation procedures.
2. Copy the Zonare US data to a temporary location on Iris, say, e:\uei\at_study\temp
3. Start Matlab on Iris, Run:" zonare_data_preprocessing". The function will open the GUI for zonare data preprocessing
4. Click "IQ Data Conversion" button. You will be asked to choose a directory where the Zonare US data were stored. Choose e:\uei\at_study\temp. All the Zonare raw US data in the directory will be converted into the so called "IQ" data format and saved in the same directory.
5. Wait till "IQ Data Conversion" is finished. Click "RF Data Extraction" button. You will be asked to choose a directory where the IQ data were stored. Choose e:\uei\at_study\temp. All the IQ data in the directory will be converted into RF data format. The RF data and its corresponding movie will be saved in the same directory.
6. Move the IQ data from PC controlled Dorsal/Plantar Flexion to :\uei\at_study\temp\control. Move the IQ data from manual Compression/Decompression to e:\uei\at_study\temp\manual.
7. For PC-controlled motion data, click "Auto" button. You will be asked to choose a directory where the PC-controlled motion IQ data were stored. Choose e:\uei\at_study\temp\control. Then enter the frame number of the RF sequence, by default, it's 16. The RF data and its corresponding movie will be stored in the same directory.
8. For manual compression/decompression data, review all the movies first. Manually select 16 frames from compression and 16 frames from decompression. Create a txt file, say framenum.txt, which contains the start/end frame numbers of each compression/decompression processes for all the data. Click "Manual" button. You will be asked to choose a directory where the manual compression/decompression IQ data were stored. Choose e:\uei\at_study\temp\manual. Then select the txt file where all the frame selection info was stored. The RF data and its corresponding movie will be then stored in the same directory.
9. Create the corresponding uei_body for the participant and copy the participant's data into the e:\uei\data directory.

Appendix 4.1: Autologous Blood Withdrawal Protocol

Volumes of ACD-A and corresponding volumes of blood to achieve anti-coagulated blood containing approximately 7 parts blood: 1 part ACD-A:

Total Volume of Anticoagulated Blood (ml)	Volume of ACD-A (ml)	Volume of Blood Drawn (ml)
30	**4.0**	**26.0**
40	**5.0**	**35.0**
50	**6.0**	**44.0**
60	**8.0**	**52.0**

Use MDK300 Magellan disposable kit

Prime the needle with the citrate anticoagulant prior to performing the venepuncture.

Draw the appropriate amount of ACD-A into 60ml BD syringe(s) at a flow rate of 1 ml per second.

GENTLY draw the blood using an 18 gauge needle or larger for peripheral vein access such as the antecubital vein. Excess force may prematurely activate the platelets and cause red blood cell haemolysis. Therefore, when using smaller gauge devices with either access site, the blood withdrawal rate should be slowed accordingly.

Invert the 60 ml blood collection syringe several times to insure adequate mixing of the blood and anticoagulant.

Mix the other syringes every 5 to 8 minutes while awaiting processing on the Magellan device.

The 60 ml blood collection syringes must be labelled with the appropriate patient information and time of collection in accordance with the 3rd Edition of AABB Standards for Peri-operative Autologous Blood Collection and Administration.

The whole blood collected in the 60 ml syringes must be processed within 8 hours of collection. Once separated, the autologous platelet rich plasma must be used within an hour.

Appendix 4.2: Platelet Rich Plasma Growth Factors Sample Preparation

1. Measure PRP volume
2. Measure Thrombin volume
3. The Magellan PRP autologous thrombin kit produces the following
    a. 6 ml PRP total volume
    b. 2.5 ml to produce Autologous thrombin
    c. 3.5 ml residual PRP
    d. PRP / Atologous thrombin ratio is 2:1
4. Empty PRP and thrombin syringes into 2 separate test tubes

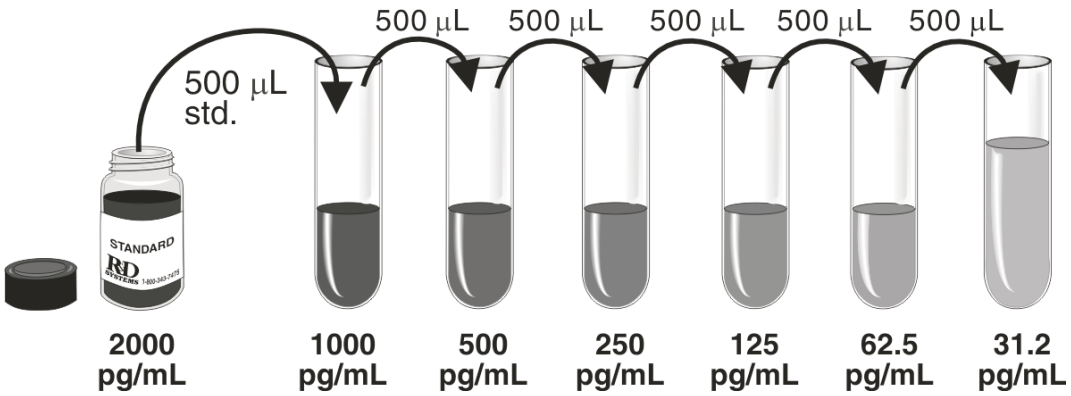
Growth Factor Sample preparation

1. In a test tube add
    a. 1.5 ml PRP
    b. 0.5 ml thrombin
2. Shake tube gently to mix
3. Incubate for 30 min at 37°c
4. When clot is formed, spin the tube in a centrifuge at 2500rpm for 20 min
5. Aspirate the serum into a small capped tube
6. Label with trial ID and date
7. Save in -80c freezer
8. GF analysis will be perfomed using ELISA kit when all samples are collected

Appendix 4.6 TGF-β1 ELISA Immunoassay

Use Quantikine Human TGF beta 1 Immunoassay. Bring all reagents and samples to room temperature before use. It is recommended that all samples, standards, and controls be assayed in duplicate.

1. Prepare all reagents according to manufacturer instruction. Prepare standard dilution as shown below. Record all samples on a chart.



2. Remove excess microplate strips from the plate frame, return them to the foil pouch containing the desiccant pack, and reseal.

3. Add 50 µL of Assay Diluent RD1-73 to each well.

4. Add 100 µL of Standard, control, or sample per well. Tap gently to mix.

5. Cover with the adhesive strip provided and incubate for 2 hours at room temperature.

6. Aspirate each well and wash, repeating the process three times for a total of four washes. Wash by filling each well with Wash Buffer (400 µL) using a pipette. Complete removal of liquid at each step is essential to good performance. After the last wash, remove any remaining Wash Buffer by aspirating or decanting. Invert the plate and blot it against clean paper towels.

7. Add 100 µL of TGF-β1 Conjugate to each well. Cover with a new adhesive strip. Incubate for 2 hours at room temperature.

7. Repeat the aspiration/wash as in step 5.

8. Add 200 µL of Substrate Solution to each well. Protect from light. For Serum/Plasma Samples: Incubate for 25 minutes at room temperature.

9. Add 100 µL of Substrate solution to each well. Incubate for 30 minutes at room temperature and protect from light.

10. Determine the optical density of each well within 30 minutes, using a microplate reader set to 450 nm. If wavelength correction is available, set to 540 nm or 570 nm. If wavelength correction is not available, subtract readings at 540 nm or 570 nm from the readings at 450 nm. This subtraction will correct for optical imperfections in the plate. Readings made directly at 450 nm without correction may be higher and less accurate.

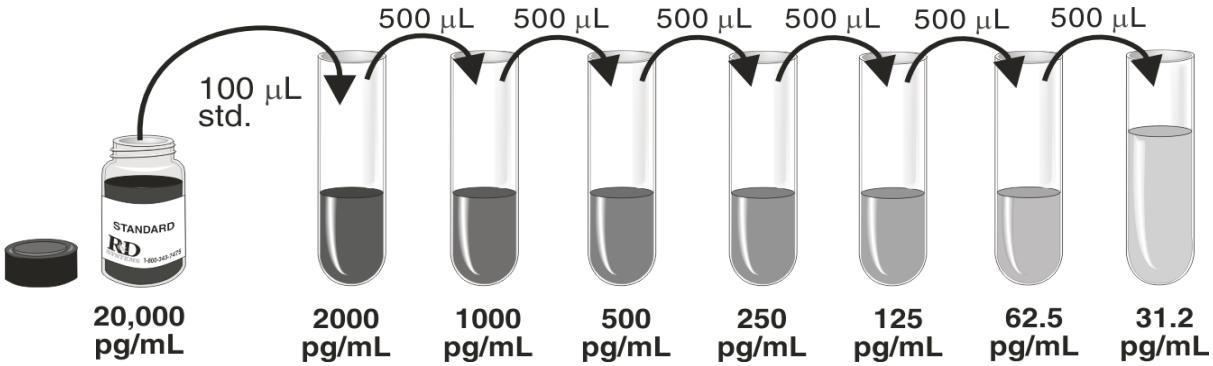
CALCULATION OF RESULTS

Average the duplicate readings for each standard, control, and sample and subtract the average zero standard optical density. Create a standard curve by reducing the data using computer software capable of generating a four parameter logistic (4-PL) curve-fit. As an alternative, construct a standard curve by plotting the mean absorbance for each standard on the y-axis against the concentration on the x-axis and draw a best fit curve through the points on the graph. The data may be linearized by plotting the log of the TGF-β1 concentrations versus the log of the O.D., and the best fit line can be determined by regression analysis. This procedure will produce an adequate but less precise fit of the data.

Appendix 4.7 PDGF-AB ELISA Immunoassay

Use Quantikine Human TGF beta 1 Immunoassay. Bring all reagents and samples to room temperature before use. It is recommended that all samples, standards, and controls be assayed in duplicate.

1. Prepare all reagents according to manufacturer instruction. Prepare standard dilution as shown below. Record all samples on a chart.



2. Remove excess microplate strips from the plate frame, return them to the foil pouch containing the desiccant pack, and reseal.

3. Add 100 µL of Assay Diluent RD1X to each well.

4. Add 100 µL of Standard, control, or sample per well. Tap gently to mix.

5. Cover with the adhesive strip provided and incubate for 3 hours at room temperature.

6. Aspirate each well and wash, repeating the process three times for a total of four washes. Wash by filling each well with Wash Buffer (400 µL) using a pipette. Complete removal of liquid at each step is essential to good performance. After the last wash, remove any remaining Wash Buffer by aspirating or decanting. Invert the plate and blot it against clean paper towels.

7. Add 200 µL of PDGF-AB Conjugate to each well. Cover with a new adhesive strip. Incubate for 2 hours at room temperature.

7. Repeat the aspiration/wash as in step 5.

8. Add 200 µL of Substrate Solution to each well. Protect from light. For Serum/Plasma Samples: Incubate for 30 minutes at room temperature.

10. Determine the optical density of each well within 30 minutes, using a microplate reader set to 450 nm. If wavelength correction is available, set to 540 nm or 570 nm. If wavelength correction is not available, subtract readings at 540 nm or 570 nm from the readings at 450 nm. This subtraction will correct for optical imperfections in the plate. Readings made directly at 450 nm without correction may be higher and less accurate.

CALCULATION OF RESULTS

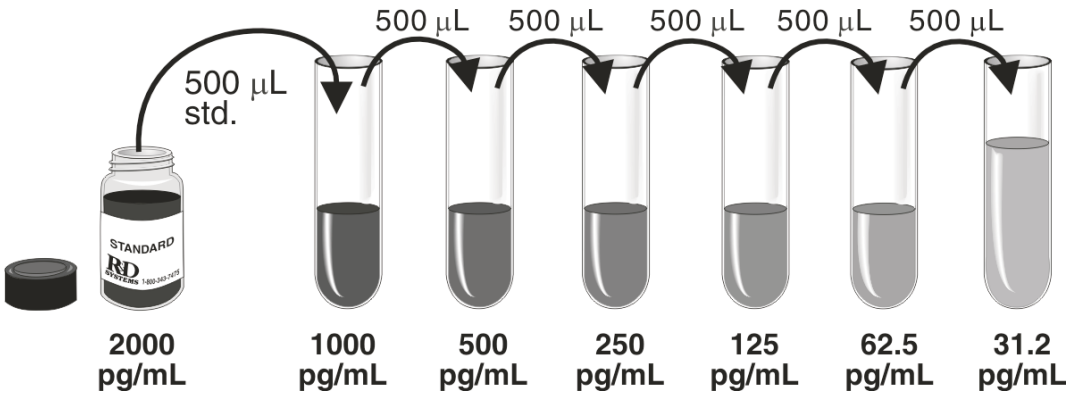
Average the duplicate readings for each standard, control, and sample and subtract the average zero

standard optical density. Plot the optical density for the standards versus the concentration of the standards and draw the best curve. The data can be linearized by using log/log paper and regression analysis may be applied to the log transformation. To determine the PDGF-AB concentration of each sample, first find the absorbance value on the y-axis and extend a horizontal line to the standard curve. At the point of intersection, extend a vertical line to the x-axis and read the corresponding PDGF-AB concentration. Because serum samples have been diluted, the measured concentrations must be multiplied by the dilution factor of 50.

Appendix 4.5 VEGF ELISA Immunoassay

Bring all reagents and samples to room temperature before use. It is recommended that all samples, standards, and controls be assayed in duplicate.

1. Prepare all reagents as shown below. Record all samples on a chart.



2. Remove excess microplate strips from the plate frame, return them to the foil pouch containing the desiccant pack, and reseal.

3. Add 100 µL of Assay Diluent RD1W to each well.

4. Add 100 µL of Standard, control, or sample per well.

5. Cover with the adhesive strip provided and incubate for 2 hours at room temperature.

6. Aspirate each well and wash, repeating the process twice for a total of three washes. Wash by filling each well with Wash Buffer (400 µL) using a pipette. Complete removal of liquid at each step is essential to good performance. After the last wash, remove any remaining Wash Buffer by aspirating or decanting. Invert the plate and blot it against clean paper towels.

7. Add 200 µL of VEGF Conjugate to each well. Cover with a new adhesive strip. Incubate for 2 hours at room temperature.

7. Repeat the aspiration/wash as in step 5.

8. Add 200 µL of Substrate Solution to each well. Protect from light. For Serum/Plasma Samples: Incubate for 25 minutes at room temperature.

9. Add 50 µL of Stop Solution to each well. If colour change does not appear uniform, gently tap the plate to ensure thorough mixing. If the colour in the wells is green or the colour change does not appear uniform, gently tap the plate to ensure thorough mixing.

10. Determine the optical density of each well within 30 minutes, using a microplate reader set to 450 nm. If wavelength correction is available, set to 540 nm or 570 nm. If wavelength correction is not available, subtract readings at 540 nm or 570 nm from the readings at 450 nm. This subtraction will correct for optical imperfections in the plate. Readings made directly at 450 nm without correction may be higher and less accurate.

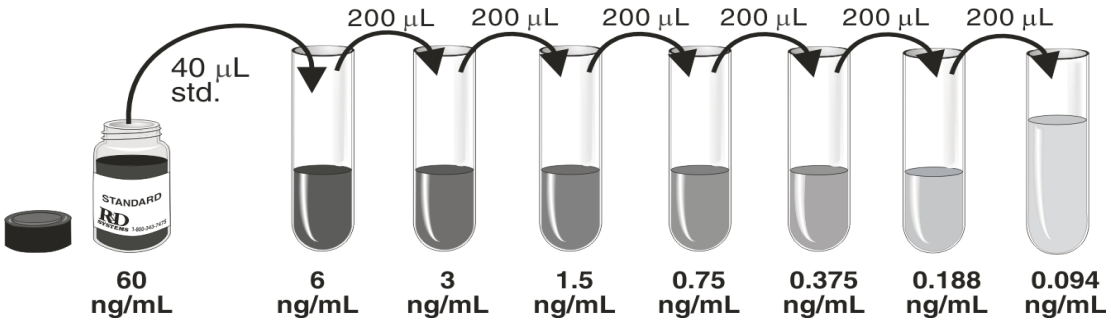
CALCULATION OF RESULTS

Average the duplicate readings for each standard, control, and sample and subtract the average zero standard optical density. Create a standard curve by reducing the data using computer software capable of generating a four parameter logistic (4-PL) curve-fit. As an alternative, construct a standard curve by plotting the mean absorbance for each standard on the y-axis against the concentration on the x-axis and draw a best fit curve through the points on the graph. The data may be linearized by plotting the log of the VEGF concentrations versus the log of the O.D., and the best fit line can be determined by regression analysis. This procedure will produce an adequate but less precise fit of the data.

Appendix 4.8 IGF-1 ELISA Immunoassay

Use Quantikine Human IGF 1 Immunoassay. Bring all reagents and samples to room temperature before use. It is recommended that all samples, standards, and controls be assayed in duplicate.

1. Prepare all reagents according to manufacturer instruction. Prepare standard dilution as shown below. Record all samples on a chart.



2. Remove excess microplate strips from the plate frame, return them to the foil pouch containing the desiccant pack, and reseal.

3. Add 150 µL of Assay Diluent RD1-53 to each well.

4. Add 50 µL of Standard, control, or sample per well. Tap gently to mix.

5. Cover with the adhesive strip provided and incubate for 2 hours at 2-8°c.

6. Aspirate each well and wash, repeating the process three times for a total of four washes. Wash by filling each well with Wash Buffer (400 µL) using a pipette. Complete removal of liquid at each step is essential to good performance. After the last wash, remove any remaining Wash Buffer by aspirating or decanting. Invert the plate and blot it against clean paper towels.

7. Add 200 µL of cold IGF-1 Conjugate to each well. Cover with a new adhesive strip. Incubate for 1 hour at 2-8°c.

7. Repeat the aspiration/wash as in step 5.

8. Add 200 µL of Substrate Solution to each well. Protect from light. For Serum/Plasma Samples: Incubate for 30 minutes at room temperature.

9. Add 50 _L of Stop Solution to each well. The color in the well should change from blue to yellow. If the color in the well is green or if the color change does not appear uniform, gently tap the plate to ensure thorough mixing.

10. Determine the optical density of each well within 30 minutes, using a microplate reader set to 450 nm. If wavelength correction is available, set to 540 nm or 570 nm. If wavelength correction is not available, subtract readings at 540 nm or 570 nm from the readings at 450 nm. This subtraction will correct for optical imperfections in the plate. Readings made directly at 450 nm without correction may be higher and less accurate.

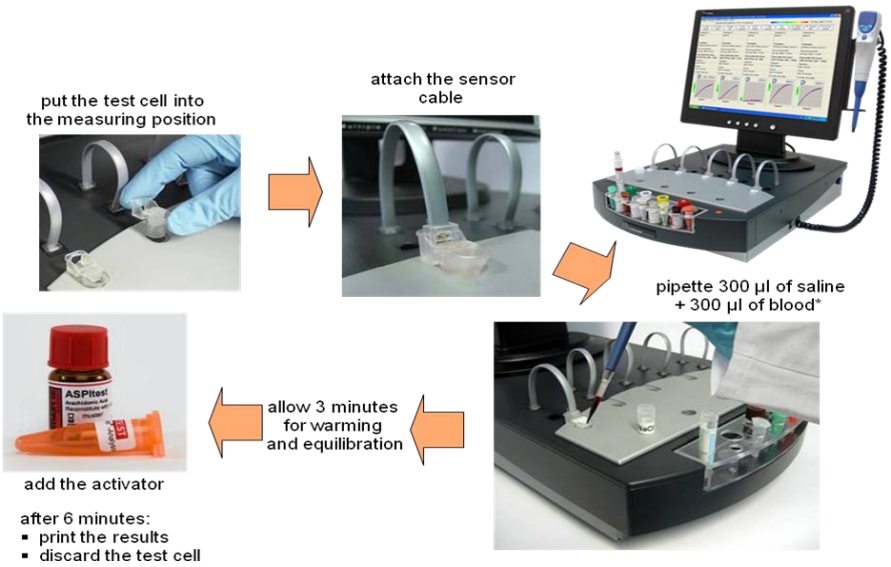
CALCULATION OF RESULTS

Average the duplicate readings for each standard, control, and sample and subtract the average zero standard optical density. Plot the optical density for the standards versus the concentration of the standards and draw the best curve. The data can be linearized by using log/log paper and regression analysis may be applied to the log transformation. To determine the IGF-1 concentration of each sample, first find the absorbance value on the y-axis and extend a horizontal line to the standard curve. At the point of intersection, extend a vertical line to the x-axis and read the corresponding PDGF-AB concentration. Because serum samples have been diluted, the measured concentrations must be multiplied by the dilution factor of 100.

Appendix 4.6 Platelet aggregation Assay Protocol

Platelet Function analysis using Multiple Electrode Aggregometry (Multiplate®)

1. Turn Multiplate Aggregometry on and wait for it to warm up to 36.6-37 c
2. Attach test cells into measuring position
3. Start electronic control and print results.
4. Attach the sensor cable to the test cell
5. Use auto-pipetting
6. Pipette **300µl of PRP into the test and control cells**
7. Pipette **300µl of warm Saline into the test and control cells**
8. Allow 3 minutes for warming and equilibration
9. Add **Thrombin** or C**ollagen reagent (ColTest) to <u>Test</u> cell**
10. Add **Saline to <u>Control</u> cell**
11. Allow the test to run for 6 minutes
12. Print results and save them on the hard disc
13. Discard the test cell



Appendix 4.7 Flow Cytometry CD62p Expression Assay protocol

1. Use capped polypropylene tubes
2. Pipette the following into the tube
    i. 150 µl PRP
    ii. 50µl GPRP (10mM)
    iii. 100µl Thrombin
3. Mix gently
4. Incubate for **10 minutes at 37®c**
5. Label four test tubes:
    i. Control-Control
    ii. Control-Test
    iii. Test-Control
    iv. Test-Test
6. Add 5 µl of the above mixture (PRP + GPRP + Thrombin) to each tube
7. Add 5 µl Control Antibodies (PE Mouse IgG1, κ Isotype Control, BD) to
    i. control-control and
    ii. Test-contol tubes
8. Add 5 µl Test Antibodies (PE Mouse Anti-Human CD62P. BD Pharmagen) to
    i. Control-test and
    ii. Test-Test tubes
9. Add 5 µl GPRP to all tubes
10. Dilute with Isoton to a total volume of 50 µl
11. Incubate for 10-15 min
12. Perform Flow cytometry measurements and print results for each test tube

APPENDIX 5.2: Dynamic USS protocol

Ultrasound Scan

Dynamic is performed by a specialist in musculoskeletal radiology on the next available list. At ultrasound:

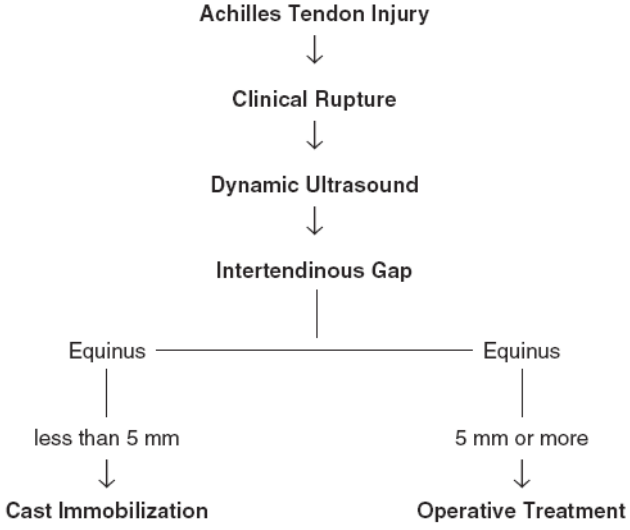
- Clinical suspicion of a TA rupture is confirmed.
- The locations of the rupture, together with measurement of the gap between the tendon ends, are recorded with the foot in the resting position (static technique).
- The foot on the injured side is then moved into as much plantar flexion as pain allowed (dynamic technique). The gap between the tendon ends is recorded and compared with that measured in the resting position.
- The site of rupture is marked on the skin.
- The patient returns to the trauma clinic the next day for a decision on the method of treatment.

Treatment Protocol

Treatment is based on the following protocol.

- Those patients with a gap between the tendon ends of 5 mm or more (dynamic technique) will receive operative treatment.
- When the tendon ends appose or the dynamic gap is measured as less than 5 mm, the patient will receive nonoperative treatment.

All patients will be informed of the advantages and disadvantages of each treatment method.
The choice of open or percutaneous repair is made by the patient after an informed discussion with the operating surgeon. Surgical repair is performed as soon as possible by or under the direct supervision of the orthopaedic surgeon. Standard approach and techniques will be used for both procedures. Postoperatively, the patient will follow the protocols out lined in the following sections.



Rohit Kotnis, Saronjini David, Robert Handley, Keith Willett and Simon Ostlere. Dynamic Ultrasound as a Selection Tool for Reducing Achilles Tendon Reruptures. *Am. J. Sports Med.* 2006; 34(9): 1395

Appendix 5.3 Sheffield Regime for Non Operative T.A Ruptures

Week 1-3

- Below knee full cast.
- NWB

Week 3-6

- Change to **below knee removable cast** at 15 degrees equinus with heel block to allow WBAT using crutches.
- Refer to **Physio.**
- Active Dorsiflexion, inversion & eversion exercises NWB
- Progress to active Plantarflexion exercises.
- Specific Soft Tissue Mobilisations (SSTM) to tendon.

Week 6-7

- Cast off into **Samson Boot** +/- heel raise if plantigrade not achievable.
- **WBAT in boot**, gait re education, wean off crutches.
- Toe & Heel raises in sitting.
- Active ankle ROM exercises.
- Passive DF stretches, PWB in sitting eg Heel slides.
- SSTM
- Basic proprioceptive exercises as appropriate.

Week 7-9

- **Wean out of boot** once DF past neutral and able to FWB in boot without crutches.
- Gait re education out of boot +/- heel raise **in shoe, FWB** no crutches.
- DF stretches in standing.
- Heel raises in standing 80/20, 50/50, 20/80
- Resisted theraband exercises all ankle movements.
- Progress proprioceptive exercises.

Week 9-12

- Aim towards single leg heel raises.
- Refer to **ankle class.**
- Eccentric & Concentric loading exercises.

Week 12 onwards

- Single leg heel raises.
- Walking on toes.
- Jogging on toes.
- Running.
- Return to sport

Use your clinical judgement to progress to each stage. Eg pain, stretch, strength.

Appendix 5.4 Protocol for Cutaneous Repair of Ruptured TA

1 week post op.

- Change from backslab to Hinged boot at 20 degrees equinus to be worn at all times
- **NWB**
- Active Dorsiflexion exercises against resistance, theraband, 10-15 /hour.
- Review 1 week

2 weeks post op.

- Check contraction of Gastroc Ms in prone.
- Check Dorsiflexion & if neutral achievable alter boot to plantigrade.
- Teach Dorsiflexion/Planterflexion exercises.
- Start Partial weightbearing in boot, if plantigrade possible, & increase WB as able.
- Wear boot at all times including sleeping.
- Review 1 week.

3 weeks post op.

- If good contraction of Gastroc ms, boot off at night.
- Increase weightbearing in boot, in & outdoors.
- Boot only when walking outdoors at 5 weeks.
- Continue PF/DF exercises.
- Review in 3 weeks.

DYNAMIC REHAB TO COMMENCE AT 6 WEEKS POST OP.

6 weeks post op

- Stop theraband exercise for DF, continue with active PF exercises.
- Boot Off.
- Heel raises in sitting.
- Careful walking FWB no boot.

7 weeks post op

- Bilateral heel raises in standing 80/20%(Good/Affected)
- Gait re education FWB

9 weeks post op 50/50 bilateral heel raises.

12 weeks post op (3 months) Single Heel Raise, aim at holding for 5 seconds.

14 weeks post op Toe walking

16 weeks post op (4 months) Jogging on toes

19 weeks post op Running.

Use your own clinical judgment to assess when patient is ready to progress onto next stage. Generally patients will be able to return to sports a few months after rehab period.

Appendix 5.5: Achilles Tendon Rupture Score (ATRS)

Trial number …… Date of Assessment ……..

All questions refer to your limitations/difficulties related to your injured Achilles tendon.

Mark with an X in the box which matches your level of limitation.

1. Are you limited due to decreased strength in the calf/Achilles tendon/foot?

0	1	2	3	4	5	6	7	8	9	10

2. Are you limited due to fatigue in the calf/Achilles tendon/foot?

0	1	2	3	4	5	6	7	8	9	10

3. Are you limited due to stiffness in the calf/Achilles tendon/foot?

0	1	2	3	4	5	6	7	8	9	10

4. Are you limited due to pain in the calf/Achilles tendon/foot?

0	1	2	3	4	5	6	7	8	9	10

5. Are you limited during activities of daily living?

0	1	2	3	4	5	6	7	8	9	10

6. Are you limited when walking on uneven surfaces?

0	1	2	3	4	5	6	7	8	9	10

7. Are you limited when walking quickly up the stairs or up a hill?

0	1	2	3	4	5	6	7	8	9	10

8. Are you limited during activities that include running?

0	1	2	3	4	5	6	7	8	9	10

9. Are you limited during activities that include jumping?

0	1	2	3	4	5	6	7	8	9	10

10. Are you limited in performing hard physical labor?

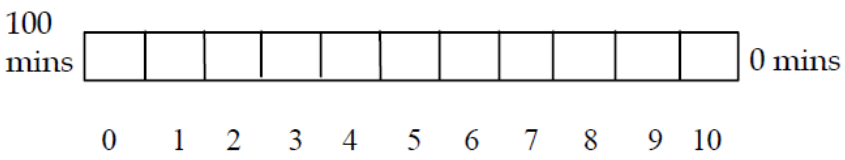
0	1	2	3	4	5	6	7	8	9	10

Initials …….. **Total:**

Appendix 5.6: VISA-A QUESTIONNAIRE

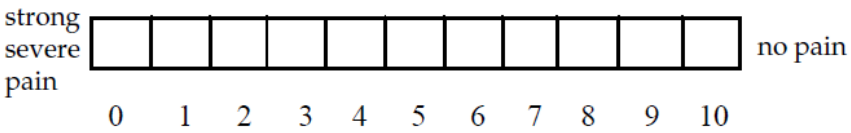
THE TERM PAIN REFERS SPECIFICALLY TO PAIN IN THE ACHILLES TENDON REGION

1. For how many minutes do you have stiffness in the Achilles region on first getting up?



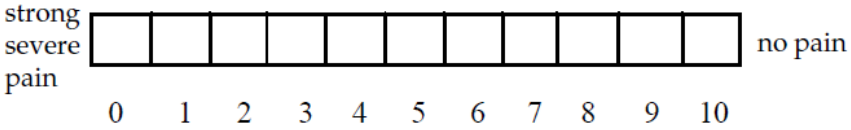
POINTS ❒

2. Once you are warmed up for the day, do you have pain when stretching the Achilles tendon fully over the edge of a step? (keeping knee straight)



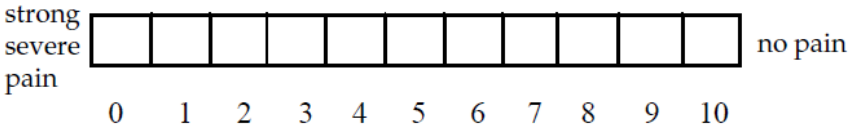
POINTS ❒

3. After walking on flat ground for 30 minutes, do you have pain within the next 2 hours? (If unable to walk on flat ground for 30 minutes because of pain, score 0 for this question).



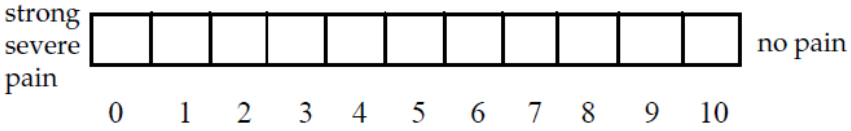
POINTS ❒

4. Do you have pain walking downstairs with a normal gait cycle?



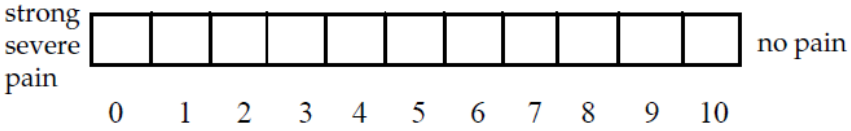
POINTS ❒

5. Do you have pain during or immediately after doing 10 (single leg) heel raises from a flat surface?



POINTS ❒

6. How many single leg hops can you do without pain?



POINTS ❒

7. Are you currently undertaking sport or other physical activity?

			POINTS
0	r	Not at all	
4	r	Modified training ± modified competition	❒
7	r	Full training ± competition but not at same level as when symptoms began	
10	r	Competing at the same or higher level as when symptoms began	

8. Please complete **EITHER A, B or C** in this question.

.

- If you have **no pain while undertaking Achilles tendon loading sports** please complete **Q8a only**.
- If you have **pain while undertaking Achilles tendon loading sports but it does not stop you from completing the activity**, please complete **Q8b only**.
- If you have **pain which stops you from completing Achilles tendon loading sports**, please complete **Q8c only**.

A. If you have **no pain** while undertaking **Achilles tendon loading sports**, for how long can you train/practise?

NIL	1-10 mins	11-20 mins	21-30mins	>30 mins	POINTS
r	r	r	r		
0	7	14	21	30	❒

OR

B. If you have some pain while undertaking **Achilles tendon loading sport**, but it does not stop you from completing your training/practice for how long can you train/practise?

NIL	1-10 mins	11-20 mins	21-30mins	>30 mins	POINTS
r	r	r	r		
0	7	14	21	30	❒

OR

C. If you have **pain that stops you** from completing your training/practice in **Achilles tendon loading sport**, for how long can you train/practise?

NIL	1-10 mins	11-20 mins	21-30mins	>30 mins	POINTS
r	r	r	r		
0	7	14	21	30	❒

TOTAL SCORE (/100) ❒

%

Appendix 5.7 Foot and Ankle Outcome Score (FAOS – UK)

Todays date: _____/_____/_____ Date of birth: _____/_____/_____
Trial ID: _____

INSTRUCTIONS: This survey asks for your view about your foot/ankle. This information will help us keep track of how you feel about your foot/ankle and how well you are able to do your usual activities. Answer every question by ticking the appropriate box, only one box for each question. If you are unsure about how to answer a question, please give the best answer you can.

Symptoms

These questions should be answered thinking of your foot/ankle symptoms during the **last week**.

S1. Do you have swelling in your foot/ankle?

Never	Rarely	Sometimes	Often	Always
☐	☐	☐	☐	☐

S2. Do you feel grinding, hear clicking or any other type of noise when your foot/ankle moves?

Never	Rarely	Sometimes	Often	Always
☐	☐	☐	☐	☐

S3. Does your foot/ankle catch or hang up when moving?

Never	Rarely	Sometimes	Often	Always
☐	☐	☐	☐	☐

S4. Can you straighten your foot/ankle fully?

Never	Rarely	Sometimes	Often	Always
☐	☐	☐	☐	☐

S5. Can you bend your foot/ankle fully?

Never	Rarely	Sometimes	Often	Always
☐	☐	☐	☐	☐

Stiffness

The following questions concern the amount of joint stiffness you have experienced during the **last week** in your foot/ankle. Stiffness is a sensation of restriction or slowness in the ease with which you move your joints.

S6. How severe is your foot/ankle stiffness after first wakening in the morning?

Never	Rarely	Sometimes	Often	Always
☐	☐	☐	☐	☐

S7. How severe is your foot/ankle stiffness after sitting, lying or resting **later in the day**?

Never	Rarely	Sometimes	Often	Always
☐	☐	☐	☐	☐

Pain

P1. How often do you experience foot/ankle pain?

Never	Monthly	Weekly	Daily	Always
☐	☐	☐	☐	☐

What amount of foot/ankle pain have you experienced the **last week** during the following activities?

P2. Twisting/pivoting on your foot/ankle

None	Mild	Moderate	Severe	Extreme

□	□	□	□	□

P3. Straightening foot/ankle fully

None	Mild	Moderate	Severe	Extreme
□	□	□	□	□

P4. Bending foot/ankle fully

None	Mild	Moderate	Severe	Extreme
□	□	□	□	□_ _ _ _ _

P5. Walking on flat surface

None	Mild	Moderate	Severe	Extreme
□	□	□	□	□

P6. Going up or down stairs

None	Mild	Moderate	Severe	Extreme
□	□	□	□	□

P7. At night while in bed

None	Mild	Moderate	Severe	Extreme
□	□	□	□	□

P8. Sitting or lying

None	Mild	Moderate	Severe	Extreme
□	□	□	□	□

P9. Standing upright

None	Mild	Moderate	Severe	Extreme
□	□	□	□	□

Function, daily living

The following questions concern your physical function. By this we mean your ability to move around and to look after yourself. For each of the following activities please indicate the degree of difficulty you have experienced in the **last week** due to your foot/ankle.

A1. Descending stairs

None	Mild	Moderate	Severe	Extreme
□	□	□	□	□

A2. Ascending stairs

None	Mild	Moderate	Severe	Extreme
□	□	□	□	□

For each of the following activities please indicate the degree of difficulty you have experienced in the **last week** due to your foot/ankle.

A3. Rising from sitting

None	Mild	Moderate	Severe	Extreme
□	□	□	□	□

A4. Standing

None	Mild	Moderate	Severe	Extreme
□	□	□	□	□

A5. Bending to floor/pick up an object

None	Mild	Moderate	Severe	Extreme
□	□	□	□	□

A6. Walking on flat surface

None	Mild	Moderate	Severe	Extreme
□	□	□	□	□

A7. Getting in/out of car

None	Mild	Moderate	Severe	Extreme
□	□	□	□	□

A8. Going shopping

None	Mild	Moderate	Severe	Extreme
□	□	□	□	□

A9. Putting on socks/stockings

None	Mild	Moderate	Severe	Extreme
□	□	□	□	□

A10. Rising from bed

None	Mild	Moderate	Severe	Extreme
□	□	□	□	□

A11. Taking off socks/stockings

None	Mild	Moderate	Severe	Extreme
□	□	□	□	□

A12. Lying in bed (turning over, maintaining foot/ankle position)

None	Mild	Moderate	Severe	Extreme
□	□	□	□	□

A13. Getting in/out of bath

None	Mild	Moderate	Severe	Extreme
□	□	□	□	□

A14. Sitting

None	Mild	Moderate	Severe	Extreme
□	□	□	□	□

A15. Getting on/off toilet

None	Mild	Moderate	Severe	Extreme
□	□	□	□	□

For each of the following activities please indicate the degree of difficulty you have experienced in the **last week** due to your foot/ankle.

A16. Heavy domestic duties (moving heavy boxes, scrubbing floors, etc)

None	Mild	Moderate	Severe	Extreme
□	□	□	□	□

A17. Light domestic duties (cooking, dusting, etc)

None	Mild	Moderate	Severe	Extreme
□	□	□	□	□

Function, sports and recreational activities

The following questions concern your physical function when being active on a higher level. The questions should be answered thinking of what degree of difficulty you have experienced during the **last week** due to your foot/ankle.

SP1. Squatting

None	Mild	Moderate	Severe	Extreme
□	□	□	□	□

SP2. Running

None	Mild	Moderate	Severe	Extreme
□	□	□	□	□

SP3. Jumping

None	Mild	Moderate	Severe	Extreme
□	□	□	□	□

SP4. Twisting/pivoting on your injured foot/ankle

None	Mild	Moderate	Severe	Extreme
□	□	□	□	□

SP5. Kneeling

None Mild Moderate Severe Extreme

Quality of Life

Q1. How often are you aware of your foot/ankle problem?

None	Mild	Moderate	Severe	Extreme
□	□	□	□	□

Q2. Have you modified your life style to avoid potentially damaging activities to your foot/ankle?

None	Mild	Moderate	Severe	Extreme
□	□	□	□	□

Q3. How much are you troubled with lack of confidence in your foot/ankle?

None	Mild	Moderate	Severe	Extreme
□	□	□	□	□

Q4. In general, how much difficulty do you have with your foot/ankle?

None	Mild	Moderate	Severe	Extreme
□	□	□	□	□

Thank you very much for completing all the questions in this questionnaire.

Appendix 5.8 Functional USS Elastography (FUSE) protocol

Use the Zonare ® Ultrasound scan machine with 12 MHz probe

Choose Path trial protocol (Musculoskeletal protocol)

Enter Trial ID

Patient is positioned prone and foot and ankle are placed in the foot and ankle device

The location of the rupture gap between the tendon ends is recorded with the foot in the resting position (static position) and during dynamic movement to full planter flexion.

The thickness and diameter of the tendon in longitudinal and transverse planes is recorded

The foot on the injured side is then moved (dorsal flexion and planter flexion) minimally (0.5-1 cm) only (lateral displacement mode).

The displacement USS data is captured and saved in the machine memory.

With the foot in resting position the USS transducer is moved gently (2-3mm) towards the tendon and then relaxed (compression decompression mode). The USS movie is captured and saved in the memory.

Using the PC-controlled foot device: capture data while the foot is moving to dorsiflexion then planter flexion. Save data to the device memory.

Data transfer to USB memory for MatLab analysis

Appendix 5.9 SF – 36 Quesionnaire

Name: **Study number:**

Date when completing form:

SF-36 Health Survey

INSTRUCTIONS: This survey asks your views about your health. This information will help keep track of how you feel and how well you are able to do your usual activities.

Please answer every question by marking the answer as indicated. If you are unsure about how to answer a question, please give the best answer you can.

When complete, please return the questionnaire in the envelope provided.

---

1. In general, would you say your health is:

(circle one)

Excellent	1
Very good	2
Good	3
Fair	4
Poor	5

2. Compared to one year ago, how would you rate your health in general now?

(circle one)

Much better now than one year ago	1
Somewhat better than one year ago	2
About the same as one year ago	3
Somewhat worse than one year ago	4
Much worse now than one year ago	5

3. The following questions are about activities you might do during a typical day. Does your health now limit you in these activities? If so, how much?

(circle one number on each line)

Activities	Yes, limited a lot	Yes, limited a little	No, not limited at all
Vigorous activities, such as running, lifting heavy objects, participating in strenuous sports.	1	2	3
Moderate activities, such as moving a table, pushing a vacuum cleaner, bowling or playing golf	1	2	3
Lifting or carrying groceries	1	2	3
Climbing several flights of stairs	1	2	3
Climbing one flight of stairs	1	2	3
Bending, kneeling or stooping	1	2	3
Walking more than a mile	1	2	3
Walking half a mile	1	2	3
Walking one hundred yards	1	2	3
Bathing or dressing yourself	1	2	3

4. During the past 4 weeks, have you had any of the following problems with your work or other regular daily activities as a result of your physical health?

(circle one number on each line)

	Yes	No
Cut down on the amount of time you spent on work or other activities	1	2
Accomplished less than you would like	1	2
Were limited in the kind of work or other activities	1	2
Had difficulty performing the work or other activities (for example, it took extra effort	1	2

5.During the past 4 weeks, have you had any of the following problems with your work or other regular daily activities as a result of any emotional problems (such as feeling depressed or anxious)?

(circle one number on each line)

	Yes	No
Cut down on the amount of time you spent on work or other activities	1	2
Accomplished less than you would like	1	2
Didn't do work or other activities as carefully as usual	1	2

6. During the past 4 weeks, to what extent has your physical health or emotional problems interfered with your normal social activities with family, friends, neighbours or groups?

(circle one)

Not at all	1
Slightly	2
Moderately	3
Quite a bit	4
Extremely	5

7. How much bodily pain have you had during the past 4 weeks?

(circle one)

None	1
Very mild	2
Mild	3
Moderate	4
Severe	5
Very severe	6

8. During the past 4 weeks, how much did pain interfere with your normal work (including both work outside the home and housework)?

(circle one)

Not at all	1
A little bit	2
Moderately	3
Quite a bit	4
Extremely	5

9. These questions are about how you feel and how things have been with you during the past 4 weeks. For each question please give the one answer that comes closest to the way you have been feeling. How much of the time during the past 4 weeks…

	All of the time	Most of the time	A good bit of the time	Some of the time	A little of the time	None of the time
Did you feel full of life?	1	2	3	4	5	6
Have you been a very nervous person?	1	2	3	4	5	6
Have you felt so down in the dumps that nothing could cheer you up?	1	2	3	4	5	6
Have you felt calm and peaceful?	1	2	3	4	5	6
Did you have a lot of energy?	1	2	3	4	5	6
Have you felt downhearted and low?	1	2	3	4	5	6
Did you feel worn out?	1	2	3	4	5	6
Have you been a happy person?	1	2	3	4	5	6
Did you feel tired?	1	2	3	4	5	6

10. During the past 4 weeks, how much of the time has your physical health or emotional problems interfered with your social activities (like visiting friends, relatives, etc.)?

(circle one)

All of the time 1
Most of the time 2
Some of the time 3
A little of the time 4
None of the time 5

11. How TRUE or FALSE is each of the following statements to you?

(circle one number on each line)

	Definitely true	Mostly true	Don't know	Mostly false	Definitely false
I seem to get ill more easily than other people	1	2	3	4	5
I am as healthy as anybody I know	1	2	3	4	5
I expect my health to get worse	1	2	3	4	5
My health is excellent	1	2	3	4	5

Appendix 6.1 : Haematoxylin Eosin Stain

Fixation: formalin fixed, paraffin embedded tissue sections.

Solutions and Reagents:

1. Harris haematoxylin
2. tap water substitute
3. acetified eosin

Procedure:

1. Bring sections to distilled water
2. Stain nuclei with the alum haematoxylin
3. Rinse in running tap water
4. Differentiate with 0.3% acid alcohol (see note)
5. Rinse in running tap water
8. Stain with eosin 1-2 mins
9. Dehydrate, clear and mount.

Results

collagen.....pale pink
muscle.....deep pink
acidophilic cytoplasm.....red
basophilic cytoplasm.....purple
nuclei.....blue
erythrocytes.....cherry red

Appendix 6.2: Alcian Blue Staining Protocol

Fixation: formalin fixed, paraffin embedded tissue sections.

Solutions and Reagents:

3% Acetic Acid Solution:
Glacial acetic acid ---------- 3 ml
Distilled water ---------- 97 ml

Alcian Blue Solution (pH 2.5):
Alcian blue, 8GX ---------- 1 g
Acetic acid, 3% solution ---------- 100 ml
Mix well and adjust pH to 2.5 using acetic acid.

Eosin counter stain:
Eosin ---------- 2-3 drops per slide

Procedure:

1. Deparaffinize slides and hydrate to distilled water.
2. Incubate in 3% Acetic acid for 3 minutes
3. Stain in alcian blue solution for 60 minutes at room temperature
4. Wash in running tap water for 10 minutes.
5. Rinse in distilled water.
6. Counterstain in Eosin for 3 minutes.
7. Wash in running tap water for 1 minute.
8. Dehydrate and through 95% alcohol, 2 changes, 3 minutes each.
9. Clear in xylene or xylene substitute.
10. Mount with resinous mounting medium.

Results:

Strongly acidic sulfated mucosubstances ---------- blue
Nuclei ---------- pink to red
Cytoplasm ---------- pale pink

Appendix 6.3 Immunohistochemistery Protocol

Solutions and Reagents

1. Xylene
2. Ethanol, anhydrous denatured, histological grade (100% and 95%)
3. Deionized water (dH_2O)
4. Haematoxylin stain
5. **Wash Buffer:**
   1X TBS/0.1% Tween-20 (1X TBST): To prepare 1 L add 100 ml 10X TBS to 900 ml dH_2O. Add 1 ml Tween-20 and mix.
6. **Antigen Unmasking:**
   10 mM Sodium Citrate Buffer: To prepare 1 L add 2.94 g sodium citrate trisodium salt dihydrate ($C_6H_5Na_3O_7 \bullet 2H_2O$) to 1 L dH_2O.

7. **3% Hydrogen Peroxide:** To prepare, add 10 ml 30% H_2O_2 to 90 ml dH_2O.
8. **Blocking Solution:** TBST/5% normal goat serum: to 5 ml 1X TBST add 250 µl normal goat serum. (provided by manufacturer)
9. Biotinylated secondary antibody (provided by manufacturer)
10. **ABC Reagent:** (Vectastain ABC Kit, Vector Laboratories, Inc., Burlingame, CA) Prepare according to manufacturer's instructions 30 minutes before use.
11. **DAB Reagent or suitable substrate:** Prepare according to manufacturer's recommendations.

Deparaffinization/Rehydration

Do not allow slides to dry at any time during this procedure.

1. **Deparaffinize/hydrate sections:**
   1. Incubate sections in two washes of Clearene for 5 minutes each.
   2. Incubate sections in two washes of 100% ethanol for 3 minutes each.
2. Wash sections twice in dH_2O for 5 minutes each.

Antigen Unmasking

Bring slides to a boil in 10 mM sodium citrate buffer pH 6.0 then maintain at a sub-boiling temperature for 10 minutes. Cool slides on bench top for 30 minutes.

Staining

1. Wash sections in dH_2O three times for 5 minutes each.
2. Incubate sections in 3% hydrogen peroxide for 10 minutes.
3. Wash sections in dH_2O twice for 5 minutes each.

NOTE: Consult product data sheet for recommended antibody diluent.

4. Wash sections twice in wash buffer for 5 minutes each.
5. Circle each section with pap pen
6. Block each section with 100-400 µl blocking solution for 20 min at room temperature.
7. Remove blocking solution
8. Add 100-400 µl primary antibody diluted in recommended antibody diluent to each section. Incubate overnight at 4°C.
9. Remove antibody solution and wash sections in wash buffer three times for 2 minutes each.
10. Add 100-400 µl biotinylated secondary antibody, diluted in TBST per manufacturer's recommendation, to each section. Incubate 20 minutes at room temperature.
11. Remove secondary antibody and wash in wash buffer three times for 2 min each
12. Prepare ABC reagent according to the manufacturer's instructions and add 100-400 µl ABC reagent to each section and incubate for 20 minutes at room temperature.
13. Remove ABC solution and wash sections three times with wash buffer for 2 minutes each.
14. Remove ABC reagent and wash sections three times in wash buffer for 2 minutes each.
15. Add 100-400 µl DAB or suitable substrate to each section and monitor staining closely (8-10 min)
16. As soon as the sections develop, immerse slides in dH_2O (for 10 min)
17. Counterstain sections in haematoxylin.
18. Wash sections in dH_2O two times for 5 minutes each.
19. Dehydrate sections:
    1. Incubate sections in 95% ethanol two times for 1 min each.
    2. Repeat in 100% ethanol, incubating sections two times for 1 min each.
    3. Repeat in Clearene incubating sections two times for 5 min each.
20. Mount coverslips.

Appendix 7.1: Tendon Explant Protocol

Equipment

1. Sterile forceps (at least 2) and either sterile scissors or scalpels.

2. DMEM F12 with 10% FBS and 1% Pennicillin/streptomycin

3. DMEM F12 with 50% FBS & 1% penn/strep

4. Sterile petri dish

5. Sterile 6- well plates

TENDON TISSUE COLLECTION

Tendon should be collected into sterile DMEM F12 with 10% FBS & 1% penicillin/streptomycin. Tendon samples were processed as soon as possible after collection (keep tendon refrigerated in the DMEM F12/ 10% FBS/ 1% penn/strep if tendon cannot be processed immediately).

EXPLANTING

DAY 1

1. Using sterile tools transfer the tissue from the collection pot to a sterile petri dish. Cover tissue with cold media (DMEM F12 with 10% FBS & 1% Penn/Strep) to prevent it drying out.

2. Using scissors (or a scalpel if preferred) dice the tissue into approx 1-3mm^3 sections. Transfer the small tendon pieces to the wells of a 6 well plate and put a small drop of media (DMEM F12 with 50% FBS & 1% Penn/Strep) on each piece to prevent them drying out (but tendon piece should not be floating). Space the tendon pieces out in each well so no more than 50% of the well is taken up by tendon pieces.

3. Incubate the explants at 37°C in CO_2 incubator.

DAY 3

1. After 48 hours gently add 1ml of warm medium (DMEM F12 with 50% FBS & 1% penicillin/streptomycin) to each well. Dribble the medium down the side of the well to avoid dislodging the explants).

2. Place plates back in 37°C CO_2 incubator.

END OF WEEK 1

1. Carefully remove approx 500µl* of media from each well and replace with the same volume of fresh DMEM F12 with 50% FBS & 1% penn/strep. * Remove as much media as possible without dislodging explants. KEEP 500µl OF THE MEDIA REMOVED FROM THE WELLS FOR MYCOPLASMA TESTING (Store at -20°C until ready to test.)

Usually between 7 and 10 days after explanting some cells have started to migrate out of the tissue and will be visible on the plate.

END OF WEEK 2 (or when a reasonable amount of cells have come out of the tissue)

1. Remove explanted tissue from 6-well plates using sterile forceps. Remove media from wells and replace with approximately 2ml/well of 10% FBS/DMEM-F12 with 1% penn/strep.

2. Media change cells 3x per week using 10% FBS/DMEM-F12 with 1% penn/strep until cells are approximately 70% confluent. This may take another 2 weeks.

END OF WEEK 4 (approximately)

1. When cells are 70% confluent, harvest cells by scraping. Transfer cells from one well in the 6-well plate to a petri dish (ie so get 6 petri dishes from one 6-well plate).

2. Grow cells in petri dishes with 10ml 10% FBS/DMEM-F12 (don't need antibiotics in media at this stage) until plates are 70% confluent. (Media change 3x per week). KEEP 500µl OF THE MEDIA REMOVED FROM THE WELLS FOR MYCOPLASMA TESTING

3. Freeze cells once 70% confluent.

FREEZING CELL STOCKS

1. Make up a 10% DMSO/90% FBS solution. Keep on ice.

2. Label cryovials (one cryovial per petri dish of cells).

3. Harvest cells by scraping.

4. Centrifuge (1400rpm for 3mins in lab centrifuge) and discard media.

5. Resuspend cells in 10% DMSO/90% FBS and immediately place in cryovials on ice.

6. Place cryovials in a polystyrene tube holder and transfer to -80°C. (As DMSO is toxic to the cells it is important to transfer them to the -80°C freezer quickly.)

7. After 24hrs, transfer cryovials to liquid nitrogen.

Disposal

- Leave any remaining tissue in the petri dish. Add Virkon to the dish and leave in the box overnight as usual. Discard any remaining solids in the petri dish by placing in a yellow bag the following morning.

- Place used scalpel into sharps bin.

- Wash forceps in Virkon being careful to remove any remaining lumps of tissue. Rinse thoroughly with water, then spray with IMS and return to the IMS pot in the primary culture hood.

- Spray the hood with IMS and wipe down. At the end of the day, spray all surfaces in the hood with barrycidal (beware - don't get biocidal by mistake!). Don't wipe off the barrycidal, turn the hood off and close the door.

- To dispose of the explants, place in a tube and add Virkon overnight. Drain off the Virkon, screw on the lid and dispose of in the yellow bag.

Appendix 7.2: Live/Dead Viability Stain Protocol

1. Tissues were previously treated with culture medium prior to assay.
2. The media was tipped out of the dish and tissues are washed prior to the assay to remove or dilute serum esterase activity generally present in serum. Wash adherent tissues gently with Dulbecco's phosphate-buffered saline (D-PBS)
3. Remove the LIVE/DEAD® assay reagents from the freezer and allow them to warm to room temperature.
4. Add 20 µL of the supplied 2 µM EthD-1 stock solution (Component B) to 10 mL of sterile, tissue culture–grade D-PBS, vortexing to ensure thorough mixing. This gives an approximately 4 µM EthD-1 solution.
5. Combine the reagents by transferring 5 µL of the supplied 4 µM Calcein AM stock solution (Component A) to the 10 mL EthD-1 solution. Vortex the resulting solution to ensure thorough mixing.
6. The resulting approximately 2 µM Calcein AM and 4 µM EthD-1 working solution is then added directly to tissue samples.
7. Add 100–150 µL of the combined LIVE/DEAD® assay reagents, using optimized concentrations, to the surface of a 22 mm square coverslip, so that samples are covered with solution. Incubations should be performed in a covered dish (e.g., 20 mm disposable petri dish) to prevent contamination or drying of the samples.
8. Incubate the samples for 30–45 minutes at room temperature. A shorter incubation time may be used if the dye concentrations or incubation temperature are increased.
9. Following incubation, add about 10 µL of the fresh LIVE/ DEAD® reagent solution or D-PBS to a clean microscope slide.
10. Using fine-tipped forceps, carefully (but quickly) invert and mount the wet coverslip on the microscope slide. To prevent evaporation, seal the coverslip to the glass slide (e.g., with clear fingernail polish). Avoid damaging or shearing tissues in the preparation of the slides.
11. View the labeled cells under the fluorescence microscope

Appendix 7.3: Alamar Blue Assay

Cells were previously treated with culture medium and incubated for 48 and 96 hours prior to assay.

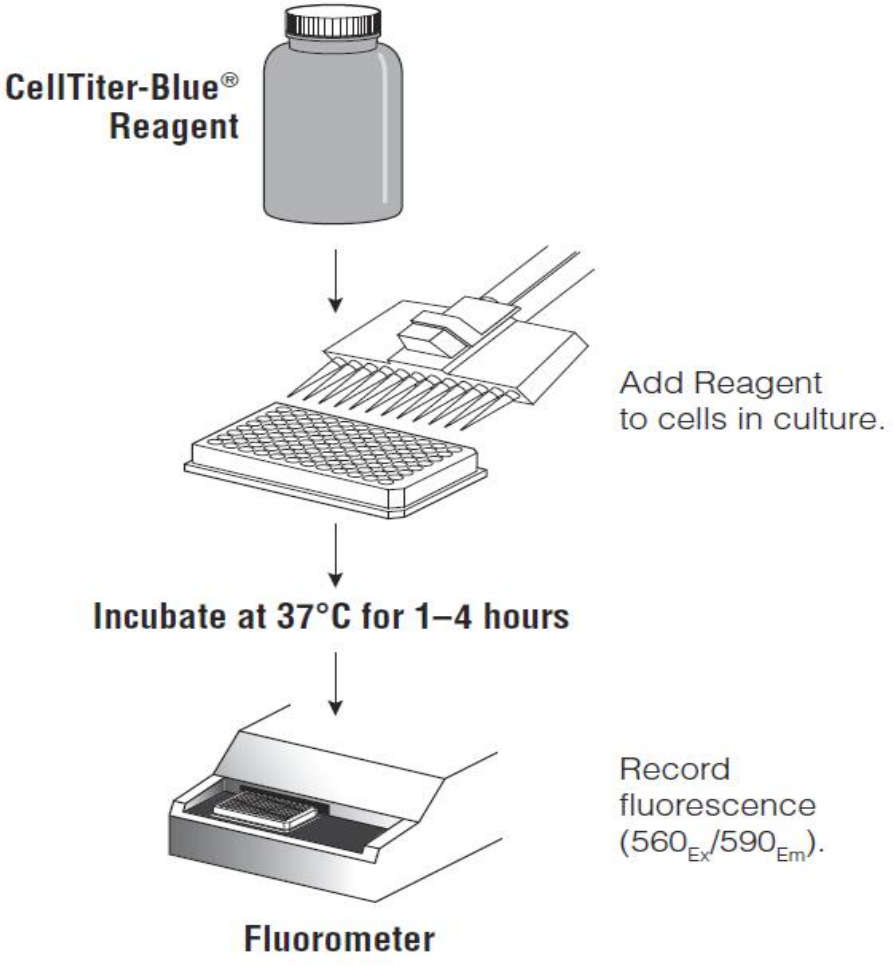
The media was tipped out of the wells and replaced with DMEM + 1% FCS, and were left for 30 minutes in the incubator.

This media was tipped out and a 1:10 dilution of Alamar Blue was added to the cultures.

Cultures were left for three hours in the incubator.

The REDOX state of Alamar Blue was measured using a Spectramax Gemini XS microplate reader, at an excitation wavelength of 530nm, and emission wavelength of 590nm, with a 570nm cut-off.

Cells can be washed and re-stained or grown some more.



Appendix 7.4: PicoGreen dsDNA Content Assay Protocol

1. Tissues were previously treated with culture medium prior to assay.
2. Allow the Quant-iT™ PicoGreen® reagent to warm to room temperature before opening the vial.
3. **Prepare assay buffer:**
    a. TE buffer (10 mM Tris-HCl, 1 mM EDTA, pH 7.5) is used below for diluting the Quant-iT™ PicoGreen® reagent, for diluting DNA samples, and in the assay itself.
    b. Because the Quant-iT™ PicoGreen® dye is an extremely sensitive detection reagent for dsDNA, it is imperative that the TE solution used be free of contaminating nucleic acids. The 20X TE buffer included in the Quant-iT™ PicoGreen® dsDNA Assay Kits is certified to be nucleic acid–free and DNasefree.
    c. Prepare a 1X TE working solution by diluting the concentrated buffer 20-fold with sterile, distilled DNase-free water.
4. **Prepare the reagent**
    a. On the day of the experiment, prepare an aqueous working solution of the Quant-iT™ PicoGreen® reagent by making a 200-fold dilution of the concentrated DMSO solution in TE.
    b. Add 100 µL Quant-iT™ PicoGreen® dsDNA reagent to 19.9 mL TE.
    c. Protect the working solution from light by covering it with foil or placing it in the dark, as the Quant-iT™ PicoGreen® reagent is susceptible to photo degradation.
5. **DNA standard curve**
    a. Prepare a 2 µg/mL stock solution of λdsDNA in TE.
    b. Prepare 5 different concentration of λdsDNA stock as shown in table below
    c. Generate standard curve and equation

Table 3. Protocol for preparing a high-range standard curve.

Volume (µL) of TE	Volume (µL) of 2 µg/mL DNA Stock	Volume (µL) of Diluted Quant-iT™ PicoGreen® Reagent	Final DNA Concentration in Quant-iT™ PicoGreen® Assay
0	1,000	1,000	1 µg/mL
900	100	1,000	100 ng/mL
990	10	1,000	10 ng/mL
999	1	1,000	1 ng/mL
1,000	0	1,000	blank

6. **Samples Analysis**
    a. Load 10 µl of samples were loaded into the 96-well plate in triplicates.
    b. Add 100 µl of 1 X TE buffer to each well containing standards and samples
    c. Add 100 µl of Picogreen dsDNA quantitation reagent to each well containing standards and samples
    d. Incubate at room temperature in the dark on a plate shaker for 30 minutes.
    e. Measure the fluorescence of samples at 490 nm excitation wavelength, emission wavelength at 540 nm and cut off at 530 nm with the Spectramax Gemini microplate spectrofluorimeter.
    f. Subtract the florescence of the reagent blank from that of each of the samples.
    g. Determine the concentration of the sample from the standard curve generated in DNA standard curve.

Appendix 7.5: Ziva™ Ultrasensitive BrdU Cell Proliferation Assay

Prepare Reagents:

1. 1X working preparation solution from the Kit 3X preparation solution
   e.g. for 12 wells:
   12 x 0.4mL x 5 = 24mL total volume of 1X prep solution needed.
   [(24mL / 3) of 3X kit prep solution) + [2 x (24mL / 3) of distilled water].
   8mL of 3X kit prep solution + 16mL distilled water = 24mL 1X prep solution.
2. Preparation of Anti-BrdU mAb-Alkaline Phosphatase Conjugate Working Solution
   e.g. for 12 wells:
   12 x 50µL = 600µL antibody conjugate diluents needed.
   Add 10µL/mL x 0.6mL = 6µL anti-BrdU Ab-AP conjugate to the specified volume of antibody conjugate diluent.

Assay Protocol

1. Grow cells to appropriate confluence and apply PRC at appropriate concentrations for the required time. Use white, flat bottom, 96-well culture dishes.
2. 24 hours prior to assay: dilute BrdU Labeling Solution stock 1:100 with 0% FCS DMEM, then pipette 10µL per well (if there was 100µL medium in the well).
3. After 24hrs remove plate from incubator. Add 200µl of preparation solution to each well. Decant and blot liquid.
4. Add 400µl preparation solution to each well. Decant and blot.
5. Add 50µl Fix solution to each well. Cover plate and incubate @ RT for 10 minutes. Decant and blot.
6. Add 200µl Stringency solution to each well. Cover plate and incubate @ RT for 10 minutes. Decant and blot.
7. Add 400µl preparation solution to each well. Cover plate and incubate @ RT for 2 minutes. Decant and blot.
8. Add 50µl of the prepared diluted anti-BrdU antibody conjugate solution to each well. Cover plate and incubate @ RT for 20 minutes. Decant and blot.
9. Add 400µl wash buffer to each well. Decant and blot. Do this 4 times.
10. Add 400µl preparation solution to each well. Decant and blot. Do this 2 times.
11. Add 50µl CDP Star Chemiluminescent substrate to each well. Read plate after 60 minutes.

ZIVA™-CPA STANDARD ASSAY PROTOCOL

